DOE/NASA/0013-80/1
NASA CR-159852
WRC 78-182

CONCEPTUAL DESIGN STUDY OF AN IMPROVED GAS TURBINE POWERTRAIN

W.I. CHAPMAN
WILLIAMS RESEARCH CORPORATION

MARCH 1980

PREPARED FOR
NATIONAL AERONAUTICS AND SPACE ADMINISTRATION
LEWIS RESEARCH CENTER
UNDER CONTRACT DEN3-13

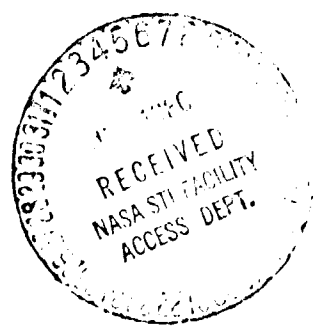

FOR
U.S. DEPARTMENT OF ENERGY
OFFICE OF TRANSPORTATION PROGRAMS
DIVISION OF AUTOMOTIVE TECHNOLOGY DEVELOPMENT

DOE/NASA/0013-80/1
NASA CR-159852
WRC 78-182

CONCEPTUAL DESIGN STUDY OF AN IMPROVED GAS TURBINE POWERTRAIN

W.I. CHAPMAN
WILLIAMS RESEARCH CORPORATION
WALLED LAKE, MICHIGAN 48088

MARCH 1980

PREPARED FOR
NATIONAL AERONAUTICS AND SPACE ADMINISTRATION
LEWIS RESEARCH CENTER
CLEVELAND, OHIO 44135
UNDER CONTRACT DEN3-13

FOR
U.S. DEPARTMENT OF ENERGY
OFFICE OF TRANSPORTATION PROGRAMS
DIVISION OF AUTOMOTIVE TECHNOLOGY DEVELOPMENT
WASHINGTON, D.C. 20545
UNDER INTERAGENCY AGREEMENT EC-77-A-31-1040

FOREWORD

This report presents the results of a Conceptual Design Study of an Improved Gas Turbine Powertrain for automotive applications under NASA Contract No. DEN3-13. The work was performed by Williams Research Corporation and AM General Corporation, a subsidiary of American Motors Corporation, as a joint effort.

The IGT powertrain design and analysis accomplished under this contract was performed by the engineering staff of Williams Research Corporation. Among the principal contributors to this work were the following:

Design Engineering Coordinator: R. Horn
Mechanical Design: R. Beland, E. Botting
Mechanical Analysis: T. Culbertson, J. Johnston
Materials: J. Carlton
Performance Analysis: D. Dorer, R. Everett, D. Svalstad
Compressor: R. Honn
Turbine: E. T. Pawl
Combustor: M. Bak
Heat Exchanger: D. Robson

The vehicle installation studies were performed by the AM General Corporation. The principal contributor was T. T. Lie.

TABLE OF CONTENTS

LIST OF ILLUSTRATIONS

LIST OF TABLES

SUMMARY

This final report summarizes the results and the work accomplished on the conceptual design study of the automotive Improved Gas Turbine (IGT) powertrain.

Task I, Powertrain Identification and Description, started with a review of basic thermodynamic cycle parameters, rotor systems, and components that could be considered for an automotive gas turbine. Characteristics of different types of components were explored in detail, using available information on current and near term technology.

Preliminary design studies were made of a typical automotive turbine installed in a passenger car to disclose and study problem areas.

From the many possible turbine engine cycles, three powertrain candidates were selected for detailed study and analysis. These were the single-rotor engine with continuously variable transmission, and dual-rotor engines using two types of turbine temperature control, variable power turbine nozzle and slip clutch power transfer.

Task II, Powertrain Analysis, made detailed comparison of selected components in the candidate powertrains to determine the effects of compressor pressure ratio, turbine inlet temperature, and turbine cooling on specific fuel consumption (SFC) at low power. The turbine cycles with lower SFC were analyzed for vehicle fuel economy at 1542 kg (3400 lb) test weight on the federal driving cycles.

In addition, sensitivity and risk analysis were performed and production cost comparisons made to guide the selection of the concept and basic cycle parameters for the IGT powertrain. All objectives for the IGT powertrain were considered, with emphasis on vehicle fuel economy in the final selection of the dual-rotor gas turbine with variable power turbine nozzle.

A two-stage centrifugal compressor is used at a design pressure ratio of 5.28 to achieve good efficiency over the operating range. The lower shaft speed with this compressor makes it possible to operate an advanced high-temperature alloy integral first stage gasifier turbine wheel at a TIT of 1422°K (2100°F). The integral second stage power turbine wheel uses a variable nozzle for turbine temperature and output torque control. A catalytic combustor is used for very low emissions and high efficiency, with the combustion air preheated by an annular ceramic recuperator. Component characteristics and matching are directed toward reducing SFC at low power to achieve good vehicle fuel economy.

Task IIIA, Powertrain Optimization and Performance, continued the vehicle performance and fuel economy analysis to optimize the powertrain/vehicle system. The engine is sized as small as practical for steady-state operation, rated at 54.8 kW (73.5 hp) at 303°K (85°F) and 152.4 m (500 ft). This engine rating meets the vehicle acceleration requirement of 0 to 60 mph in 15.0 seconds with ambient temperature below 288°K (59°F). Water injection is used at higher ambient

temperature to maintain the power and acceleration. This optimized IGT powertrain is estimated to achieve a vehicle fuel economy of 11.9 km/l (28.0 mpg) on the combined driving cycle, 43 percent over the 1976 compact automobile.

The IGT powertrain is packaged into a compact, axisymmetric arrangement made possible by the annular recuperator. A concentric rotor arrangement is used with a common gearcase for the power turbine reduction gear and gasifier driven accessory drive train. The powertrain is packaged into an American Motors Concord 2-door sedan, using a 3-speed automatic transmission for conventional rear drive.

Task IIIB, Vehicle Cost Analysis, estimated the IGT vehicle to have a 10 percent cost penalty over the piston engine vehicle. Less than half of the cost penalty is in the turbine engine; the remainder is due to the adaptation of the current pro-duction vehicle and systems. The fuel economy improvement and reduced maintenance and repair result in an overall life cycle cost saving of 9 percent for the IGT vehicle.

Task IV, Powertrain Development Plan, generated the overall development plan for the IGT powertrain to bring it from the conceptual design study through vehicle testing of prototype powertrains.

INTRODUCTION

Williams Research Corporation and the AM General Corporation, subsidiary of American Motors Corporation, have completed the conceptual design study of an Improved Gas Turbine Powertrain under NASA Contract No. DEN3-13. This design study was on an automotive gas turbine powertrain for a compact size vehicle to meet the following objectives:

1. A 20 percent improvement in powertrain thermal efficiency compared to a conventional 1976 powertrain. This shall result in at least a 20 percent fuel economy improvement over a 1976 model year automotive vehicle over the EPA composite driving cycle. For the study, a compact class [~1406 kg (~3100 lb) curb weight] vehicle shall serve as the basis of comparison.

2. The powertrains considered should be ready to enter the production engineering phase of development as soon as possible.

3. Reliability, and life features comparable with powertrains currently in the market.

4. Driveability acceptable to the consumer.

5. Meet or exceed the Federal Emissions Standards of 0.4 gm/mi, 3.4 gm/mi., 0.40 gm/mi, for $HC/CO/NO_x$.

6. Meet noise and safety levels that are currently legislated.

7. Have competitive initial cost and a life cycle cost no greater than conventionally-powered automotive vehicles.

Williams Research Corporation was the prime contractor and performed the design and analysis on the turbine engine, based on their extensive experience since 1955 designing and developing small gas turbines for a wide variety of aircraft, marine, industrial, and vehicle applications.

AM General did the vehicle installation studies, and supplied vehicle, transmission, drivetrain, and accessory characteristics to Williams Research for incorporation with the vehicle performance and fuel economy analysis.

The major objective of the study was 20 percent minimum improvement in vehicle fuel economy on the EPA composite driving cycle. A preliminary analysis was made of the federal driving cycle based on an American Motors Gremlin at 1542 kg (3400 lb) test weight to indicate the power requirement (to the drivetrain) and the relative time spent at different power levels. This breakdown is shown in Figure 1. On the urban cycle, 40 percent of the time is spent with the engine at idle, with the vehicle decelerating or stopped. Only 10 percent of the time is over 15 kW (20 hp), with no requirement over 37 kW (50 hp). This breakdown emphasizes the need for low fuel consumption at idle and at low power. The engine cycle and components must be selected and characteristics tailored with the fuel economy objective always in mind.

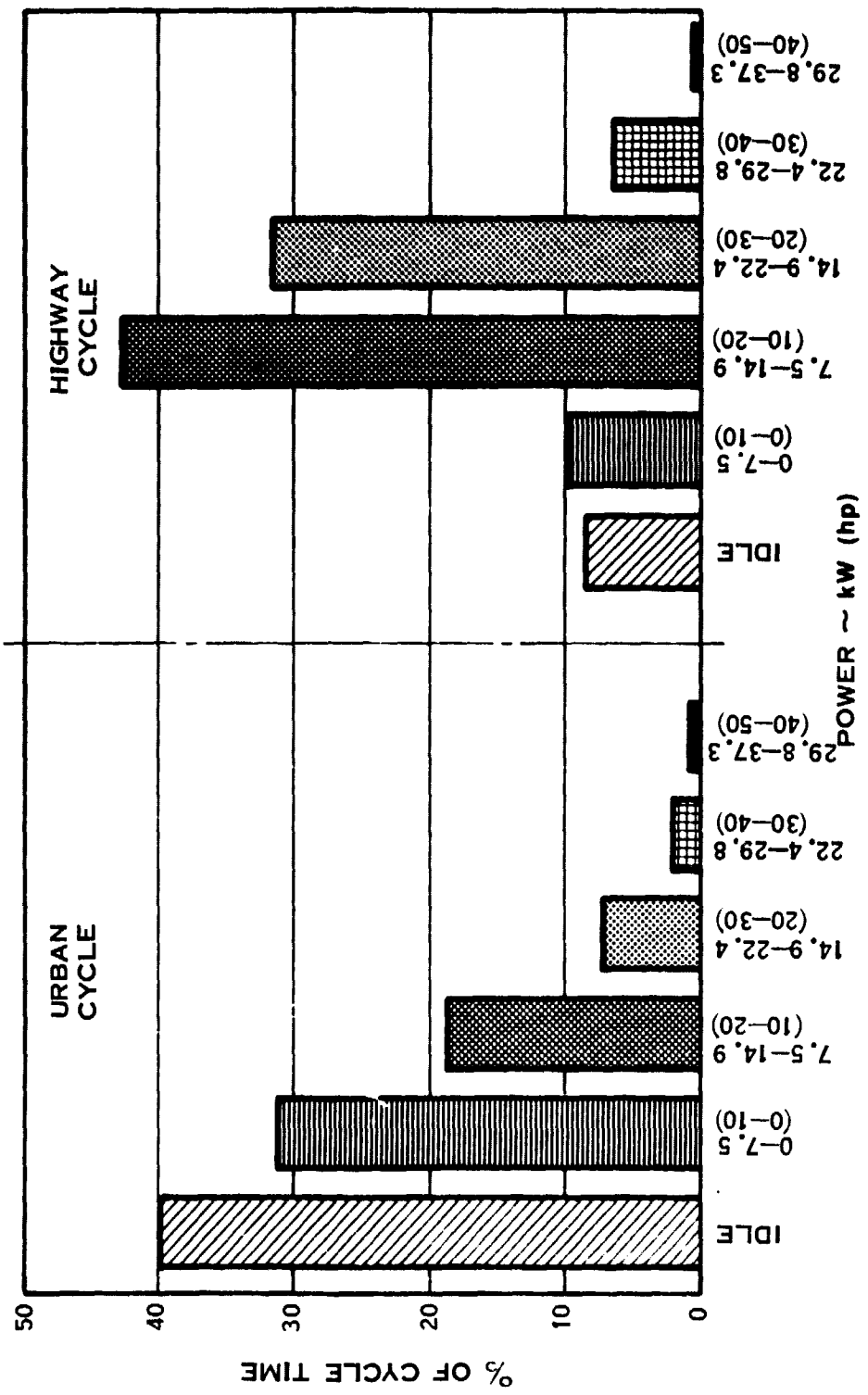

Figure 1. Power Requirements for Federal Driving Cycles

The design study was divided into six tasks, summarized as follows:

Task I - Powertrain Identification and Description

Investigate various powertrain concepts, describe inherent physical and performance characteristics, and select concepts for further analysis that have the most potential for meeting program objectives.

Task II - Powertrain Analysis

Analyze component and system performance of selected powertrain concepts, with supporting sensitivity, production cost, and risk analyses. Select powertrain concept appropriate for development.

Task IIIA - Powertrain Optimization and Performance

Optimize and define component and system performance characteristics for selected powertrain concept. Complete design study of powertrain integrated into the vehicle, with supporting mechanical analysis.

Task IIIB - Vehicle Cost Analysis

Estimate the difference in initial (sticker) price and life cycle cost between the IGT vehicle and the baseline vehicle.

Task IV - Powertrain Development Plan

Prepare complete development plan to bring the IGT powertrain through vehicle test of prototype powertrains. This plan was submitted separately as WRC Report No. 78-152 and is also summarized in this report.

Task V - Identification of Long-Lead Research and Development Requirements

Identify and report areas requiring long-lead research and development effort. This report was submitted separately as WRC Report No. 78-151.

Task VI - Reporting Requirements

Submit monthly technical progress and financial management reports, and prepare final report reviewing the work accomplished and the results from the conceptual design study.

1.0 TASK I - POWERTRAIN IDENTIFICATION AND DESCRIPTION

1.1 CYCLE PARAMETERS

The basic gas turbine cycle is a steady-flow process with a working fluid undergoing compression, heating, expansion, and exhaust (or cooling if a closed cycle). The compression and expansion processes can occur in one or more stages, using different types of turbomachinery with one or more rotors to couple the driving and driven components and to provide accessory and output power. Heat exchangers may be inserted at different points of the cycle to improve cycle performance, increase output, and improve efficiency.

Table I lists the thermodynamic cycle parameters, rotor systems, and typical components that might be used in an automotive gas turbine powertrain. Every possible powertrain concept based on these cycle parameters, rotor systems, and components could be identified and tabulated, but this would involve much detail repetition and duplication of effort. A more practical approach is to examine individually the cycle parameters, rotor systems, and components.

This preliminary list (Table I) was used as a working list to develop candidate powertrain concepts. Each item was considered to some degree, and additional items were discovered and/or developed during the course of the study.

The contribution of each item to achieving the program objectives was assessed and ranked. The items with the highest rankings were then combined logically into several powertrain candidate concepts for detailed analysis and comparison during Task II, Powertrain Analysis.

WORKING FLUID

Open cycle gas turbines using atmospheric air as the working fluid have been used exclusively in automotive applications. Closed-cycle gas turbines permit the use of other working fluids such as inert gases with perhaps more favorable thermodynamic properties, but require the addition of two heat exchangers to the cycle, an indirectly fired heater for the maximum cycle temperature at the turbine inlet, and a cooler for the minimum cycle temperature at the compressor inlet. The added heat exchangers severely restrict the thermodynamic cycle, since the turbine inlet temperature (TIT) must be below the temperature level that the heater can withstand, and the compressor inlet air must be above ambient temperature with any finite cooler. The performance, size, weight, and cost penalties of the heat exchangers and associated equipment make the closed-cycle turbine unsuitable for automotive application.

TURBINE INLET TEMPERATURE (TIT)

The IGT must be designed for the highest TIT possible throughout the operating range to achieve the best fuel economy. At the same time, the powertrain must be comparable in durability and reliability and competitive in initial cost to conventionally-powered automotive vehicles. To demonstrate achievement of these requirements by 1983, only commercially available high-temperature metal alloys are being considered for the turbine rotors.

TABLE I. GAS TURBINE CYCLE AND COMPONENT CHARACTERISTICS

CYCLE PARAMETERS

Working Fluid - Open System
- Closed System

Pressure Ratio

Turbine Inlet Temperature

Regeneration

Intercooling

Reheat

Water Injection - Hot Day
- Power Boost
- Cooling

ROTOR SYSTEM

Single-Spool
Two-Spool - PT First
- PT Second

Three-Spool - PT Second and Third

Three-Spool With Two-Stage Compressor
- PT Second
- PT Third

Rotor Interconnection - Clutch
- Gear and Clutch
- Differential Gear
- Variable Ratio
- Electric

DRIVE TRAIN

Single-Spool - Multispeed Gearbox
- Variable Ratio Mechanical
- Hydrodynamic
- Hydrostatic
- Electric

Free PT Rotor - Multispeed Gearbox
- Variable Ratio Mechanical
- Hydrodynamic
- Hydrostatic
- Electric

AUXILIARY AND ACCESSORY DRIVE

Gasifier Drive

Power Turbine Drive

Mechanical - Gear Train
- Worm Gear
- Chain
- Belt
- Direct

Electrical - Generator on Rotor
- Motor Drive

COMPRESSOR

Radial

Axial and Radial

Axial

Variable Stator

TURBINE

Radial

Radial and Axial

Axial

Variable Stator

COMBUSTOR

Annular

Can - Single
- Multiple

Reheat

HEAT EXCHANGER

Regenerator - Single
- Dual
- Concentric
- Metallic
- Ceramic

Recuperator - Single
- Multiple
- Concentric
- Metallic
- Ceramic

Intercooler With Two-Stage Compressor

MAR-M 247 high-temperature alloy was the initial choice as the material for the first stage turbine rotor of the IGT powertrain, with stress rupture strength the highest available in an easily cast conventional nickel base superalloy (Figure 2). During the course of the design study, preliminary mechanical properties data were generated on an advanced high-temperature alloy made by the rapid solidification rate (RSR) process. This alloy has significantly higher stress rupture properties than MAR-M 247 alloy as shown in Figure 2, with the potential for correspondingly higher TIT.

With these turbine rotor alloys, the TIT at maximum power is expected to be in the range of 1311 to 1422°K (1900 to 2100°F). A tentative design point was selected at 1311°K (1900°F) for the preliminary cycle analysis.

REGENERATION

Due to the many complexities associated with regeneration, it is of prime importance to determine if regeneration can be avoided. Reasonably low levels of SFC at design point conditions can be obtained without regeneration if high TIT and compressor pressure ratio are used. However, the nonregenerative engine has a part-load SFC curve which rises rapidly with decreasing power even when devices to maintain high TIT are incorporated. A part-load analysis was made to demonstrate this effect. Design point compressor pressure ratios up to 15 and TIT from 922 to 1367°K (1200 to 2000°F) were selected for the analysis.

The resultant minimum part-load SFC versus output power is shown in Figure 3. From this figure it can be seen that, even with optimistic assumptions, the resultant part-load SFC is much too high for a viable automotive engine. Some degree of heat recovery or regeneration is therefore required to obtain acceptable part-load fuel economy.

PRESSURE RATIO

To determine how high the compressor pressure ratio should be to optimize the cycle for part-load, a single-rotor engine configuration was analyzed with three compressor pressure ratios and efficiencies. This configuration has a single-stage centrifugal compressor, recuperator, combustor, two-stage axial flow turbine, ideal variable ratio transmission, and no accessory load. The three compressor pressure ratios examined were 3.5, 4.5, and 5.5 at the design point, with compressor efficiencies of 0.81, 0.79, and 0.772, respectively. All other characteristics of the engine were kept constant for the three cycles. The design point and part-load performance were calculated as shown in Figure 4.

Clearly, up to a design pressure ratio of 5.5, the higher the pressure ratio, the better the part-load fuel consumption.

Design point pressure ratio	3.5	4.5	5.5
SFC at 10 percent power with 1311°K (1900°F) TIT	0.60	0.54	0.50
SFC at 10 percent power with 1089°K (1500°F) TIT	0.65	0.59	0.53

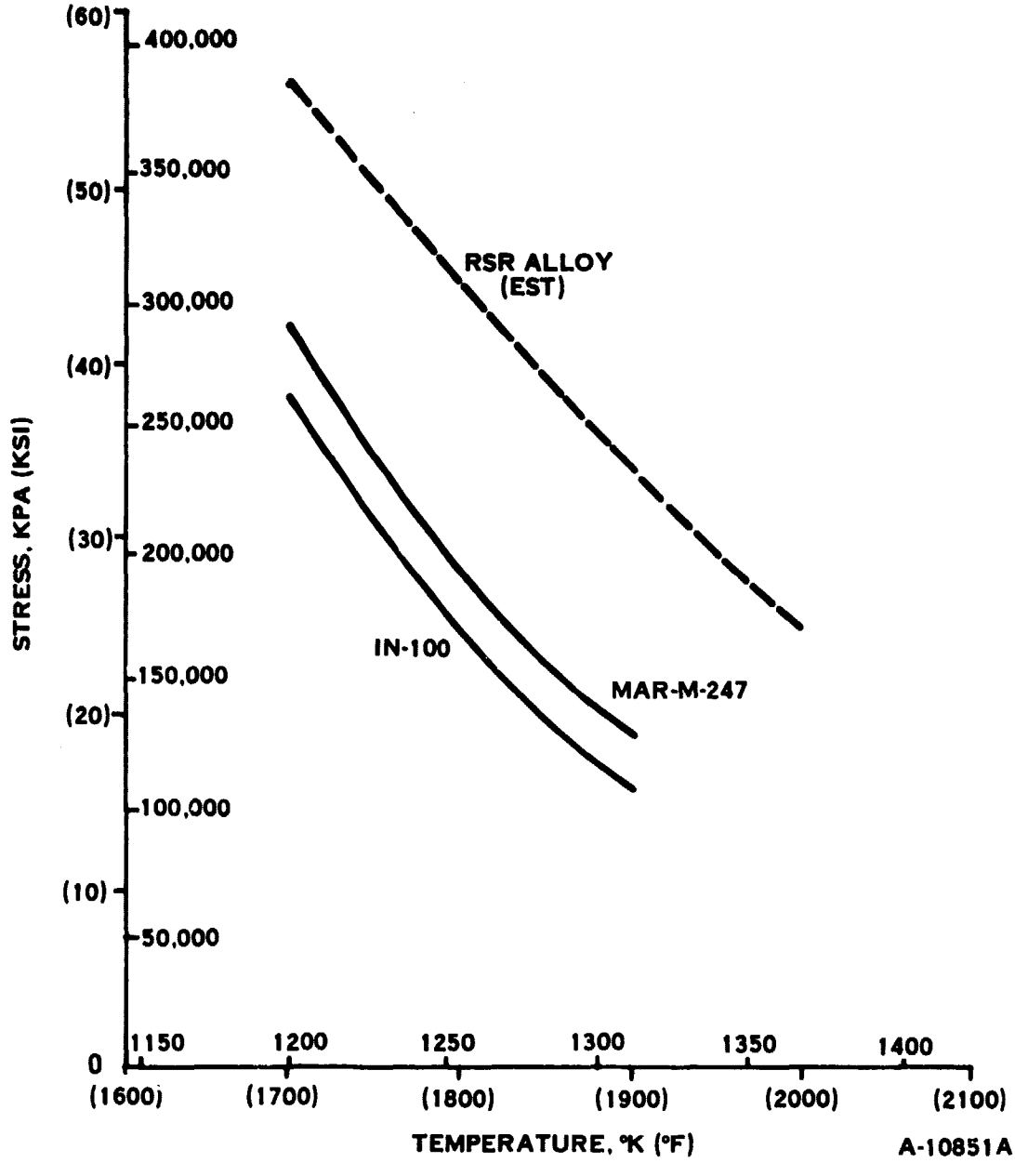

Figure 2. Turbine Alloy 100-Hour Rupture Strength

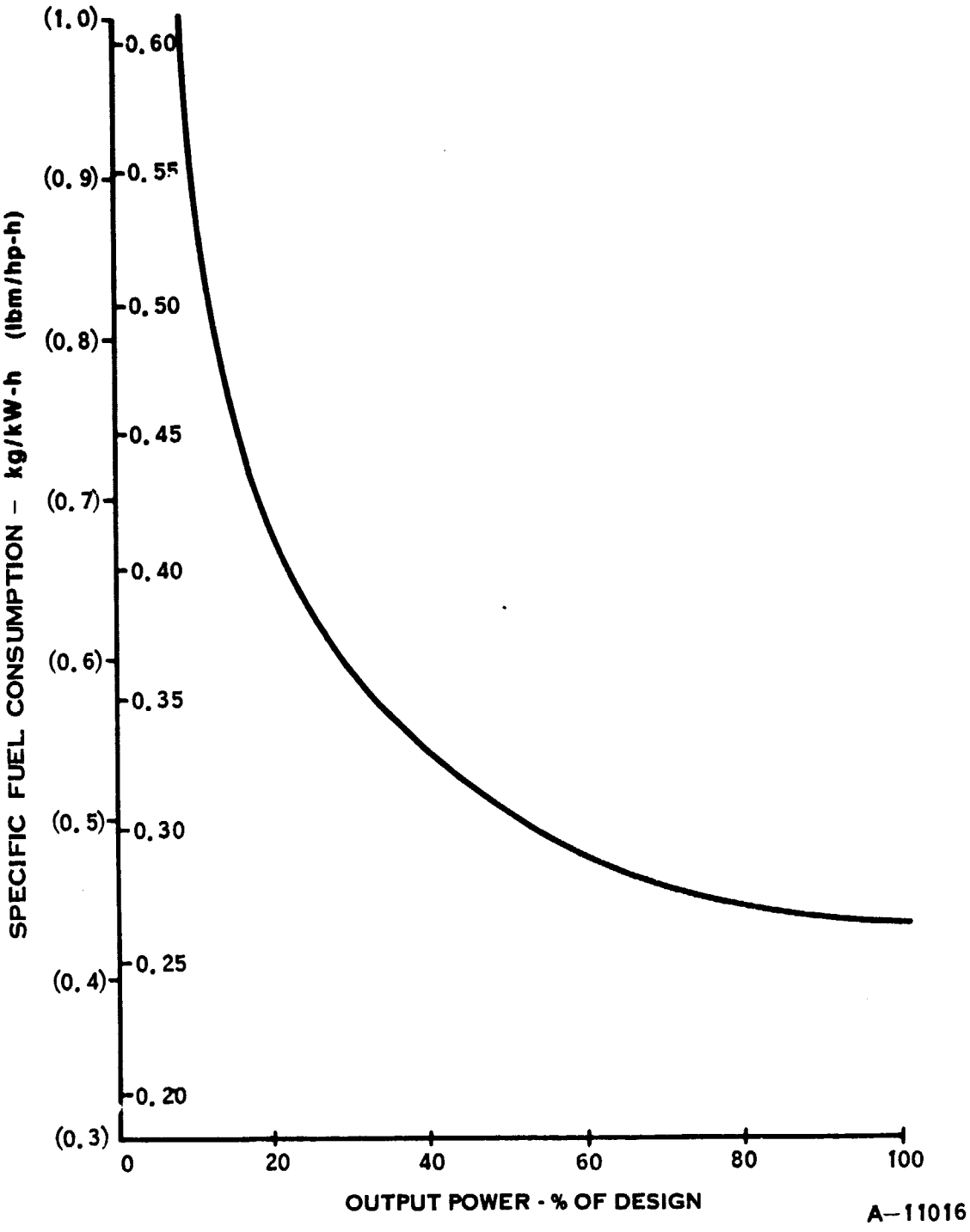

Figure 3. SFC versus Output Power for Nonregenerated Engine

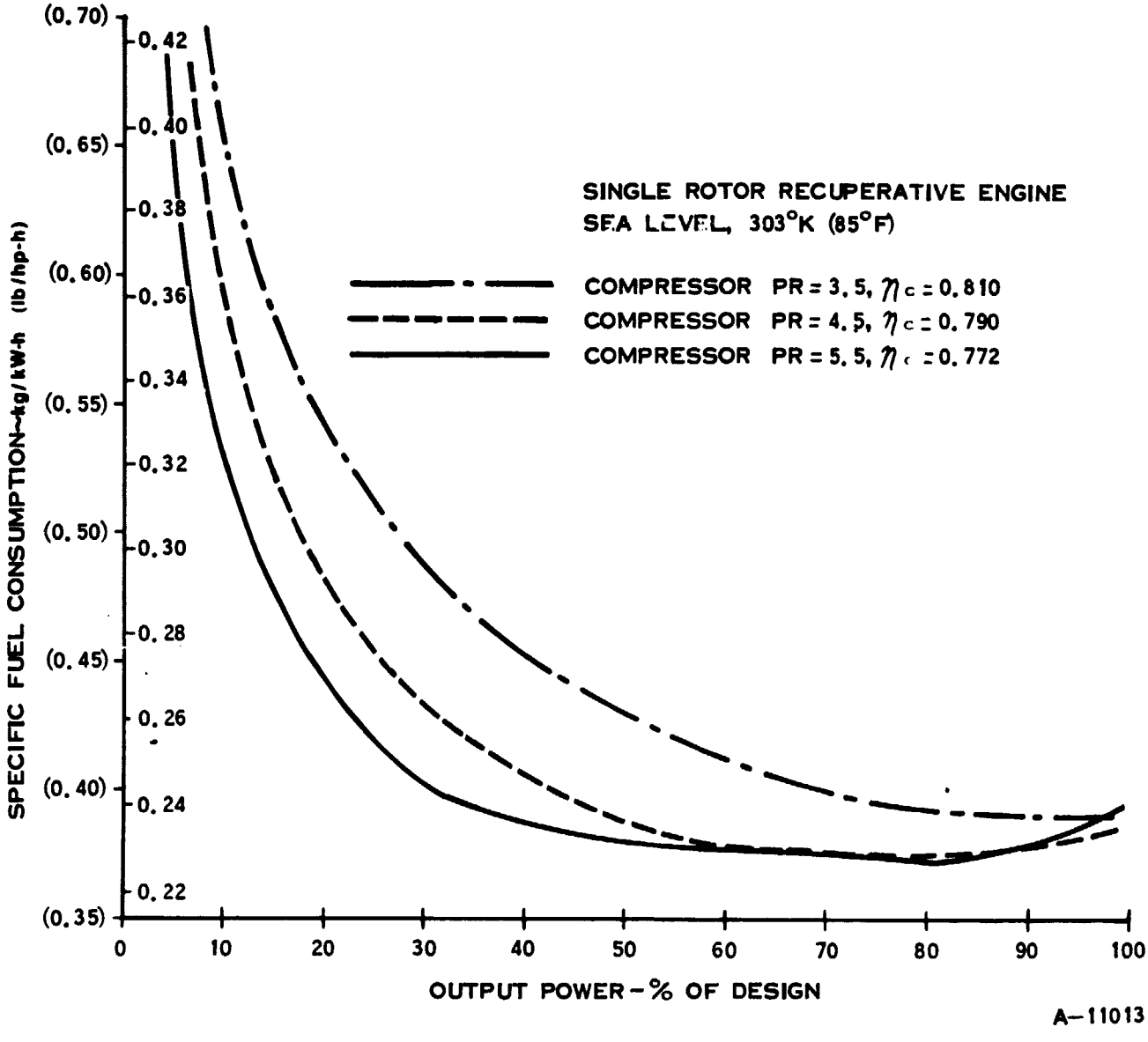

Figure 4. SFC for Compressor Pressure Ratio of 3.5, 4.5, and 5.5

The pressure ratio of 5.5 was selected as a tentative design point. On the final design, the cycle analysis will increase the maximum power pressure ratio as high as practical, consistent with TIT, turbine rotor stresses, and life. Then engine size will be adjusted to achieve the vehicle performance objective. This will minimize road load and idle fuel flow for best fuel economy.

INTERCOOLING

Intercooling between compression stages is a classical method of increasing overall compressor efficiency with significant improvement in cycle efficiency and specific output. The requirement of two stages, and the cost and complexity of the intercooler and associated hardware eliminated the intercooler from the IGT study.

REHEAT

Reheat between turbine stages increases output of the following stage; for the IGT application, it would be used only for maximum acceleration and would not be active for road load operation. The pressure losses of the reheat combustor and ducting increase part-load SFC. The poorer part-load SFC and the added cost, control, and emissions requirements indicate that reheat should not be considered further for the IGT.

POWER TRANSFER

Power transfer between gas generator and power turbine shafts was considered as a means of improving part-load fuel consumption. Preliminary analysis shows that power transfer is an effective means of reducing part-load SFC. It also has secondary features, such as engine braking and overspeed prevention. Therefore, further study of power transfer was continued during Task II.

VARIABLE GEOMETRY

Use of a variable power turbine nozzle is a second means of maintaining high TIT at part-load conditions. It has been widely used in past automotive gas turbine engines and has been found to be an effective means of reducing part-load SFC. The variable nozzle also has additional capability, providing engine braking, improving starting and acceleration, trimming the engine for maximum output, overspeed protection, and rapid response control of output torque. Trade studies were made during Task II comparing this approach and power transfer in engines which use free power turbines.

A variable first stage (or gasifier) turbine nozzle can also be effective in changing the turbine flow area relative to the compressor flow characteristics. It could be used to vary component matching, moving the operating line to optimize compressor efficiency and/or avoid compressor surge. Variable geometry in both compressor and turbine could be an effective way of modifying engine size, reducing air and fuel flow at idle while increasing maximum output. However, a variable first stage turbine nozzle is not as practical as the power turbine nozzle because of higher operating temperatures and pressures, greater losses due to

clearances and flow passage compromises, and greater effect of losses on cycle efficiency. The variable first stage nozzle has not been demonstrated in an automotive application and was not considered in the IGT study.

The variable diffuser for the centrifugal compressor also has problems with the effect of clearance on compressor and cycle efficiency.

Variable stators will be considered with the axial compressor, and variable inlet guide vanes with the centrifugal compressor as demonstrated methods of improving surge characteristics and varying the effective flow size to minimize idle fuel flow and maximize engine output.

WATER INJECTION

One way to reduce fuel consumption is to reduce the size of the engine. Passenger cars operate at low power levels during normal city and highway use, but the minimum size of the engine is determined by the acceleration requirement, namely, vehicle acceleration from 0 to 96.6 km/h (0 to 60 mph) within 15 seconds.

With water injection, the engine could be smaller and thereby use less fuel under part-load conditions and still meet the peak power requirement. The engine can be sized for normal city and highway use. Then, for a rapid acceleration, water is injected to increase the peak power output. This use of water injection will be considered for reducing engine size and part-load fuel consumption.

1.2 ROTOR SYSTEMS

The individual gas turbine components require mechanical connections for shaft power as well as flow connections for the working fluid to function as a complete gas turbine system. Every gas turbine engine has one or more rotor systems, with the turbine stages(s) driving the compressor stage(s) and/or the output shaft and accessories, with the use of reduction gears or other power transmission devices to provide power at a usable speed.

SINGLE-ROTOR ENGINE

The simplest gas turbine engine has a single rotor, with the turbine driving the compressor, accessories, and the output shaft. This simple engine cannot deliver useful torque at low speed, as needed for the automobile application, without the help of a complex variable ratio transmission system. The variable ratio drive system must have high efficiency to meet the vehicle performance and fuel economy objectives. Turbine temperature is controlled for steady-state operation by loading the engine through the variable ratio drive.

DUAL-ROTOR ENGINE

The dual-rotor engine has a gasifier rotor, with the first stage(s) turbine driving the compressor, and the second stage(s) turbine driving the vehicle. The engine has high torque at low speed, well suited to automotive requirements. Engine and vehicle accessories may be driven from either rotor, depending on the accessory loading and drivetrain design.

A variant of the dual-rotor engine uses the first turbine stage(s) as the power turbine, and the second stage(s) drives the compressor. This arrangement has not shown up in hardware, probably because the turbine design is more difficult in this arrangement.

THREE-ROTOR ENGINE

The simplest version of the three-rotor engine adds a third turbine stage used to drive accessories or, through suitable differential gearing, connecting with the other turbine stages to assist in driving the output shaft and compressor. References 1 and 2 show higher torque at low speed, but also indicate higher specific fuel consumption in the normal driving range. The design is complicated, requiring a great deal of attention to many parameters to achieve the desired overall characteristics. It also requires more hardware, increasing the initial cost.

Another type of three-rotor engine uses the twin-spool compressor with a separate power turbine between or after the gasifier turbine stages. This arrangement is well suited to a high pressure ratio cycle.

ROTOR INTERCONNECTION

Some turbine cycles require connections between rotors to transfer power to control turbine temperature and provide engine braking. In the dual-rotor engine, transfer from the gasifier to the power turbine (or output shaft) through a slipping clutch can load the gasifier turbine to control inlet temperature and improve specific fuel consumption. The clutch can also trim the engine to run at rated temperature at rated gasifier speed, maximizing the output for a given set of hardware, regardless of production tolerances and discrepancies. Since the clutch transmits only a small fraction of the output power, the losses due to slip can be accepted. A variable ratio drive could be used, but the potential efficiency improvement is small compared to the complexity and cost increase. The clutch can also be locked up for engine braking; equivalent braking through a variable ratio drive would be much more difficult.

The three-rotor engine (References 1 and 2) also requires rotor interconnection through a differential gear train to realize the advantages of the system. For example, the gasifier turbine can be designed for lower loading and inertia by using the auxiliary turbine to assist in driving the compressor. Another feature is transferring inertia energy from the auxiliary turbine to the gasifier rotor to aid acceleration.

Rotors may also be interconnected electrically, using a high-speed, variable-frequency, alternating current generator/motor on each rotor, with suitable frequency-changing accomplished electrically. The alternator output can also be used to drive accessories, with or without frequency-changing.

DRIVETRAIN

The IGT powertrain must meet specified fuel economy and acceleration requirements, delivering power from the turbine engine to the vehicle in an efficient manner over a wide speed range.

The drivetrain requirements are most difficult with the single-rotor engine; a variable ratio drive with a wide range is a must. This could be a multispeed gearbox with clutches for startup and ratio changes. Continuously variable mechanical transmissions such as variable ratio belt, chain, or traction drive were considered, (Reference 3); hardware with adequate performance, durability, and reliability is not available in the power range of interest and would require extensive development.

Equivalent hydraulic transmissions include hydrodynamic torque converters, with or without variable geometry, and hydrostatic transmissions with or without differential geartrains to extend speed range and improve road-load efficiency. The Orshansky hydromechanical transmission has demonstrated adequate performance and durability for a vehicle development program.

An electric transmission, using a high-speed, direct drive or geared alternator is another possibility. This approach is ideally suited to a hybrid vehicle, using batteries to meet peak power demand, and reducing engine size to just meet maximum steady-state requirements, maximizing fuel economy. This approach was not allowed by the ground rules of the IGT design study.

The dual-rotor engine has torque characteristics readily adaptable to vehicle propulsion. The output shaft torque rises as speed decreases to a stall torque about twice that at rated conditions. This torque characteristic is roughly equivalent to a piston engine equipped with a torque converter, and can give acceptable vehicle performance with a conventional three-speed automatic transmission. The usual torque converter is not required, since the dual-rotor engine inherently has the equivalent characteristics; it has been used in some automotive turbines to maintain a minimum power turbine speed to drive accessories.

ACCESSORY DRIVE

Engine and vehicle accessories must be driven at high enough speed under all driving conditions to supply enough fuel and lubricant, keep the battery charged, and provide adequate air conditioning and power assist for steering and brakes.

The single-rotor engine has a simple solution, driving all accessories from the single reduction geartrain. The speed range is about 2 to 1, so that accessories sized for adequate capacity at idle run about twice that fast at rated power.

The dual-rotor engine has more options for accessory drive. Accessories may be driven from the gasifier rotor with an accessory drive geartrain, with the same speed range as the single-rotor engine. Limitations here are the effect of accessory power loading on turbine inlet temperature and acceleration away from idle and low power; for example, the power steering pump at maximum pressure is a high load that must be handled momentarily. The alternator and air conditioning compressor may be cut out electrically on demand for rapid gasifier acceleration.

Accessories may also be driven from the power turbine rotor. With the simplest drivetrain, automatic transmission without torque converter, the accessories would stop when the vehicle stops. This may be satisfactory with the alternator and air conditioning compressor, which can stand momentary interruption, provided a transmission neutral (manual or automatic) permits accessory operation for standing.

A conventional hydrodynamic torque converter ahead of the automatic transmission can be set up for a minimum power turbine speed at idle, equivalent to a piston engine in speed range from idle. Conventional automotive (piston engine) accessories are built to run over this speed range, say 6 or 8 to 1, but do absorb more power at the higher speeds. Engine fuel and lubricant pumps may be run from this system, with other provisions during starting.

Three-rotor engines are similar to the dual-rotor engines. The auxiliary turbine with differential geartrain will provide additional options for accessory drive that must be carefully considered in the detail design.

With any of these systems, a speed reduction and shaft spacing is needed to mount and drive conventional accessories. Spur and helical (for lower noise) geartrains are flexible in design and acceptable in cost. Bevel or worm gears may be considered to suit packaging or ratio requirements. Lubricated chain and sprockets or belt and pulley, V or toothed, provide design flexibility of accessory location.

Another approach is direct drive, such as a high-speed alternator on the gasifier rotor. This would be rectified as usual for battery charging, but could also be used as variable frequency alternating current in a high-speed motor to drive other accessories. Direct current motors could obviously also be used.

With all accessory systems, provision must be made for starting the engine. The usual method of a direct current motor operating from the vehicle battery has proven to be an acceptable solution. This requires a drive connection to the rotor, clutched directly or through the accessory geartrain. A hydraulic or pneumatic motor could replace the starter, but energy storage equivalent to the battery is not normally available in the automobile. Compressed air could also be used with direct impingement on the turbomachinery, but again the energy storage problem exists.

ROTOR SYSTEMS COMPARISON

The dual-rotor system with the free power turbine is ranked highest for the IGT because the good output torque characteristics minimize transmission requirements. The single-rotor system will also be considered for performance comparison, using a commercially available variable ratio transmission. The three-rotor system will not be used, due to the considerable increase in cost and complexity with no clear improvement in performance or fuel economy.

For rotor interconnection on the dual-rotor engine, slip clutch power transfer is ranked highest because of its low cost, proven performance, and engine braking capability. The variable ratio drive or electrical drive is much more expensive with little potential for better performance.

The drivetrain choice for the dual-rotor system is the conventional three-speed automatic transmission, without torque converter. The torque converter does provide power turbine rotation with the automobile standing still, but this is not needed with gasifier driven accessories. The torque converter does not improve vehicle acceleration or fuel economy, and does increase initial cost. For the single-rotor system comparison, the hydromechanical variable ratio transmission is ranked highest, since it has demonstrated adequate performance and durability. Other variable ratio transmissions require extensive development.

The highest ranking accessory drive arrangement for the dual-rotor system is the geartrain from the gasifier rotor. This provides adequate capacity while minimizing accessory speed range and power requirements. The geartrain from the power turbine is less desirable because of the wider accessory speed range, higher power requirements, and the need for torque converter or clutch for idle operation.

1.3 COMPONENT TECHNOLOGY ASSESSMENTS

The accuracy of the assessment of component performance capabilities plays a very important role in the selection of an automotive gas turbine engine thermodynamic cycle. A thorough understanding of manufacturing and life cycle operating requirements and costs is also essential when various engine component configurations are being studied. For example, an overly optimistic projection of compressor efficiency at high pressure ratios may cause an investigator to reason that a simple non-regenerative engine is an obviously better choice than a lower pressure ratio regenerative engine. This conclusion, though false, would divert significant effort to dealing with the design and fabrication problems associated with a costly, high-sensitivity compressor component.

Likewise, overly conservative estimates of component performance or engine parasitic losses could lead, in the search for fuel efficiency, to the selection of excessively high values of cycle temperature, unwarranted mechanical risk, and possibly reduced engine life capabilities. Hence, a prerequisite to achieving optimum thermal efficiency, within the bounds of reasonable risk and cost, is the ability to accurately predict and achieve state-of-the-art levels of aerodynamic component performance.

This segment of the Task I study effort is devoted to a review of candidate components within four distinct classes: compressor, turbine, combustor, and heat exchanger. Relative ranking of candidate configurations within each of the four classes was conducted to ascertain which components deserve further analyses in Task II.

Table II summarizes the candidate configurations. To permit an accurate ranking of the candidates for an automotive gas turbine of the IGT size, preliminary aerodynamic sizing was done between pressure ratios of 2 and 12 and airflow rates of 0.091 to 0.680 kg/sec (0.2 to 1.5 lbm/sec).

TABLE II. COMPONENT CONFIGURATIONS STUDIED

Component	Basic Configuration	Variation
Compressor	Multistage Axial	Low vs High Speed
	Centrifugal	Radial vs Backswept, Variable IGV
	Axial-Centrifugal	
	Two-stage Centrifugal	
Turbine	Radial	Variable Geometry
	Axial	Variable Geometry
	Radial-Axial	
	Multistage Axial	
Combustors	Diffusion	Staged, Water Injected, Ram Induction
	LPP	Jet Induced Circulation, Vortex Air Blast, Porous Plate, Multi-element
		Ceramic
	Catalytic	
Heat Exchangers	Recuperator	Ceramic vs Metallic
	Regenerator	Ceramic vs Metallic

COMPRESSOR

The selection of a centrifugal compressor has been the traditional choice of designers from the inception of automotive gas turbine engines. This selection was chiefly motivated by the inherent simplicity, ruggedness, and low cost of this compressor. In the last 4 years, developments related to the sources and supply of hydrocarbon fuels have rearranged and changed the significance of the basic objectives of automotive gas turbine engine designs. Now, fuel efficiency is of paramount importance, and the achievement of optimum levels of compressor performance is a necessary goal.

The objective of the Task I compressor study is to describe the physical and performance characteristics of those compressor configurations that could satisfy the principal requirements of an automotive gas turbine powertrain design. Furthermore, each of these candidates will be ranked based on chosen thermodynamic and mechanical qualities, with the leading contenders being selected for a more detailed Task II study. Table III summarizes the features on which each compressor configuration will be assessed.

TABLE III. COMPRESSOR QUALIFICATIONS

1. Efficiency Potential (Part Load, Peak)
2. Range of Operation
3. Insensitivity to Size
4. Complexity/Cost
5. Manufacturing
6. Durability

Two basic classes of compressor were identified for performance projection purposes: axial and centrifugal. Hybrid compressors such as axial-centrifugal and two-stage centrifugal compressors were examined in terms of their individual axial or centrifugal stages, and overall performance was projected.

Range and stage matching considerations are addressed qualitatively, but detail calculations were reserved for the Task II effort. Devices capable of producing moderate variations in compressor flow range and pressure ratio such as variable geometry, water injection, and interstage bleeds are considered cycle requirements but were not included in the configurations in Task I because of the general nature of this phase of the study.

Devices which are capable of massive shifts in compressor airflow, such as variable diffuser geometry or multiple variable stator rows, were not considered in this study. These devices are not only complex in their own right, but are only effective when used in conjunction with a nearly completely variable engine, including inlet guide vanes, combustor geometry, gasifier turbine nozzles, and power turbine nozzle (if a two-spool configuration is selected). The problems associated with variable geometry become compounded when the size of the typical automotive gas turbine engine is considered. The clearance spaces or end wall gaps cannot be effectively scaled with blade and vane size and consequently represent a greater proportion of the flow passage height for small machines than for large machines. The effects of extensive variable geometry on centrifugal compressor performance is reported on by Rodgers (Reference 4). This machine, whose full speed pressure ratio was near 4:1 but whose flow was two to four times that required for automotive gas turbine application, demonstrated reductions in peak efficiency of over 15 percent when flow was reduced by 50 percent at a given speed.

Simulated variable diffuser testing at WRC corroborates these trends. In this program, two fixed geometry variants of a basic diffuser design were tested. The diffuser throat area variation of 10 percent was achieved by rotating diffuser vanes about their leading edge until the required throat opening was achieved. Significant reductions in compressor performance were noted. Correlations indicated 0.3 percent loss in peak efficiency for each 1.0 percent reduction in flow achieved through restaggering diffuser vanes. These losses, which did not include end wall leakage effects, are not considered acceptable when considered in light of the much smaller size requirements of the automotive gas turbine compressor. Consequently, the extensively variable compressor was not included in the Task I review.

Compressor Candidates

Candidate compressor configurations examined in Task I of the IGT program were a multiple-stage axial, a multiple-stage axial supercharging a single-stage centrifugal (same spool), a single-stage centrifugal, and a two-stage centrifugal (same spool). Preliminary engine sizing studies indicated that a compressor with a corrected flow of slightly less than 0.45 kg/s (1.0 lbm/s) and a pressure ratio (total-to-static) of 5.5 would be about that needed for the IGT.

Single-Stage Centrifugal Compressor

Initial centrifugal compressor studies concentrated on a single-stage compressor with a 40 degree backward curved impeller. The design point used for the study, based on early IGT engine cycle modeling, was as follows:

- Corrected Flow ($W\sqrt{\theta}/\delta$) = 0.442 kg/s (0.974 lbm/sec)
- Stage Total-to-Static Pressure Ratio = 5.500
- Stage Total-to-Static Efficiency = 0.754

The stage efficiency was based on Figure 2-1 in Reference 5, which presented state-of-the-art centrifugal compressor adiabatic (total-to- total) efficiency versus pressure ratio as a function of corrected flow. Figure 5 shows the total-to-static efficiency calculated from these data based on a stage exit Mach number of 0.2, compatible with combustor or heat exchanger requirements. The surge margin at which the efficiencies are presented is unspecified; it is possible that the efficiencies are higher than would be attained at a usable design point. The stage efficiency used for the single-stage centrifugal compressor thus represents a slight advancement of the state of the art but is thought to be attainable while meeting compressor range requirements.

Two-Stage Centrifugal Compressor

The high rotational speed of the single-stage impeller, resulting in a supersonic relative Mach number at the inducer shroud and an exit tip speed almost certain to result in stress problems, prompted an examination of a two-stage centrifugal compressor. Although little published technical data exists for such a configuration in gas turbines, with the notable exception of Reference 6, they are being used in at least two Garrett AiResearch engines (TPE331 and GT601) and are being proposed for or developed for use in other gas turbines. The design point, based on early IGT cycle modeling, was:

- Corrected Flow ($W\sqrt{\theta}/\delta$) = 0.446 kg/s (0.983 lbm/s)
- Overall Compressor Total-to-Static Pressure Ratio = 5.585
- Overall Compressor Total-to-Static Efficiency = 0.713
- First Stage Corrected Flow ($W\sqrt{\theta}/\delta$) = 0.446 kg/s (0.983 lbm/s)
- First Stage Total-to-Total Pressure Ratio = 2.754
- First Stage Total-to-Total Efficiency = 0.729
- Second Stage Corrected Flow ($W\sqrt{\theta}/\delta$) = 0.196 kg/s (0.431 lbm/s)
- Second Stage Total-to-Static Pressure Ratio = 2.028
- Second Stage Total-to-Static Efficiency = 0.758

At the design point, the overall compressor efficiency was reduced from that of the single-stage compressor even though the design points are virtually identical. This resulted from the match of the two compressor stages; the first stage is operating towards choke and away from peak efficiency, while the second stage is operating near peak efficiency. The value of peak efficiency for each stage of the two-stage centrifugal compressor at design speed was initially set in accordance with the data of Figure 5. Those levels were then degraded to reflect efficiencies of unpublished test data and for expected impeller efficiency loss due to a cast (versus a machined) impeller. Due to the automotive application of the two-stage centrifugal compressor, which carries with it the necessity for low-cost components, it is envisioned that the two impellers would be cast and the crossover duct between them would be die-cast.

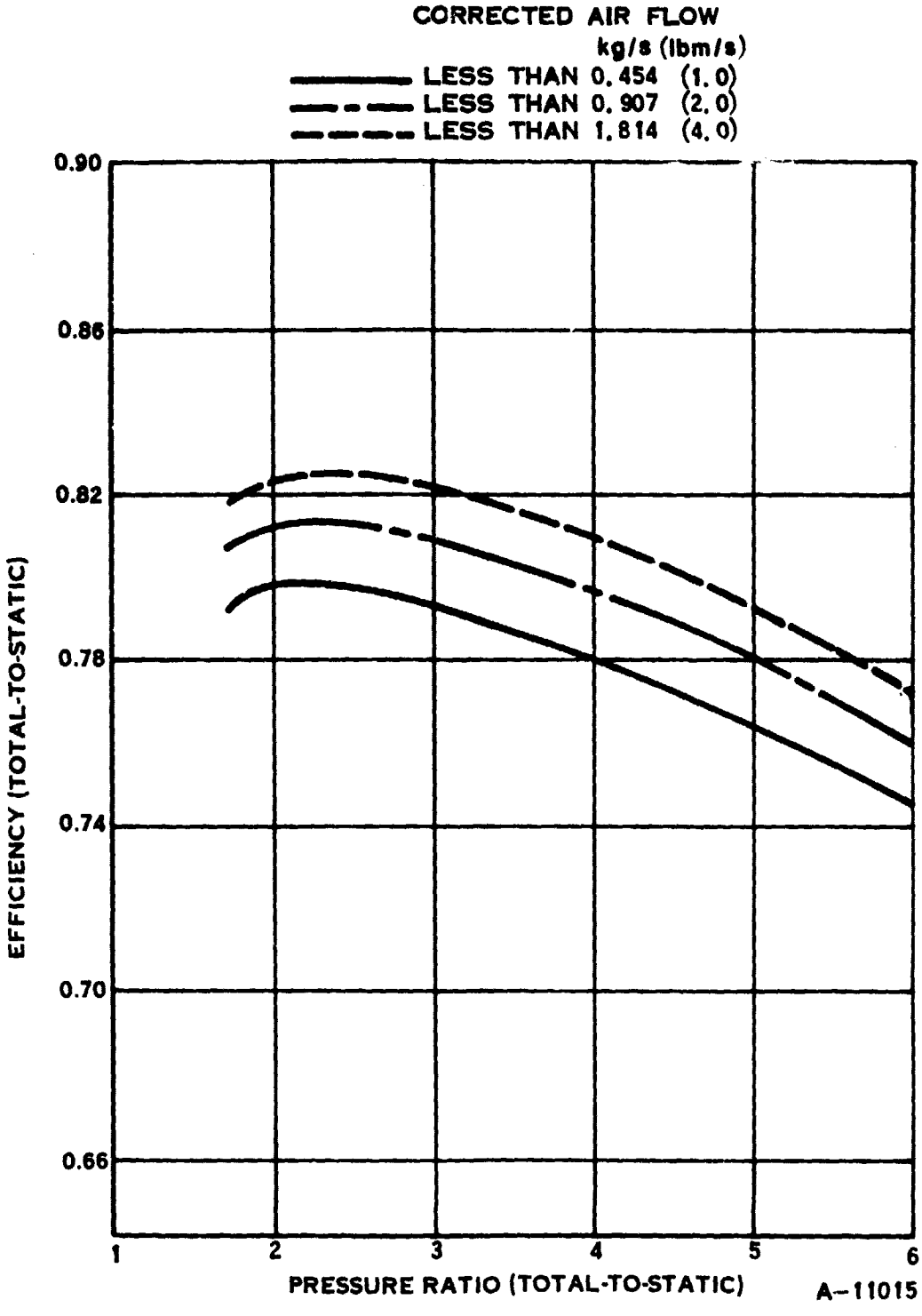

Figure 5. Compressor Efficiency versus Pressure Ratio

Multistage Axial Compressor

To establish the performance potential of the axial compressor as applied to the IGT requires the consideration of design parameters not considered critical in the larger gas turbine engines for aircraft or industrial use. The requirements of the IGT result in a compressor airflow in the range of 0.318 to 0.454 kg/s (0.7 to 1.0 lbm/s). This small size makes the parameters of Reynolds number, tip clearance, and manufacturing tolerances critical in the assessment of the performance potential of a candidate compressor configuration.

To establish the state of the art in axial compressor performance, the available test data have been reviewed. These data are primarily single-stage results, although some multistage data are included. These data, along with a previous correlation from Reference 7, are shown in Figure 6. The airflow of the compressors shown range from 1.13 to 440 kg/s (2.5 to 970 lbm/s). Also shown is a WRC estimate of fan performance potential based on the single-stage data. A general agreement of both the data and the WRC correlation with that of Reference 7 has encouraged the use of this procedure for evaluating various multistage configurations. An alternative method outlined in Reference 8 requires preliminary design information not generally available during the engine cycle parametric study. This method has been used at WRC to evaluate specific configurations and has been found to verify the Wiggins and Waltz correlation (Reference 7).

Recent WRC experience with a low cost six-stage compressor designed for a pressure ratio of 3.7 has provided a basis for considering use of an axial compressor in the IGT. This low tip speed (259 m/s, 850 ft/s) compressor applied manufacturing techniques which make the axial compressor a mechanically practical candidate but result in extensive aerodynamic compromises. At the design point the airflow was 1.59 kg/s (3.5 lbm/s). The design details are documented in Reference 9. At the test conditions the measured peak efficiency was 77 percent (Reference 10). With additional aerodynamic development and manufacturing improvements, a 3.6 percent improvement in performance is projected.

Using these characteristics, the performance level of an axial compressor suitable for use in the IGT was estimated for a variety of configurations. Assuming an airflow of 0.408 kg/s (0.9 lbm/s), 0.35 Mach number at the compressor exit to set the blade height, and a constant clearance of 0.127 mm (0.005 inch), the performance levels of Figure 6 can be degraded to those achievable in the IGT. Figure 7 is a replot of the Figure 6 data including the aforementioned performance degradations coupled with an additional 3.6 percent loss which has been subtracted for the manufacturing process and its associated tolerances. These results are summarized in Table IV. The results are assumed applicable to all airflows suitable for the IGT cycle because of the narrow range in Reynolds number involved.

Preliminary IGT cycle studies indicated that a total-to-static pressure ratio of 5.5 was required. Based on the stage loading of the six-stage axial compressor, the work required in the IGT cycle could be achieved in seven stages. Assuming an

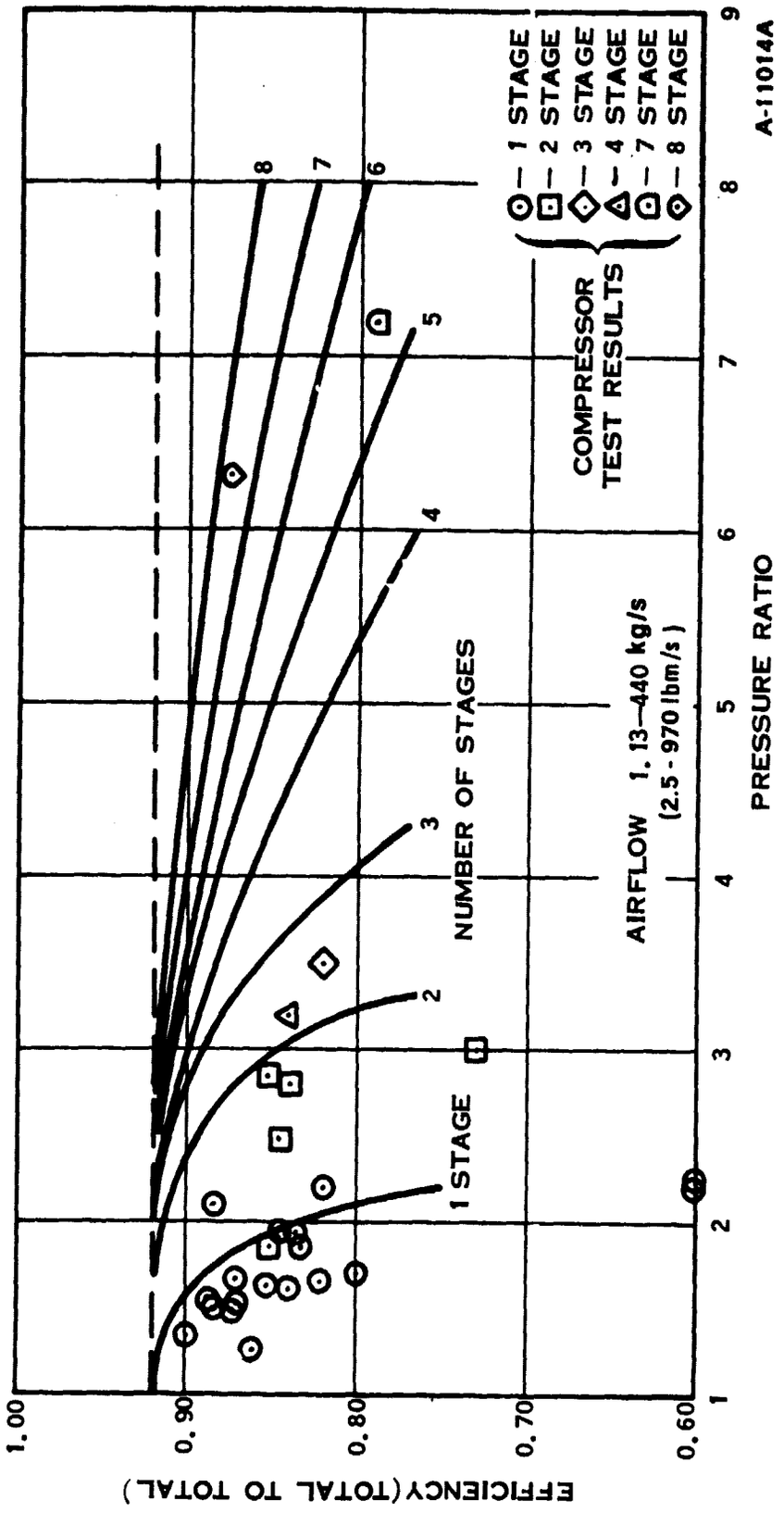

Figure 6. Axial Compressor Performance

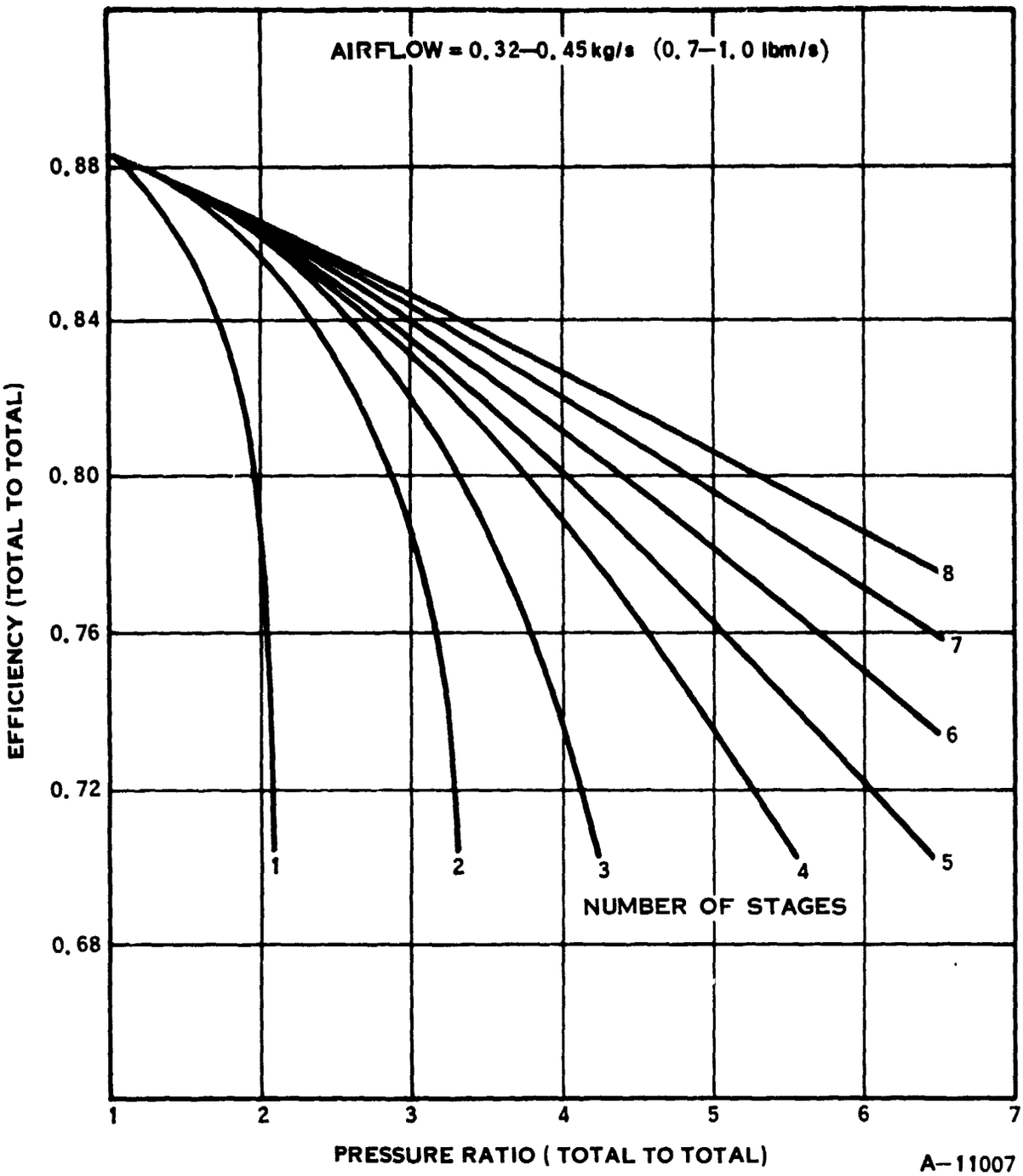

Figure 7. Axial Compressor Efficiency Potential

TABLE IV. COMPRESSOR CANDIDATES

AXIAL				CENTRIFUGAL			OVERALL***	
PR_{t-t}	STAGES	η_{t-t}	ΔT*	PR_{t-s}	η_{t-s}	ΔT	ΔT	η_{t-s}
-				5.50	0.750	450	450	0.750
1.25	1	0.872	41	4.40	0.767	400	441	0.767
1.50	1	0.858	78	3.67	0.775	359	436	0.774
2.00	1	0.787	151	2.75	0.770	301	451	0.749
	2	0.856	139	2.75	0.770	295	434	0.779
2.50	1	0.830	195	2.20	0.764	243	438	0.771
	2	0.844	192	2.20	0.764	242	434	0.779
3.00	1	0.786	254	1.83	0.756	198	452	0.748
	2	0.821	243	1.83	0.756	195	438	0.771
	3	0.830	240	1.83	0.756	194	434	0.778
5.66**	5	0.733	468				468	0.722
	6	0.762	453				453	0.746
	7	0.780	442				442	0.764
	8	0.793	435				435	0.776

*T_{inlet} = 303°K (85°F)

**Total-to-Total Required with M_e = 0.35 and Diffuser Recovery (Cp) = 0.65.

***Total-to-Static PR = 5.50

exit Mach number of 0.35 and a diffuser recovery of 0.65, the required total-to-total pressure ratio is 3.66. From Table IV the estimated efficiency is 78 percent and results in a total-to-static efficiency of 76.4 percent.

Axial-Centrifugal Compressor

This is essentially a hybrid of the seven-stage axial compressor and the two-stage centrifugal compressor already discussed, and incorporates the best features of both. The small stages at the back of the multistage axial compressor, whose performance is very sensitive to radial clearance, are replaced by a centrifugal compressor. The high efficiency front stages of the axial compressor replace the front centrifugal stage, whose efficiency is not as high, especially at part speed where the IGT operates extensively.

The preliminary configuration uses the first three stages of the multistage axial compressor coupled with the second stage of the two-stage centrifugal. The performance estimates for both stages were based on published information. Table IV presents a summary of performance estimates for axial-centrifugal compressor combinations based on the performance of pure axial and pure centrifugal compressors. The axial efficiencies were taken from Figure 7. The centrifugal efficiencies were taken from Figure 5, which is a replot of data presented in Reference 5 with total-to-static efficiency based on a stage exit Mach number compatible with heat exchanger requirements (0.2 Mach). The surge margin at which the efficiencies are presented is unspecified; it is possible that efficiencies are higher than would be attained at a usable design point. The centrifugal stage efficiency thus represents a slight advancement of the state of the art, but is thought to be attainable while meeting compressor range requirements.

It is envisioned that the axial compressor (rotors and stators) will be cast in the same way as the six-stage axial compressor is fabricated for the WRC WR33 low-cost engine. The rotor blades will be cast integral with a one-piece drum, and the stator assembly will have vanes cast in place in a clamshell arrangement to fit around the rotor drums. The centrifugal impeller will be cast, but the diffuser will probably require machining.

This design of cast axial compressor does present a problem with selecting the shaft speed to create a near optimum specific speed for the centrifugal stage. An axial rotor maximum tip speed of 280 m/s (950 ft/s) is imposed on the cast rotor for stress reasons. This limits the specific speed of the centrifugal stage to a number smaller than desirable, which introduces risk in meeting the performance levels previously quoted for the centrifugal stage. This will have to be taken into account when the final compressor selection is made.

Centrifugal Compressor Selection

After completion of the preliminary design analysis, a comparison of the two centrifugal compressor configurations, single-stage and two-stage, was in order to determine if either one or both should be examined further in Task II. Areas of concern were examined and a discussion of these follows.

A. Confidence in Performance Levels

The two-stage centrifugal compressor has sufficient data support to give confidence in meeting performance goals, although it appears that one has not been tested in this size.

The single-stage compressor performance prediction is substantially less solid. The rotational speed of the impeller, necessary to run a specific speed compatible with the quoted performance, presents several problems. First, the value of impeller inducer tip relative Mach number is beyond the level of the vast majority of existing impellers. This introduces a severe obstacle to attaining both the quoted performance and necessary surge margin. The surge margin problem is further intensified by the impeller exit tip speed being at a level almost certain to result in a reduction of the backward curvature, impeller speed, or both, due to high stress levels. A reduction in backward curvature would reduce part-speed surge margin and force a rematch of the impeller and diffuser, resulting in a reduction in compressor efficiency (due to "low flowing" the impeller). A reduction in impeller speed would, in this application, possibly increase impeller efficiency because of the shock loss associated with the inducer tip relative Mach number. However, a reduction in speed will increase the swirl angle into the vaneless space resulting in possible separation with the resultant efficiency penalty, and the impeller exit tip speed will still be of concern. Thus, the performance confidence lies with the two-stage compressor rather than the single-stage compressor.

B. Design Complexity

The single-stage compressor would appear to have the advantage here because of the fewer pieces to be designed and matched. However, because of the rotational speed of the impeller, the blade design will be very critical in the inducer area, and the impeller design may be compromised by stress considerations. The impeller would almost certainly require splitter blades, which increase the complexity of the part, especially if the splitter blades are set for equal throats. Conversely, the two-stage compressor will have subsonic flow into the impellers, and the impeller speed is low enough that the impeller designs will not be compromised for stress considerations. Only full blades should be required for the impellers, and a castable thickness distribution would not cause high incidence losses with the subsonic flow. Thus, their design should be straightforward.

The diffusion system of the single-stage compressor presents less design work than that of the two-stage compressor, but the two-stage design will be done using proven methods. Because of the complex single-stage impeller design, the overall two-stage design appears little, if any, more complex than the single-stage design.

C. Manufacturability

For high-volume production, it is certainly desirable to fabricate the compressor at the lowest possible cost, such as by casting. The single-stage compressor impeller does not appear to be a good candidate for casting. The level of inducer shroud relative Mach number will make the impeller performance very sensitive to

blade-setting accuracies. Cast impellers exhibit more nonuniformity in blade-setting angles than does a machined part at the present state of the art. The biggest problem seems to be blade droop after heat treat, which becomes hard to control with a part as complex as the single-stage impeller. The performance quoted for the single-stage impeller was based on a machined part because of the anticipated casting problem already discussed. The two-stage compressor impellers and crossover duct, on the other hand, seem to be quite castable.

As previously discussed, the projected performance of the two-stage centrifugal compressor included the efficiency decrement known to occur for a cast configuration of this type relative to machined parts. The crossover duct can be die-cast quite accurately with no expected performance decrement, as has been demonstrated on other similar configurations (AiResearch TPE331, IE831, GTPF 990 and GT601 gas turbines). In fact, it gives repeatability equal to or better than a machined part. The only parts machined on the compressor would be the first stage radial diffuser vanes (made from sheet stock) and the second stage radial diffuser. Thus, the two-stage compressor seems to have the advantage in this area.

D. Performance Repeatability and Consistency

This area of concern focuses on both the initial performance of the engine as manufactured and changes in performance in the field. With proper tooling and equipment, both compressors can be manufactured consistently. The sensitivity of each compressor to foreign object damage during field usage of the IGT would favor the two-stage compressor, as its performance would be less affected by any damage because of the low inducer tip relative Mach number.

Two areas where the two-stage centrifugal compressor may experience problems are in attaining desired axial clearances between the shroud and impeller and in part mismatch. More parts mean more chance to have tolerances create clearances wider or closer than desired, and to have flowpath mismatches between components.

E. Size Effects

These have already been taken into account during the performance prediction effort, as portrayed in Figure 5. One area deserving mention is that, if the engine goes to a higher turbine inlet temperature than those compressors were sized for, recontouring would probably be required to retain the engine power. This would detrimentally affect the performance of the single-stage impeller more than that of the two-stage configuration.

F. Noise

The two-stage would appear to have a decided advantage here because of the lower inducer relative Mach numbers on the first stage.

G. Development Effort Required

Because of the anticipated problems in achieving the desired performance from the single-stage compressor, it is expected that the two-stage centrifugal compressor will be less costly to develop.

H. Rotational Speed

The two-stage centrifugal compressor runs about 70 percent of the rotational speed of the single-speed compressor, since the work is divided between the two stages, reducing the tip speed requirement. An axial gasifier turbine driving the two-stage compressor then has about half the blade stress of one driving a single-stage centrifugal compressor. This permits a significant increase in TIT, 83 to 111°K (150 to 200°F) for a typical advanced nickel base alloy. If fully utilized to decrease engine size and improve low power SFC, this higher TIT will result in a significant improvement in vehicle fuel economy.

In conclusion, based on the comparison of the two centrifugal compressors, the two-stage centrifugal compressor offers the following advantages over the single-stage compressor:

1. Greater certainty of attaining the desired performance
2. Lower cost to manufacture in automotive production
3. Better repeatability of performance from unit to unit on initial engine assembly and less decay in performance over time of use
4. Easier recontouring without excessive performance loss
5. Lower noise
6. Less development effort anticipated
7. Lower rotational speed permits 83°K (150°F) or more increase in TIT

The major overriding consideration is the lower rotational speed permitting higher TIT. Therefore, Task II concentrated on the two-stage centrifugal compressor.

Axial Compressor Selection

Due to the 1GT preliminary cycle compressor airflow and pressure ratio, the back stages of the multistage axial compressor become quite small and, as such, are very performance-sensitive to radial clearance. As a solution to this problem, the axial-centrifugal compressor configuration was examined where the small back stages of the axial were replaced by a single-stage centrifugal. This would certainly enhance the consistency of performance, especially in production, as it is difficult to hold the very tight radial clearances on the axial airfoils. Stage matching becomes more of a problem on the axial-centrifugal than on the multistage axial, but WRC has experience in this area based on the WR24-7 axial-centrifugal compressor and it is anticipated that the required operating range can be met. The axial-centrifugal compressor would be slightly higher on inertia than the multistage axial compressor, but would be much more insensitive to performance losses based on size effects. Both axial compressor configurations are roughly equivalent in complexity, cost, manufacturability, and durability. Based on the necessity for the compressor to achieve consistently good performance in production engines, the axial-centrifugal compressor was carried into Task II.

TURBINE

Recent significant developments in turbine technology have been paced by, and are associated with, advancements in high-temperature materials technology. These improved turbine capabilities, while not improving the aerodynamic performance of the turbine itself, have benefited the gas turbine engine by permitting cycles to be designed for the improved SFC and higher specific power that results from higher values of TIT. The recent renewed interest in fuel-efficient, small gas turbine engines for rotorcraft, light aircraft, cruise missiles, and automotive propulsion applications has promoted increased interest in the development of small, uncooled high-temperature turbine capability. This interest has accelerated the development and application of a wide variety of advanced materials concepts. The turbine designer working on the next generation of engines has a wide variety of high-temperature materials to consider, ranging from ceramics (silicon nitride, silicon carbide) to metallics [RSR (rapid solidification rate) materials, coated molybdenum] to composites (carbon-carbon). Obviously there are limitations and varying degrees of risk associated with the use of these materials. Some are in limited supply and others still have a considerable number of development hurdles to overcome before they can be considered for long-life engine applications.

The Task I study of small turbine performance capability was undertaken with due consideration for high-temperature operation. Other typically automotive engine performance-related considerations included optimum performance, insensitivity to small size and mass production manufacturing techniques, polar moment of inertia, minimum reliance on variable geometry, and low cost.

Two classes of turbine were studied in detail: radial inflow and axial. The evaluation was initiated with a thorough review of recent NASA, ASME, SAE, and related technical documents. These data were used to establish a baseline of performance and to verify WRC computerized turbine performance prediction routines.

Projections of axial and radial turbine performance are also presented. These performance estimates relate stage efficiency to blade loading, assuming that Reynolds number and real blade geometry effects are negligible. Additional curves focusing on the effects of Reynolds number, face/tip axial and radial running clearance, blade height, trailing edge thickness, and specific speed are then presented. These curves summarize the trends generated within WRC's computerized turbine performance prediction models. Additional description of the computerized models is also provided.

Turbine Candidates

Twelve turbine configurations were selected for the purpose of detailed comparison. They include single-shaft, two-shaft, and three-shaft designs, and radial inflow, single-stage axial, multistage axial and radial-axial combinations. In addition, variable turbine inlet geometry and the effects of power transmission between shafts were considered. The configurations are shown in Figure 8.

SINGLE SHAFT
SINGLE STAGE AXIAL
(A)

SINGLE SHAFT
TWO STAGE AXIAL
(B)

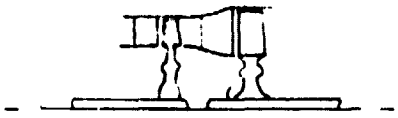

TWO SHAFT
TWO STAGE AXIAL
VARIATIONS (C) VARIABLE SECOND NOZZLE
(D) POWER TRANSFER
BETWEEN SHAFTS

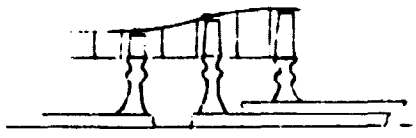

THREE SHAFT
THREE STAGE AXIAL
(E)

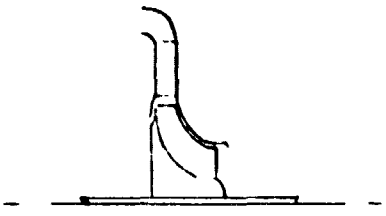

SINGLE SHAFT
RADIAL TURBINE
(F) FIXED NOZZLE
(G) VARIABLE NOZZLE

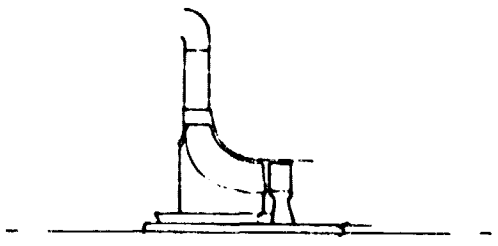

TWO SHAFT
RADIAL TURBINE WITH
POWER EXDUCER
(H)

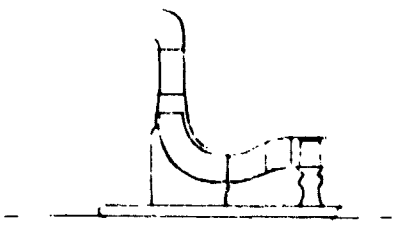

SINGLE SHAFT
RADIAL–AXIAL TURBINE
COMBINATION
(I)

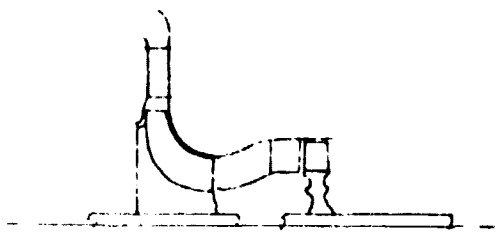

TWO SHAFT
RADIAL–AXIAL TURBINE
COMBINATION
VARIATIONS (J) VARIABLE SECOND
NOZZLE
(K) POWER TRANSFER
BETWEEN SHAFTS

A-11290 B

Figure 8. Turbine Configurations

A. Single-Shaft, Single-Stage Axial Turbine (Figure 8-A)

The single-shaft, single-stage axial turbine configuration is the lowest cost axial turbine configuration due to the fact that it has the fewest turbine parts. The small size of a single-stage axial turbine for a compact automotive engine affects axial turbine efficiency. Tip clearance as a percentage of blade height has a direct, adverse effect on small axial turbines (Figure 9).

B. Single-Shaft, Two-Stage Axial Turbine (Figure 8-B)

The single-shaft, two-stage axial turbine configuration has basically the same benefits and constraints as the single-stage axial turbine; however, the two-stage design would cost approximately twice as much to manufacture since it requires two turbine wheels and nozzles. Conversely, this configuration has the potential of achieving higher efficiency for the following reasons:

- Two turbine stages can achieve higher efficiency because of the reheat effect between stages. Basically, energy that is not used in the first stage is not lost to the cycle. It can still be used in the second stage. Further, the work split between stages causes a lower ($\Delta H/U^2$) loading, resulting in the potential for higher efficiency.

- A two-stage turbine designed to replace a single-stage turbine has higher blade heights than the single-stage turbine. Hence, the efficiency loss due to tip clearance is less in a two-stage than the single-stage turbine. However, stress levels in the last stage are larger because of the increased area of the annulus as related to an AN^2 blade root stress relationship.

C. Two-Shaft, Two-Stage Axial Turbine with Variable Geometry (Figure 8-C)

The use of the variable area power turbine nozzle is one method to improve part-load fuel consumption. Basically, decreasing flow area by closing the power turbine nozzle blades increases the TIT with a resulting decrease in SFC. Main disadvantages of the variable turbine geometry are the added cost and complexity involved in this system. Further, as smaller powerplants are required for smaller vehicles, the use of variable geometry becomes less attractive, since the benefits obtained from variable geometry have to be weighed against the additional aerodynamic and leakage losses due to the additional clearances required to rotate the vanes.

D. Two-Shaft, Two-Stage Axial Turbine with Power Transfer (Figure 8-D)

The two-shaft, two-stage power transfer system is another approach to maintaining TIT during part-load application. Basically, such a system uses either a clutch or an electric motor-generator set to transfer scheduled amounts of power between the gas generator and power turbine rotors. As power is reduced during part-load operation, the clutch or motor set is engaged, loading the gas generator rotor. This increases the TIT and shifts the operating line until compressor surge is approached. Higher TIT, coupled with the higher compressor pressure ratio,

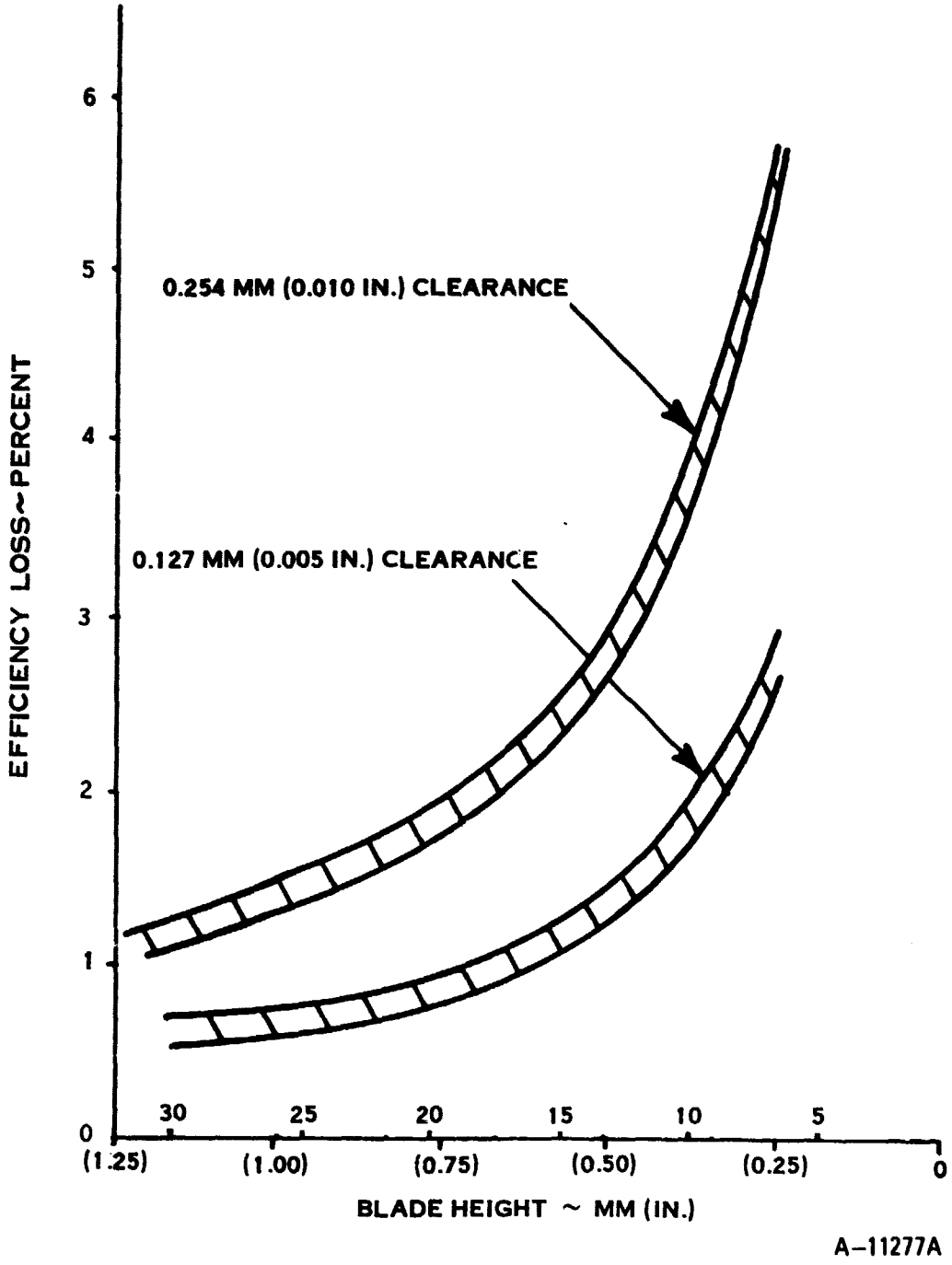

Figure 9. Effort of Axial Turbine Clearance on Efficiency

improves part-load fuel consumption significantly. The power transmission mechanism does introduce extra complexity and cost to the system. However, it eliminates need for variable geometry in the turbine. The operating mechanism is not exposed to the hot gas stream, hence there are no associated aerodynamic losses.

E. Single-Shaft, Radial Inflow Turbine (Figure 8-F)

The single-shaft, radial inflow turbine offers low cost and high efficiency. Again, as with the single-shaft axial turbines, an infinitely variable transmission must be utilized to achieve the desired driveability. The radial inflow turbine offers the potential for high efficiency in the smaller engine sizes, since radial turbines are not as sensitive to tip or shroud clearances as axial turbines.

F. Single-Shaft, Radial Inflow Turbine with Variable Geometry (Figure 8-G)

Variable inlet geometry as applied to the radial inflow turbines operates the same as for axial turbines. Cost and complexity are the main considerations. Here again, cycle improvements must be compared against additional aerodynamic and leakage losses from the clearances required to rotate the vanes and leakage through the control mechanism. These losses may be less than for an axial turbine because the vane surfaces for the radial turbine are flat instead of spherical as required for the axial turbine.

G. Radial-Axial, Two-Stage Turbine (Figure 8-I)

An alternative configuration to those previously discussed is a radial-axial, two-stage turbine. Such a configuration could be used where the work ratio is such that the first axial stage of a two-stage axial turbine would be too small to provide good efficiency, and where the work would require single-stage radial turbine inlet tip speeds that exceed good mechanical design practice. This combination of turbines could be used for either a single-shaft (Figure 8-I) or two-shaft (Figures 8-J, 8-K) designs and provide relatively high efficiency levels for small size and high work. However, an additional loss is incurred by this system because of interstage duct losses.

H. Three-Shaft, Three-Stage Axial Turbine (Figure 8-E)

The three-shaft, three-stage axial turbine configuration is an interesting concept that allows for separate shafts for compressor turbine, power turbine, and auxiliary turbine. The auxiliary turbine powers all accessories and related equipment and hence removes accessory inertia from the power turbine. This concept is designed so that fast acceleration, low idling speed, and low part-load fuel consumption can be obtained. However, the cost of such a system is greater than any of those previously described and the system is significantly more complex. It is felt that for small vehicle applications the use of such a system would be prohibitive since turbine component cost and complexity are high.

I. Two-shaft Radial Inflow Turbine with Power Exducer (Figure 8-H)

This configuration is similar to the radial-axial turbine with the exducer section used as the free power turbine. This configuration is considered high risk because of a strong potential for the occurrence of high vibration levels caused by interaction between the two rotating components as the two shaft speeds vary.

Turbine Candidate Analysis

The candidate turbine configurations were reviewed and refined in order to evaluate the merits and drawbacks of the performance characteristics. Each system was evaluated on its potential to improve the state-of-the-art efficiency in small turbines. Size effects such as those shown in Figures 9 and 10 were observed and special emphasis was placed on avoiding high losses due to chord size, blade height, secondary losses, and profile losses. The analysis techniques consisted of various WRC and NASA-developed computer programs.

In addition to the in-depth aerodynamic component performance analysis performed, practical considerations were also addressed. Such items as tip clearances, minimum practical leading edge and trailing edge thicknesses, wheel sizes, inertia, realistic tip speeds, and other physical considerations were fixed so that the analysis was representative of production automotive type hardware. Furthermore, complexity factors were also evaluated. Such items as realistic flow path shapes between turbine stages, exhaust ducting, variable geometry, and power transfer mechanisms were all looked at with an eye toward functionalism. Matching of the components (i.e., compressors, combustors, and turbines) was continually rechecked to minimize the potential problems involved in putting the engine configuration together.

For the turbine components, inlet, outlet and interstage ducting are required. The exact nature of the ducting will depend on the engine arrangement and the design concepts employed for combustor, turbines, turbine exhaust, and heat exchanger. For example, if radial-axial turbine stages are employed, then an annular interstage transition duct is required. The turbine inlet configuration may be designed for either can-type or annular-type combustors. The can-type combustor may require the use of an inlet volute or plenum. The annular-type combustor requires only an annular nozzle ring.

In the preliminary design phase, duct designs are guided by rules-of-thumb, and approximate loss coefficients in the form of $\Delta P/P$ or $\Delta P/q$ are applied for the preliminary design performance analysis. Primary rules-of-thumb are:

- Minimized velocities and duct length to minimize skin friction losses
- Minimal diffusion and/or local diffusion ratio to minimize separation losses

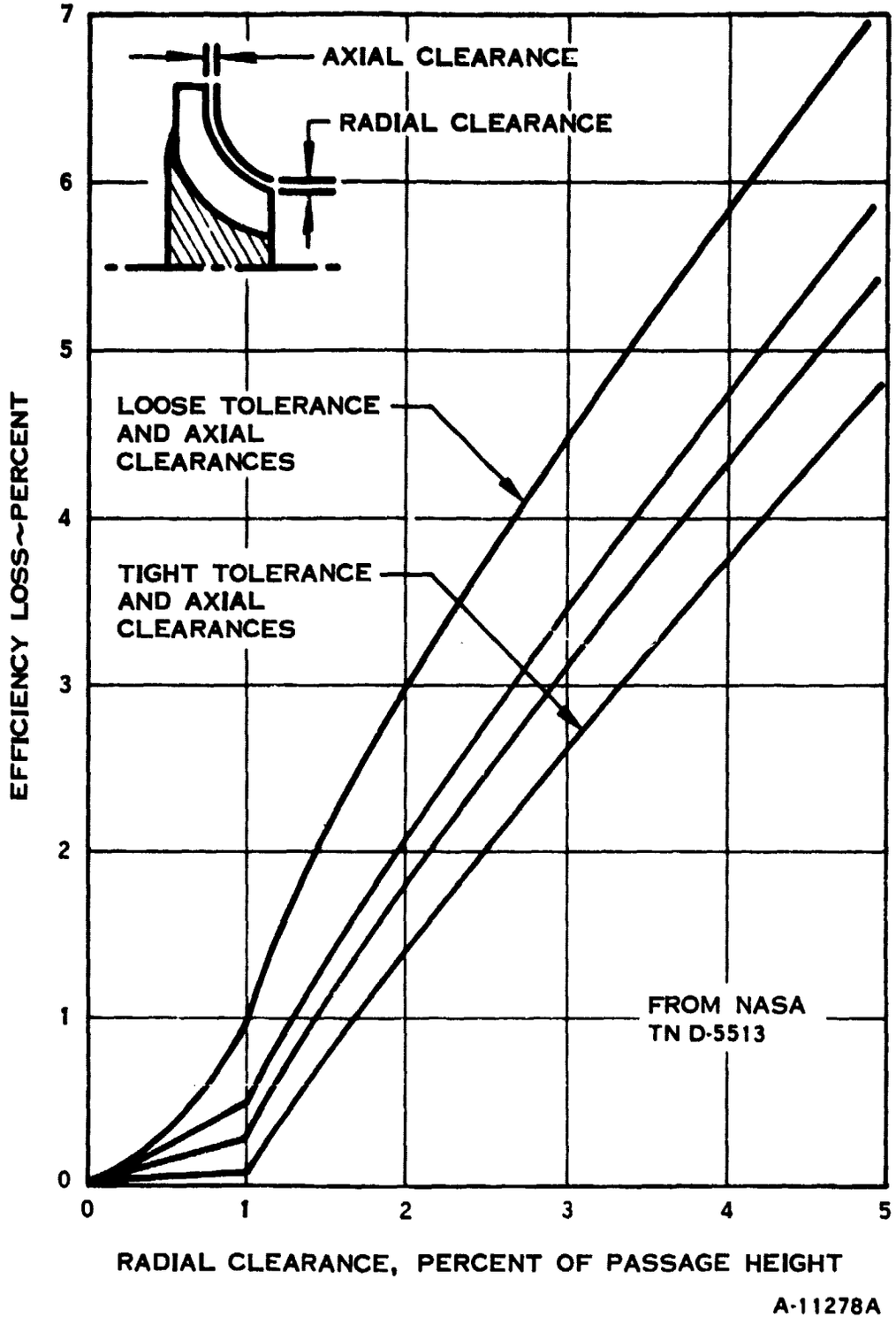

Figure 10. Effect of Radial Turbine Clearance on Efficiency

Following the preliminary design, more sophisticated flow analyses are applied to those ducting components which represent moderate risk performance losses. An iterative streamline curvature program is employed to estimate surface and internal flow velocities in the duct. This program is used to reshape the duct to optimize surface velocity profiles within the duct.

Turbine Candidate Comparison

The turbine candidate configurations were evaluated based on design point conditions prescribed by the various compressor configurations; pressure ratio, TIT, and operating range. Turbine candidates were designed with the intent of achieving maximum efficency at less than maximum operating speed. This was done so that higher efficiencies could be maintained at road-load operation in the automotive turbine application. The turbine candidates were evaluated based on component performance maps, producibility, inertia, adaptability to variable geometry, and adaptability to high-temperature materials such as ceramics, etc.

Four of the twelve candidates were eliminated from consideration prior to the performance mapping. These four are listed below:

1. Single-shaft, single-stage, axial configuration. Power and sizing requirements made this an impractical candidate. (Figure 8-A)

2. Three-shaft, three-stage, axial configuration. Size, cost, and complexity made this configuration unacceptable. (Figure 8-E)

3. Two-shaft, radial inflow turbine with power exducer configuration. Mechanical and basic vibration problems make this an impractical candidate for the wide range of operation of an automotive turbine. (Figure 8-H)

4. Single-shaft, radial and axial configuration. This configuration was determined to be impractical when the single-shaft, radial-only configuration was calculated to be sufficient. (Figure 8-I)

From a turbine cost standpoint, the following ranking occurs (lowest to highest cost):

1. Single-stage, radial inflow turbine
2. Single-stage, axial turbine
3. Two-stage, radial-axial combination turbine
4. Two-stage, axial turbine
5. Three-stage, axial turbine

Variable inlet geometry and power transfer will add similiar costs to each of the configurations.

From an engine size standpoint, the following ranking occurs (smallest to largest size):

1. Single-stage, radial inflow turbine
2. Single-stage, axial turbine
3. Two-stage, axial turbine
4. Two-stage, radial-axial combination turbine
5. Three-stage, axial turbine

From an engine response time standpoint based on component inertia, the following ranking occurs (fastest to slowest):

1. Three-stage axial turbine
2. Two-stage axial turbine
3. Single-stage axial turbine
4. Two-stage radial-axial combination turbine
5. Single-stage radial inflow turbine

From a utility standpoint, either the two-stage axial or two-stage radial-axial combination would provide design flexibility. These configurations could be used on a single-shaft configuration or a two-shaft configuration. From a single shaft only standpoint, the single-stage radial turbine would be the most economical if inertia can be reduced through the use of ceramic materials.

Performance Projection (1978-1985)

Configuration studies that require a prediction of performance to 1985) cannot be concluded without an assessment of probable improvements to materials, manufacturing tolerances, and analytical techniques. Each of these probable improvements has an impact on the performance prediction. Figure 11 shows the probable effects of improvements in materials, in the form of reduced running clearances due to low coefficients of expansion for the ceramic and carbon-carbon composite materials, improvements in manufacturing tolerances in the form of reduced trailing edge thicknesses, and improvements in analytical techniques in the form of 3-D viscous flow analysis methods. In addition to the improvement in turbine efficiency, the improved materials will permit higher TIT with a corresponding improvement in vehicle fuel economy.

COMBUSTOR

Combustor Candidates

Combustor technology for low-pollution combustion has undergone considerable change in the last 5 years. An assessment of the various types of combustion processes is required to establish criteria for designing an IGT combustor. Ten combustor types were studied but several were dropped from consideration because they could not meet the NO_x specification. A brief description of the potentially acceptable combustor types is given below. The description is based on a simple can-type combustor. Similar configurations can be developed for the annular-type combustor. Discussions of the types of fuel injectors and combustor geometry are also given.

PROJECTION OF SMALL
RADIAL TURBINE PERFORMANCE

1978 METALLIC 0.51MM (0.020IN.) EDGE THICKNESS
1985 CERAMIC 0.76MM (0.030IN.) EDGE THICKNESS
1985 METALLIC 0.51MM (0.020IN.) EDGE THICKNESS
1985 COMPOSITE 0.51MM (0.020IN.) EDGE THICKNESS
0.227 KG/S (0.5 LB/S) FLOW RATE
IMPROVED MANUFACTURING TOLERANCES DUE TO COMPOSITE MOLDING, IMPROVED CLEARANCES DUE TO LOWER EXPANSION, NEW 3-D VISCOUS DESIGN TECHNIQUES, HIGHER TIP SPEEDS

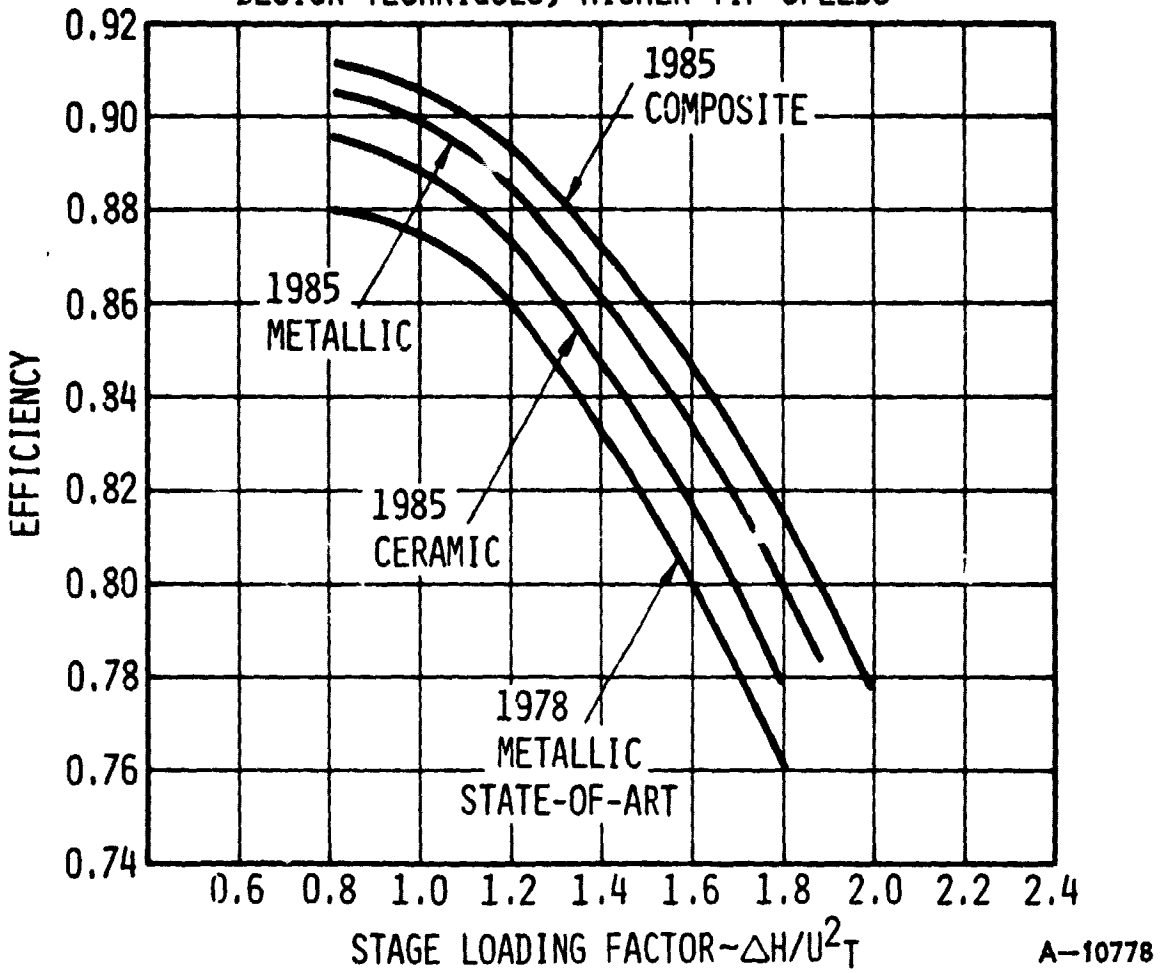

Figure 11. Projection of Radial Turbine Performance

A. Diffusion Flame Combustor (Figure 12)

The diffusion flame combustor is not capable of meeting proposed emission specifications, but it was included in this study because it is the accepted standard of reference for gas turbine combustors. The diffusion flame combustor operates on the principle of direct combustion of fuel droplets after injection of the fuel into the primary zone of the combustor. The flame is aerodynamically stabilized by recirculation of burned products caused by jets of air in the primary zone. The flame temperature in the primary zone can reach the adiabatic limit. Hot gases leaving the primary zone are cooled to TIT by the addition of dilution air. This type of combustor has good efficiency over a wide range of fuel-air ratios. Emission of NO_x is usually high at high power level due to the high primary zone temperature.

B. Lean Premixed Prevaporized (LPP) Combustor (Figure 13)

Lean, premixed, and prevaporized fuel-air mixtures have been found to burn at temperatures well below the adiabatic flame temperature for a given fuel. Combustors have been built which have an external vaporizer in which the fuel/air charge is mixed and vaporized prior to entering the primary zone of the combustor. The stability limits of this type of combustor are very narrow. Extreme care in design and fabrication is required to prevent flashback or autoignition of the fuel/air mixture in the vaporizer. NO_x concentrations in the exhaust gas increase almost exponentially when primary zone temperatures exceed 1922°K (3000°F).

C. Jet-Induced Circulation (JIC) Combustor (Figure 14)

The jet-induced circulation (JIC) combustor is a type of premixed, prevaporized combustor which uses strong aerodynamic circulation to aid in prevaporizing and stabilizing the lean fuel/air mixture. The fuel is mixed with air in the jet tubes and is vaporizing as it enters the combustor. The mixture continues to vaporize as it penetrates into the combustion chamber. A flow reversal in the combustion chamber adds to the turbulence and improves the stability of this combustor. Flashback into the jet tubes can cause the tubes to burn out. This type of combustor has low NO_x emissions and slightly better stability than the more conventional LPP-type combustor.

D. Vortex Air Blast (VAB) Combustor (Figure 15)

The vortex air blast (VAB) is a type of LPP combustor. Primary zone airflow is controlled by a variable angle, radial inflow swirler. Fuel is injected into the higher velocity airstream at the swirler and is allowed to mix and vaporize in the annular duct prior to entering the combustion chamber. The angle of the swirl vanes controls the swirl velocity, which in turn controls the residence time of the fuel/air mixture in the vaporizer. Heat is transferred into the fuel/air mixture through the walls of the annular duct to aid in vaporization of the fuel. The efficiency and NO_x emission level are approximately equal to those of the JIC-type combustor.

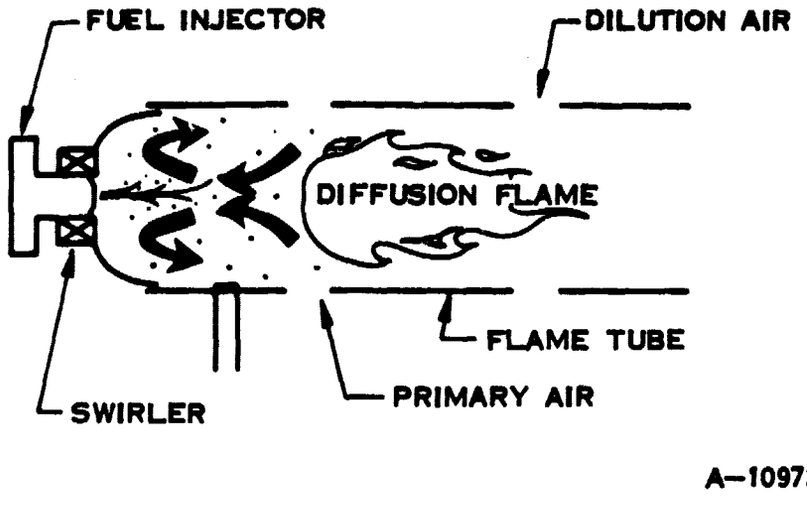

Figure 12. Diffusion Flame Combustor

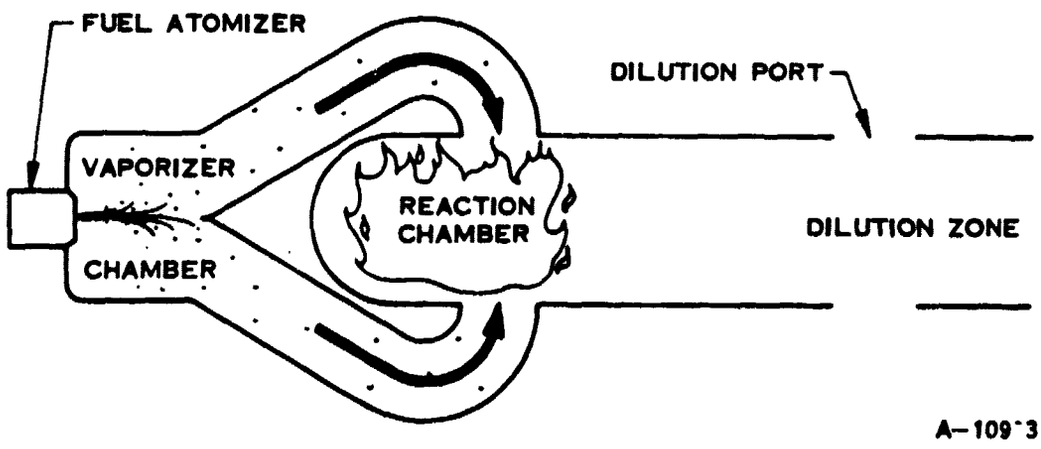

Figure 13. Lean Premixed Prevaporized Combustor

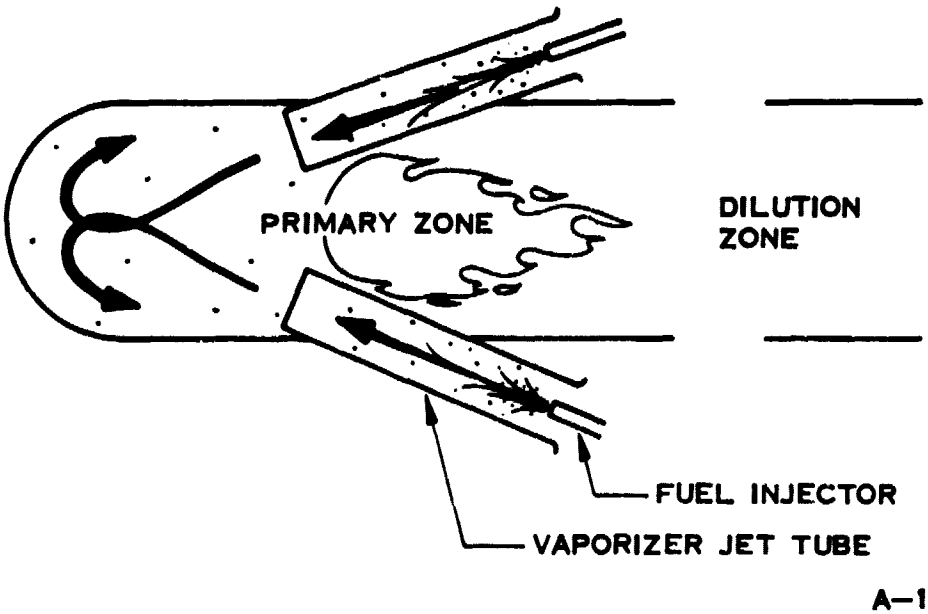

Figure 14. Jet-Induced Circulation Combustor

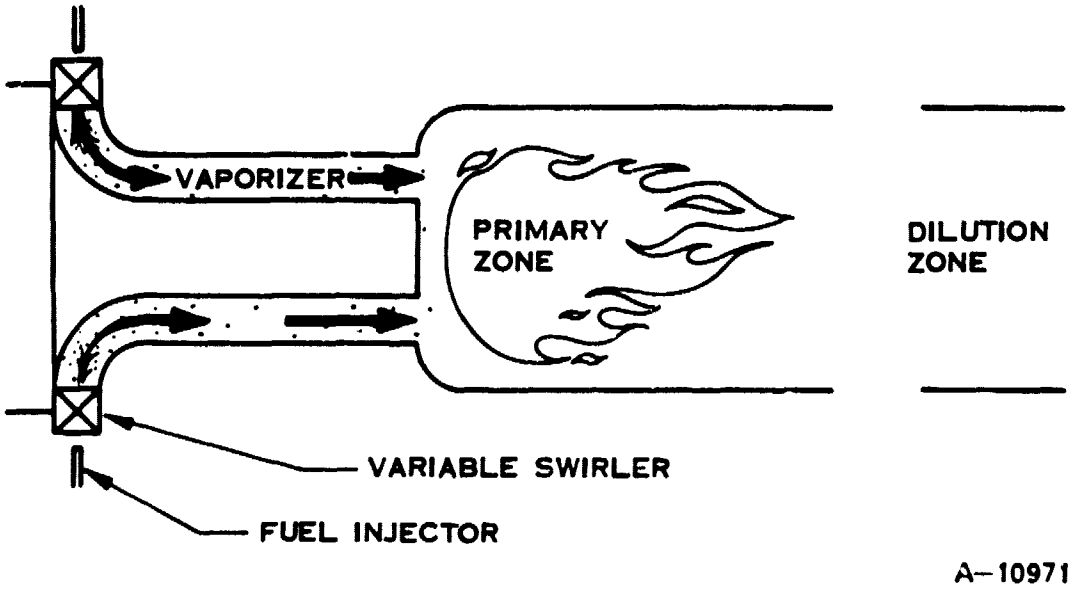

Figure 15. Vortex Air Blast Combustor

E. Multielement Ceramic Combustor (Figure 16)

The multielement ceramic combustor is a type of surface combustor. The primary zone of this combustor is composed of several stepped ceramic tubes which serve as flame holders. The fuel/air mixture is injected into the small diameter end of the ceramic flame tube. As the mixture flows through the tube, the fuel is mixed, vaporized, and preheated. Heat convection from the hot walls of the ceramic tube aids in vaporization of the fuel and preheating the mixture to allow lean mixtures to be burned. As the mixture passes into the larger diameter section of the flame tube, the velocity drops and combustion begins. The step forms an aerodynamic flame holder to aid in stabilization of the flame. The combustion efficiency and NO_x emission levels are equivalent to those of the LPP-type combustors.

F. Catalytic Hybrid Combustor (Figure 17)

Catalytic combustion of hydrocarbon fuels is a very low pollution method for burning fuels in gas turbine engines. The catalyst bed can be made from a metal or ceramic honeycomb. The surface of the honeycomb is treated with a material to increase its surface area. The catalytic material is then applied over the surface. Materials such as platinum and palladium are efficient catalysts for hydrocarbon fuels. The catalytic bed must be preheated to approximately 589°K (600°F) for the catalytic reaction to be self-sustaining. A small pilot combustor can be used for starting. The fuel/air mixture must be well atomized before entering the catalytic bed. A premixer or vaporizer section is required upstream of the catalytic bed. The catalytic combustor is extremely efficient when the combustor exit temperature is maintained above 1366°K (2000°F). It would be ideally suited to a constant TIT cycle.

Fuel Injection Methods

Several methods for fuel injection are available for automotive-type combustors. A brief description of several types of fuel injectors is given below.

A. Rotating Fuel Slinger (Figure 18)

The rotating fuel slinger is used on several of the WRC folded annular combustors. Fuel is injected into the rotating fuel slinger at relatively low pressure. The fuel forms a thin annular film on the interior of the slinger as it is accelerated up to shaft speed. A pressure head is developed because of the centrifugal force acting on the fuel film. The fuel is discharged through a number of small orifices on the periphery of the slinger. As the fuel exits from the slinger, it has a very high tangential and radial velocity which aids in the rapid atomization of the fuel droplets.

B. Air Blast Atomizer (Figure 19)

The air blast atomizer uses very high shear velocity between the fuel droplets and the atomizing airflow to achieve atomization. The atomizing airflow is generated by the combustor liner pressure drop. Fuel is injected into the atomizing air stream at very low pressure. The air blast atomizer is not effective at low burner pressure drop operating conditions such as during engine starting.

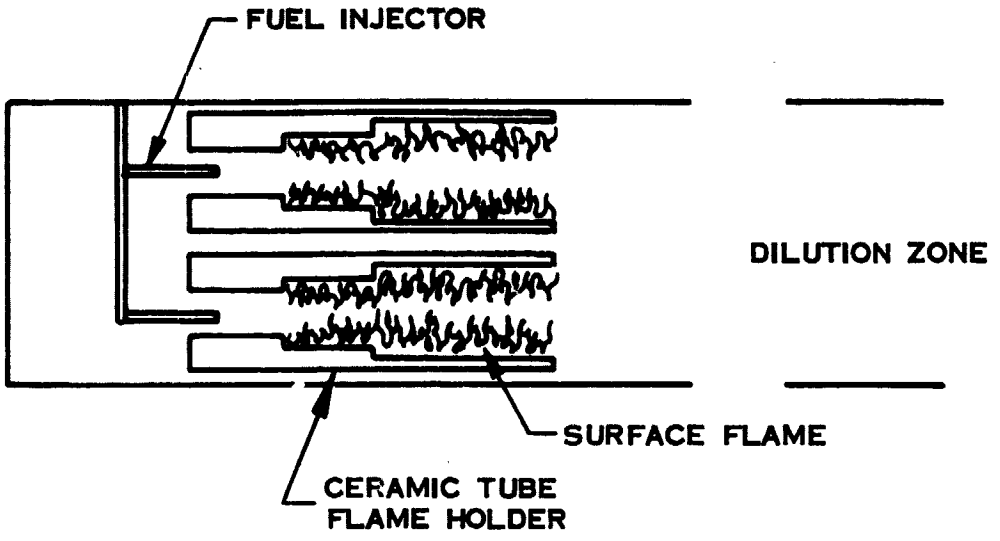

Figure 16. Multielement Ceramic Combustor

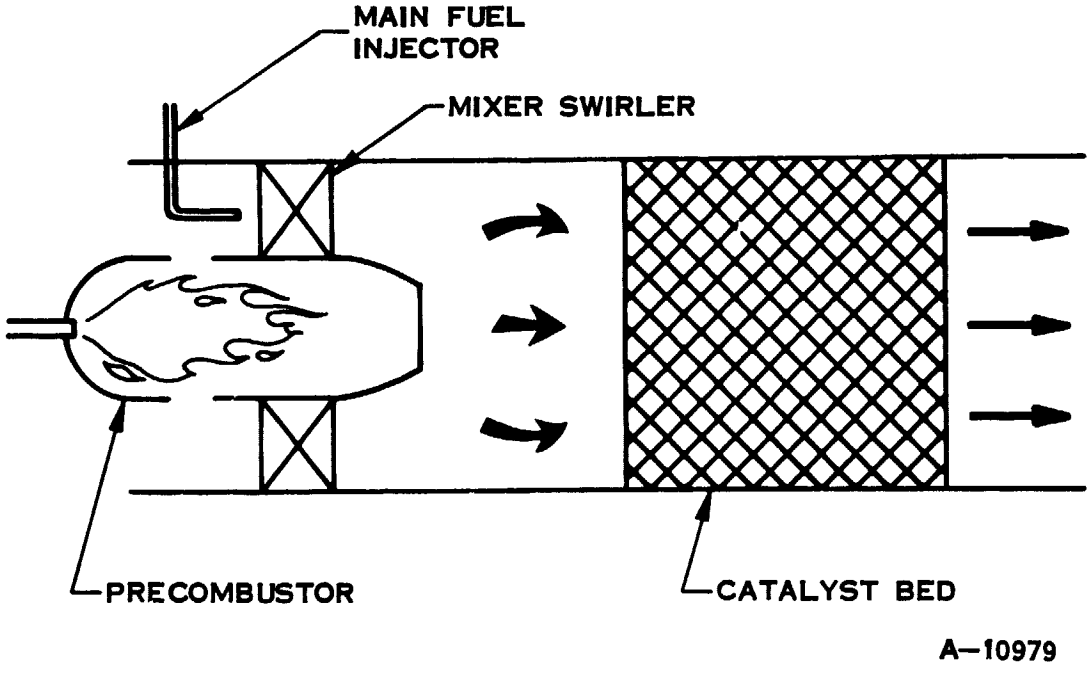

Figure 17. Catalytic Hybrid Combustor

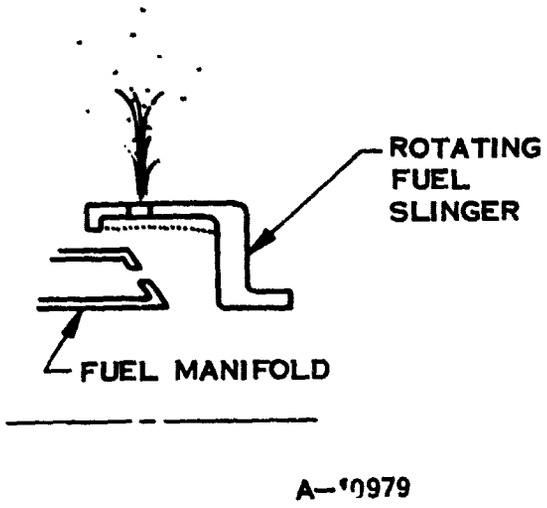

Figure 18. Rotating Fuel Slinger

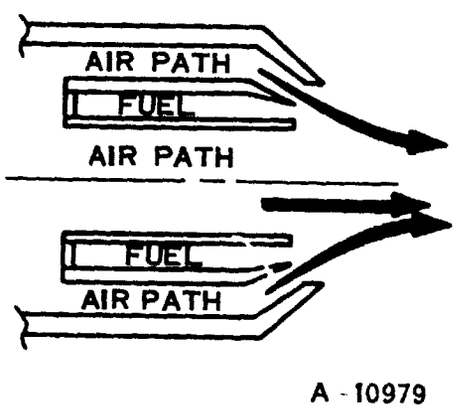

Figure 19 Air Blast Atomizer

C. Air Assist Atomizer (Figure 20)

The air assist atomizer works on a principle similar to the air blast atomizer except that the atomizing airflow is provided by an auxiliary air supply instead of the normal engine primary zone airflow. The air assist atomizer is not dependent on engine operating conditions to achieve good atomization because the atomizing airflow is externally supplied.

D. Pressure Atomizing Fuel Nozzle (Figure 21)

The pressure atomizing fuel nozzle uses high fuel pressure to force fuel through a small orifice, which causes ligaments to form that atomize into fine droplets due to surface tension of the fuel. All components of the fuel system must be designed to withstand the higher operating pressures required. The combustor gas pressure affects the quality of atomization and the diffusion angle of the fuel spray from the pressure atomizing nozzle.

E. Flash Vaporization (Figure 22)

Flash vaporization is a technique in which heat is added to the fuel prior to injection into the combustor. The fuel is heated to a temperature well above the distillation temperature, but is kept liquid by application of high pressure. When the fuel is injected into the combustor, it vaporizes immediately, since all the energy necessary for vaporization is already stored in the fuel.

Combustor Liner Geometry

Several different combustor geometric configurations are available to the engine designer. Several of the common configurations are described below.

A. Single Can Combustor (Figure 23)

The single can combustor generally uses a cylindrical outer casing with a simple inner cylindrical flame tube liner. Flow in the liner can be in the same direction or opposite in direction to the flow of air in the outer casing. The combustor liner generally has some type of head or dome which supports the fuel injection device.

B. Annular Combustor (Figure 24)

The annular combustion chamber is formed by a cylindrical outer casing with an annular liner which is usually wrapped around the engine shaft. Several fuel injectors are installed in the forward end of the liner.

In applications where weight and engine size are critical, the folded annular combustor can be used. The advantage of the folded annular combustor is that a long flow path length can be squeezed into a small area. The flow path can be folded to give flow in either the axial or radial direction. The axial flow folded annular combustor is shown in Figure 25, and the radial flow, folded annular combustor is shown in Figure 26.

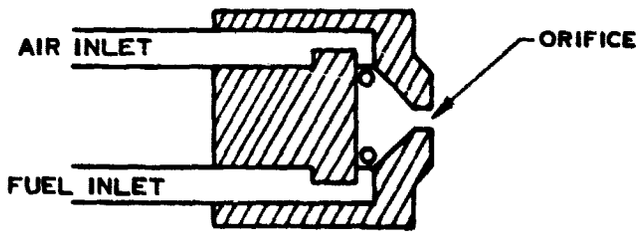

Figure 20. Air Assist Atomizer

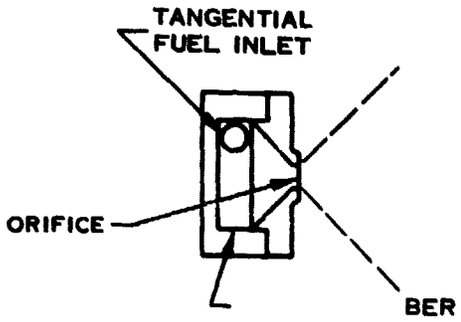

Figure 21. Pressure Atomizing Fuel Nozzle

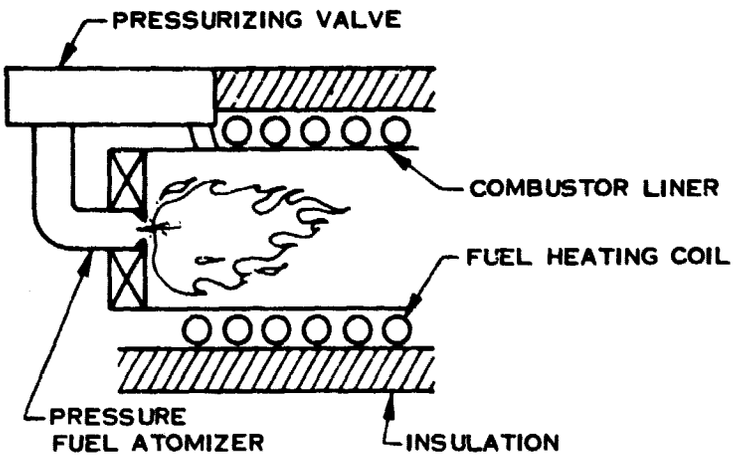

Figure 22. Flash Vaporization

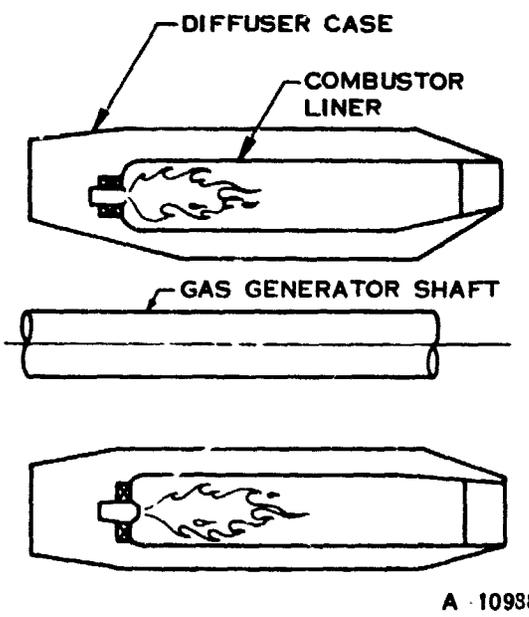

Figure 24. Annular Combustor

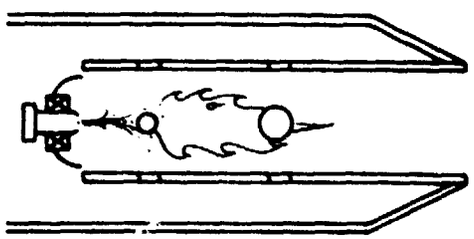

Figure 23. Single Can Combustor

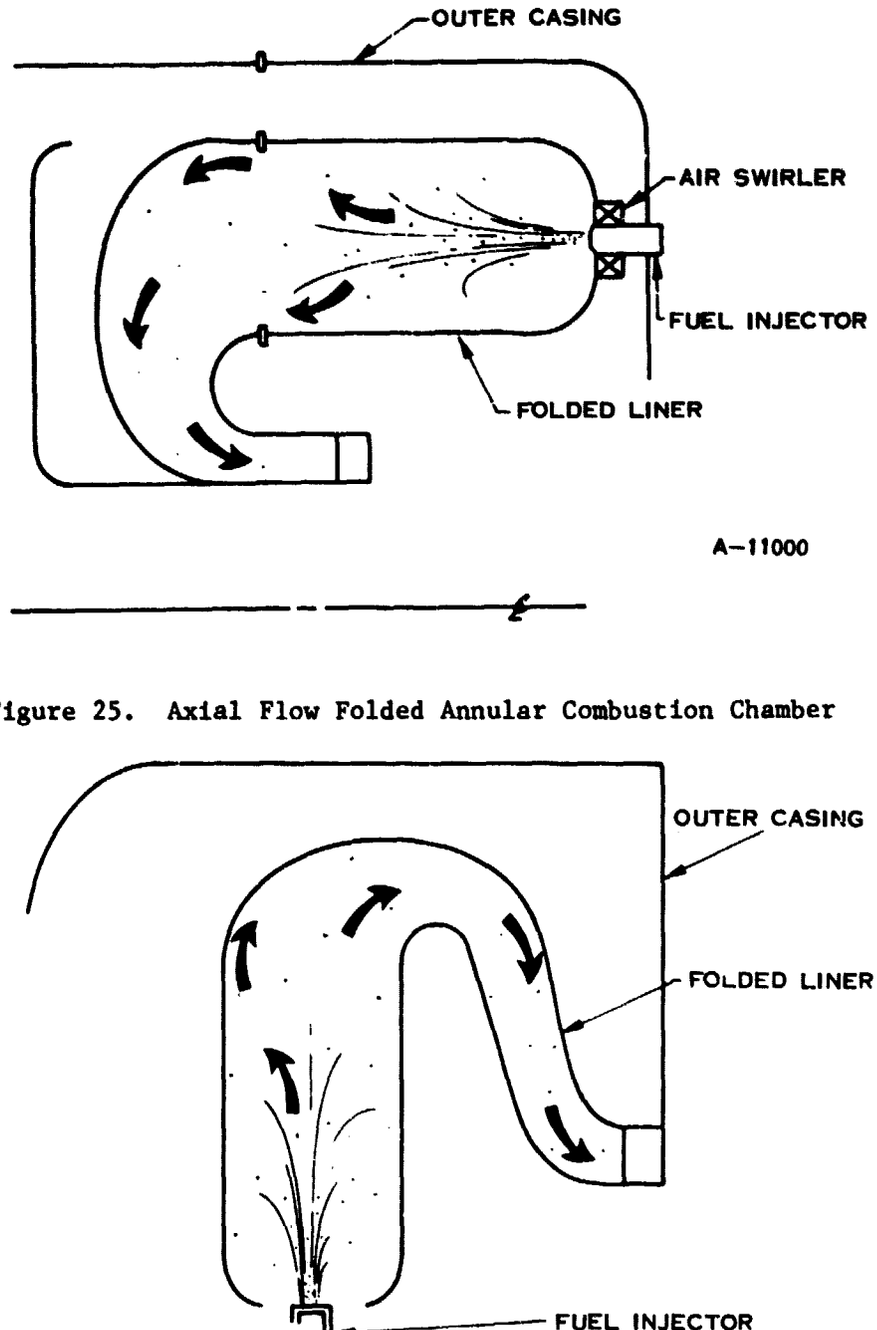

Figure 25. Axial Flow Folded Annular Combustion Chamber

Figure 26. Radial Flow Folded Annular Combustor

Combustor Comparison

Many constraints were placed on the operation of the combustor which forced the elimination of many of the combustor concepts early in the evaluation. Table V lists the rating criteria for selection of the most desirable configurations for further study. The major factor in the elimination of many of the combustor types was the inability to meet the 0.35 g/km (0.4 g/m) NO_x emission limit. All combustors which have primary zone flame temperatures above 2033°K (3200°F) were dropped because of this emission limit. Mechanical complexity and durability were also used to rate the combustor concepts. Variable geometry with moving hot parts is much less desirable than a fixed geometry combustor from both a complexity and durability standpoint. Control of the combustor is the final major criterion for evaluating the combustor types. A simple single-point fuel delivery system operating at low pressure is the most desirable system. Staging multiple nozzle and high-pressure atomization are less desirable.

Combustor Selection

The primary candidate selected for use as the IGT combustor is the premixed, prevaporized catalytic combustor. For the advanced cycle selected for the IGT engine, the catalytic combustor is well suited because of its high efficiency and low emission characteristics. The lean premixed prevaporized combustor and the multielement ceramic combustor were also selected for further study.

HEAT EXCHANGER

Heat Exchanger Performance Requirements

Preliminary cycle analysis indicated that a heat exchanger was required for good part-load specific fuel consumption (SFC). It was next necessary to determine the heat exchanger performance that must be achieved to attain or surpass the fuel economy objective.

To achieve good fuel economy, the fuel flow must be low at low power and idle. The basic performance parameters for the heat exchanger are effectiveness, pressure drop, and air loss. A high effectiveness heat exchanger, whether regenerator or recuperator, is very effective in improving SFC at low power. The ideal heat exchanger with 100 percent effectiveness can never be achieved, but 90 to 95 percent can be accomplished practically, although with cost and size limitations.

A given level of effectiveness can be achieved in a smaller package by increasing pressure drop, but with an increase in SFC. The resulting fuel economy and the trade-offs in package size and cost are compromises required in the design process.

The rotary regenerator has an inherent air loss from the high pressure passage due to seal leakage and the rotated air volume. This leakage shows up in two ways: (1) bypassing the turbine stages with significant loss in output power, and (2) reducing regenerator low pressure passage inlet temperature, with a corresponding increase in fuel flow to the combustor. The stationary recuperator should have much lower air loss, although there could be some leakage through wall porosity, bonding imperfections, or at static seals.

TABLE V. COMBUSTOR TECHNOLOGY RANKING

Type	NO_x Emission	Mechanical Complexity & Durability	Controls
Diffusion Flame	High NO_x	Simple Fixed Geometry	Single System
External LPP	Acceptable NO_x	Variable Geometry	Control for Variable Geometry Required
Jet Induced Circulation	Acceptable NO_x	Vaporizer Tube Burn-out	Fuel Staging Required
Vortex Air Blast	Acceptable NO_x	Variable Geometry	Geometry Controls
Multi-element Ceramic	Very Low NO_x	Well-Developed Ceramic Structure	Simple Fuel System
Catalytic	Lowest NO_x of All Combustors Surveyed	Precombustor Required for Starting	Dual Fuel System Required

Heat Exchanger Comparison

The heat exchanger for the IGT powertrain can be either a rotary regenerator or stationary recuperator, Table VI. In either case, a low expansion ceramic material will be used, based on the extensive development experience with ceramic regenerators. A ceramic recuperator should have the same temperature capability, up to 1273°K (1832°F), although stress conditions are entirely different. In either case, ceramic has the potential for low cost and availability in production compared to a metal fabrication requiring nickel-base or equivalent alloys and exotic bonding in order to function at these temperature levels.

The heat exchanger effectiveness at part-load must be as high as practical, in the 90 to 95 percent range. The pressure drop will be a compromise to obtain high effectiveness with a reasonable package size, with additional losses in the recuperator due to integral manifolds. Regenerator leakage may be held below 4 percent with careful design and development, with much lower leakage for the recuperator.

The regenerator configuration would be a single circular disk, with the axis perpendicular to the turbomachinery. Lateral ducts are required to form the flowpath, with traditional problems in flow distribution.

The recuperator could be one or more rectangular modules, or could be an annular ring. In either case, the basic heat transfer surface would be counterflow, with face area, flow length, and passage size similar to the regenerator. Integral manifolds are required to connect alternating high-pressure and low-pressure passages, designed for good flow distribution across the face of the core. The annular recuperator with axisymmetric flow passages to and from the ring should be particularly good on flow distribution.

Initial cost of the regenerator system includes the rubbing seals and a high reduction ratio (about 3000:1) drive. The recuperator has additional cost for the integral manifolds, dependent on the cost of the ceramic material.

Maintenance for the regenerator will include inspection and replacement of the rubbing seals and drive components. The recuperator requires no equivalent service.

Fouling problems have occasionally been reported with recuperators, although usually associated with a combustion problem. The catalytic combustor for the IGT should operate with very high efficiency and very low emissions, properties not conducive to fouling.

The final consideration is vehicle fuel economy. The heat storage, leakage, and flow distribution effects are worse in the rotary regenerator, making it more difficult to achieve the high level of effectiveness needed for good fuel economy.

TABLE VI. HEAT EXCHANGER COMPARISON

	Rotary Regenerator	Stationary Recuperator
Material	Ceramic	Ceramic
Temperature	1273°K (1832°F)	1273°K (1832°F)
Effectiveness	90-95%	90-95%
Pressure Drop	3-6%	5-10%
Leakage	2-4%	<0.5%
Configuration	Single Disk	Rectangular Modules Annular Ring
Initial Cost	Added seal and drive cost	Added ceramic manifold cost
Maintenance	Seal inspection and replacement	Possible fouling problem
Fuel Cost	TBD	TBD

Heat Exchanger Selection

Present-day regenerators have demonstrated acceptable performance and durability, but there are problems and limitations. Leakage may easily range up to 6 percent, with a significant power loss. These leakage effects and flow distribution problems make it difficult to get an installed effectiveness much over 90 percent. The recuperator projected for 1983/1985 should be capable of higher effectiveness, approaching 95 percent at low power, with very low leakage.

The decision was made to explore the ceramic recuperator thoroughly as part of Task II. The decision would be verified by comparing powertrain performance with recuperator with an equivalent powertrain with regenerator.

1.4 VEHICLE CONCEPT STUDIES

Preliminary design studies were made by AM General on different automobile concepts suitable for marketing in 1985-1990. These studies used an existing conceptual design layout of a 60 kW (80 hp) regenerative automotive gas turbine. This conceptual design layout was developed as part of an automotive gas turbine economic analysis, WRC Report No. WR-ERh1, December 1972, performed for the Environmental Protection Agency (EPA). The conceptual design was based on the Williams Research Corporation WR26 engine, which had been installed in an American Motors Corporation (AMC) Hornet automobile.

These vehicle concept studies were based on the AMC Concord 2-door sedan. A comparison between the AMC Concord and baseline vehicle reveals discrepancies in the following areas:

	AMC Concord	Baseline
Roominess Index	680.44 cm (267.89 in)	694.43 cm (273.40 in)
Wheelbase	274.32 cm (108.00 in)	278.13 cm (109.50 in)
Vehicle Curb Weight	1448.32 kg (3,193 lb)	1406.14 kg (3,100 lb)
Trunk Space	0.305 m^3(10.76 ft^3)	0.453 m^3(16.00 ft^3)
Frontal Area	1.872 m^2(20.15 ft^2)	1.997 m^2(21.50 ft^2)
Tires	DR78-14	ER78-14

Some of these differences can be accommodated as part of the vehicle design in Task III. Others, such as wheelbase, frontal area and trunk space, may not be achievable within the restrictions of the AMC Concord design. The IGT powertrain should weigh considerably less than the six-cylinder piston engine in the conventional AMC Concord, enough to be under the baseline weight.

Design studies were made of three drive arrangements, the conventional front-engine installation with rear drive, front-engine with front drive, and rear-engine with rear drive.

FRONT-ENGINE INSTALLATION WITH REAR DRIVE

The conventional front-engine installation with rear drive easily fits into the engine compartment with adequate clearance and the driveline at the standard location. The air intake is behind the grille, with large ducts to the engine intake at the rear. The engine exhausts to the rear of the vehicle through two 6.35 cm (2.5 inch) diameter pipes; an alternate system exits ahead of the rear axle. Oval-shaped pipes were considered for a single pipe system, but exhaust system manufacturers advised against them because of high tooling costs. Both steel and aluminum pipes are under consideration. Aluminum is attractive because of the lighter weight, but steel is less costly.

FRONT-ENGINE INSTALLATION WITH FRONT DRIVE

The basic requirement for the front-engine, front-drive arrangement is the availability of front-drive components. The Hydramatic Division of GM was working on front-drive units for future models, but detailed information was not available at the time of the study. One possible drivetrain arrangement was studied. Other installation requirements such as intake and exhaust systems are similar to the front-engine, rear-drive arrangement.

REAR-ENGINE INSTALLATION WITH REAR DRIVE

The rear-engine installation with rear drive uses drivetrain components similar to the front drive. This arrangement results in more vehicle changes than the other two. The air intake is from the sides of the vehicle, opposite the engine intakes. The exhaust ducts are short, direct to the side or to the rear.

VEHICLE CONCEPT COMPARISON

The principal characteristics of the three vehicle concepts are summarized in Table VII. The installed weight of the WR26 engine was approximately the same as the six-cylinder piston engine. The lower weight of the IGT powertrain will improve the weight distribution.

VEHICLE CONCEPT SELECTION

The conventional front-engine, rear-drive arrangement was chosen for the vehicle concept studies during Tasks II and III. This arrangement minimizes vehicle changes, and eliminates major development of components such as front axle, steering, suspension, transmission, and body structures.

1.5 POWERTRAIN CONCEPT STUDIES

The review and evaluation of the basic cycle parameters, rotor systems, and components provide the basis for selection of a small number of powertrain concepts

TABLE VII. PRINCIPAL CHARACTERISTICS OF THE IGT POWERTRAIN INSTALLATION

Exhaust - 77.4 cm^2 (12 in^2)
Intake - 361.3 cm^2 (56 in^2)

Engine Location	Axle Driven	Weight Distribution	Advantages	Disadvantages	Problem Areas	Research and Development Area
Front	Rear	Frt. - 55% RR - 45%	. Improved traction on grades . Good stability . Minor modifications required to the body . Existing automatic transmission can be utilized	. Harder steering (manual) . Exhaust piping and insulation is more complex . Tunnel protrusion for driveshaft in passenger compartment	. Exhaust	
Front	Front	Frt. - 58% RR - 42%	. Good stability . Good handling characteristic . No driveshaft tunnel required . Drive train (axle and transmission) can be made more compact	. Harder steering (manual) . Loss of traction on grades . Major modifications required to body, steering, suspension . New axle and transmission required . Driveshaft C.V. joints more complex . Reduced wheel cut (turn radius)	. Exhaust . Body . Steering and suspension . Axle and transmission . Drive lines	. Steering and suspension . Axle and transmission . Drive lines
Rear	Rear	Frt. - 45% RR - 55%	. Good traction on ice & snow . Improved traction on grades . Simpler exhaust system . Drive train (axle and transmission) can be made more compact . Lighter steering . No driveshaft tunnel required	. Poor stability . Major modification required to body, suspension and fuel system . New axle and transmission required . Reduced luggage room . More complex control system for engine, transmission, heating, power steering & brakes	. Body . Suspension . Axle and transmission	. Suspension . Axle and transmission

NOTE

This study was based on a WRC engine approximately the same weight as the six-cylinder gas engine. Engine contour same as turbine engine installed in an AMC Hornet in 1975.

for detailed study during Task II. Achieving the prime objective of improved fuel economy immediately points to the regenerative cycle with as high TIT and pressure ratio at rated power as practical, with a means of maintaining high TIT at part load. The engine should be sized as small as practical, with a continuous rating adequate for steady-state operation, and use variable geometry and/or water injection to maintain performance on hot days.

The dual-rotor engine with free power turbine is an excellent system, meeting all control and operational requirements. This engine functions well with a simple, efficient drivetrain. The single-rotor engine is also a viable candidate, if a satisfactory continuously variable transmission is available.

In the review of component candidates, the two-stage centrifugal compressor stands out for good efficiency with wide range and high pressure ratio capability. The axial-centrifugal compressor is an alternative with comparable performance. Axial turbines are favored for good efficiency and low inertia, particularly with the two-stage requirement of the dual-rotor engine. A catalytic combustor has the potential of very low emissions and high efficiency, keeping the lean premixed, prevaporized combustor as a backup. The ceramic recuperator is the choice over the ceramic rotary regenerator, eliminating the seals and drive with their associated leakage and durability problems. The regenerator with its proven performance and durability can be used as an alternate heat exchanger until the recuperator can be developed to operational capability.

The three candidate powertrains shown in Table VIII were selected to provide a base for combining these selected components into a practical, functional engine. Final adjustments on cycle parameters, component tailoring and matching, and drivetrain characteristics were performed as part of Task II.

TABLE VIII. POWERTRAIN CONCEPT CANDIDATES

A - SINGLE-ROTOR
- Combined Gear Train for Accessories and Output
- Transmission - Variable Ratio Hydromechanical

B - DUAL-ROTOR WITH VARIABLE POWER TURBINE NOZZLE
- Gasifier Gear Train for Accessories
- Transmission - 3-speed Automatic without Torque Converter

C - DUAL ROTOR WITH SLIP CLUTCH POWER TRANSFER
- Gasifier Gear Train for Accessories
- Transmission - 3-speed Automatic without Torque Converter

2.0 TASK II - POWERTRAIN ANALYSIS

2.1 COMPONENT ANALYSIS

COMPRESSOR

Two compressor configurations from Task I were subjected to further analysis in Task II. These were the two-stage centrifugal compressor and the multiple-stage axial coupled with a single-stage centrifugal compressor. Task II effort concentrated on establishing design point efficiency, generation of performance maps for the two configurations for input to the IGT cycle analysis, and monitoring of the resultant cycle match to ensure that the compressors were aerodynamically satisfactory.

Two-Stage Centrifugal Compressor

The approach used in establishing the design point efficiency for this configuration was to initially match the two stages to achieve peak efficiency at the unaugmented IGT peak power point. Figure 5, a replot of Figure 2-1 from Reference 2, which presented centrifugal compressor stage performance as a function of size, was used as the basis for the peak efficiency projection for each stage. A performance improvement is not projected for the 1983 to 1985 time frame. The first stage compressor was reduced from the Figure 5 projected efficiency based on a cast impeller and the ducting loss up to the second stage impeller leading edge.

The second stage was reduced in efficiency from the Figure 5 projection based on a cast impeller. A projected performance map was produced for each stage and input to the cycle in that manner. This enabled cycle rematching of the compressor stages to assist in establishing the best operating line performance without surging. Due to the uncertainty of the conclusion in Reference 4 about the first stage compressor running past its surge point during testing, the conservative approach was taken to not include that feature in the performance projection. The projected performance maps were used in subsequent cycle analysis efforts with adjustments to the maps made by scalars.

The basic maps were not redone during either the remainder of Task II or Task III. The efficiency level of each stage was also not adjusted, as flow and speed changes for the compressors were made within a narrow band and, in addition, were felt to be conservative enough to remain unchanged. It should be emphasized that the compressor performance was slanted towards a conservative approach to ensure meeting IGT performance goals in production.

Axial-Centrifugal Compressor

The approach used in setting the axial compressor performance was to establish a consistent method to predict the performance of the ideal compressor and then estimate the degradation from this performance level due to the small size. This enabled a multistage axial compressor to be sized that, in combination with the second stage compressor of the two-stage centrifugal compressor, would be a viable IGT compressor candidate.

To establish the state of the art in axial compressor performance, the available test data have been reviewed. These data are primarily single-stage results, although some multistage data are included. These data, along with a previous correlation from Reference 4, are shown in Figure 6. The airflow of the compressors shown range from 1.13 to 440 kg/s (2.5 to 970 lbm/s). Also shown is a WRC estimate of fan performance potential based on single-stage data. A general agreement of both the data and the WRC correlation with that of Reference 7 has encouraged the use of this procedure for evaluating various multistage configurations. An alternative method outlined in Reference 8 requires preliminary design information not generally available during the engine cycle parametric study. This method has been used at WRC to evaluate specific configurations and has been found to verify the Wiggins and Waltz correlation (Reference 7).

The effects of the low Reynolds number, generally associated with low airflow, have been discussed by several authors including those in References 7,8, 11,12 and 13. The studies show that the performance loss due to Reynolds number can be given by the following expansion:

$$1 - \frac{\eta_{Rey}}{\eta_{id}} = K_{Rey} \log (N_{Rey})$$

where η_{id} and η_{Rey} are the ideal and Reynolds number corrected overall efficiency, respectively. The proportionability constant, K_{Rey}, has been placed in the narrow range of $0.167 < K < 0.2$. Depending on the configuration and using the Reynolds number based on a typical rotor chord, an efficiency penalty of from 5 to 8 percent can be expected.

Blade tip clearances effects have been modeled in References 8, 13, 14, and 15. When these models are isolated for tip clearances only, they generally reduce to the following form:

$$1 - \frac{\eta\Delta}{\eta_{id}} = K_4 \frac{\Delta}{h_{ave}}$$

where the efficiency at the nominal clearance, $\eta\Delta$, is proportional to the tip clearance, Δ, as a fraction of the blade height, h. For a multistage compressor, the average value of Δ/h is used. The proportionability factor, K_4, is estimated to be in the range of $1.0 < K_4 < 1.5$ with the consensus being the smaller value. Depending on the dynamic characteristics of the IGT, the clearances could be as small as 0.127 mm (0.005 inch) or as great as 0.381 mm (0.015 inch). Using estimated blade heights, an efficiency penalty of 2 to 5 percent may result.

Recent WRC experience with a six-stage compressor designed for a pressure ratio of 3.7 has provided data on the effect of manufacturing tolerances on performance. This low tip speed [250 m/s (850 ft/s)] compressor applied manufacturing techniques which make the axial compressor a cost-effective mechanically practical candidate but result in some undesirable aerodynamic compromises. The design details are documented in Reference 9. At the design point, the airflow was 1.59 kg/s (3.5 lbm/s) and the Reynolds number at the first rotor tip was 115,000. During the component test program, the Reynolds number was reduced to 72,000, thus providing data at conditions comparable to the estimated Reynolds number of 80,000 in the IGT compressor. At these test conditions, the measured peak efficiency was 77 percent (Reference 12). Applying the previously discussed corrections for the test Reynolds number and the measured tip clearance to the correlation of Wiggins and Waltz in Figure 6, the predicted efficiency of the compressor was 84.2 percent.

This difference of 7.2 percent has been assumed to be the result of three sources. The manufacturing tolerances controlling such items as blade spacing, setting angle and surface contour and roughness of both the airfoil and flowpath were excessive. Additional development of the manufacturing process will reduce these to values more typically associated with turbomachinery. The manufacturing process, even in its developed form, demands certain compromises from aerodynamic optimum airfoil shapes. Some of these compromises required in the initial configuration may be relaxed in later configurations. Finally, the test article from which the original performance data were obtained has had no aerodynamic development. Interstage data are available to optimize the match of the stages and improve the overall performance. At this point, an exact estimate of the potential of such a design cannot be made, but a conservative estimate is that one-half the difference between the ideal and the measured efficiency, or 3.6 percent, will be achieved. No additional improvement beyond this is expected for the 1983 to 1985 time frame.

Using the results from this discussion, the performance level of an axial compressor suitable for use in the IGT was estimated for a variety of configurations. Assuming an airflow of 0.408 kg/s (0.9 lbm/s), a Mach number of 0.35 at the compressor exit to set the blade height and a constant clearance of 0.127 mm (0.005 inch), the performance levels of Figure 6 can be degraded to those achievable in the IGT. An additional 3.6 percent has been subtracted for the manufacturing process and its associated tolerances. These results are summarized in Table IV. The results are assumed applicable to all airflows suitable for the IGT cycle because of the narrow range in Reynolds number involved.

The preliminary compressor design point, based on IGT cycle requirements when this particular configuration was analyzed, was as follows:

- Corrected Flow ($W\sqrt{\theta}/\delta$) = 0.441 kg/s (0.973 lbm/s)
- Overall Compressor Total-to-Static Pressure Ratio = 5.500
- Overall Compressor Total-to-Static Efficiency = 0.821

The approach used in establishing the efficiency level was the same as for the two-stage centrifugal. The stages were initially matched to achieve peak efficiency at the unaugmented IGT peak power point. Performance maps for the multistage

axial and the centrifugal compressor were input as separate entities into the cycle. This enabled rematching of the compressor to best meet IGT cycle requirements. The IGT cycle-dictated match yielded an efficiency below that initially set at the peak power design point, a result identical to that of the two-stage centrifugal match. In general, the efficiencies along the operating line were similar to those of the two-stage centrifugal compressor.

As was the case for the two-stage centrifugal compressor, scalars on pressure ratio and flow were applied to the basic performance maps. Efficiency was held constant because of the small range of flow and pressure ratio excursions necessary to meet cycle requirements.

TURBINE

Each of the turbine component configurations that were described in Task I was reviewed and evaluated based on the merits and drawbacks of each system's mechanics and performance. The axial turbines were compared based on the resulting location on the efficiency correlation graph shown in Figure 27, which relates stage loading factor, efficiency, and stage flow factor prior to subtracting the clearance and Reynolds losses. The radial turbines were compared using the graph provided in Figure 28, which relates efficiency to specific speed and identifies the contributions of the various loss systems.

In addition to the in-depth aerodynamic component performance analysis, other practical considerations were also addressed. Items such as tip clearances, minimum practical leading and trailing edge thicknesses, wheel sizes, inertia, tip speeds, and other physical considerations were kept consistent and representative of production automotive hardware. Furthermore, complexity factors were also evaluated. Items such as flowpath shapes between turbine stages, exhaust ducting, inlet ducting, variable geometry and power transfer mechanisms were studied functionally. The selection of the final configuration was based on the varying degrees of risk associated with each of the described variables and on adaptability to various materials and vehicle drivetrains expected for the 1983 time frame.

The conclusion of the evaluation resulted in the selection of the two-stage axial turbine configuration which will be optimized for use in Task III. This configuration was preferred based on the following criteria:

1. The turbine system does not require a continuously variable transmission.

2. The low inertia of this configuration does not require a materials breakthrough or development of ceramic or other composite materials.

3. A decrease in SFC at part power can be expected from the use of a variable area power turbine nozzle.

4. This turbine configuration results in a convenient packaging of the combustor, turbine, recuperator, and exhaust system, minimizing related ducting.

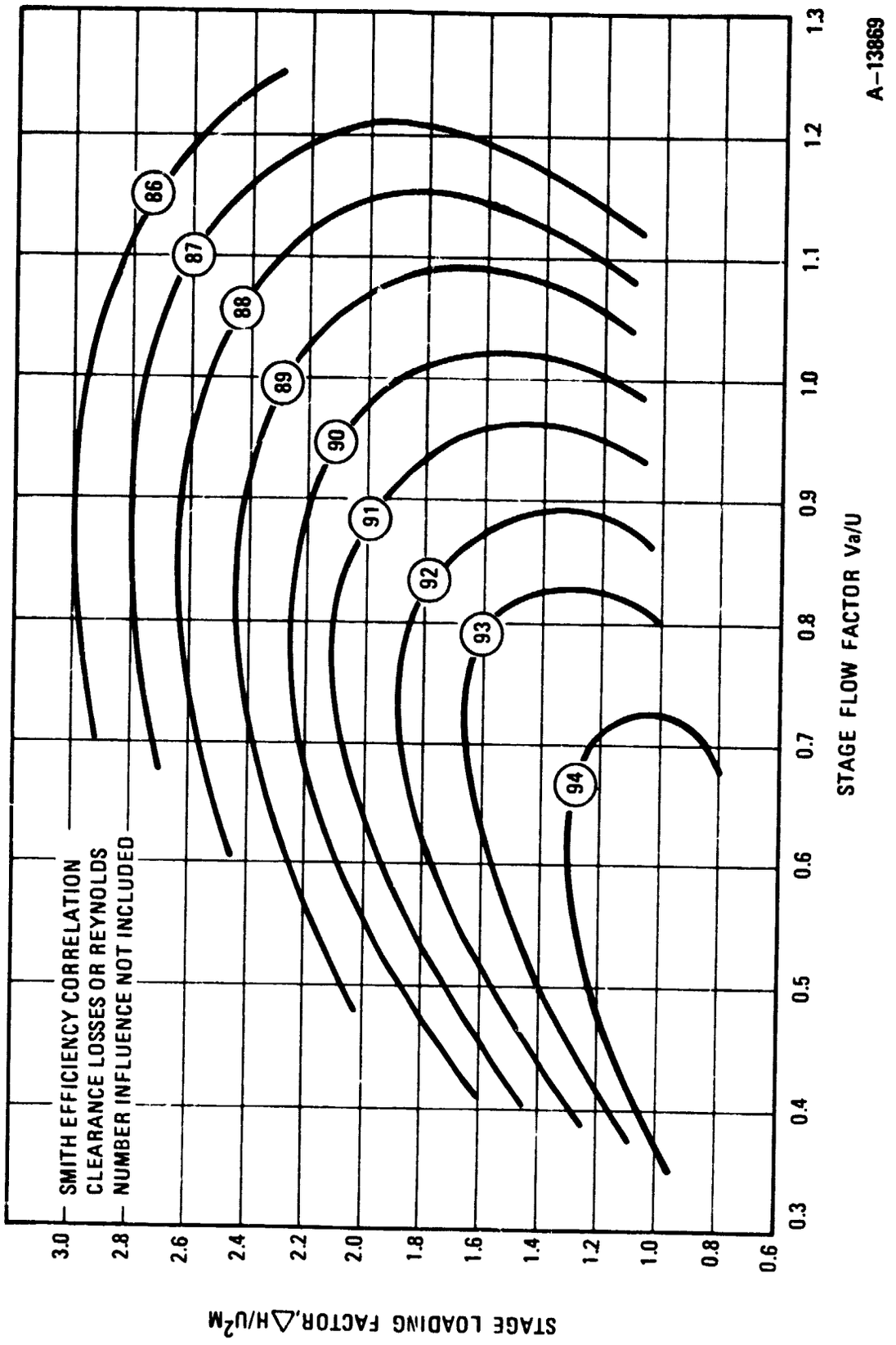

SMITH EFFICIENCY CORRELATION

Figure 27. Axial Turbine Efficiency Correlation

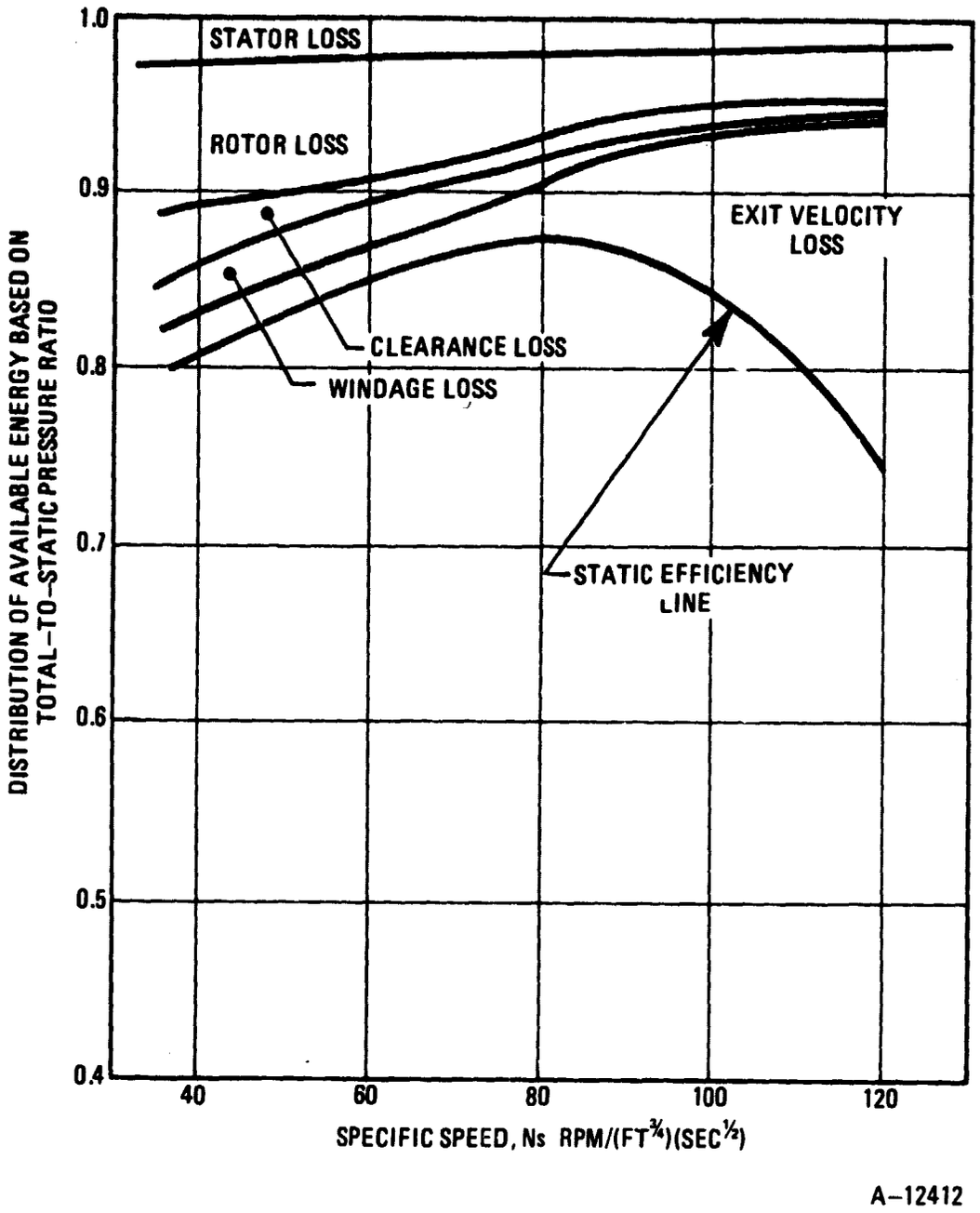

Figure 28. Radial Turbine Loss Distribution

COMBUSTOR

The catalytic combustor is a relatively new development for use in gas turbine engines, but the state of the art has progressed very rapidly. Current technology has demonstrated essentially 100 percent efficient combustion of fuel at reaction temperatures above 1350°K (1970°F). The emission levels demonstrated by current technology catalytic combustors are less than half of the 1978-allowed emission levels for carbon monoxide and unburned hydrocarbons and approximately 0.1 of the oxides of nitrogen limit. Current catalytic combustors have run in excess of 1,000 hours at 1570°K (2380°F) and shown little change in combustion efficiency using diesel No. 2 fuel, Reference 16.

Sizing of a Catalytic Combustor

Flow velocities are the most critical parameters used for sizing the prevaporizer and catalyst bed in a catalytic combustor system. The inlet or reference velocity of the fuel/air mixture into the catalyst bed controls the diffusion rate of reactants to the catalyst surface and of combustion products to the exit of the flow channel. The reference velocity selected for the IGT engine is 15 m/s (49 ft/s) at maximum power. This velocity gives the required diffusion rate for efficient combustion without having an excessively large combustor cross section. The velocity of the flow through the premixer must be selected such that mixing and vaporization are complete but residence time is short enough to prevent autoignition. Experimental data will be required to substantiate the flow velocity selected. A velocity of 65 m/s (213 ft/s) has been selected which gives a residence time of approximately 4 milliseconds. The vaporization rate for the slowest vaporization condition is approximately 2 milliseconds and the autoignition delay time is approximately 5 milliseconds; therefore, the 65 m/s (213 ft/s) velocity through the premixer should operate satisfactorily.

At the cycle temperatures planned for the IGT engine, no need for combustor variable geometry is anticipated. The fuel/air ratios required to meet the cycle specification range from 0.004 at idle to 0.011 at maximum power. Operation over this range of fuel/air ratios has been demonstrated in tests performed by NASA, Reference 17.

Combustor Complexity

The catalytic combustor draws heavily on technology developed for ceramic regenerator cores. The catalyst substrate is made of corrugated ceramic materials similar to a regenerator disk. The basic combustor is relatively simple, with the major components being a fuel atomizer, a premixing duct, the combustor support structure, and the catalyst substrate. The major design problem to be solved is the integration of the high-temperature ceramic component into the metallic structure of the engine.

Maturity of Component Technology

Like all low-emission combustor technology, the catalytic combustor is a relatively new concept. The technology has been explored by both private industry and the federal government. Significant advances in combustion efficiency, operating

range, and component durability have been documented. Further advances in ceramic durability and catalyst technology will aid in improving overall operating durability of the catalytic combustor.

Adaptability to High-Temperature Operation

Catalytic combustion is ideally suited to the high-temperature regenerative gas turbine cycle. The catalyst bed becomes essentially 100 percent efficient at 1350°K (1970°F) and maintains high efficiency up to the point that the substrate fails at approximately 1900°K (2960°F). The combustor can also operate at fuel/air ratios well below the normal lean extinction limit for hydrocarbon fuels.

Ease of Development

The catalytic combustor will be less difficult to develop than other types of lean premixed, prevaporized combustors. The catalyst bed is somewhat standardized by the available fabrication technology of the ceramic manufacturers. The catalyst support and fuel preparation devices are the components which will require concentrated development effort. These devices would be required in some form by any combustor used.

Flexibility of Concept

The current plan is to flow 100 percent of the combustor airflow through the catalyst bed. This limits the operation of the combustor in a pure catalytic mode to conditions at which the combustor exit temperature exceeds 1350°K (1970°F). At temperatures below this level, the combustor becomes inefficient in the catalytic operating mode. A precombustor will be utilized to operate the engine at the idle and very low power end of the operating envelope where temperatures are low.

The design is flexible enough to allow changes to be made in the flow path. If it is found advantageous to bypass some of the combustor airflow around the catalyst bed and inject it as diluent downstream of the catalyst bed to allow the bed to run hotter at higher fuel-air ratio, it can easily be accomplished with the current design.

Precombustor

Over most of the operating range of the IGT engine, the catalytic combustor will operate efficiently with no augmentation. However, at very low power level the combustor inlet and outlet temperature will drop below the range of efficient operation of the catalytic combustor. For this portion of the engine operating range and for starting, a small supplemental diffusion flame pilot combustor will be required. This combustor will be ignited when the outlet temperature of the catalyst bed is below 1340°K (1950°F). The pilot combustor will be designed to operate with primary zone flame temperature below the NO_x formation threshold of 2033°K (3200°F). For the very narrow operating range of the pilot combustor, a lean burning fixed geometry combustor is feasible. The combustor fuel supply can be scheduled to control primary zone temperature based on combustor inlet temperature and airflow rate. The pilot combustor must be designed to operate without exceeding the temperature at which the combustor liner oxidizes rapidly. For current high-temperature alloys, skin temperatures of 1366°K (2000°F) are feasible.

Hydrogen Conversion

A possible alternate method to achieve efficient catalytic combustion at the low temperature idle operating condition is to convert the hydrocarbon fuel to a more reactive hydrogen and carbon monoxide gaseous fuel. The fuel can be converted by a chemical process called reformation. A very rich (five times stoichiometric) fuel-air mixture is passed over a hot nickel catalyst, which causes the fuel to decompose into hydrogen and carbon monoxide. Nitrogen from the air and small quantities of carbon dioxide and unconverted fuel are also found in the converter exhaust products. The converted fuel would then be burned in a small segment of the catalytic combustor using only 14 percent of the total engine airflow. The remaining 86 percent of the air would flow through the combustor unfueled and would be used to dilute the combusted products. This, in effect, is a staging method for a catalytic combustor. The use of the hydrogen converted fuel allows operation at lower inlet temperatures due to the low catalytic ignition temperature of hydrogen. Running with only a small portion of the catalyst bed fueled allows that section of the bed to run at or above the 1350°K (1970°F) minimum temperature for efficient catalytic combustion.

Technology Risk

The technology risk for development of a catalytic combustor is greater than for conventional diffusion flame combustors but only slightly greater than for other non-polluting combustor types. Most low-emission combustors use some form of premixing and prevaporization of the fuel. The catalytic combustor will also require a fuel premixing device. Many lean premixed, prevaporized combustors need a stability augmentation device such as a continuously burning torch to keep the reaction zone burning stably during throttle transients. The catalytic combustor will require a similar device to serve as a precombustor for starting and during low power operation. The catalyst bed is the only part of the combustion system which has a higher development risk than other types of combustors which could be utilized. The catalyst industry has been very active in the research area, and the risk of development for the catalyst bed has been significantly reduced.

Conceptual Limitations

The catalytic combustion system is basically limited by its performance at low temperature. The catalyst does not become sufficiently active to sustain a reaction until a temperature of approximately 700°K (800°F) is reached at the inlet to the catalyst bed. Optimum efficiency is not reached until the outlet temperature reaches 1350°K (1970°F). The low temperature operating characteristics necessitate the use of a pilot burner to provide preheating to start the reaction in the catalyst bed. If the engine cycle is such that at some conditions the combustor outlet temperature will drop below 1350°K (1970°F), the pilot burner may need to be reignited to ensure fast throttle response on demand. High-temperature operation is limited by the properties of the substrate material. The catalyst bed is not cooled; therefore, the substrate must be able to retain its strength and shape at the maximum operating temperature of the engine. Materials such as silicon carbide can operate to temperatures as high as 1900°K (2960°F). The catalytic material may tend to erode off the substrate material at very high temperatures.

However, new catalytic materials such as rare earth oxides and improved wash coat processes are improving the high temperature capabilities. Operation in the 1500°K (2250°F) temperature range presents no problem for current catalyst technology. A 1000-hour durability test using grade 2 diesel fuel was completed at 1316°K (2400°F) by Engelhard Industries.

Driveability

The driveability of a vehicle using a catalytic combustor should present no problems on initial cold start-up. A 10-second warm-up period will be required to bring the catalyst bed up to temperature. Any lean premixed, prevaporized combustor would need a similar warm-up period to allow the recuperator outlet temperature to stabilize. The lean premixed, prevaporized combustor depends on high inlet temperature to expand the flammability limits of the fuel/air mixture.

Backup Combustor Configurations

The lean premixed, prevaporized combustor would be the alternate combustor for the IGT in the event that an insurmountable development problem on the catalytic combustor arises. The technology developed on fuel atomization and prevaporization will be directly applicable to the lean premixed, prevaporized combustor design The development of a variable geometry air metering device for the reaction chamber will be the most difficult task involved with the development of a lean premixed, prevaporized combustor. It is desirable to run the reaction chamber with no liner cooling in order to reduce wall quenching effects which lower combustion efficiency. Ceramic materials will be needed for the reaction chamber since the temperature in the primary zone will be approximately 1900°K (2960°F), which is well above the melting point of nickel or cobalt alloy materials. Combustion stability of the LPP combustor is difficult to achieve, especially in the transient operating mode typical of automotive usage. A method used to aid in stabilization of the LPP combustor is to have a torch or pilot burner discharging into the reaction chamber. If combustion instability causes a flameout, the mixture is reignited by the torch.

The multielement stepped ceramic combustor is the second choice for a back-up combustor configuration. The fuel atomization data acquired in development of a catalytic combustor would not be applicable to a multielement ceramic combustor. The multielement ceramic combustor may present a difficult fuel metering problem. The operating fuel/air ratio limits of the individual flame tubes is quite narrow.

This suggests that the fuel would be staged such that only a limited number of the flame tubes would receive fuel at off-design operating points. As the engine load increased, the fuel flow would start near the lean limit for each flame tube which was receiving fuel. Fuel flow would then increase to the rich limit, at which time another tube would be brought on line and fuel flow to all tubes would return to lean limit flow again.

Summary

The catalytic combustor has been selected as the primary combustor type for the IGT engine for the following reasons:

1. High combustion efficiency
2. Low emissions
3. Good combustion stability
4. Ease of development
5. Good durability
6. Simple variable geometry if required

The catalytic combustor with a precombustor and/or hydrogen converter for starting should meet all requirements for the IGT engine.

RECUPERATOR

The design effectiveness level of the heat exchanger was governed by an acceptable level of pressure loss within the recuperator, system packaging, and manufacturability.

Pressure Loss

The level of pressure loss was determined by carefully balancing the effects of poor flow distribution and performance penalties associated with various levels of pressure loss.

Poor flow distribution can reduce the recuperator effectiveness, but the additional thermal stresses which result from larger material temperature differentials cause more concern since they can easily lead to cracking and leakage. Flow distribution which results in a cold material area is highly undersirable because the cold sections are prone to the deposit of soot. If soot does form, the operating temperatures of the affected material will decrease, which will attract more soot. Once the flow passages become completely blocked, extreme material temperature differentials will create thermal stresses which could cause cracking and leakage.

Poor flow distribution can be improved by increasing the pressure loss within the recuperator or reducing the variations in the kinetic head of the flow as it enters and leaves the heat exchanger. The variations in the kinetic head of the entering and exiting fluid are minimized by using large flow areas and generous turn radii. The axisymmetric flow passage with the annular recuperator will also contribute to good flow distribution.

The pressure loss chosen for the hot side of the recuperator was 7.4 percent at full load, which results in a 2.75 percent loss at the 15 percent power level. The 2.75 percent hot side pressure loss will provide an even hot flow distribution over the face of the recuperator at the low output level to offset the effects of inherent ducting imperfections.

The percentage of pressure loss on the cold side of the recuperator is approximately constant over the full range of operation because the average cold side temperature within the recuperator and the high-pressure turbine inlet flow parameter are nearly constant. The pressure loss on the cold side of the recuperator is 3.0 percent over most of the operating range, and 2.5 percent at the 15 percent power level.

A plot of hot and cold side pressure losses as a function of power output is given in Figure 29. The discontinuity shown in the curves at the 10 percent power level indicates a change in the compressor operating line as the power turbine nozzle opens to reduce TIT.

A lower pressure loss could have been selected for both the hot and cold flows to show a theoretical improvement in performance, assuming that an even flow distribution would occur. The option of using the higher selected levels of pressure loss will assure an even flow distribution and increase the durability of the recuperator.

System Packaging and Manufacturability

The volume of the heat exchanger is controlled by the required heat transfer surface area, hydraulic diameter, and porosity. The hydraulic diameter will strongly influence the overall size of the heat exchanger. The minimum allowable hydraulic diameter is controlled by the fouling and plugging tendencies of the passages and by the mechanical processes which are available to manufacture the product. The fouling and plugging limits on hydraulic diameter are controlled by the efficiency of the burner and the operating temperature of the heat exchanger material. The automotive emission standards strictly limit the allowable amounts of unburnt hydrocarbons, which tend to form soot in the heat exchanger. However, the cycle operating temperatures are elevated at part-load, which will tend to burn away the carbon deposits.

The material type selected for the recuperator is ceramic instead of metallic. A ceramic construction allows the engine to maintain high gasifier inlet temperatures at part power. This is necessary to obtain low specific fuel consumptions.

The minimum flow path dimension for a ceramic core was set at 0.381 mm (0.015 inch), which results in a hydraulic diameter of 0.5867 mm (0.0231 inch) for the selected matrix configuration. Figure 30 illustrates a typical matrix configuration section in the counter-flow area of the recuperator. This level of hydraulic diameter is comparable to those successfully used in current regenerators. The technology for manufacturing small hydraulic diameter with sufficient accuracy is currently available.

The material thickness used in the heat exchanger will also be influential in determining the area-to-volume ratio and the porosity of the recuperator because of the relatively small hydraulic diameter. The minimum allowable material thickness for a mass-produced heat exchanger is limited by the requirement of low-cost manufacturability. Ceramic recuperators can be made with material thicknesses down to 0.0762 mm (0.003 inch) using low-production methods which may be considered unpractical for the automotive volume requirements. The anticipated range of practical material thickness is 0.127 to 0.178 mm (0.005 to 0.007 inch).

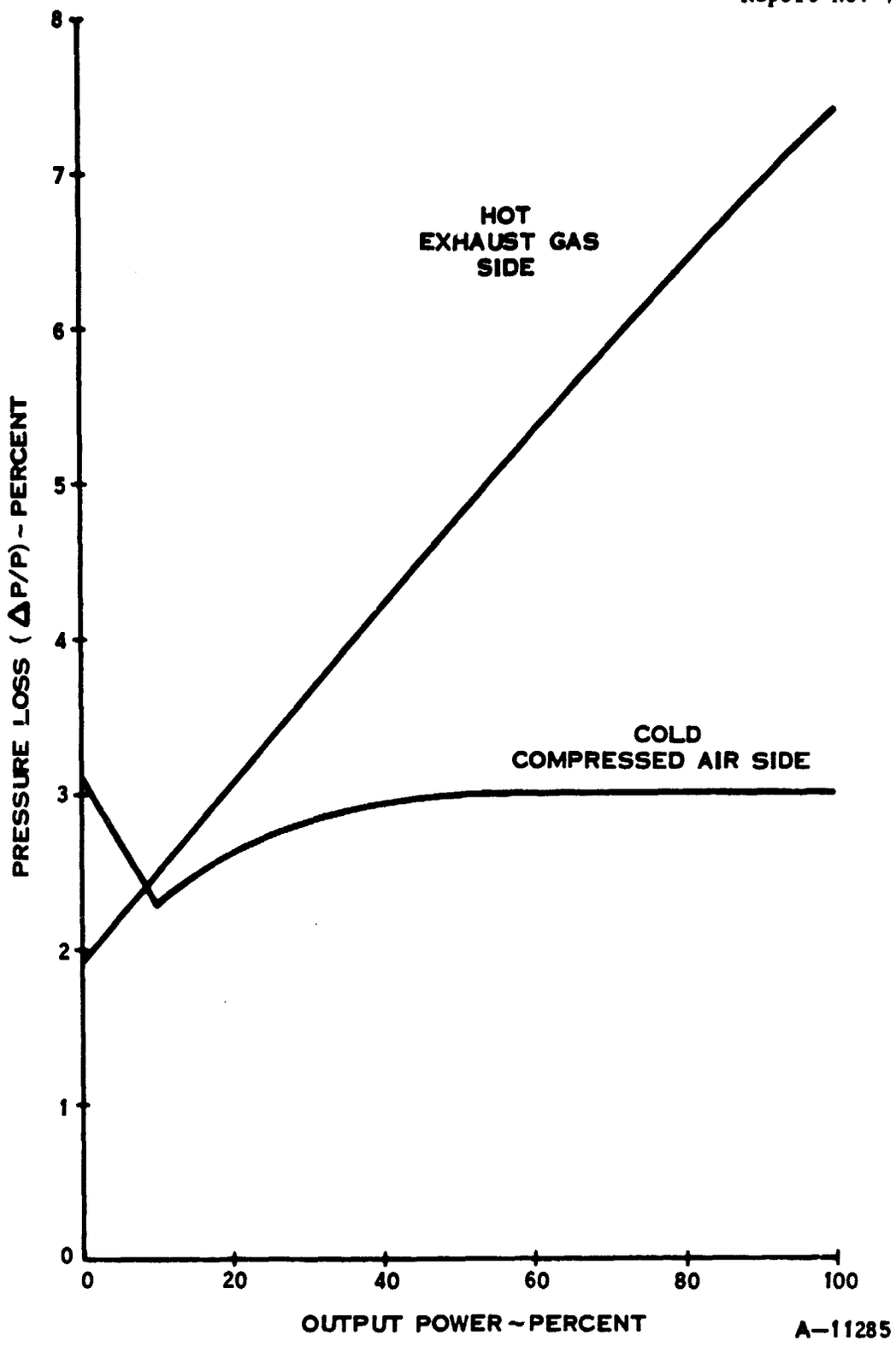

Figure 29. Hot and Cold Side Pressure Losses

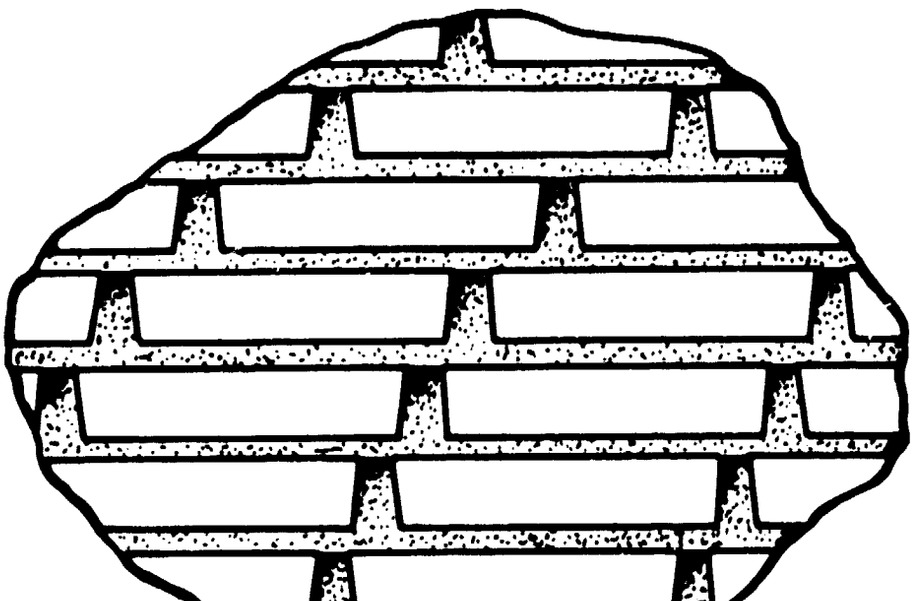

A—11201

Figure 30. Typical Matrix Configuration Section

The frontal area and length of the heat exchanger are essentially defined as a function of effectiveness, since the design levels of pressure loss, hydraulic diameter, porosity, heat transfer surface-area-to-volume ratio, and material type and thickness have been established. A plot of frontal area and length versus effectiveness is given in Figure 31 for a counterflow heat exchanger with a "Z" flow path configuration on the cold, high-pressure side.

The shape of the heat exchanger could be rectangular or annular, as illustrated in Figure 32. The rectangular configuration can be remotely mounted from the engine, which could offer some packaging advantages. The annular configuration has the advantage of drastically reducing the volume and mass of the manifolds and ducts. The annular configuration also offers an inherent even flow distribution which must be obtained for high effectiveness, especially at part-load.

2.2 POWERTRAIN PERFORMANCE ANALYSIS

The powertrain concepts that were specified for detailed study during Task II are summarized as powertrain concepts 1 through 10 in Table IX.

Powertrain concept No. 1 is the dual-rotor engine with free power turbine. The engine has a two-stage centrifugal compressor and two-stage axial flow turbine, using a variable power turbine nozzle to control turbine inlet temperature. The ceramic recuperator and the catalytic combustor are used. The drivetrain uses the conventional three-speed automatic transmission, with accessories gear-driven from the gasifier rotor.

Powertrain concept No. 2 is the same as concept No. 1 except for slip clutch power transfer to control turbine inlet temperature in place of the variable power turbine nozzle. Shaft power is taken from the gasifier rotor and transferred to the output shaft, forcing the gasifier turbine to run at a higher inlet temperature. Clutch slipping permits power transfer over a range of rotor speeds.

Powertrain concept No. 3 is the same as concept No. 1 except for the axial-centrifugal compressor in place of the two-stage centrifugal compressor.

Powertrain concept Nos. 4 through 8 are the same as concept No. 1 except for different compressor pressure ratio and turbine inlet temperature.

Powertrain concept No. 9 is a single-rotor engine, using the same aerodynamic components as concept No. 1. The accessories are gear-driven from the reduction geartrain, with a hydromechanical variable ratio transmission for the drivetrain.

Powertrain concept No. 10 is the same as concept No. 8 except for the ceramic rotary regenerator as an alternate heat exchanger in place of the ceramic recuperator.

POWERTRAIN PERFORMANCE ANALYSIS PROCEDURE

The performance analysis of each engine began with the conceptual definitions such as component selections, overall pressure ratio, turbine inlet temperature and type of temperature control. From this the design point characteristics of

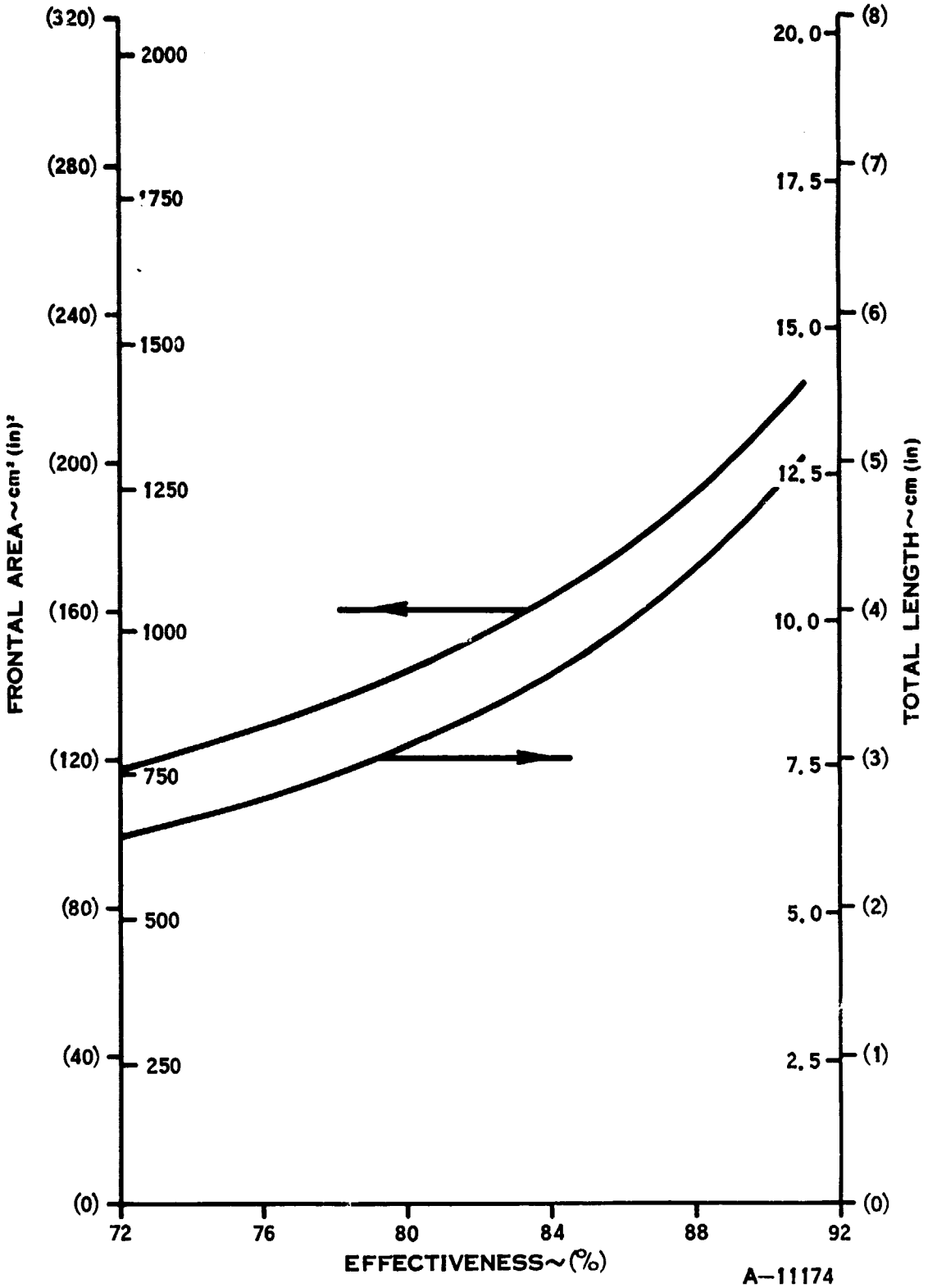

Figure 31. Frontal Area and Length versus Effectiveness, Counterflow Heat Exchanger

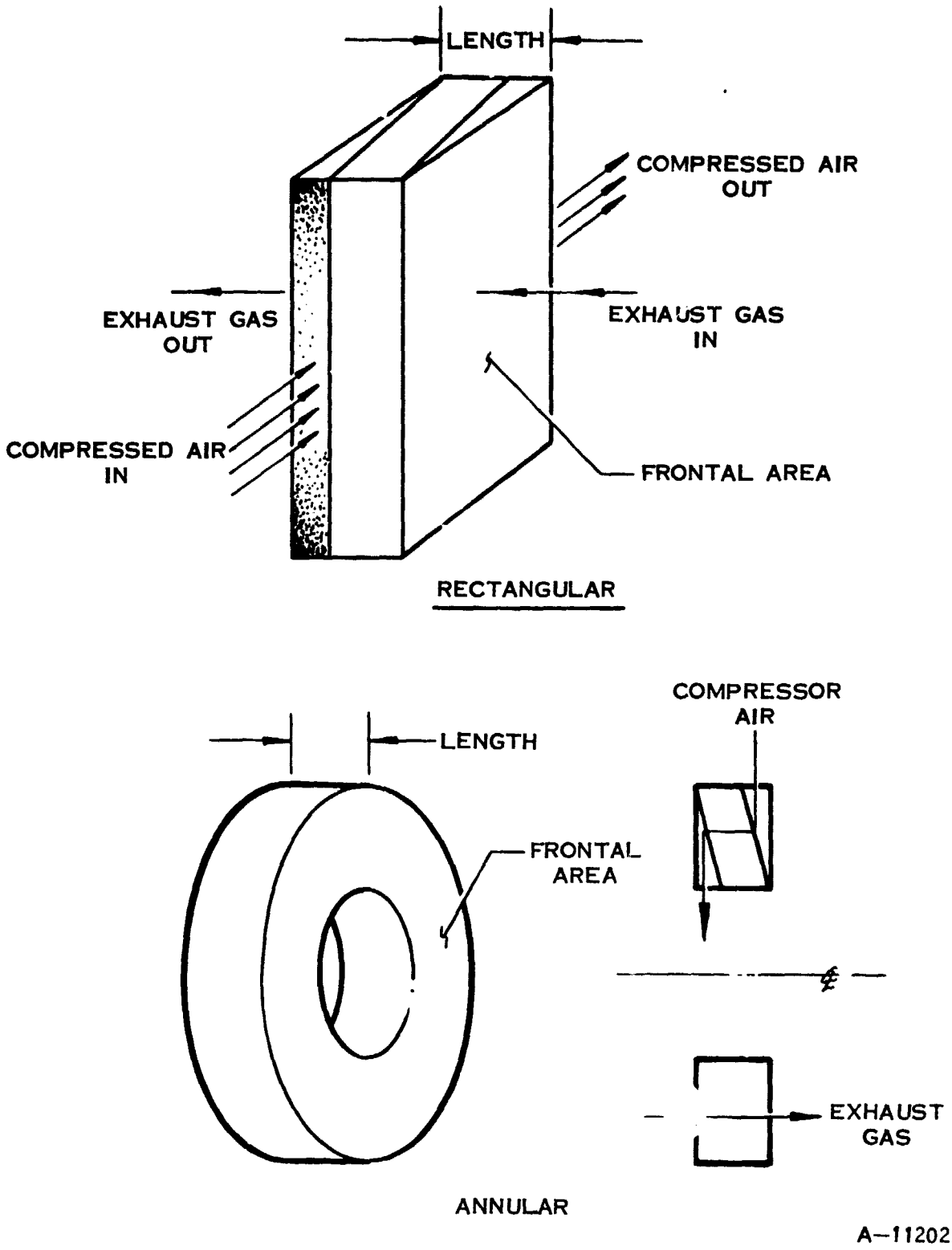

Figure 32. Rectangular and Annular Heat Exchanger Configurations

TABLE IX. POWERTRAIN CONCEPTS

POWERTRAIN CONCEPT NO.	1	2	3	4	5	6	7	8	9	10
TURBINE INLET TEMPERATURE	2250°F					1900°F	2500°F	2100°F	2250°F	2100°F
TIT CONTROL	VARIABLE PT NOZZLE	SLIP CLUTCH POWER TRANSFER	VARIABLE POWER TURBINE NOZZLE						VARIABLE RATIO TRANSMISSION	VARIABLE PT NOZZLE
COMPRESSOR	TWO-STAGE CENTRIFUGAL		AXIAL CENTRIFUGAL	TWO - STAGE CENTIFUGAL						
COMPRESSOR PRESSURE RATIO	5.00			5.58	6.21	4.74	6.00	5.28	5.58	5.27
HEAT EXCHANGER	ANNULAR RECUPERATOR									ROTARY REGENERATOR
ROTOR SYSTEM	TWO SHAFT FREE POWER TURBINE								SINGLE SHAFT	TWO SHAFT FREE TURBINE

A-11997

the engine were evaluated. Compressor characteristics were obtained from the Task II analysis. Leakage, heat losses, bearing losses, duct losses, and other secondary effects were based on past experience and published literature. These secondary effects are defined in the following performance analysis assumptions. The values assigned to these parameters were then used in the design point program.

The design point program takes all of the operating parameter design values and calculates the engine design point performance. It calculates the conditions at each station using thermodynamic energy and continuity balance relationships. The steady-state operating point is found by balancing the total work demand on each rotor. The program prints the performance based on an inlet flow of 0.45 kg/s (1.0 lbm/s); from this, all of the information needed to run the partload engine simulation program is calculated. Component map scalars, flow loss coefficients and so on, are found by scaling the design point performance to the required output power. The recuperator has its own design point program which provides the physical dimensions that the part-load program uses to simulate the recuperator. Once the scalars and coefficients are calculated, the part-load program is used to simulate the engine. When all of these inputs plus the component performance maps are fed into the part-load program, the program can duplicate the scaled design point program performance.

The part-load engine simulation calculates engine performance over a wide range of operating conditions. Internally, the program works like the design point program except it matches compressor and turbine maps in an iterative process. However, the basic thermodynamic operations are the same. Where the design point program uses an input value for each parameter, the part-load program uses a mathematical model to predict the operating characteristics at any point. The assumptions used for this modeling of the engine hardware are explained in the following section.

Most of the engines studied used a variable power turbine nozzle for controlling turbine inlet temperature. This was modeled by using a turbine performance map that was input as a function of nozzle area and required no special treatment in the program. However, some of the concepts selected required special modeling.

Powertrain concept 2 incorporated a slipping clutch as a means of controlling turbine inlet temperature. To model this, it was assumed that the mechanical efficiency of the power transfer system was equal to the speed ratio of the two clutch disks, with power transferred only from the faster-moving disk to the slower-moving disk.

Another engine that required special treatment was powertrain concept 4A. This engine used 2 percent of its inlet airflow for cooling the high-pressure turbine rotor. To model the effects of this cooling on engine performance, two assumptions were made. First, the high pressure turbine efficiency was reduced by 1 percent to account for cooling effects and second, the cooling air was assumed to mix completely with the high-temperature gas between the two turbine stages.

For the single-rotor engine, powertrain concept 9, the power characteristic was based on the fixed design point nozzle area, and the power turbine rotor was forced to run at the same speed as the gasifier rotor.

POWERTRAIN PERFORMANCE ANALYSIS ASSUMPTIONS

A schematic diagram of the engine arrangements analyzed is shown in Figure 33, with the stations used for performance analysis shown.

A. Ambient total pressure and temperature.

Ambient pressure = 99.526 kPa (14.435 psia) 152.4 m (500 ft altitude).
Ambient temperature = 303°K (85°F, 545°R).

B. Inlet system pressure drop.

The inlet system pressure ratio at 100 percent power varied from 0.990 to 0.994. For all the engines, the inlet loss at part-load was proportional to the velocity head.

C. Compressor design point efficiency and the method of generating off-design performance.

The compressor design point efficiency levels and the off-design performance were obtained by considering individually the axial and centrifugal compressor requirements.

The axial compressor efficiency potential was obtained from the information in Reference 18. These data include the effects of stage loading, size, and tip clearance. The levels from this source were then tempered, based on WRC experience in low-cost compressor technology. The total-to-static off-design compressor map was obtained by direct scaling of the WR33 compressor total-to-total efficiency and pressure ratio to meet the design point requirements. A moderate level of diffuser recovery (Cp = 0.65) was assumed to convert to the total-to-static map presented in the analysis.

The centrifugal compressor design point total-to-total efficiency was estimated based in the data in Reference 19. It was assumed that the appropriate exit Mach number was 0.2 for these data to obtain the total-to-static design point efficiency. The off-design compressor performance map was estimated based on the analysis of range and speed versus flow characteristics of similar compressors. These data are available in the published literature and through extensive WRC experience.

For compressor configurations requiring considerable matching efforts, such as the axial-centrifugal combination and the two-stage centrifugal, the overall performance maps were calculated by a direct combination of the appropriate maps.

D. Compressor bleed flows, bleed flow paths, and percent flow to each path.

One percent of inlet airflow leakage was removed from the compressor discharge to the atmosphere to represent the combined effects of shaft seal leakage, static seal leakage, and cooling airflow.

E. Pressure drop associated with each transition section and/or duct in the system.

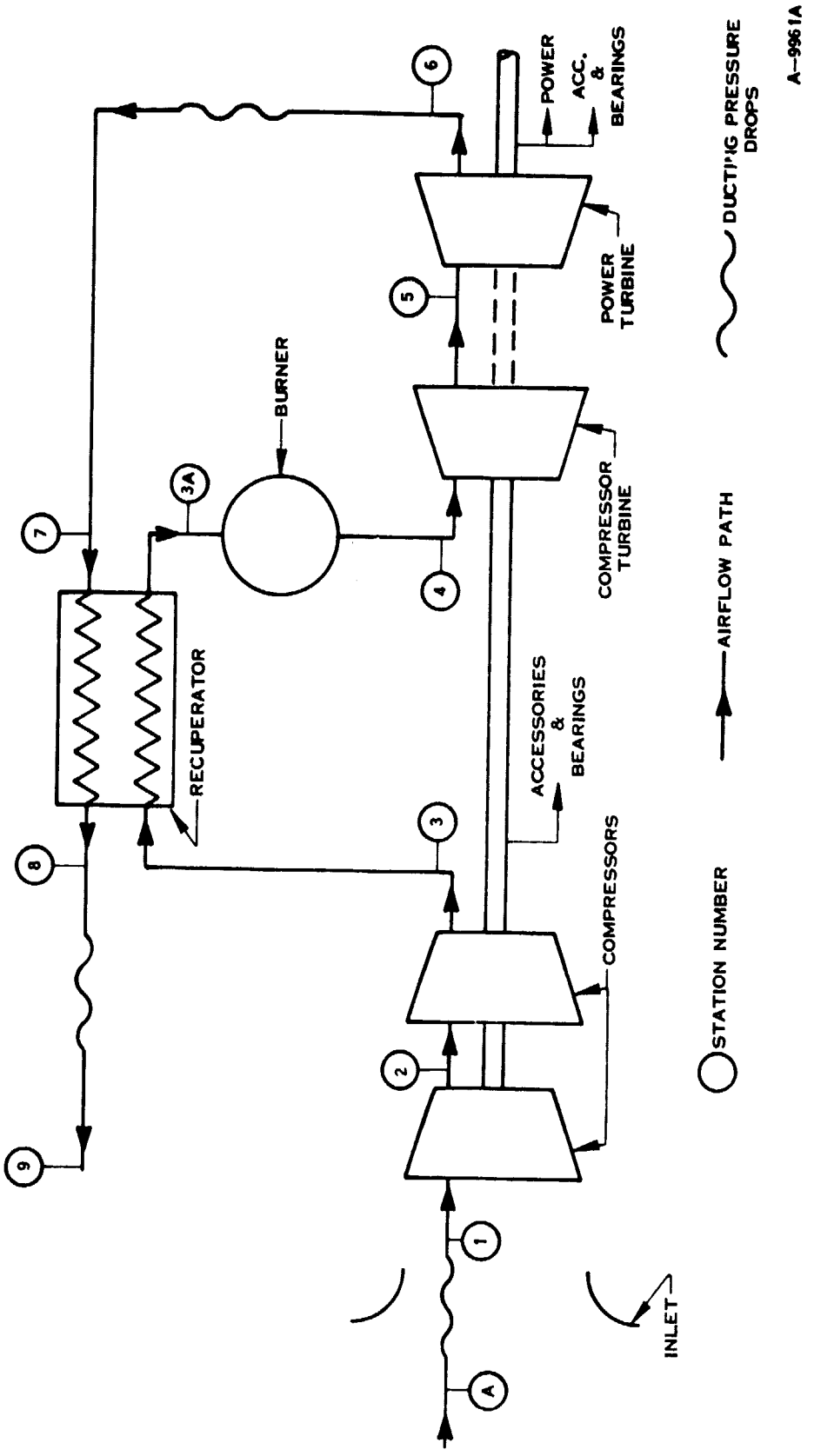

Figure 33. Engine Schematic Diagram with Station Identification

1. The inlet system pressure drop is covered in item B.

2. The pressure drop for the ducting to and from the cold side of the recuperator is included in the recuperator pressure loss, item G.

3. The power turbine diffuser is covered in item M.

4. The hot side recuperator manifolding is included in the recuperator pressure loss item G.

5. The exhaust system pressure ratio at 100 percent power varied from 0.990 to 0.994. The part-load exhaust loss was proportional to the velocity head.

F. Combustor efficiency and pressure drop on and off design.

The combustor efficiency was assumed to be 0.998 at all conditions. The combustor pressure ratio was 0.970 at 100 percent power, and at part-load, the pressure loss was proportional to the combustor inlet velocity head.

G. Heat exchanger effectiveness and pressure drop on and off design.

The effectiveness of a fixed geometry counterflow heat exchanger is derived from equation 1 if the capacity ratio is not equal to unity.

$$(1)\quad \text{EFFECTIVENESS} = (1 - X)\ \frac{1 - e^{-NTU\ (1\ -\ C_{min}/C_{max})}}{1 - (C_{min}/C_{max})\ e^{-NTU\ (1\ -\ C_{min}/C_{max})}}$$

and

$$X = (0.73 - 5.2 \times 10^{-8}\ NTU^{4.55})\ [A\ frontal\ (1\text{-}POR)\ K/(L\ C_{min})]^{0.975}$$

where

$NTU = UA/C_{min}$ - number of transfer units

U - overall heat transfer coefficient

A - heat transfer area

$C_{min} = (W\ Cp)\ min$ - minimum fluid capacity rate

$C_{max} = (W\ CP)\ max$ - maximum fluid capacity rate

W - mass flow

Cp - gas specific heat

X - correction factor for axial conduction

A frontal - frontal area

POR - porosity

K - material conductivity

L - heat transfer length

If the capacity ratio is equal to unity, effectiveness is defined by equation (2).

$$(2)\quad \text{EFFECTIVENESS} = (1 - X)\frac{NTU}{NTU + 1}$$

The overall heat transfer rate was related to individual heat transfer coefficients by equation (3).

$$(3)\quad U = \frac{1}{\left(\frac{1}{h_h} + \frac{\Delta X}{K} + \frac{1}{h_c}\right)}$$

where

h_h - hot side heat transfer coefficient

ΔX - material thickness

K - material conductivity

h_c - cold side heat transfer coefficient

The heat transfer coefficients were defined by equation (4).

$$(4)\quad h = a\,\frac{K_g}{D_H}\left(\frac{W D_H}{A_F \mu}\right)^b Pr^{0.4}$$

where

a - constant depending on core configuration

K_g - gas conductivity

D_H - hydraulic diameter

A_F - flow area

μ - viscosity

Pr - Prandtl number

b - constant depending on core configuration

It can be seen from the above equations that the effectiveness of a fixed geometry heat exchanger is primarily a function of mass flow. The physical properties of the fluids also influence effectiveness, and they are controlled by temperature.

The pressure drop of the gas flow through the heat exchanger is calculated from equation (5).

$$(5) \quad \Delta P = C_D + \frac{f\,L}{D_H} \quad \frac{\rho\,V^2}{2\,g\,P}$$

where

ΔP - pressure drop

P - inlet pressure

C_D - loss coefficient

$f = a + b\,Re^c$ - friction factor

a, b and c - friction factor coefficients depending on core matrix

Re - Reynolds number

L - core length

D_H - hydraulic diameter

ρ - density

V - velocity

g - gravitation constant

H. Heat exchanger leakage and leak paths over the range of operation.

Zero leakage was assumed for the recuperator. A leakage of 4 percent of inlet airflow was assumed for the rotary regenerator (Engine 10) at 100 percent power. At part-load, the regenerator leakage was calculated assuming a constant leakage area.

I. Total pressure drop from burner to turbine.

This pressure drop is part of the combustor pressure drop, item F.

J. Turbine inlet temperature (TIT) and station definition.

The TIT ranged from 1311°K (1900°F) for Engine 6 to 1644°K (2500°F) for Engine 7. TIT was defined at station 4.

K. Turbine efficiency and the method for predicting off-design performance.

Turbine efficiencies were based on total-to-total turbine pressure ratio.

Axial turbine off-design performance was based on programs developed by Williams Research Corporation in cooperation with Dr. John Stanitz. The axial turbine methods include a loss assessment based on the works of Ainley and Mathieson (Reference 20) and the improved models of Dunham and Came (Reference 21).

L. Turbine total pressure ratio, inlet total to rotor exit total.

Turbine total pressure ratio varied from 4.02 for Engine 6 to 5.09 for Engine 5. The turbine total pressure ratio was based on the ratio of inlet total pressure to rotor exit total pressure.

M. Turbine diffuser total pressure drop.

The turbine diffuser total pressure ratio ranged from 0.965 to 0.976 at 100 percent power, based on a pressure recovery coefficient Cp = 0.76. At part-load, the pressure loss changed proportionately to the diffuser inlet velocity head.

N. Exhaust duct Mach number at design point.

The exhaust duct Mach number at 100 percent power for Engine 8B was 0.31 at the hub and 0.45 at the tip with an average of 0.4. A Mach number of 0.4 was assumed for the turbine diffuser performance estimate. All of the engines had similar exhaust duct Mach numbers.

O. Engine system and reduction gear moment of inertia.

1. The engine system moment of inertia changed throughout the study.

For the driving cycle studies, the gasifier rotor inertia was 0.000482 Nm/s^2 (0.00427 $in\text{-}lb/s^2$) for Engines 4, 6, and 9. All the others used 0.0011 Nm/s^2 (0.0097 $in\text{-}lb/s^2$). The inertia value of 0.0011 Nm/s^2 (0.0097 $in\text{-}lb/s^2$) was used for the gasifier acceleration study. The power turbine rotor inertia used was 0.00075 Nm/s^2 (0.0066 $in\text{-}lb/s^2$).

2. The reduction gear moment of inertia was neglected. The effect was small compared to the engine rotor inertias due to the slower rotating speeds of the gears.

P. Engine accessory loads, parameter losses over the operating range, and which shaft they are run off.

1. The engine and vehicle accessories loads are shown in Figures 34 and 35. Figure 34 shows the accessories for all the engines except 8A and 8B. Figure 35 shows the accessories for 8A and 8B. The only difference was in the

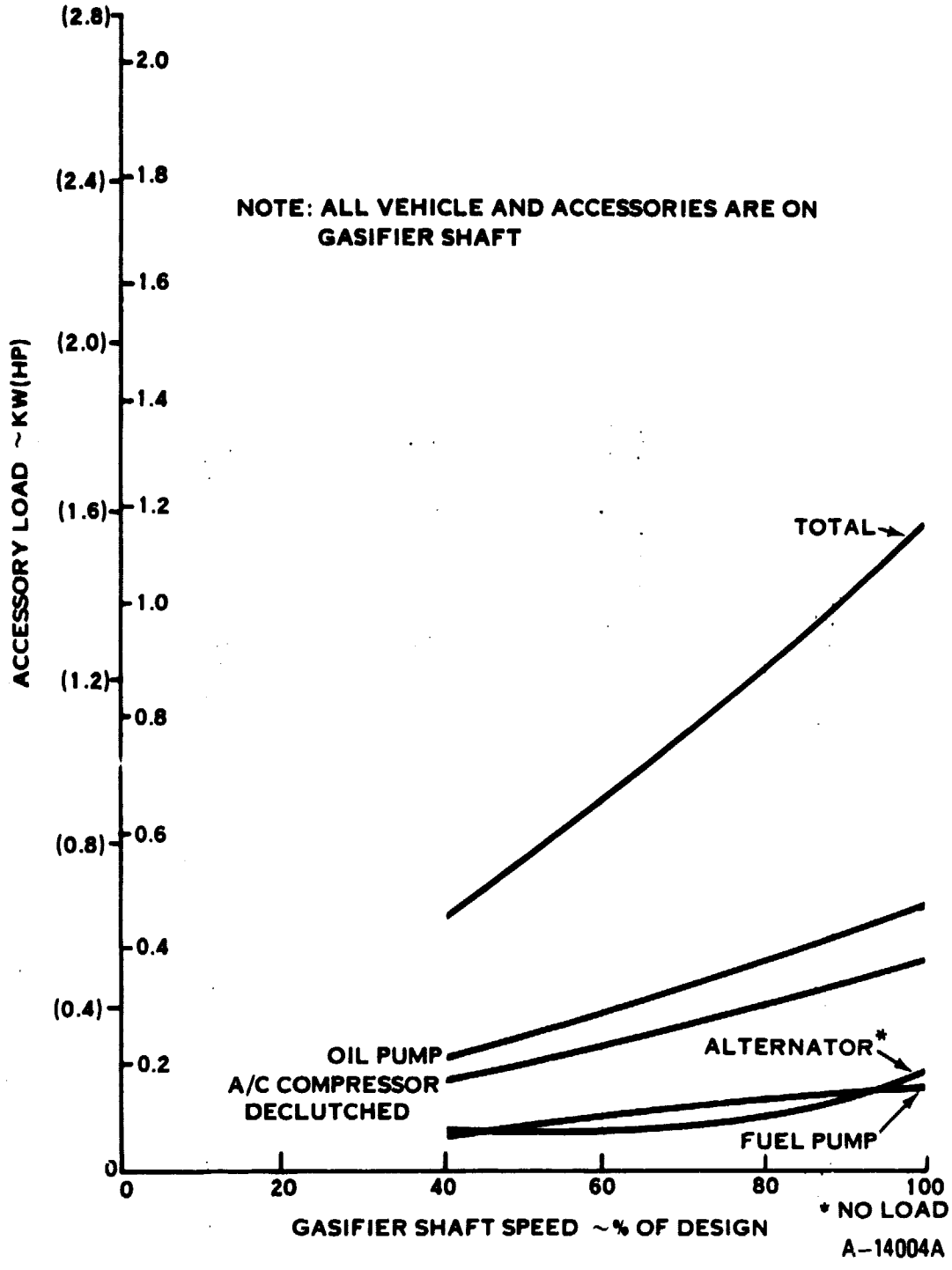

Figure 34. Accessory Loads versus Gasifier Shaft Speed, Engine 1-10, 4A

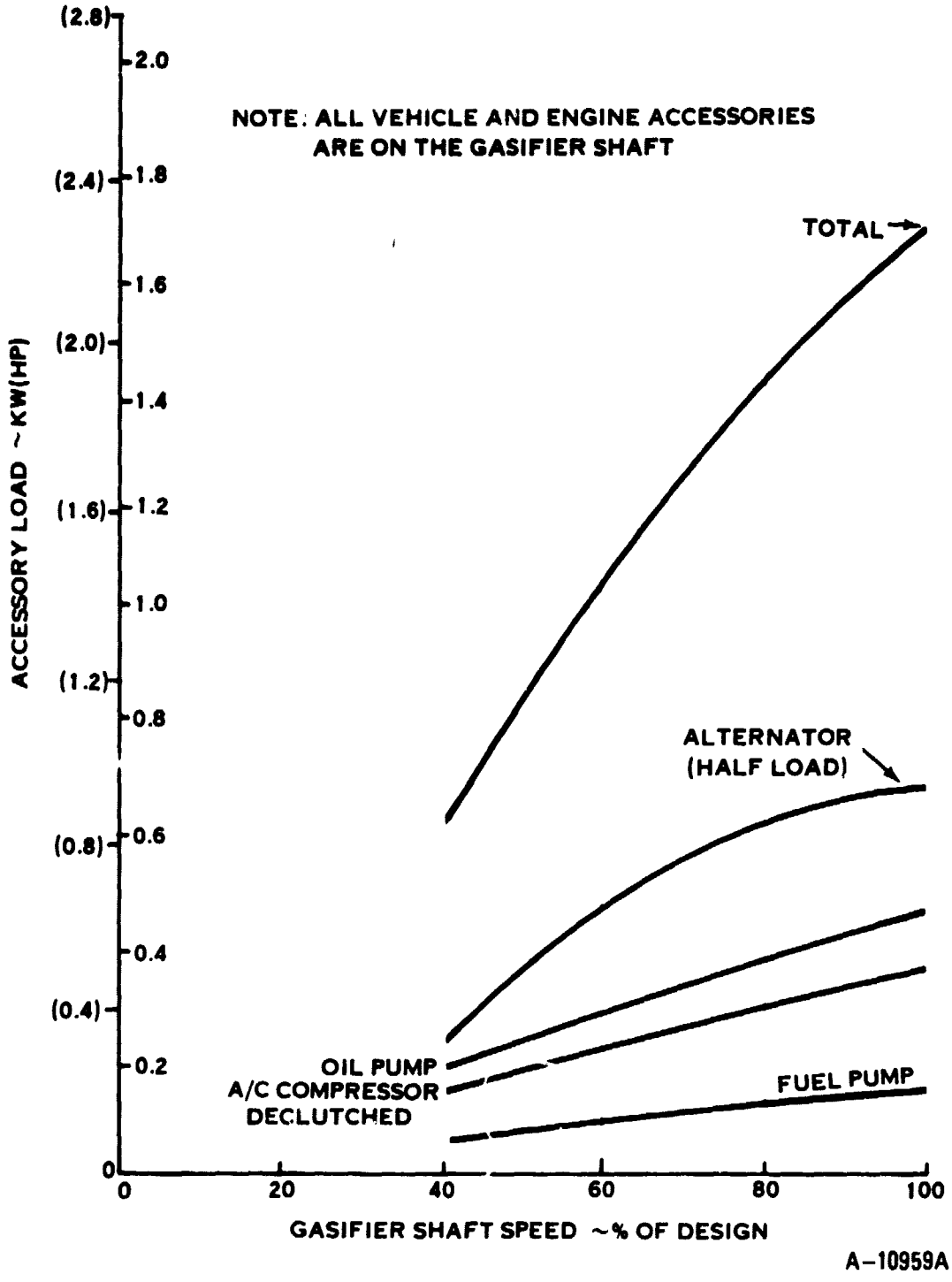

Figure 35. Accessory Loads versus Gasifier Shaft Speed, Engines 8A and 8B

alternator curve. Engines 8A and 8B used an alternator under half load and all the other engines used an alternator under no load. All accessories were driven from the gasifier rotor.

2. The bearing losses are shown in Figure 36.

3. The reduction gear loss was assumed to be 2 percent of the input power for all conditions. This loss was handled in the driving cycle analysis and was not included in the engine tabulations except for Engines 8A and 8B. The data listed for the rest of the engines show performance with no reduction gear loss; Engines 8A and 8B show performance with the reduction gear loss included.

Q. Engine system design power and design philosophy.

1. All of the study engines were designed to or scaled to a 74.6 kW (100 hp) output except for Engine 8B. Engine 8B had a design power level of 54.8 kW (73.5 hp).

2. The design philosophy is twofold:

a. Reduce the engine SFC by optimizing the components and cycle at a part load condition; and

b. Reduce the engine fuel consumption by minimizing the engine design power consistent with the acceleration requirements.

R. Idle fuel flow was determined differently for each of the four main engine configurations. For the dual-rotor engine with power transfer, idle occurred at a 50 percent gasifier rotor speed with the power turbine at zero speed and no power transferred between shafts. For the dual-rotor engine with a variable power turbine nozzle, idle occurred at a 50 percent gasifier rotor speed with the power turbine at zero speed and the nozzles opened to 140 percent of design area Idle fuel flow for the single-rotor engine occurred at a 50 percent rotor speed.

Deceleration fuel flow was assumed to be the same as idle fuel flow.

S. Fuel properties

LHV = 44194 kJ/kg (19,000 Btu/lbm) = 31493 kJ/l (113,000 Btu/gal)
Fuel density = 0.7126 kg/l (5.947 lbm/gal)

POWERTRAIN PERFORMANCE ANALYSIS

The powertrain performance analysis was organized to select the cycle parameters and the powertrain concept. Table X shows how the powertrain concepts, Table IX, were analyzed and compared in sequence, with the selections made at each step. The first choice was the variable power turbine nozzle versus the slip clutch power transfer for turbine inlet temperature control, using 1505°K (2250°F) turbine inlet temperature and a compressor pressure ratio of 5. The second choice was the two-stage centrifugal compressor versus the axial-centrifugal compressor. The third choice was overall compressor pressure ratio, using compressors with nominal design point pressure ratios of 5.0, 6.0, and 7.0.

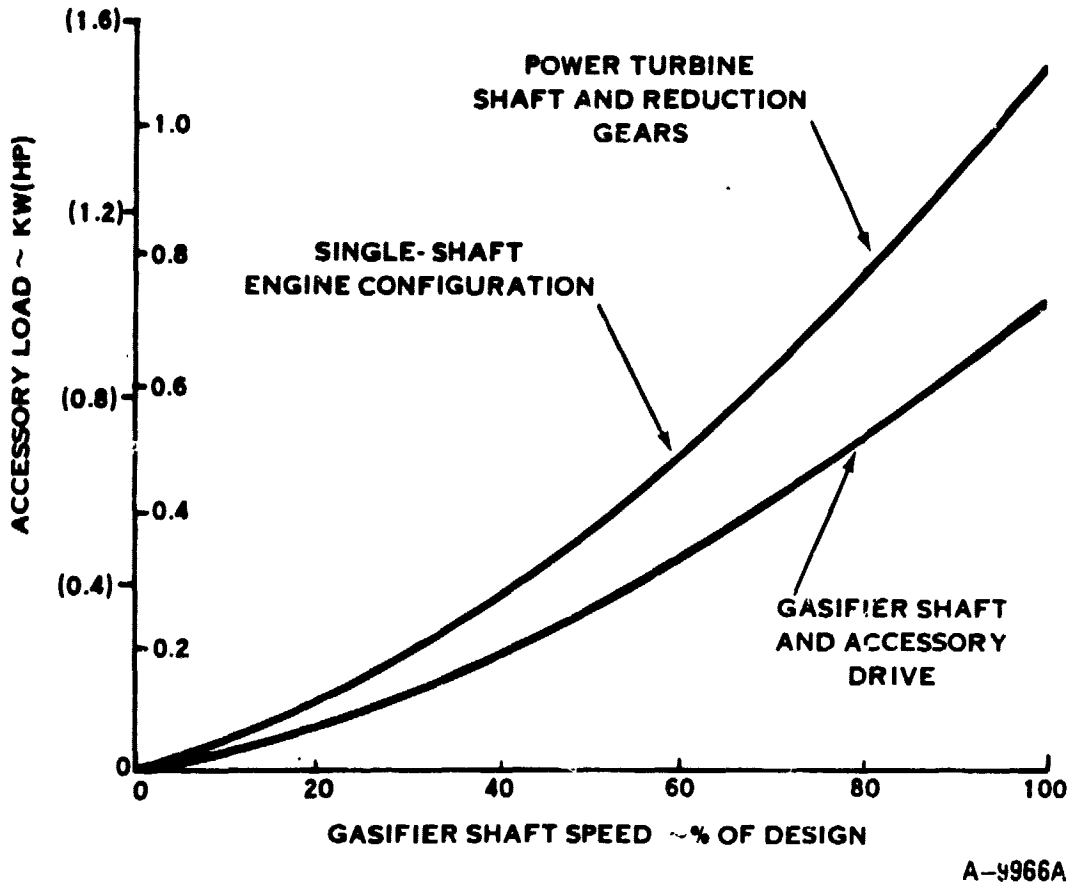

Figure 36. Bearing Power Losses versus Shaft Speed

TABLE X. IGT CONCEPT SELECTION (SHEET 1 OF 2)

A. Turbine Inlet Temperature Control Selection.

TIT - 1505°K (2250°F)
Compressor - Two-stage centrifugal
Compressor pressure ratio - 5.0

Engine	TIT Control
1	Variable power turbine nozzle
2	Slip clutch power transfer

B. Compressor Selection.

TIT - 1505°K (2250°F)
TIT control - variable PT nozzle
Compressor pressure ratio - 5.0

Engine	Compressor
1	Two-stage centrifugal
3	Axial - centrifugal

C. Compressor Pressure Ratio Selection.

TIT - 1505°K (2250°F)
TIT control - variable PT nozzle
Compressor - Two-stage centrifugal

Engine	Compressor Pressure Ratio
1	5.0
4	6.0
5	7.0

D. TIT Comparison

TIT control - variable PT nozzle
Compressor - Two-stage centrifugal
Compressor pressure ratio - 6.0

Engine	TIT
4	1505°K (2250°F)
4A	1505°K (2250°F) with turbine cooling
6	1311°K (1900°F)
7	1644°K (2500°F)
8	1422°K (2100°F)

C-2

TABLE X. IGT CONCEPT SELECTION (SHEET 2 OF 2)

E. Rotor System Comparison

TIT - 1505°K (2250°F)
Compressor - Two-stage centrifugal
Compressor pressure ratio - 5.58

Engine	Rotor System	TIT Control
4	Dual	Variable PT nozzle
9	Single	Variable ratio transmission

F. Heat Exchanger Comparison

TIT - 1422°K (2100°F)
TIT control - variable PT nozzle
Compressor - Two-stage centrifugal
Compressor pressure ratio - 5.28

Engine	Heat Exchanger
8	Rotary regenerator
10	Annular recuperator

The choices up to this point were based primarily on specific fuel consumption at low power. The comparisons that followed required vehicle driving cycle analysis to evaluate the effect on fuel economy and life cycle cost. These included the effect of turbine inlet temperature, using 1311°K (1900°F), 1422°K (2100°F), 1505°K (2250°F), and 1644°K (2500°F), with the effect of additional turbine cooling air at 1505°K (2250°F). A comparison of the single-rotor and dual-rotor systems was then made, followed by a heat exchanger comparison, the rotary regenerator versus the annular recuperator.

Tables XX through XLV in Appendix A summarize the performance of each powertrain at 100, 50, and 10 percent power and at idle.

Turbine Inlet Temperature Control Selection. Two methods of controlling turbine inlet temperature are compared in Figure 37, Engine 1 with variable power turbine nozzle and Engine 2 with slip clutch power transfer, both at 1505°K (2250°F) TIT and a compressor pressure ratio of 5. The driving cycle power requirement is below 50 percent, so the variable power turbine nozzle is the obvious choice for fuel economy. It also has good control response, with direct control of output shaft torque at any engine condition. It can assist starting and gasifier acceleration, and provides adequate engine braking. The SFC with the slip clutch is shown in Figure 38, along with the power being transferred from the gasifier rotor and the corresponding mechanical efficiency of the clutch. Characteristics of an ideal power transfer system with 100 percent efficiency are also shown as reference. The speed ratio for the clutch was set up to provide turbine temperature control at maximum power with about 3 kW (4 hp) transferred. This should provide for variation in production engine due to tolerances. The power transfer system can provide more engine braking by locking up the clutch, but this system lacks the flexibility that the variable nozzle provides.

Compressor Selection. Figure 39 compares the two-stage centrifugal compressor, Engine 1, with the axial-centrifugal compressor, Engine 3. The comparison is made at an overall pressure ratio of 5.0, using the variable power turbine nozzle to hold 1505°K (2250°F) TIT. Here the difference in SFC is much smaller, favoring the higher efficiency axial compressor. However, the performance of the compressor in the engine depends greatly on the matching, how the operating lines fall on the compressor map, and how the characteristics, particularly efficiency, change. The matching must also provide adequate surge margin at any expected steady-state or transient condition. Analysis cannot define these detailed matching characteristics with the precision required for comparison and selection. It is proposed that both types of compressors be developed as components until the detailed characteristics can be thoroughly defined and compared before making the final selection.

Compressor Pressure Ratio Selection. Figure 40 shows the initial comparison at nominal overall compressor pressure ratios of 5.0, 6.0, and 7.0 of Engines 1, 4, and 5, using the two-stage centrifugal compressor with variable power turbine nozzle to hold 1505°K (2250°F) TIT. Engines 4 and 5 have gone past the power peak, with higher SFC and shorter life. These engines were then backed off in speed and pressure ratio to 5.58 and 6.21. This final comparison in Figure 41 shows that Engine 4 with 5.58 pressure ratio has slightly better specific fuel consumption than the other two; 2 percent better at 10 percent power, Tables XX,

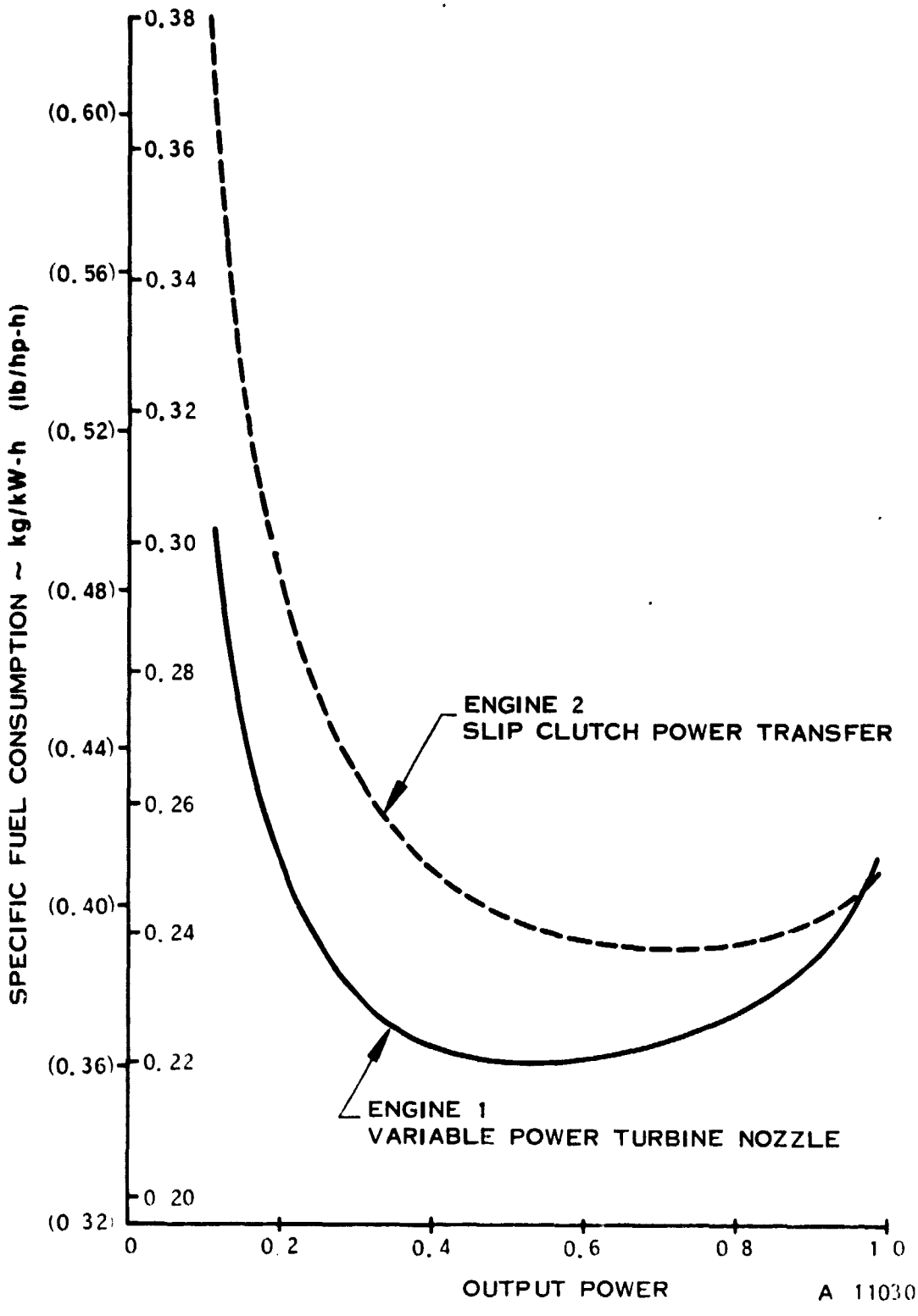

Figure 37. Comparison of SFC Between Two Methods of Controlling TIT

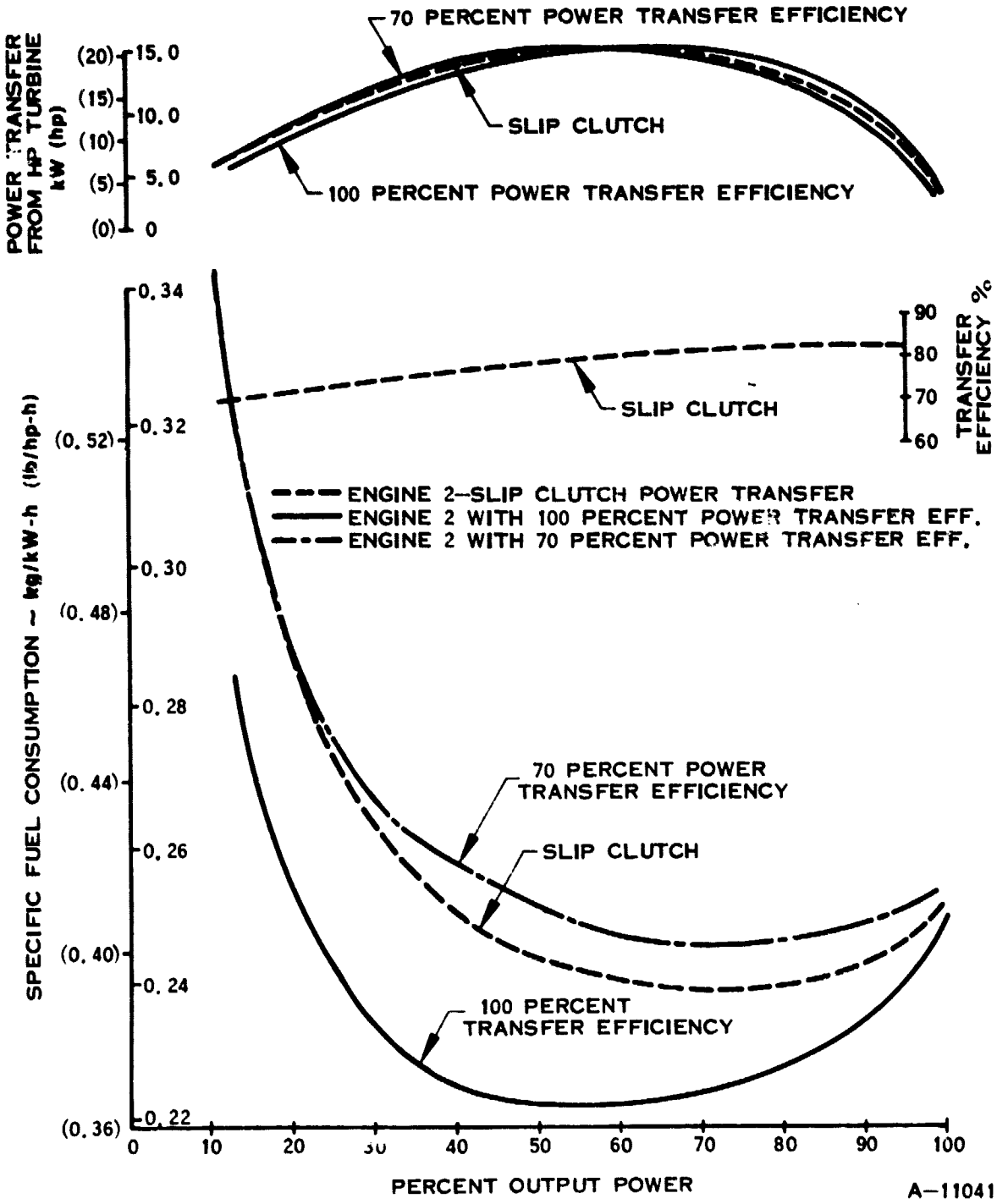

Figure 38. Power Transfer Comparison

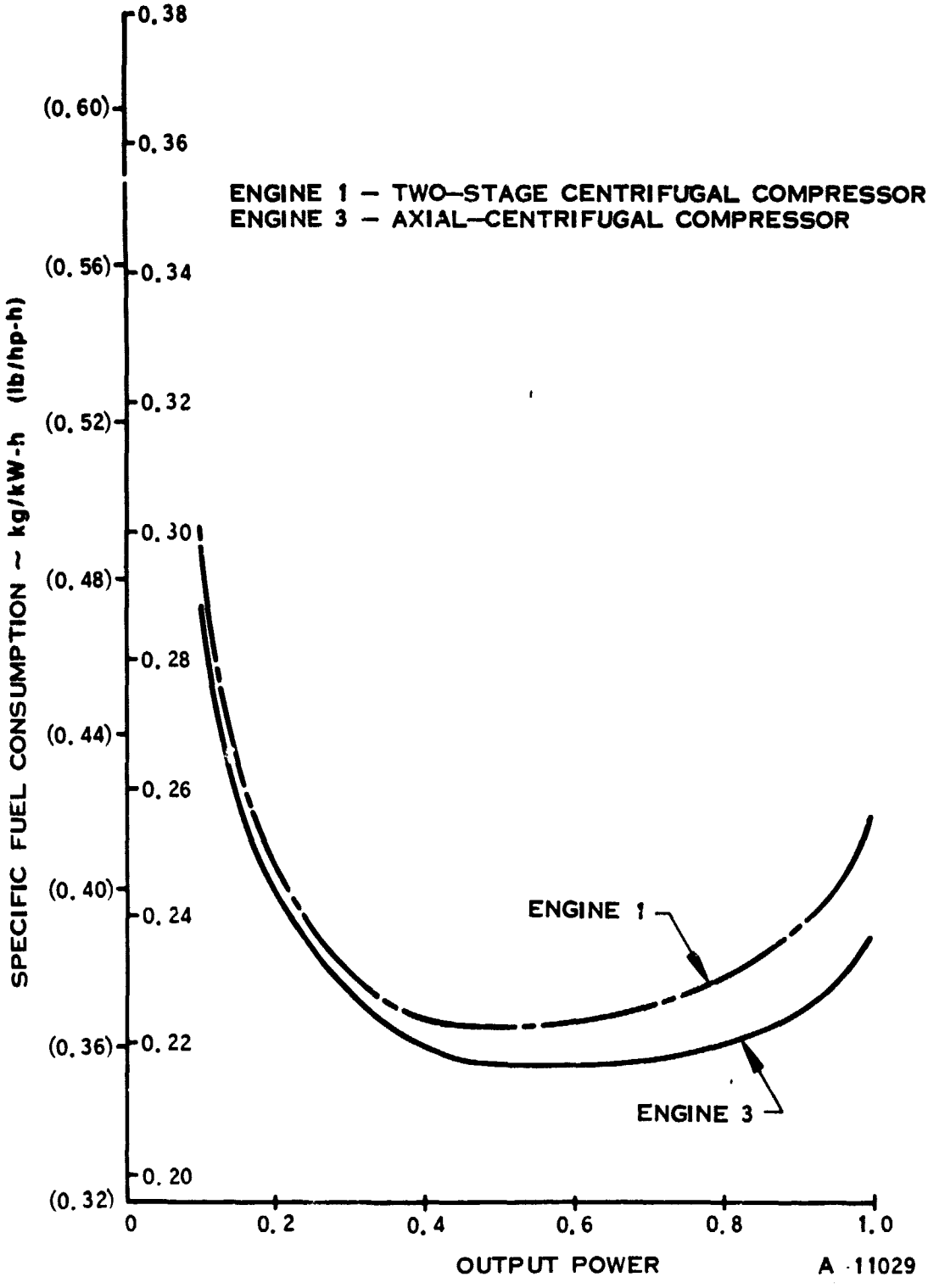

Figure 39. Comparison of SFC Between Two-Stage Centrifugal and Axial-Centrifugal Compressors

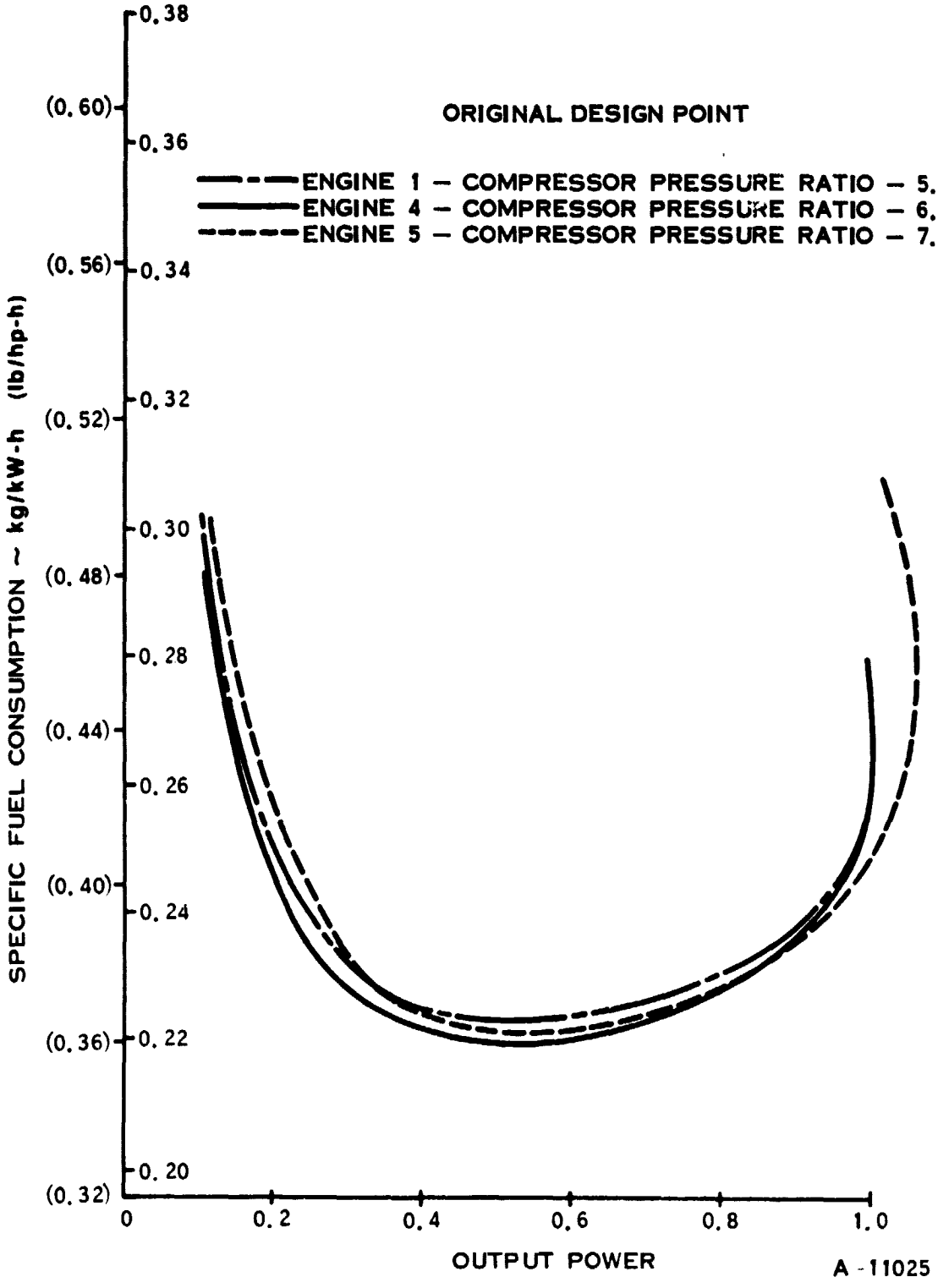

Figure 40. Pressure Ratio Comparison, Initial

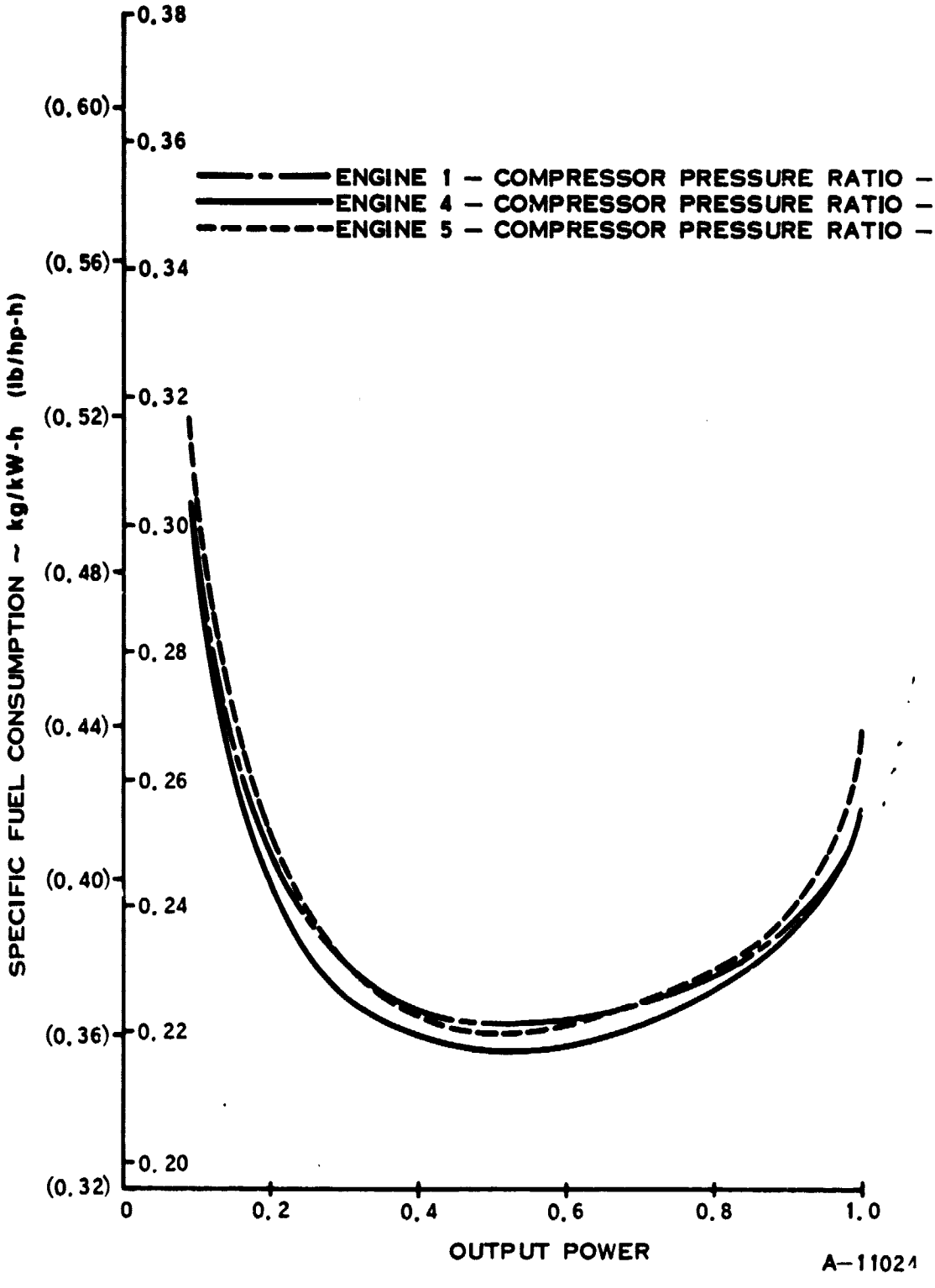

Figure 41. Pressure Ratio Comparison, Final

XXVI, and XXX. Engine 4 also has 4 percent lower idle fuel flow compared to Engine 1, Tables XXVI and XX. The fuel consumption of Engine 5 is higher except for idle fuel flow, making the nominal 5.58 pressure ratio a good choice for the 1505°K (2250°F) temperature level.

Turbine Inlet Temperature Study. Figure 42 compares turbine inlet temperatures at 1311°K (1900°F), 1422°K (2100°F), 1505°K (2250°F), and 1644°K (2500°F) in Engines 6, 8, 4, and 7, respectively, all using the two-stage centrifugal compressor with the variable power turbine nozzle. Cycle analysis started with the same nominal 6.0 overall compressor ratio that Engine 4 had started with, but Engines 6 and 8 also had to be backed down to the following compressor pressure ratios at rated power.

Engine	TIT °K, (°F)	Pressure Ratio
6	1311°K (1900°F)	4.74
8	1422°K (2100°F)	5.28
4	1505°K (2250°F)	5.58
7	1644°K (2500°F)	6.00

These changes in pressure ratio illustrate the effect of TIT on optimum pressure ratio for power. As expected, higher TIT improves SFC.

Engines 4, 6, 7, and 8 were run with the same minimum cooling airflow, a total of 1.0 percent of the airflow for all shaft seals and cooling. Operation at higher temperature would probably require additional turbine rotor cooling air. Specifications for Engine 4 using 1505°K (2250°F) TIT included a composite first stage turbine rotor with ceramic blades attached mechanically to a metal disk. The preliminary design called for 2 percent of the compressor discharge air to cool the turbine rotor. A modified cycle analysis was run as Engine 4A, returning the cooling air to the cycle downstream from the first stage turbine rotor, mixing before the power turbine. The first stage turbine efficiency was ratioed down 1.0 percent to account for the disturbance of the working fluid by the cooling airflow. The performance is summarized in Table XXVIII, and the specific fuel consumption is compared to Engine 4 in Figure 43. The SFC is considerably higher--13.5 percent at 10 percent power--due primarily to the lower turbine outlet (recuperator inlet) temperature and the corresponding effect on burner inlet temperature and fuel flow.

Rotor System Comparison. Engine 9 was modeled as a single-rotor engine at 1505°K (2250°F) TIT, similar to Engine 4 except that a fixed power turbine nozzle was used and the two turbine stages were forced to run at the same speed. The performance characteristics are summarized in Table XXXII and the specific fuel consumption is compared to Engine 4 in Figure 44. The SFC for Engine 9 is slightly better at high power, but worse at the low power level used during the driving cycles.

The better SFC at high power is due to the lower losses with the fixed power turbine nozzle compared to the variable nozzle, resulting in 0.03 higher stage efficiency. The turbine stage efficiencies were compared to the optimum stage efficiencies in Figure 45. This shows a significant efficiency reduction in both

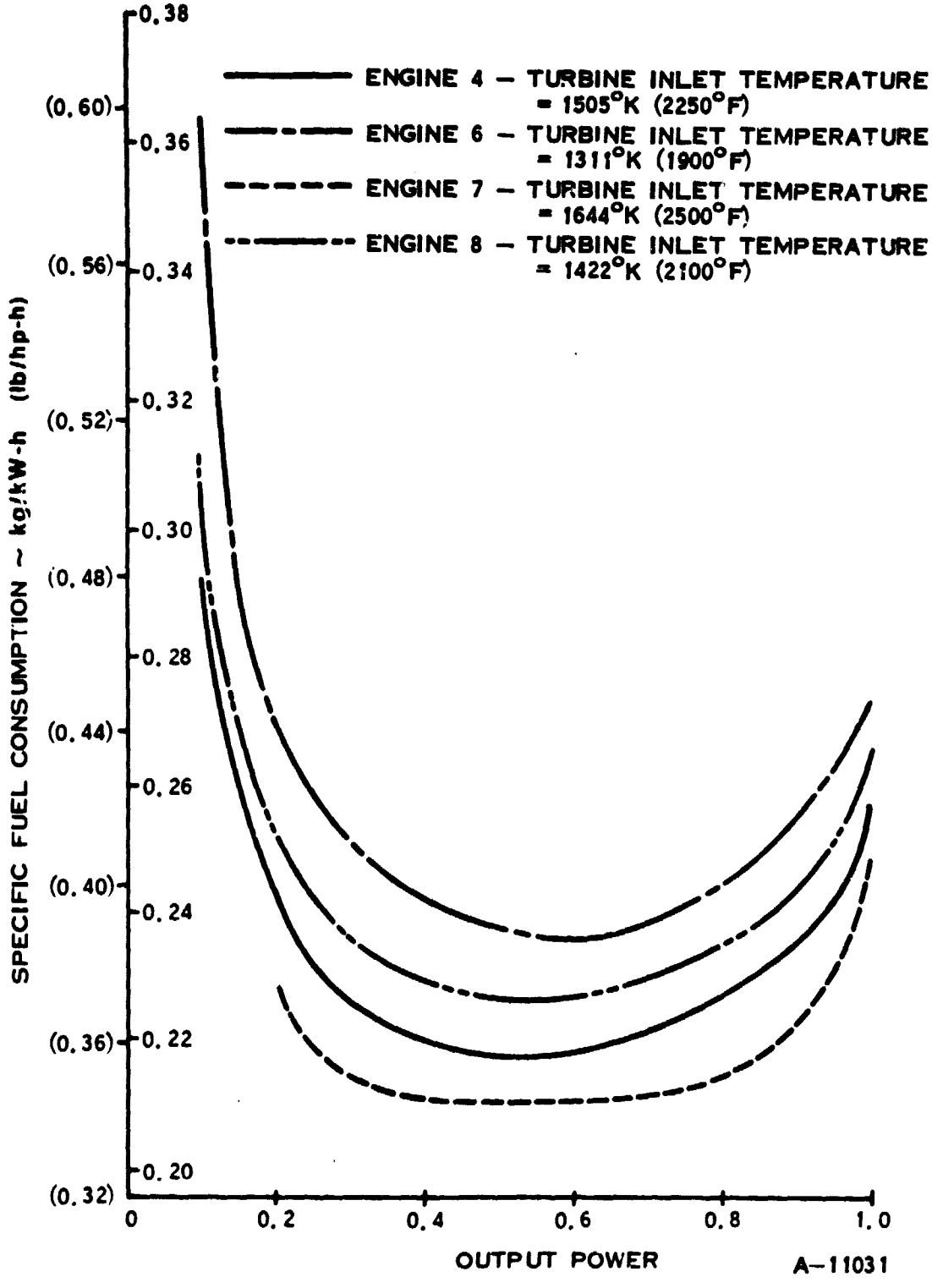

Figure 42. Effects of TIT on SFC

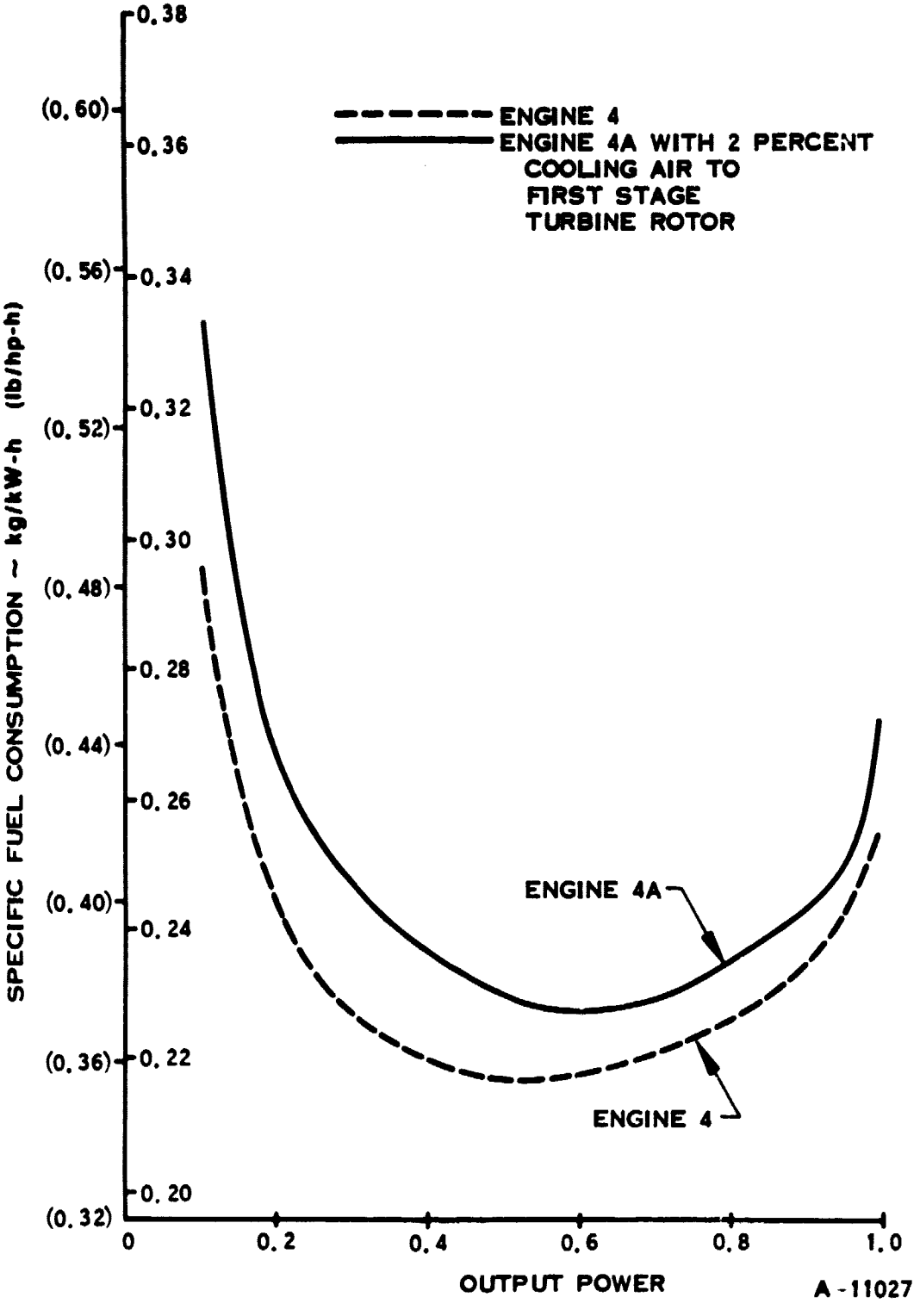

Figure 43. Effect of Cooling Airflow on SFC

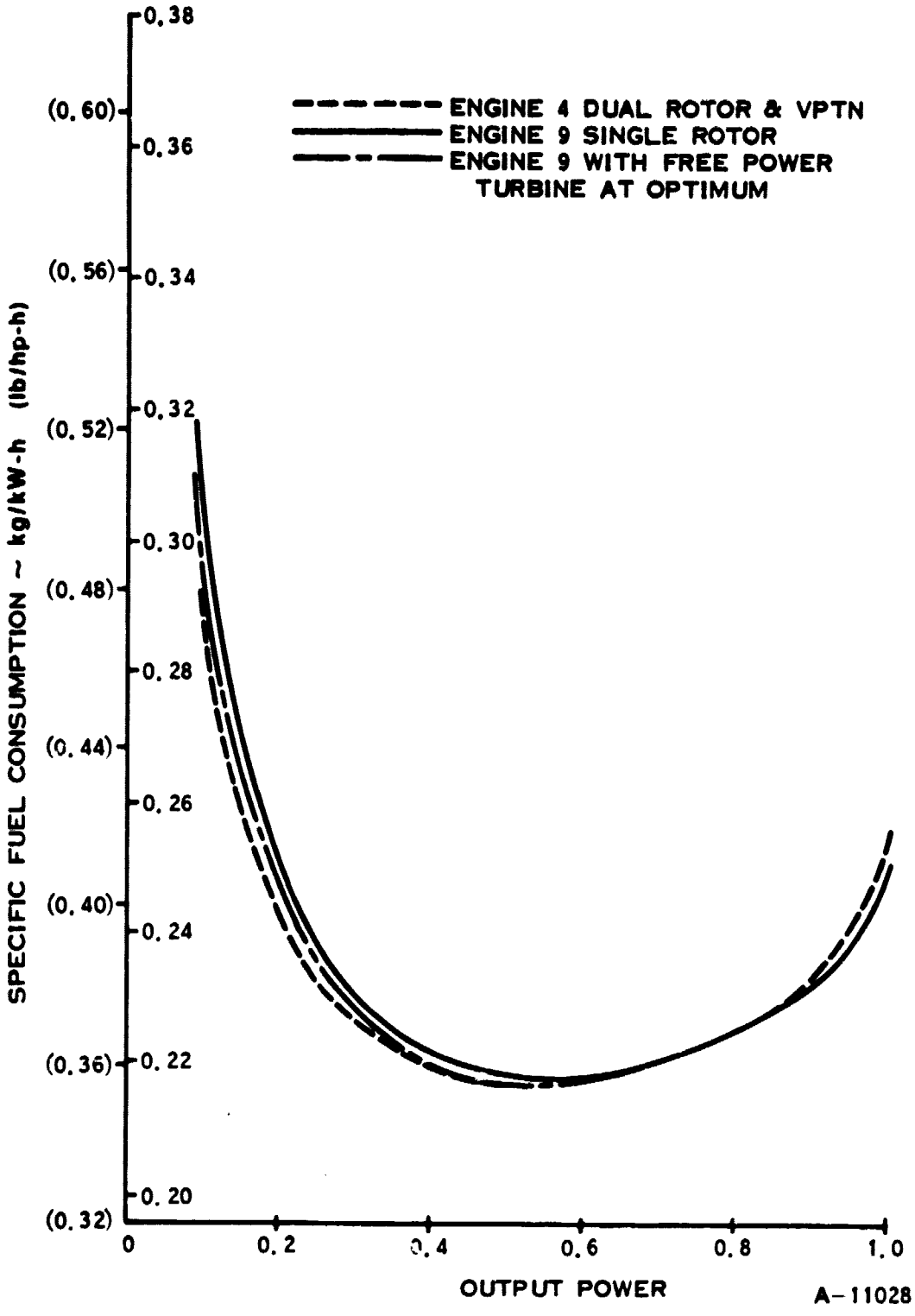

Figure 44. Rotor System Comparison

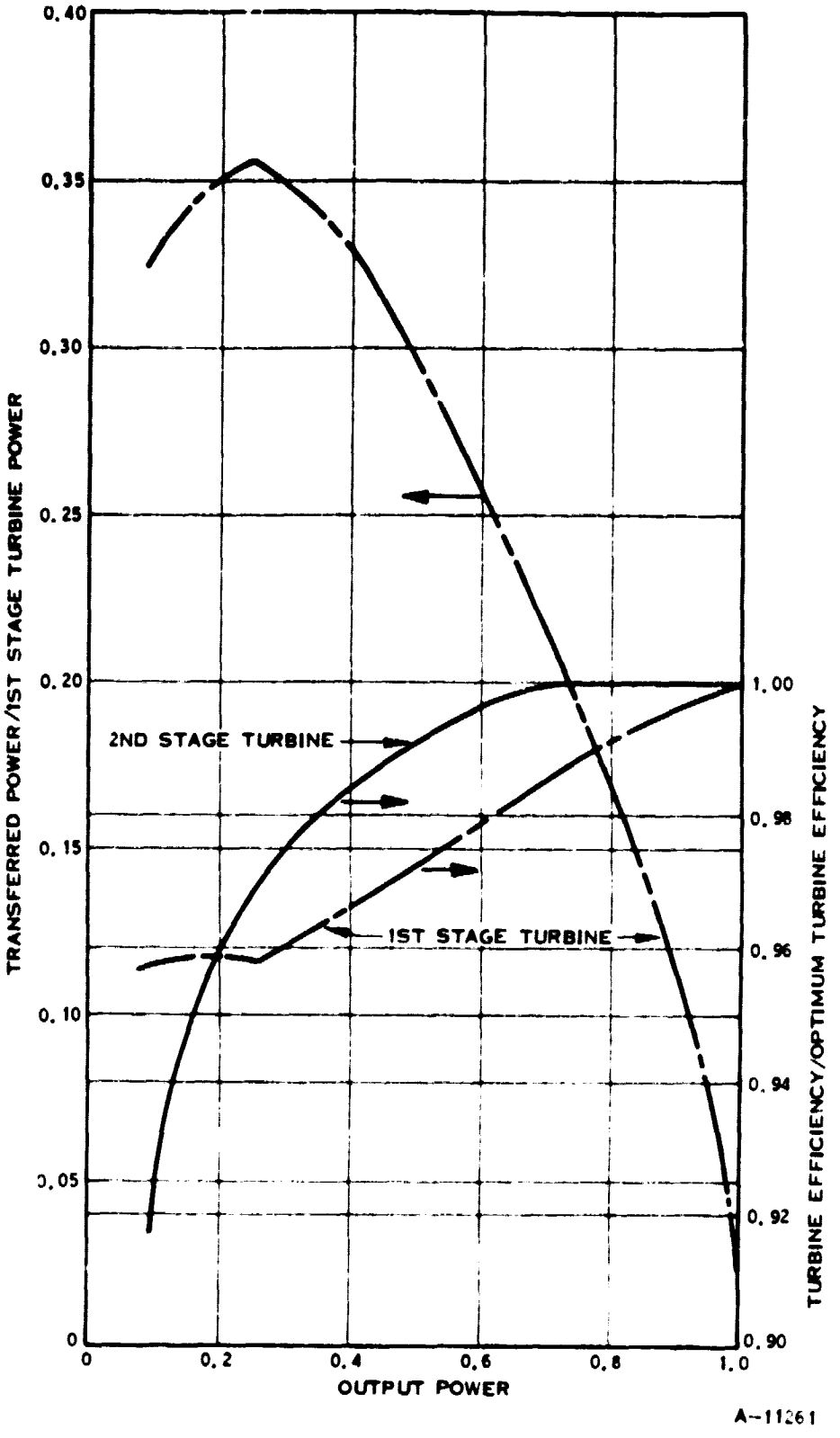

Figure 45. Effect of Turbine Mismatching with Single-Rotor Engine

stages at part load, along with the increased loading of the first stage turbine. To improve the power turbine efficiency, a run was made with a free power turbine at optimum speed with ideal power transfer as shown in Figure 44. This improves the SFC, but it is still not as good as the dual-rotor engine with variable power turbine nozzle. It appears that the turbine design for a single-rotor engine should be analyzed carefully for part-load efficiency and optimized for best fuel economy.

Heat Exchanger Comparison. Cycle analysis was completed on Engine 10 with a rotary ceramic regenerator. Except for its heat exchanger, Engine 10 is the same as Engine 8; it has a two-stage centrifugal compressor, operates at 1422°K (2100°F) TIT, and uses the variable power turbine nozzle for turbine temperature control. The rotary ceramic regenerator in Engine 10 was sized for the same effectiveness and pressure drop at rated power as the annular ceramic recuperator in Engine 8. Engine 10 performance is summarized in Table XXXIV. The engine airflow in Engine 10 is 13 percent greater than in Engine 8 due to the 4 percent leakage and carryover from the high pressure side of its rotary regenerator This leakage also affects the SFC, which is about 8 percent higher at 10 percent power, as shown in Figure 46.

This comparison did not include the effect of the regenerator seals leaking colder compressor discharge air into the power turbine exhaust duct, reducing the average regenerator inlet temperature, with a corresponding effect on burner inlet temperature and fuel flow. It also did not assess the effects of flow distribution with the regenerator performance. This has been a traditional problem with the regenerator, making it very difficult to achieve the last bit of heat transfer for the desired high effectiveness.

Performance Trade-Off Studies. Initial performance trade-off studies have been completed as part of this powertrain performance analysis. These include the effect of varying thermodynamic cycle parameters--pressure ratio, turbine inlet temperature, turbine cooling, heat exchanger effectiveness, and pressure drop Component matching has been explored as part of the part load performance analysis

The variable turbine nozzle has been compared with slip clutch power transfer as methods of controlling turbine inlet temperature. Comparisons have been made between regenerator and recuperator, and between single-rotor and dual-rotor powertrains. Performance trade-off studies continued as part of the vehicle fuel economy analysis and again in the powertrain optimization during Task III.

2.3 VEHICLE FUEL ECONOMY ANALYSIS

VEHICLE FUEL ECONOMY ANALYSIS PROCEDURE

A computer program was set up to simulate the operation of the vehicle through the urban and highway driving cycles. The program models the various powertrain components with input maps which define the component characteristics. All of the vehicle component maps, including the Chrysler Model 904 3-speed automatic transmission, and the referenced 232 cid piston engine performance characteristics were obtained from AM General. The turbine engine performance characteristics were generated as described previously. The driving cycles are input along with

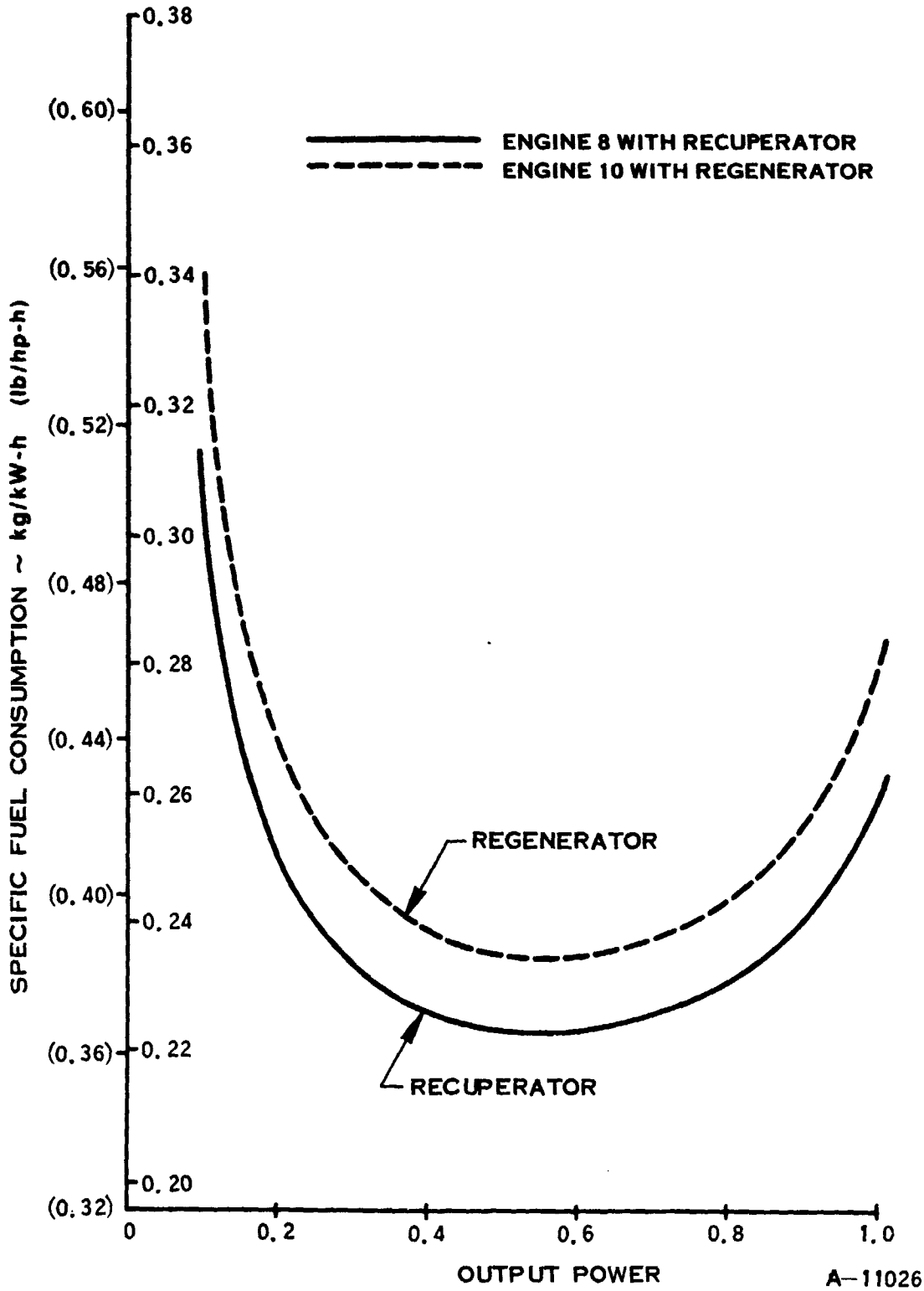

Figure 46. Comparison of Recuperator (SFC)

the component maps. The program drives the vehicle through the driving cycle, calculating the vehicle performance at one-second intervals. The program starts by finding the average velocity and acceleration for the one-second time interval. Speed and power demand is found by calculating the vehicle road load and acceleration powers. The program moves forward from the wheels to the engine, calculating component rotational speeds and power losses. At the transmission, a gear ratio is arbitrarily selected and the input torque calculated from the appropriate gearing map. Torque converter performance (where used) is found by varying the torque converter speed ratio until the engine and torque converter characteristics balance. Fuel flow is determined by the engine speed and power demand. The effect of engine inertia is then added.

Next, the program picks another gear and runs through the drivetrain calculations again. Whichever gear gives the lowest fuel flow is the gear chosen for that interval. The fuel used during each interval is added together to obtain the total fuel consumed. The driving cycle fuel economy is calculated from this total.

An allowance was made for the initial start in the urban cycle by estimating the heat stored in the engine at idle and lost at shutdown, requiring a corresponding fuel increment on the next start. The fuel equivalent of the heat stored at idle varied from 0.41 kg (0.90 lb) for Engine 4A down to 0.24 kg (0.53 lb) for Engine 10.

The vehicle simulation program was first used to calculate the driving cycle fuel economy for the American Motors Gremlin and Concord automobiles. Both cars were run with the AMC 232 cid 6-cylinder engine and the Chrysler Model 904 3-speed automatic transmission. The results are shown in Table XI, along with the EPA driving cycle data. Correlation is excellent for the urban cycles, with computed fuel economy being about 10 percent less than the EPA test for the highway cycle.

TABLE XI. DRIVING CYCLE FUEL ECONOMY

Vehicle Model	Driving Cycle	Fuel Economy km/l (mpg)	
		EPA Test	WRC Simulation
Gremlin	Urban	7.82 (18.4)	7.81 (18.38)
	Highway	10.76 (25.3)	9.73 (22.88)
	Combined	8.92 (21.0)	8.57 (20.16)
Concord	Urban	7.78 (18.3)	7.64 (17.97)
	Highway	10.42 (24.5)	9.42 (22.16)
	Combined	8.76 (20.6)	8.35 (19.64)

VEHICLE FUEL ECONOMY ASSUMPTIONS

A. Vehicle test weight.

The vehicle operating test weight = 1542 kg (3400 lbm).

B. Driving cycle description.

The driving cycles used for the fuel economy ratings were the EPA highway and urban driving cycles defined in The Federal Register, Vols. 41 and 42. The cycles are presented by a given vehicle velocity at each second time interval for the duration of each cycle. The urban cycle was 1371 seconds long; however, the first 505 seconds of the cycle were driven twice, once from a cold start and once with the engine already hot. The fuel consumed during the first 505 seconds was a weighted average of the hot and cold runs. The calculated fuel was found by adding 43 percent of the cold run fuel and 57 percent of the hot run fuel. The fuel for the last 866 seconds was then added to the weighted average from the first 505 seconds to obtain the total urban cycle fuel consumption. The highway cycle was 763 seconds long and was driven just once from a hot start. The combined cycle rating is defined by the equation:

$$\text{Combined k/l (mpg)} = \frac{1}{\frac{0.55}{\text{urban k/l (MPG)}} + \frac{0.45}{\text{highway k/l (mpg)}}}$$

C. Transmission efficiency vs speed.

The transmission characteristics were dependent on the engine configuration. The two-shaft configuration used a three-speed automatic transmission without a torque converter. The first, second, and third gear characteristics are shown in Figures 47, 48, and 49, respectively. The single-shaft configuration used a continuously variable transmission whose characteristics are shown in Figure 50.

D. Rear end efficiency over operating range.

The rear axle power loss is shown in Figure 51.

E. Vehicle road load power.

The road load power required for the American Motors Concord 2-door sedan at 1542 kg (3400 lb) is shown in Figure 52, derived from coastdown test data.

VEHICLE FUEL ECONOMY

Effect of Turbine Inlet Temperature. The effect of TIT on vehicle fuel economy was evaluated using Engines 6, 8, and 4 at 1311°K (1900°F), 1422°K (2100°F), and 1505°K (2250°F) TIT, as shown in Table XII.

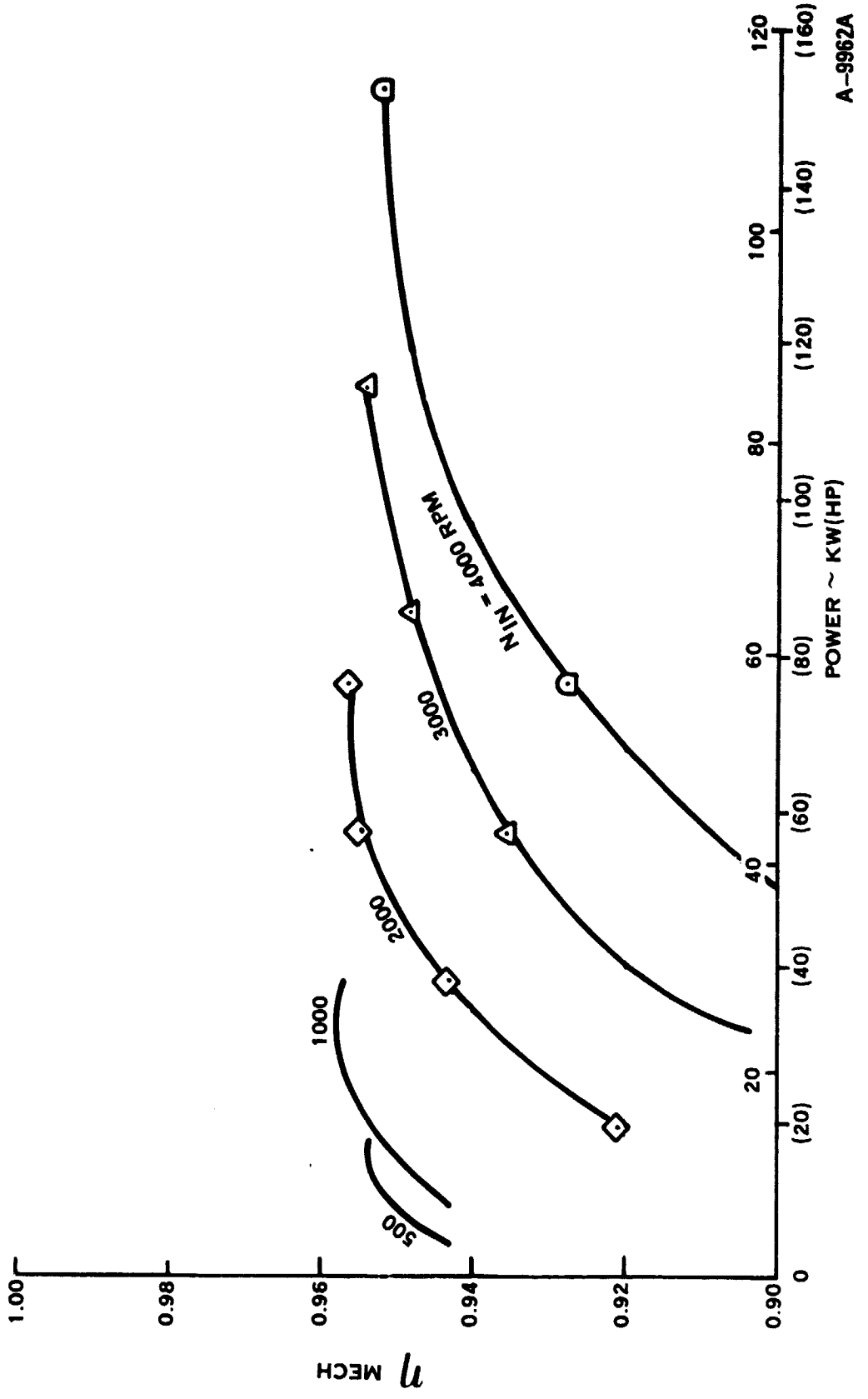

Figure 47. Transmission Efficiency versus Input Power, First Gear, Gear Ratio = 2.45

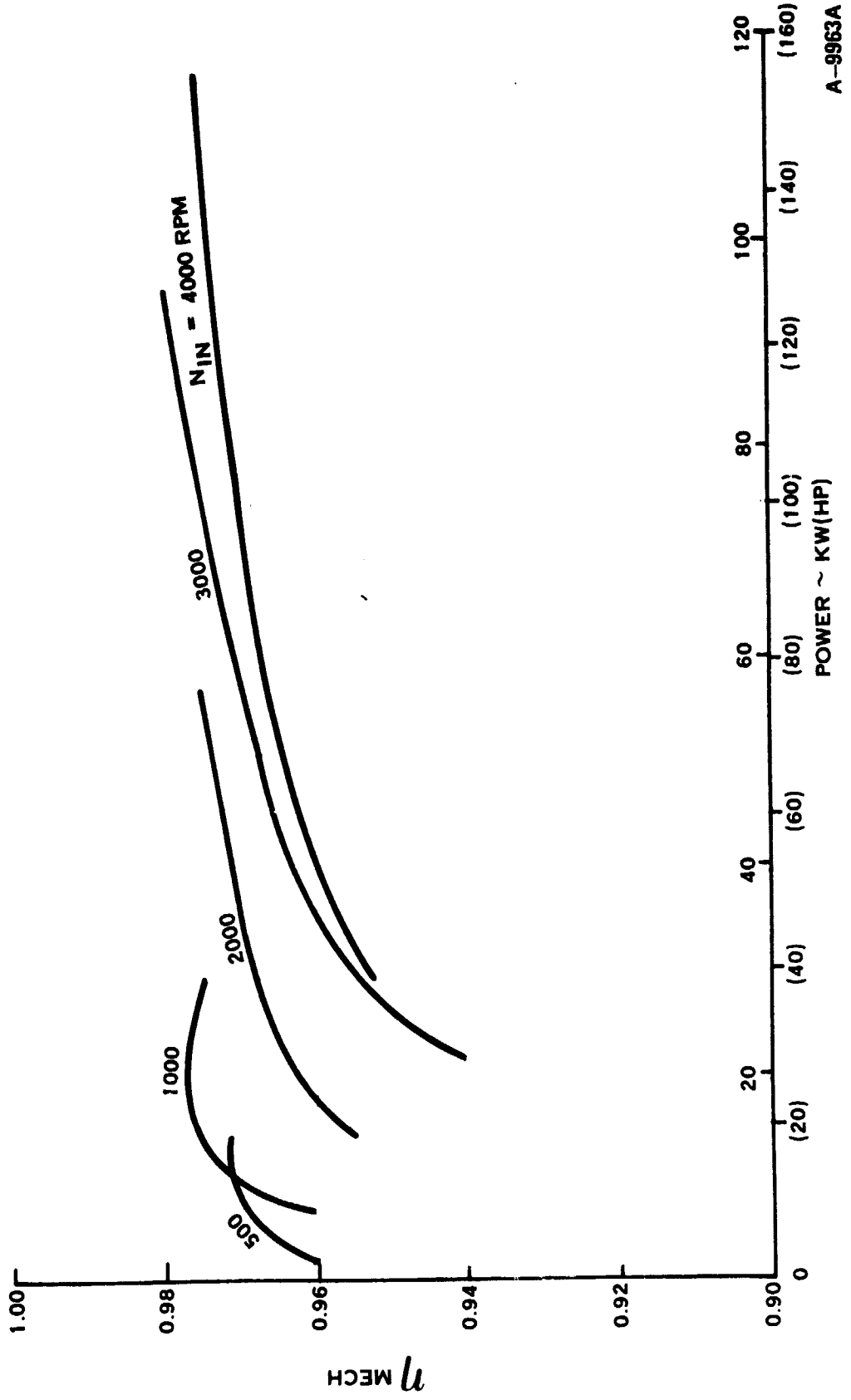

Figure 48. Transmission Efficiency versus Input Power, Second Gear, Gear Ratio = 1.45

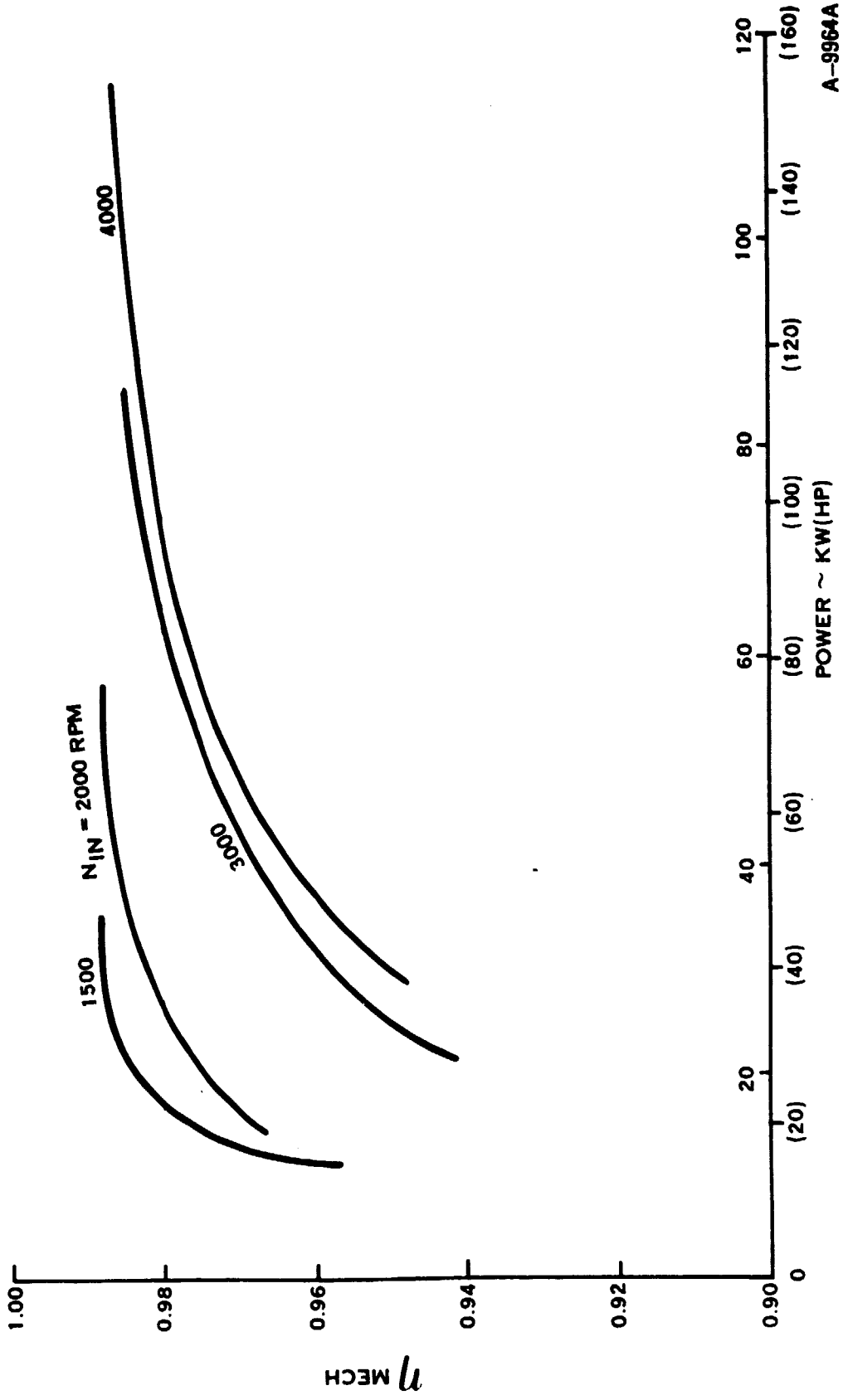

Figure 49. Transmission Efficiency versus Input Power, Fluid Gear, Gear Ratio = 1.00

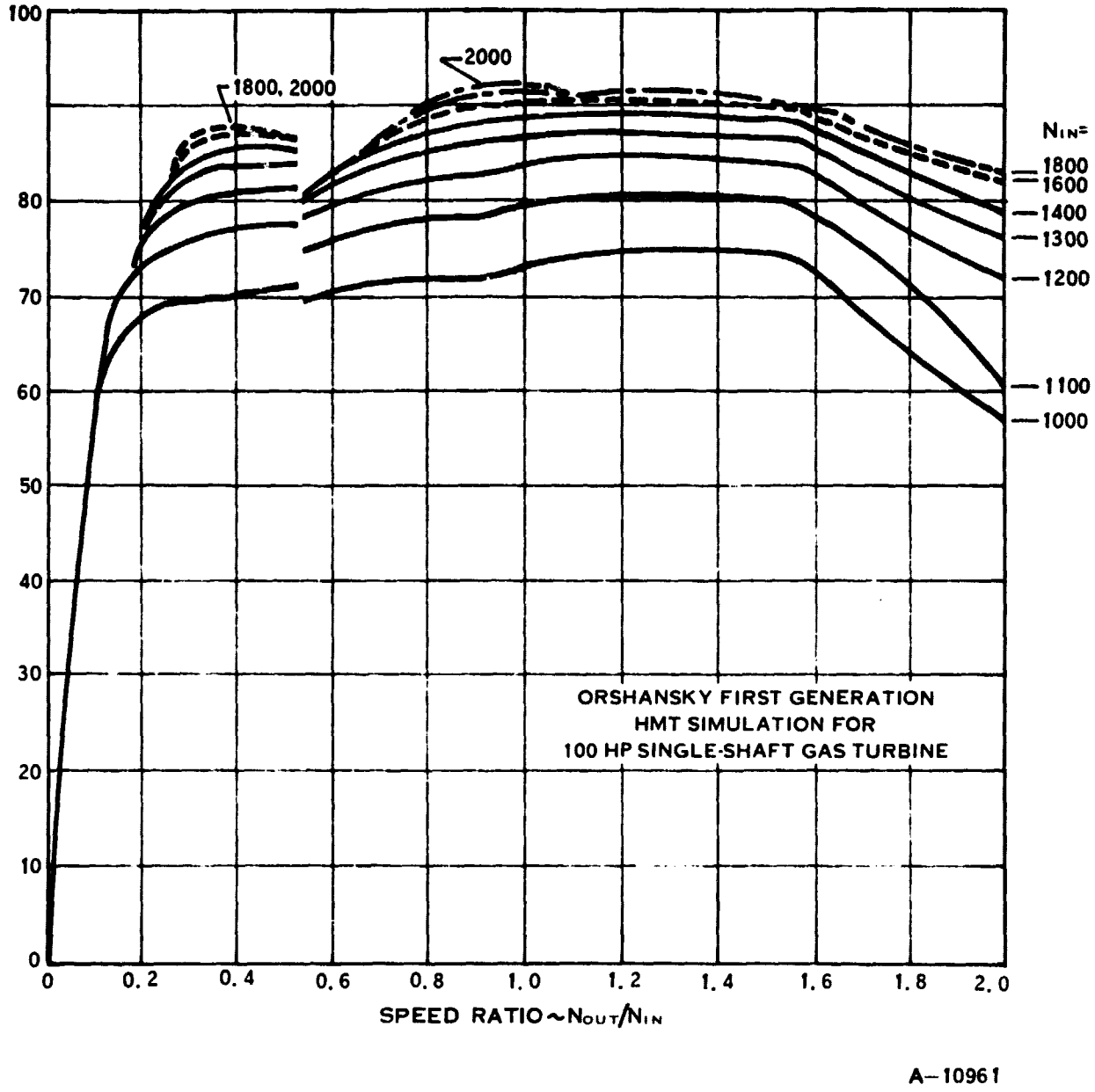

Figure 50. Orshansky Hydromechanical Transmission Efficiency

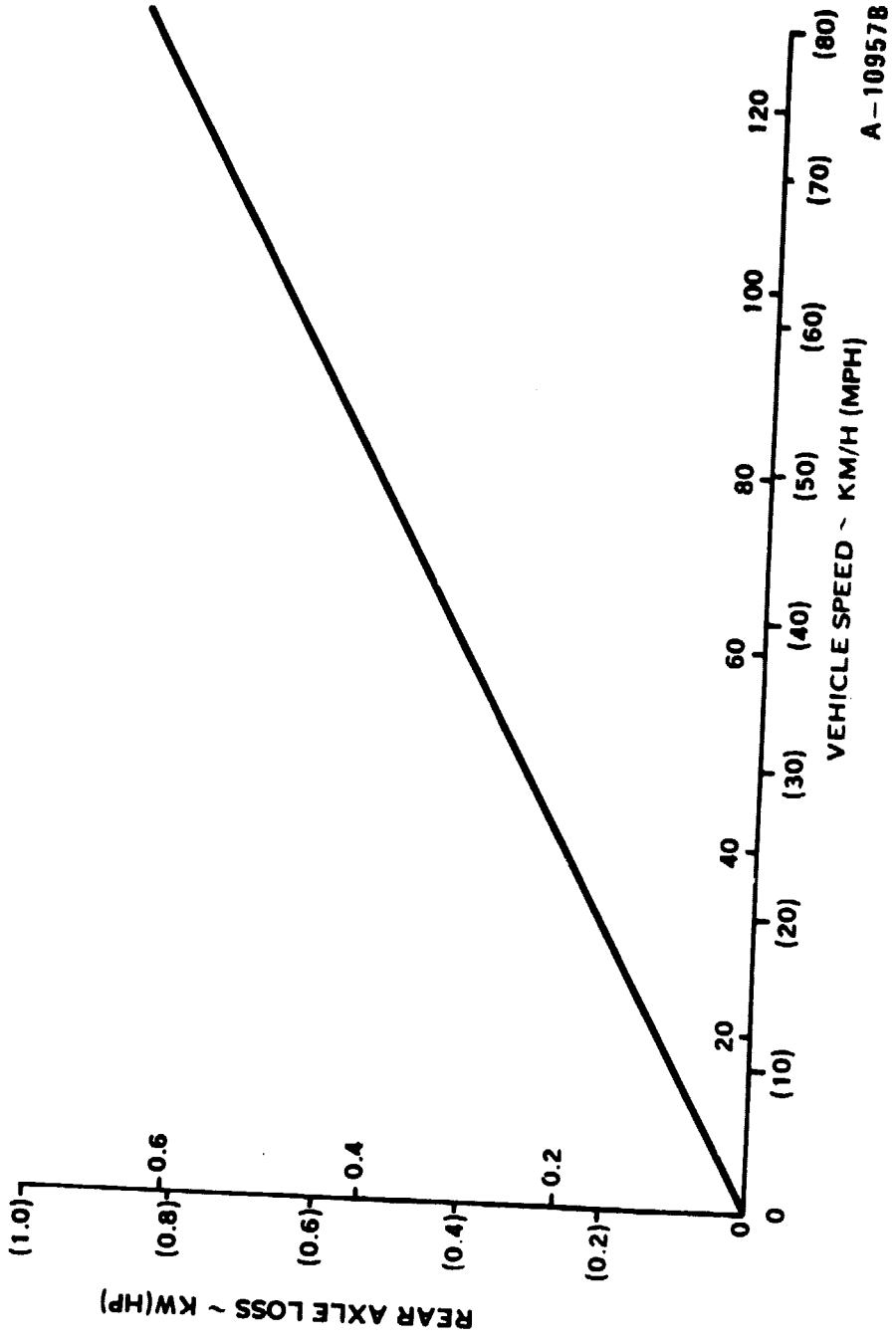

Figure 51. Rear Axle Loss versus Vehicle Speed, Rear Axle Gear Ratio = 3.58

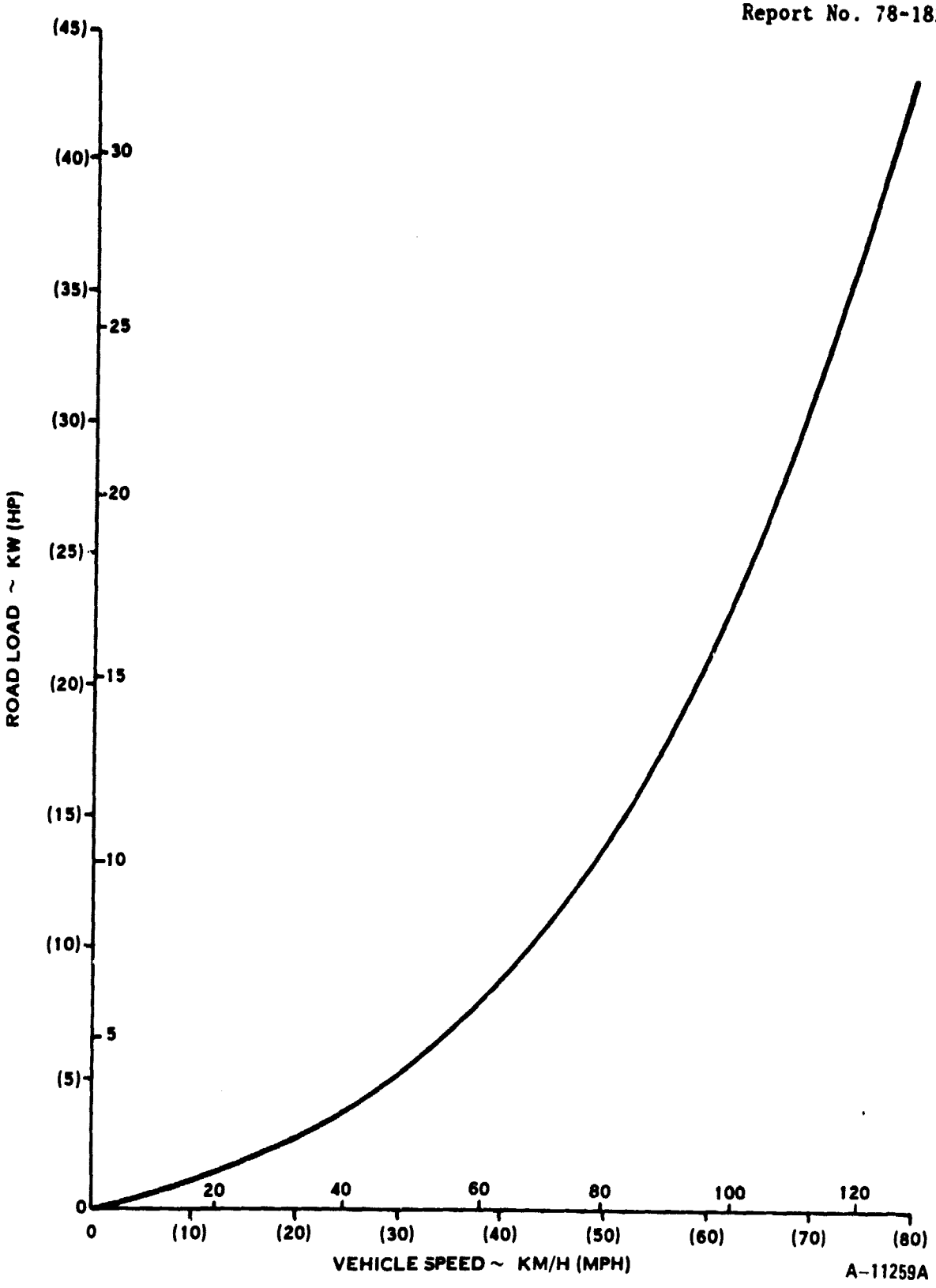

Figure 52. Vehicle Road Load Power

TABLE XII. EFFECT OF TIT AND COOLING ON FUEL ECONOMY

ENGINE NO.	6	8	4	4A
TIT, °K (°F)	1311 (1900)	1422 (2100)	1505 (2250)	1505 (2250)
Air Loss, Percent	1.0	1.0	1.0	3.0*
Urban Cycle, km/l (mpg)	7.92 (18.62)	8.66 (20.38)	9.17 (21.56)	8.08 (19.0)
Highway Cycle, km/l (mpg)	15.37 (36.16)	15.88 (37.34)	16.52 (38.86)	15.09 (35.5)
Combined Cycle, km/l (mpg)	10.13 (23.82)	10.89 (25.62)	11.46 (26.96)	10.20 (24.0)
Ratio to 8.3 km/l (19.6 mpg)	1.215	1.307	1.376	1.224

NOTES: Concord at 1542 kg (3400 lbm) test weight
Ambient weight on first urban cycle

*1.0 percent loss plus 2.0 percent cooling air to first stage turbine rotor

Initial analysis was done at a fixed overall speed ratio, power turbine rotor to drive wheels, but was expanded for Engine 4 over a range of reduction gear ratios from 16 to 28 as shown in Figure 53. The fuel economy is not sensitive to gear ratio, but the ratio of 14.83 used previously was far from optimum. A gear ratio of 22 gives 3 percent better combined driving cycle fuel economy, and at the same time improves vehicle acceleration.

Effect of Turbine Cooling. The effect of cooling the first stage turbine wheel was analyzed by modifying Engine 4. This Engine 4 is specified for operation at 1505°K (2250°F) turbine inlet temperature, using a composite first stage turbine rotor with ceramic blades attached mechanically to a metal disk. The preliminary design called for 2 percent of the compressor discharge air to cool the turbine rotor. A cycle analysis was made of modified Engine 4A, returning the cooling air to the cycle downstream from the first stage turbine rotor, mixing before the power turbine.

The first stage turbine efficiency was ratioed down 1.0 percent to account for the disturbance of the working fluid by the cooling airflow. The specific fuel consumption is considerably higher as shown in Figure 43, 13.5 percent at 10 percent

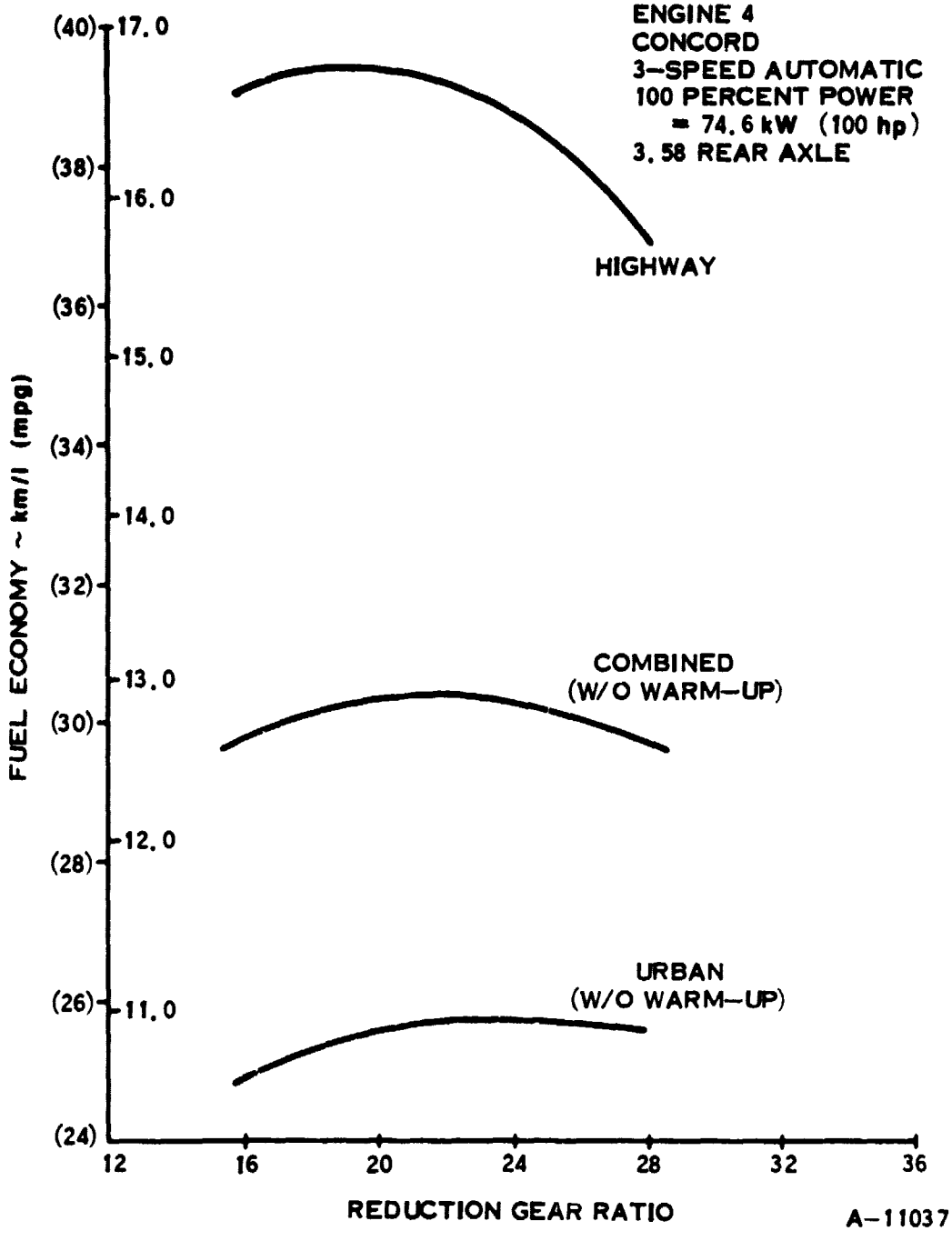

Figure 53. Fuel Economy Versus Reduction Gear Ratio, 3-Speed Automatic

power -- due primarily to the lower turbine outlet (recuperator inlet) temperature and the corresponding effect on burner inlet temperature and fuel flow.

The estimated fuel economy with and without cooling is shown in Table XII, and compared with similar uncooled analyses at 1311°K (1900°F) and 1422°K (2100°F) turbine inlet temperatures. With no turbine wheel cooling (1.0 percent air loss for labyrinth seals), higher turbine inlet temperature shows a significant improvement in fuel economy. When the turbine wheel is cooled, fuel economy at 1505°K (2250°F) turbine inlet temperature drops to within 1 percent of that attainable at 1311°K (1900°F) without cooling. This comparison supports the selection of the integral metal first stage turbine rotor for operation in the 1422°K (2100°F) range.

Comparison of Single-Rotor and Dual-Rotor Concepts. The driving cycle simulation program was modified to handle the single-rotor engine and the variable ratio transmission. The Orshansky hydromechanical transmission chosen for this study was modeled as shown in Figure 50, using a computer simulation supplied by Orshansky for a 100 hp single-rotor turbine transmission. A reduction gear ratio of 39.61 was chosen to fit the 2000 rpm input for the transmission, and the rear axle ratio was varied from 1.95 to 3.6. Again, the fuel economy as shown in Figure 54 is not sensitive to axle ratio, but the combined driving cycle fuel economy at the optimum ratio of 2.25 is 5.3 percent below the equivalent dual-rotor engine.

Comparison of Regenerator and Recuperator. The effect of the type of heat exchanger was shown by estimating the fuel economy for Engine 10 with the regenerator and comparing it to Engine 8 with the recuperator. The SFC of Engine 10 is shown in Figure 46 and the vehicle fuel economy is compared to Engine 8 in Table XIII. The highway driving cycle fuel economy of Engine 10 is 4 percent lower than that of Engine 8, but the urban cycle fuel economy of Engine 10 is higher than that of Engine 8 because the lower weight of the regenerator compared to the recuperator (approximately 0.6 ratio) reduces the warm-up effect in the urban cycle. This results in a net 0.5 percent lower combined cycle fuel economy with the regenerator.

As noted in the discussion of Engine 10, a more realistic analysis of the regenerator would have included the influence of heat storage, flow distribution, and leakage on regenerator effectiveness. An estimate of these effects would reduce the fuel economy with the regenerator to about 8 percent below that with the equivalent recuperator.

2.4 SENSITIVITY ANALYSIS

This sensitivity study is an indicator of the effect of variation in cycle parameters on overall engine performance, i.e., fuel consumption and maximum power. Magnitudes of change in parameters were chosen large enough to ensure resolution between effects and are not necessarily indicative of either possible development program shortcomings or production engine tolerances.

The procedure used in the analysis was to change the desired cycle parameter by the selected amount at the maximum rating and allow the engine to rematch. Thus, efficiency changes for a given component are generally constant over most of the

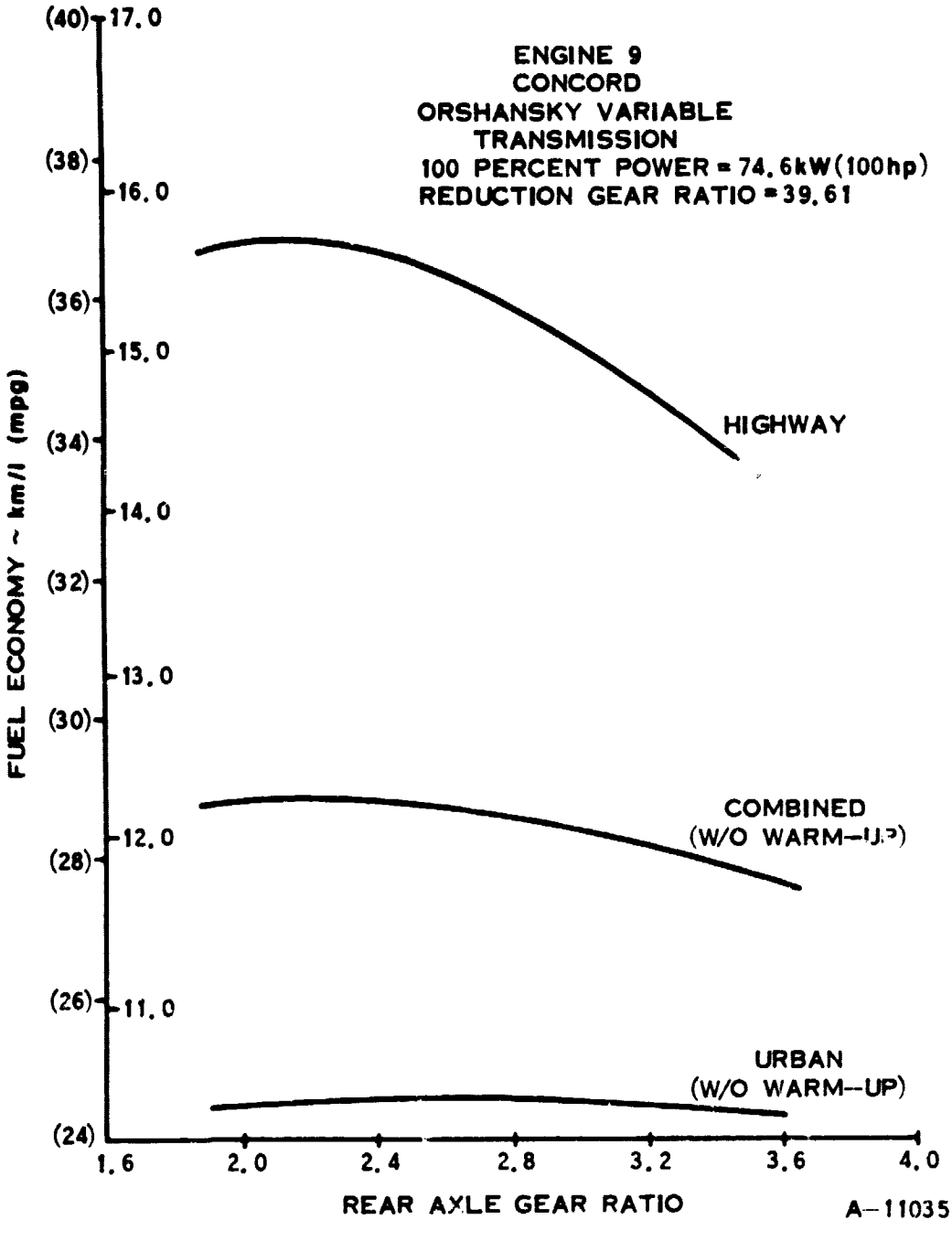

Figure 54. Fuel Economy versus Reduction Gear Ratio, Orshansky Variable Transmission

TABLE XIII. FUEL ECONOMY COMPARISON

ENGINE NO.	8	10
TIT, ^{o}K (^{o}F)	1422 (2100)	1422 (2100)
Heat Exchanger	Recuperator	Regenerator
Urban Cycle, km/l (mpg)	8.44 (19.85)	8.50 (20.0)
Highway Cycle, km/l (mpg)	15.85 (37.27)	15.18 (35.7)
Combined Cycle, km/l (mpg)	10.69 (25.14)	10.63 (25.0)
Ratio to 8.3 km/l (19.6 mpg)	1.283	1.276

NOTES: Concord at 1542 kg (3400 lbm) test weight
Ambient start on first urban cycle

power range, but pressure and power loss changes (functions of flow parameters and speeds) will not remain constant.

Table XIV presents the effects of changes in the cycle parameters on the drive cycle fuel economy for the urban, highway, and combined cycles and on the maximum output power. The baseline IGT powertrain is Engine 4 with 1505^{o}K (2250^{o}F) turbine inlet temperature, installed in a Concord. The urban and combined cycle fuel economies do not include the warm-up effect.

The following is a description of the extent and effects of varying the cycle parameters:

Efficiencies

- Two point changes in overall compressor, HP turbine, or LP turbine efficiency have similar effects on fuel economy and maximum power.
- Recuperator effectiveness is the parameter having the strongest effect on fuel economy. It has no effect on maximum power.

Leakage

- Two percent leakage air from the compressor exit has a fuel flow effect very similar to a rotating component efficiency change, but an even more significant drop in maximum power.

TABLE XIV. EFFECTS OF CHANGES TO CYCLE PARAMETERS ON FUEL ECONOMY AND OUTPUT POWER*

	Baseline Engine 4	-2 pts Overall Compressor Efficiency	-2 pts HP Turbine Efficiency	-2 pts Power Turbine Efficiency	-2 pts Recuperator Effectiveness	+2% Compressor Discharge Air Leakage	Inlet/Exhaust** Pressure Loss	Combustor** Pressure Loss	Turbine Diffuser** Pressure Loss	Recuperator** Pressure Loss	Increased** Bearing Loss	Increased** Accessory Power	Road Load +10%	Vehicle Weight -90.72 kg (-200 lb)
Urban (km/l)	10.44	10.27	10.28	10.30	9.64	10.28	10.43	10.16	10.38	10.15	9.71	10.00	10.22	10.63
Urban (mpg)	24.56	24.16	24.19	24.22	22.67	24.17	24.54	23.89	24.4.	23.87	22.83	23.51	24.05	25.01
%Δ Urban	-	-1.6	-1.5	-i.4	-7.7	-1.6	-0.1	-2.7	-0.6	-2.8	-7.0	-4.3	-2.1	+1.8
Highway (km/l)	16.52	16.15	16.24	16.24	15.34	15.38	16.50	15.95	16.37	15.93	15.50	15.90	15.61	16.63
Highway (mpg)	38.86	37.98	38.20	38.20	36.07	36.18	38.81	37.51	38.51	37.46	36.46	37.39	36.72	39.12
%Δ Highway	-	-2.3	-1.7	-1.7	-7.2	-1.8	-0.2	-3.5	-0.9	-3.6	-6.2	-3.8	-5.5	+0.6
Combined (km/l)	12.51	12.28	12.32	12.33	11.57	12.31	12.50	12.14	12.43	12.13	11.67	12.00	12.10	12.70
Combined (mpg)	29.43	28.89	28.97	29.00	27.22	28.95	29.41	28.56	29.23	28.53	27.45	28.22	28.47	29.86
%Δ Combined	-	-1.8	-1.6	-1.5	-7.5	-1.7	-0.1	-3.0	-0.7	-3.1	-6.7	-4.1	-3.3	+1.4
Max Power (kW)	74.6	71.3	71.5	72.7	74.6	70.2	73.2/73.8	72.4	71.4	70.3	72.6	73.4		
Max Power (hp)	100.0	95.6	95.9	97.5	100	94.2	98.1/99.0	97.1	95.8	94.3	97.4	98.4	-	-

*Data based on Powertrain No. 4 - 1505°K (2250°F) TIT

**See text for actual change in parameter.

Pressure Losses

- Inlet/Exhaust: Both the inlet and the exhaust pressure losses were doubled; however, both were initially very small. The change in inlet $\Delta P/P$ was 0.0087 at maximum power and 0.0007 at 10 percent power. The change in exhaust $\Delta P/P$ was 0.0082 at maximum power and 0.0004 at 10 percent power.

- Combustor: This pressure loss was increased by a factor of two at a given flow parameter with rematch effects.

	Maximum Power	10% Power
Change in $\Delta P/P$ / Base $\Delta P/P$	0.0271 / 0.0303	0.0253 / 0.0277

- Turbine Diffuser: This pressure loss was increased by a factor of two at a given flow parameter, but engine rematch changes the flow parameter at a given percent power.

	Maximum Power	10% Power
Change in $\Delta P/P$ / Base $\Delta P/P$	0.0284 / 0.0309	0.0041 / 0.0028

- Recuperator: Hot and cold side losses were both increased by a factor of 1.5 at a given flow parameter. As noted above, engine rematch results in a somewhat different pressure loss.

	Maximum Power	10% Power
Change in $\Delta P/P$ / Base $\Delta P/P_{hot\ side}$	0.0278 / 0.0744	0.0162 / 0.0237
Change in $\Delta P/P$ / Base $\Delta P/P_{cold\ side}$	0.0138 / 0.0298	0.0136 / 0.0234

Power Losses

- Bearing Loss: Bearing losses for both rotors were increased by a factor of two at a given speed with rematch changing speed slightly at given percent power.

	Maximum Power	10% Power
Total Change in Bearing Loss kW (hp) / Total Base Bearing Loss kW (hp)	1.86 (2.49) / 1.88 (2.52)	0.75 (1.0) / 0.78 (1.04)

- Accessories: The accessory power required is increased by a factor of two.

	Maximum Power	10% Power
Change in Access. kW (hp) / Base Access. kW (hp)	1.10 (1.48) / 1.10 (1.48)	0.53 (0.71) / 0.53 (0.71)

- Road Load: Both coefficients in the road load power required equation were multiplied by a factor of 1.1.

- Vehicle Weight: The total vehicle weight was decreased by 90.7 kg (200 lb). It should be noted that this result reflects only the inertial effect of the weight. The reduction in steady-state road-load power required which would be expected is not included.

PRODUCTION ENGINE TOLERANCES

Gas turbine engine thermodynamic and mechanical performance can be broadly altered by variations in production engine tolerances. The problems associated with variations in production engine tolerances can range from degraded fuel economy to reductions in engine life to violent surges that render the engine inoperable. Consequently, it is important that a thorough understanding of the source, impact, and avoidance of these problems exist when preliminary designs leading to cycle selection and engine configuration are being made.

Variations in production tolerances are traceable to many sources. Chief among these are: methods selected for fabrication and assembly, choice of materials, size of the part in question, and level of tolerances required. For a viable automotive gas turbine engine design, mass production techniques must be considered if acceptable unit costs are to be achieved. Generally, this means heavy reliance on castings, complete part interchangeability, minimizing the steps in the fabrication and assembly process, and designing parts that are durable enough to withstand the rigors of the production line. Each of these considerations indicates the desirability of durable parts whose performance is relatively unaffected by wide tolerance bands. Consideration must also be given to field service and repair functions. Components must be designed and toleranced so they can be replaced as easily accessible individual units that will not require entire engine teardowns when only individual components need replacement. An example would be part toleranceing for balance. Replacing a damaged compressor rotor should not require complete removal of the gasifier shaft for dynamic balancing. Components should be toleranced so they can be balanced and replaced as individual units.

Another consideration that affects production tolerance control is the selection of engine materials. Some materials are inherently hard to machine and hold within specified tolerances. Hard materials that accelerate tool wear often are the first parts within an engine to experience out-of-tolerance problems. These materials are often the more costly ones and, consequently, dependency on them should be

avoided if possible. All design approaches that tend to reduce stress levels must be considered if this problem is to be minimized. Multistage component configurations that can function at lower speeds are a good example of how reduced stress levels, common, easy-to-machine materials, and less critical balancing techniques can be utilized to good advantage.

The overall size of a part or special details of the part are also often sources of engine production tolerance problems. Tolerances do not scale as easily as aerodynamic performance. Although close tolerances can be achieved with small parts, the fabrication and quality control steps necessary are usually more expensive in production line volume. Hence engine design approaches that tend to maximize part size will inherently reduce production engine tolerance problems.

The last significant source of production tolerance problems is in the selection of the allowable range of tolerance variations. Designs that are highly dependent on tight tolerances will often be the first to experience problems associated with tolerance deviation. Trends in aerodynamic design that rely on precision high Mach number blading or small controlling throat areas should be avoided to the greatest extent possible.

Since every design represents some form of aerodynamic and mechanical design compromise, the problems associated with production engine tolerances will have to be dealt with. An important factor in reaching the right design compromise is an understanding of the performance or mechanical impact of specified production tolerance deviations. A good understanding of these impacts is largely related to an engine designer's experience in dealing with the aerodynamic and mechanical design interactions. The impact of production tolerances on engine performance is chiefly a function of and varies with the engine components in question. Once a given geometric change can be reliably related to a shift in component performance, the overall effect on the engine operating characteristics can be determined using computerized engine simulation performance projections. Out-of-tolerance dimensions on compressors may not only degrade component efficiency but often shift surge line location. These shifts could result in excessive acceleration time, overtemperature of hot end parts, or violent surge and engine failure. Experience at WRC has produced correlations indicating surgeline sensitivity to inducer blade angle and the variations in impeller tip blade passage height. Similar correlations relating turbine nozzle throat size variations to stage work sharing, exit swirl, and rotor performance have also been made. Many of these cause and effect relationships are analytically predictable but can only be quantified for use as design guidelines when high quality data from a wide range of test programs are available for analysis. Experience in working with small gas turbine engines is essential here.

Once the source and impact of production engine tolerance problems is understood, minimizing their effects follows easily. Approaches that minimize close tolerances and apply them only to critical areas must be considered early in the design process. Multicomponent designs that minimize speeds, stresses, and Mach numbers must be traded off against more sensitive but sometimes simpler approaches. To be effective, engine development programs must utilize prototype parts that are representative of production hardware, lest false impressions of true performance result. Finally, it is important to remember that when long life is required, such

as in automotive engine applications, new part tolerances, no matter how precise, will not be preserved when exposed to the continual abuse of the erosion, corrosion, and thermal cycling that are normal to the engine's duty cycle. Consequently, engine designs that are sensitive to production tolerance variations when new will never endure the test of time and operation.

2.5 RISK ANALYSIS

The IGT powertrain concepts, Table VIII, use essentially identical aerodynamic components, with variations in the method of TIT control, drivetrain, and accessory drive. The risk associated with the selected basic components is discussed first, followed by the powertrain concept risk.

COMPRESSOR

The two-stage centrifugal or axial-centrifugal compressor is very low risk. The rotors operate at low tip speed and stresses, permitting design for high efficiency. Design variations in axial blading, inducer, exducer, and diffuser should permit the tailoring of compressor characteristics to best suit engine requirements.

Compressor design techniques are well established, and performance goals are modest, making a high probability of success. The original design task will include consideration of design variations, so that alternate hardware will be available for evaluation early in the compressor development program. All centrifugal components will be machined to minimize procurement time, and the axial components will be fabricated by WRC, using well-developed, low-cost techniques.

Considering all factors, there should be no problem demonstrating acceptable compressor characteristics prior to initial engine testing.

TURBINE

The aerodynamic design of the turbine section is also well established; the risk is in the TIT chosen and the materials and construction to operate at that temperature.

The inlet temperatures chosen originally for the study were 1311°K (1900°F), representing an integral metal rotor cast in a commercially available high-temperature alloy, and 1644°K (2500°F), a goal for integral ceramic turbine rotors. The 1311°K (1900°F) rotor is low risk, though requiring careful attention to detail design and extensive development to demonstrate adequate durability. The 1644°K (2500°F) ceramic rotor, on the other hand, is very high risk. A practical ceramic rotor has not been demonstrated to date, in spite of extensive effort. Successful demonstration by 1983 may be achieved, but at unknown effort and cost.

An interim selection was made of a composite first stage turbine rotor, with ceramic blades assembled to a metal disk, for operating at 1505°K (2250°F). This reduces risk significantly, since the ceramic must meet the blade mechanical requirements only, not both blade and disk, and all blades can be proof-tested before assembly into a rotor, eliminating early failures. Even with this reduced risk, development effort and cost cannot be defined.

Finally, analysis using preliminary data on an advanced RSR (rapid solidification rate) high-temperature alloy indicated that a TIT of 1422°K (2100°F) or higher is feasible with adequate blade life. The driving cycle fuel economy is well over the specification and is within 4 percent of the 1505°K (2250°F) cycle. Therefore, the metallic rotor in the 1422°K (2100°F) TIT range can meet all requirements at an acceptable risk level.

WRC is also working on advanced turbine rotors in other programs. Information generated from these programs will help support the IGT program and could act as a base for a backup design. One program for the United States Air Force is for dual property turbine wheels, using cast disks with mechanically alloyed oxide dispersion-strengthened, single-crystal, and RSR blades. A second program for TARADCOM is studying ceramic thermal barriers and blade cooling techniques with integral cast rotors. A third program has completed initial demonstration testing of an integral molybdenum rotor.

In addition, turbine rotor and nozzle castings from commercially available alloys can be used to run engines at reduced temperature level and/or life, so that engine development can proceed even with unforeseen difficulty with the selected rotor materials.

COMBUSTOR

After study of many combustor configurations, the catalytic combustor has been chosen for its potential for very low emissions and high efficiency. NASA and others have done extensive testing of catalytic combustors, but the automotive fuel application involves a wide range of conditions, from ambient temperature starting, fast warm-up, minimum idle fuel flow, high temperature cruising, and very rapid transients over the power range, with very low emissions and high efficiency throughout.

For normal steady-state operation, the high-performance recuperator provides high temperature air to the combustor, which then requires a very low overall fuel/air ratio, conditions conducive to catalytic combustion. On the other hand, when the engine is started from ambient conditions, temperatures are low and fuel/air ratio must be relatively high to get a fast start with a practical automotive starting system. Warm-up and transients such as full throttle acceleration and closed throttle deceleration expand the range of operating conditions. At the same time, reliability and durability must meet automotive standards, and production cost must be acceptably low.

The risk involved in developing a catalytic combustor to meet all these conditions is high. Fortunately, the engine arrangement permits extensive changes in combustor configuration since the combustor section is at one end of the engine assembly. Length, diameter, and geometry may be changed without affecting other engine hardware.

All initial development will take place in a combustor test rig, permitting controlled test and development at steady-state operating conditions. The rig will also be used to simulate transients such as starting and acceleration, but final evaluations will be made during powertrain and vehicle development.

Optional combustor designs will be provided to back up the catalytic combustor. A simple can-type combustor with fuel nozzle will be used for initial engine testing and for continuing engine development regardless of combustor problems. A more refined lean premixed, prevaporized combustor will also be designed, with the potential for meeting emission requirements, as a possible development replacement for the catalytic combustor.

HEAT EXCHANGER

The high-performance heat exchanger is required for high fuel economy. The ceramic annular recuperator selected to meet the powertrain goals is a high-risk component, and will require extensive development, including the manufacture of the recuperator. The initial design of the recuperator will include the design and development of the entire manufacturing process to make sure the design and process are compatible. The first pieces fabricated will be small samples of the flow passages, followed by modules using the heat transfer configuration, including the internal manifolds. Initial testing with samples and modules will demonstrate heat transfer and flow characteristics, as well as material capability up to engine pressures and temperatures. After these smaller sections have been developed to demonstrate adequate strength and low leakage, complete recuperators will be fabricated for component and powertrain development tests.

Component testing may disclose problem areas, such as fouling, increased leakage, or structural failure due to temperature gradients and pressure loading. Cyclic tests may also aggravate these problems, but the test program will detect problem areas and guide changes in design, material and processing to improve performance and durability. Fouling problems must be evaluated in the complete engine, since fouling depends primarily on combustion characteristics. The catalytic combustor, after development to high efficiency and very low emissions, is expected to minimize any fouling tendencies.

Alternative heat exchanger designs have been considered as backup to the annular ceramic recuperator, but the resulting product is not as attractive. They would not be used unless a major problem developed, with no solution in sight. These alternative designs are as follows:

1. A modular construction, assembling several smaller modules, could simplify the manufacture and reduce stresses. However, additional hardware is required to assemble the modules, resulting in a bulkier design and additional joints to seal. The annular arrangement is the eventual goal for packaging and vehicle installation.

2. Another alternative is the rotary regenerator. The ceramic rotary regenerator has demonstrated adequate material properties, performance and life, and can be integrated into the powertrain design. The powertrain packaging and vehicle installation are entirely different, requiring extensive redesign throughout.

POWERTRAIN CONCEPT NO. 1

The added risk with this dual rotor engine with free power turbine is in the variable power turbine nozzle mechanism. This system has been developed with acceptable durability and reliability at 1311°K (1900°F) TIT, and will require development for the higher 1422°K (2100°F) TIT. Provisions have been made in the design for cooling the nozzle mechanism, using compressor discharge air to minimize additional development and risk. The engine can still operate with nozzle mechanism problems, so engine development can proceed.

The three-speed automatic transmission (without torque converter) is adapted from current automotive production, at almost no risk for durability and reliability. It will require some redesign and development to achieve smooth shifts with the turbine powertrain characteristics, but should always be operable for vehicle development.

POWERTRAIN CONCEPT NO. 2

The slip clutch power transfer system used with this dual-rotor engine is very low risk. The clutch can be designed for adequate life at the torque and speed ratios required for turbine temperature control, as well as high lock-up torque capacity for engine braking.

POWERTRAIN CONCEPT NO. 3

This dual-rotor powertrain is the same as concept No. 1 except for the axial-centrifugal compressor in place of the two-stage centrifugal compressor. Risk is considered comparable and acceptable, as discussed in the compressor component section.

POWERTRAIN CONCEPT NOS. 4-8

These dual-rotor engines with free power turbine are similar to concept No. 1 except for changes in compressor pressure ratio and turbine inlet temperature. The compressor pressure ratio should not significantly affect risk since the analytical procedure and criteria for the compressor and turbine stages included consistent pressure ratio effects in the performance analysis.

The effect of turbine inlet temperature has a great effect on risk, as noted in the turbine component risk discussion. Operation at 1644°K (2500°F) requires a ceramic turbine rotor, considered very high risk for the planned development schedule. Reducing TIT to 1505°K (2250°F) reduces risk, although still not to an acceptable level, by permitting a composite turbine rotor, with ceramic blades assembled to a metal disk. Metal turbine rotors do not have the problems of ceramic or ceramic-bladed rotors. Commercially available alloys have been very acceptable in the 1311°K (1900°F) range, and the advanced RSR high-temperature alloy should be capable of 1422°K (2100°F) TIT with acceptable risk.

POWERTRAIN CONCEPT NO. 9

Combining the selected components into the single-rotor powertrain introduces little additional risk except for the variable-ratio transmission. The Orshansky hydromechanical transmission was chosen for fuel economy analysis, since it has had extensive development with the piston engine. It should be readily adaptable to the single-rotor turbine engine at low risk, but requires redesign to reduce production cost, along with development work to reduce noise. Mechanical variable-ratio transmissions such as the Excelermatic may have lower production cost but have not demonstrated performance and durability to meet turbine requirements.

POWERTRAIN CONCEPT NO. 10

This dual-rotor engine with free power turbine is similar to concept No. 1 except for the regenerator in place of the recuperator. As noted in the heat exchanger component discussion, the ceramic rotary regenerator has demonstrated adequate performance and life and is a low-risk backup heat exchanger.

2.6 POWERTRAIN DESIGN STUDIES

Powertrain design studies performed as part of Task II consisted of sketches and layouts of component arrangements (primarily as engine cross section drawings), outline drawings of the candidate powertrain assemblies, and installation design studies of the powertrain assemblies in the selected vehicle, the 1978 American Motors Concord 2-door sedan.

POWERTRAIN CONCEPT DESIGN STUDIES

Preliminary sketches and layouts were made of component arrangements to explore the different candidate powertrains. These included many layouts of rotor systems, single and dual, to study the mechanical design requirements that accompanied the aerothermodynamic design and selection of the turbomachinery.

Many studies started from the preliminary powertrain arrangement sketched in Figure 55. This is a dual-rotor system using the variable power turbine nozzle for turbine temperature control. The sketch is based on a single-stage centrifugal compressor and two axial turbine stages using four rectangular recuperator modules boxing the turbine section. A can-type combustor was used with conventional fuel injection. The two rotors were on the same axis with the power turbine drive to the reduction gear at the rear of the engine. The powertrain assembly based on this arrangement, Figure 56 (P7810), was used for vehicle installation studies.

Variations on this four-recuperator module arrangement were made to represent a single rectangular recuperator module, Figure 57 (P7821), and a single rotary regenerator, Figure 58 (P7812). Another version, Figure 59 (P7828), uses an annular recuperator of the stacked plate design and a can-type combustor with a volute to the turbine inlet.

ANNULAR RECUPERATOR POWERTRAIN STUDIES

The recuperator concept studies had developed the annular recuperator design with spiral plates to form a counterflow recuperator with Z-shaped integral manifolds on

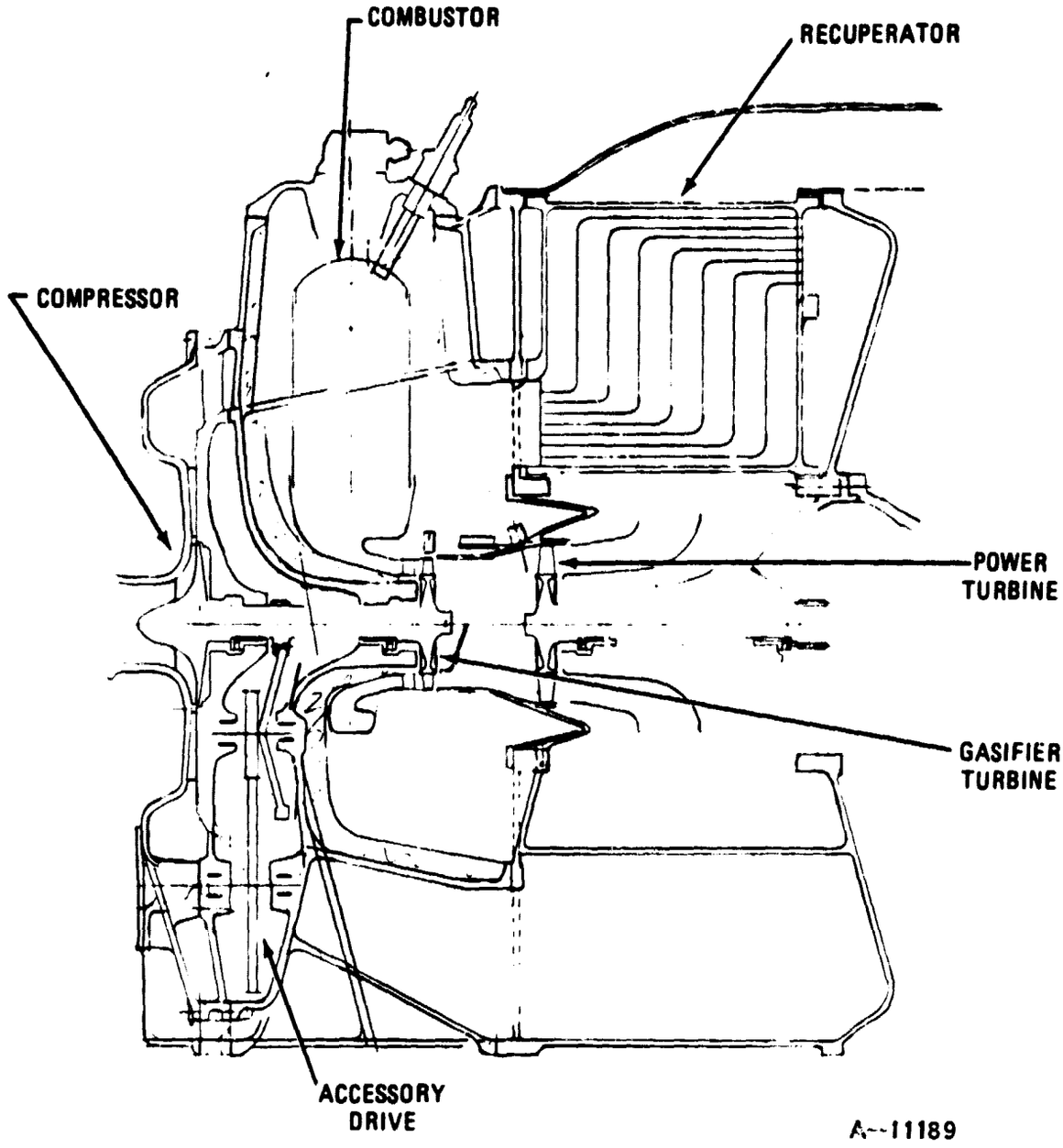

Figure 55. Dual-Rotor Engine Arrangement - Four Recuperator Modules

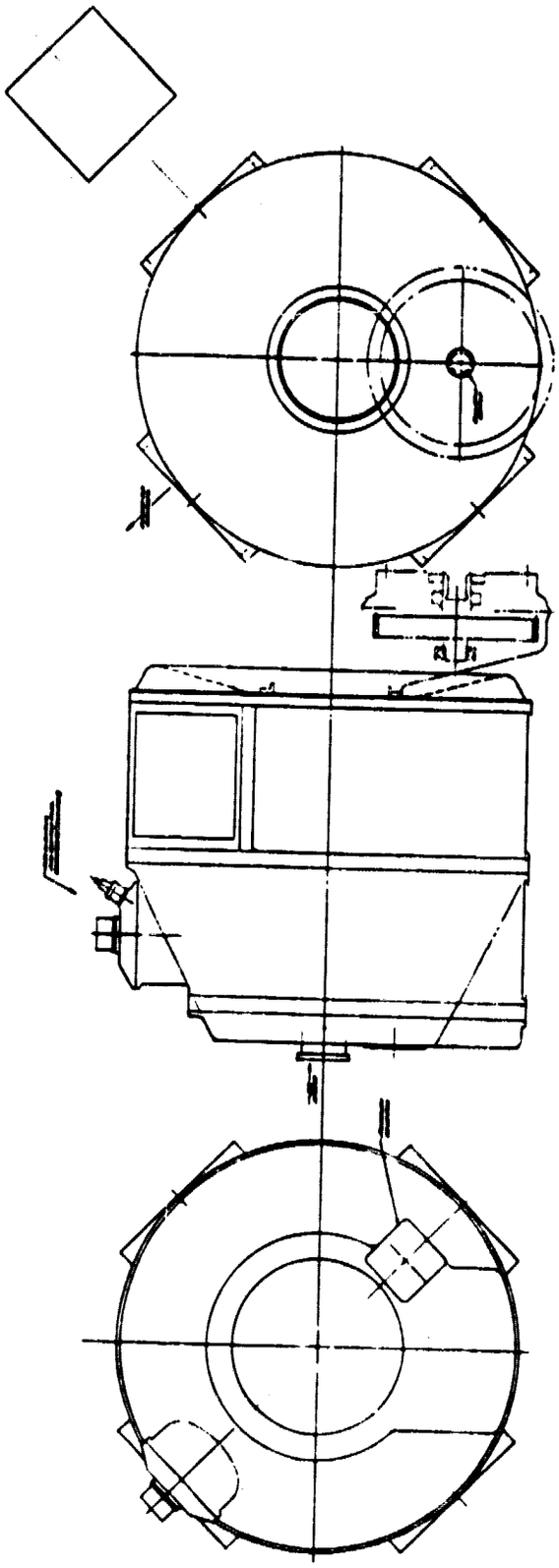

A-11181

Figure 56. Dual-Rotor Engine - Four Recuperator Modules

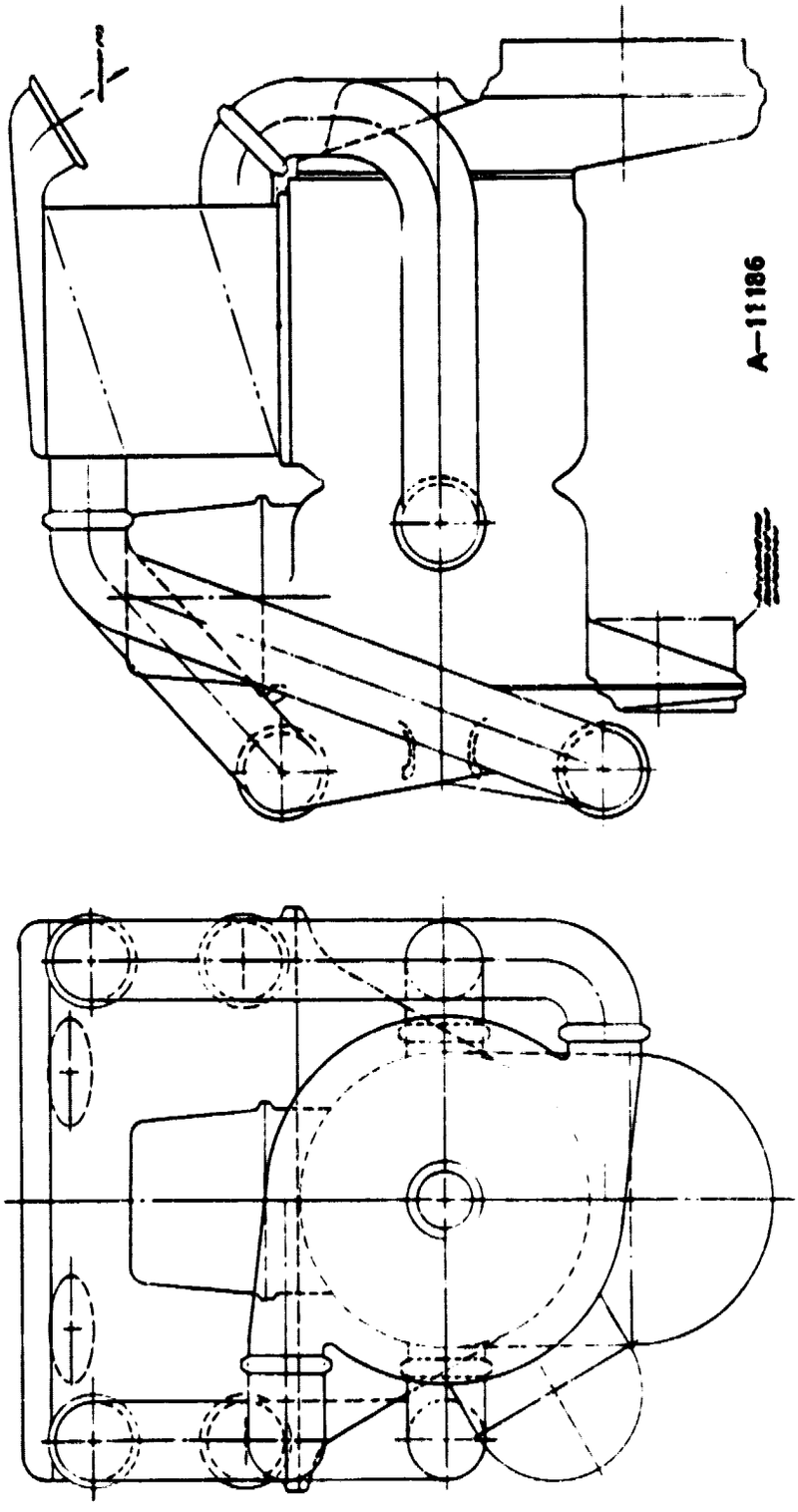

Figure 57. Dual-Rotor Engine - Single Rectangular Recuperator

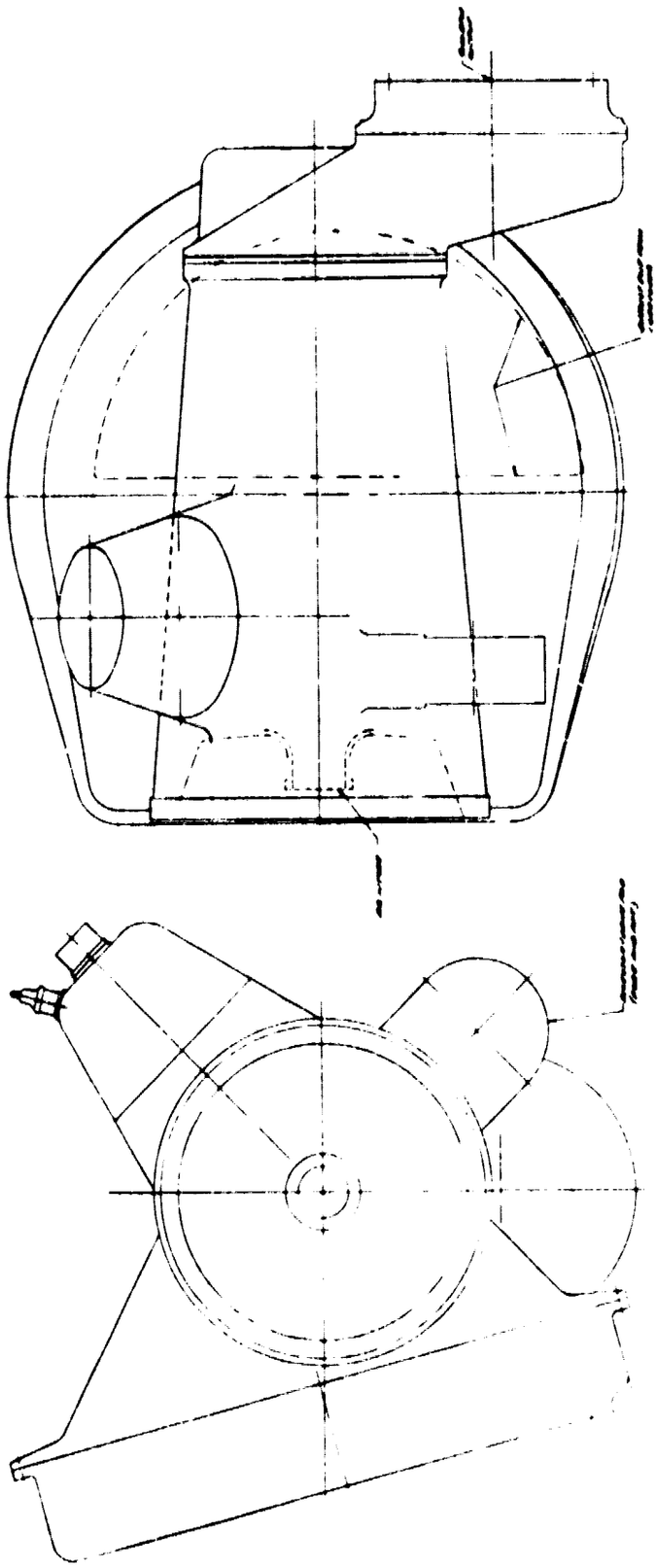

Figure 58. Dual-Rotor Engine - Single Rotary Regenerator

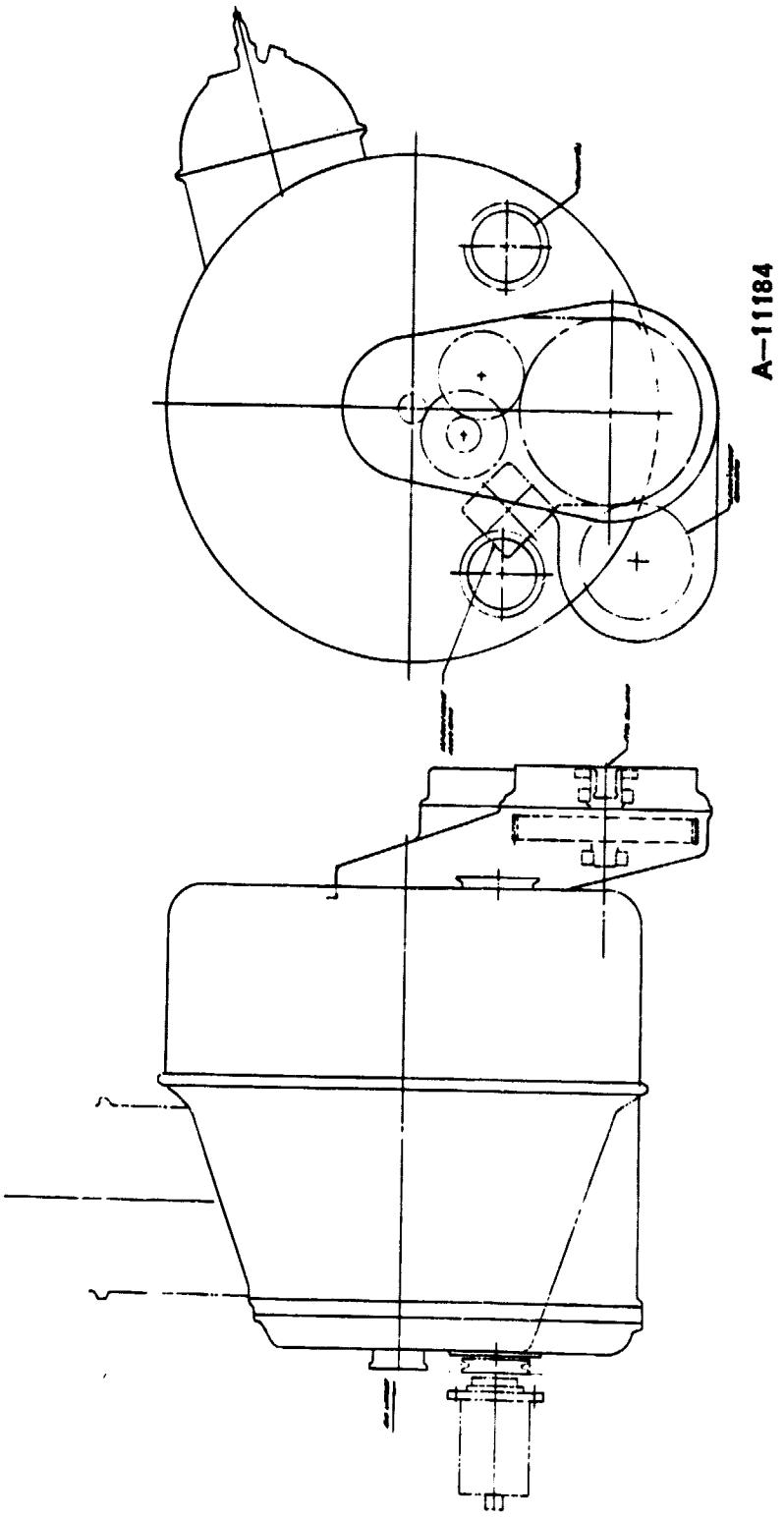

Figure 59. Dual-Rotor Engine - Annular Recuperator

the high pressure side. This construction can be used with different orientations, resulting in different engine flow paths. A matrix approach was used to explore all possible flow paths.

Figure 60 shows the possible flow paths with the flow direction in the turbine section away from the compressor, used in all powertrain arrangements described previously. Eight flow paths are possible, with flow radial or axial, either direction, and high-pressure inlet on either side. All eight arrangements require the flow paths to cross at one point. The cold high-pressure path crossing the cold low-pressure path can be handled by ducting compressor discharge air across or around the engine exhaust. The high-pressure hot path (recuperator high-pressure outlet) crossing the low-pressure hot air (power turbine outlet) is considered impractical to accommodate, since it must be accomplished inside the hot section of the engine, with both paths connected to the recuperator, and with nearly maximum pressure difference across pressure walls and joints.

A second group of eight flow paths is shown in Figure 61 with the flow in the turbine section toward the compressor. In this case, four of the flow paths do not cross; the other four cross on both cold and hot paths, and are again not considered practical.

Of these 16 arrangements, eight arrangements with the recuperator flow in the axial direction have high-pressure air on the outside and inside diameters. By judicious location of joints or seals to the high-pressure manifolds, the recuperator ring can be pressurized to place the ring as a structure in compression. This is considered advantageous, particularly with the ceramic recuperator, minimizing the formation and propagation of cracks.

In comparing the 16 possible flow paths, two are most desirable, 7B and 8B, with external pressurizing and no flow paths crossing, permitting annular connecting ducts. Of these two, flow path 7B permits close spacing between compressor and turbine sections, favoring shaft dynamics, and was used for the following studies.

Figure 62 sketches the component arrangement for the selected flow path, using a reduction gear train between the compressor and power turbine. A dual-rotor system is used, with the first stage turbine driving the compressor through a concentric power turbine rotor. The reduction gear is located behind the two-stage centrifugal compressor, with a separate accessory drive gearbox at the compressor inlet. A return flow annular catalytic combustor is shown, with centrifugal fuel injection from a slinger on the gasifier turbine rotor, and with a precombustor inside the catalytic combustor.

Other design variations considered in this arrangement included different catalytic combustor concepts, axial relocation of the recuperator, common gearcase including accessory drive and output gear trains, and output shaft drive to either end of the engine. These design studies culminated in the final engine configuration described in Task III.

VEHICLE INSTALLATION STUDIES

Installation studies by AM General concentrated on the conventional front-engine installation with rear-axle drive in the 1978 American Motors Concord 2-door sedan.

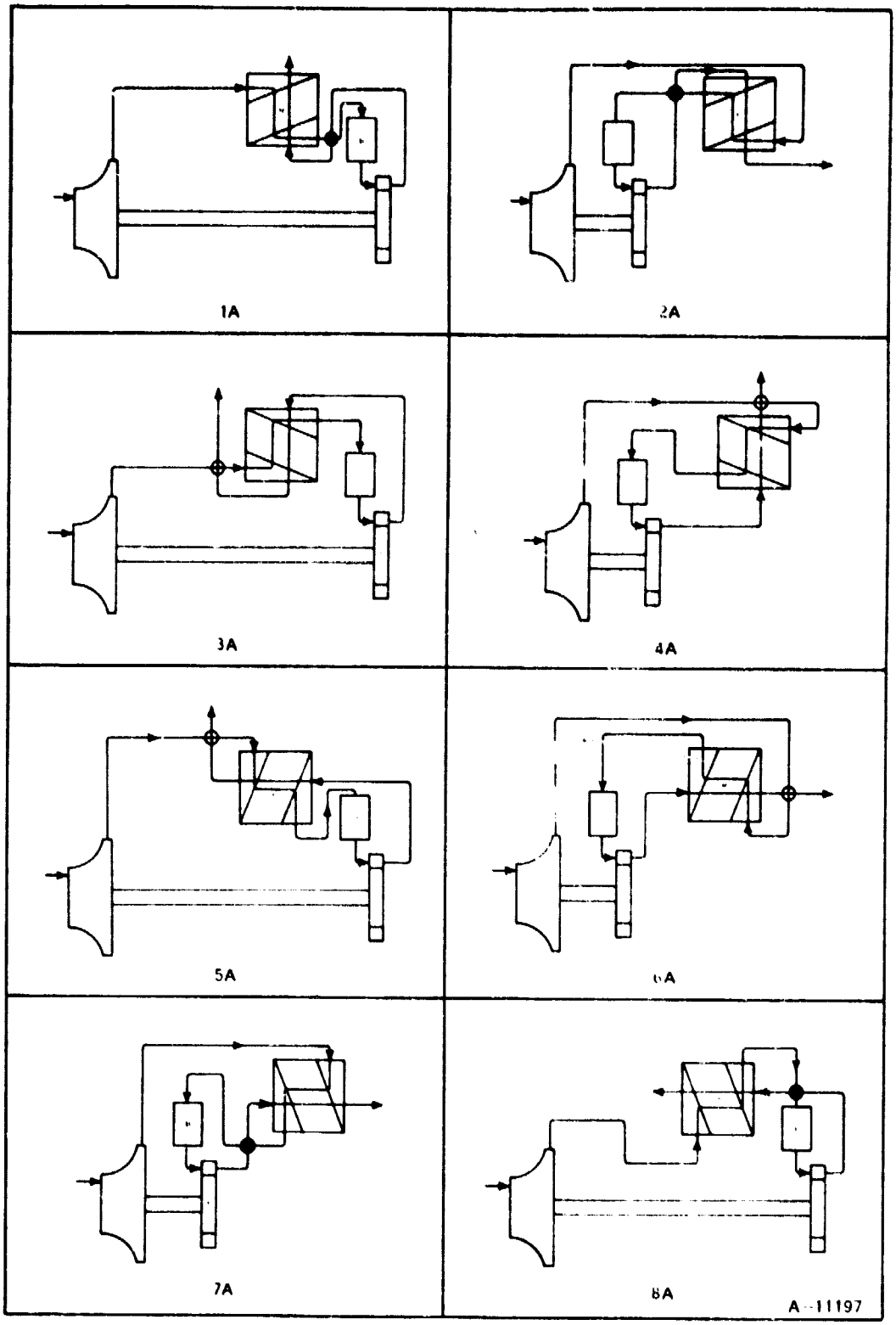

Figure 60. Flow Paths, Turbine Flow Direction Away From Compressor

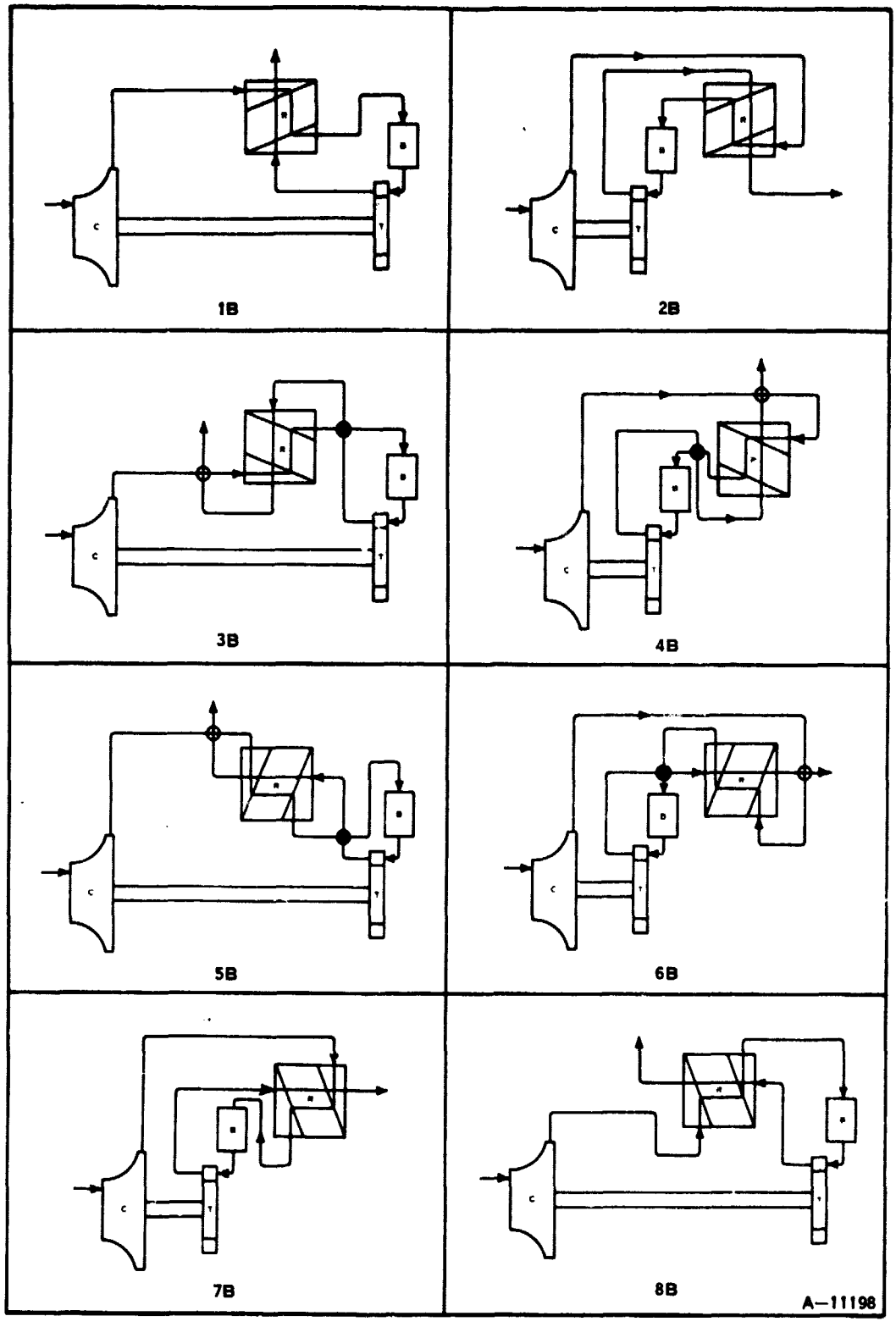

Figure 61. Flow Paths, Turbine Flow Direction Toward Compressor

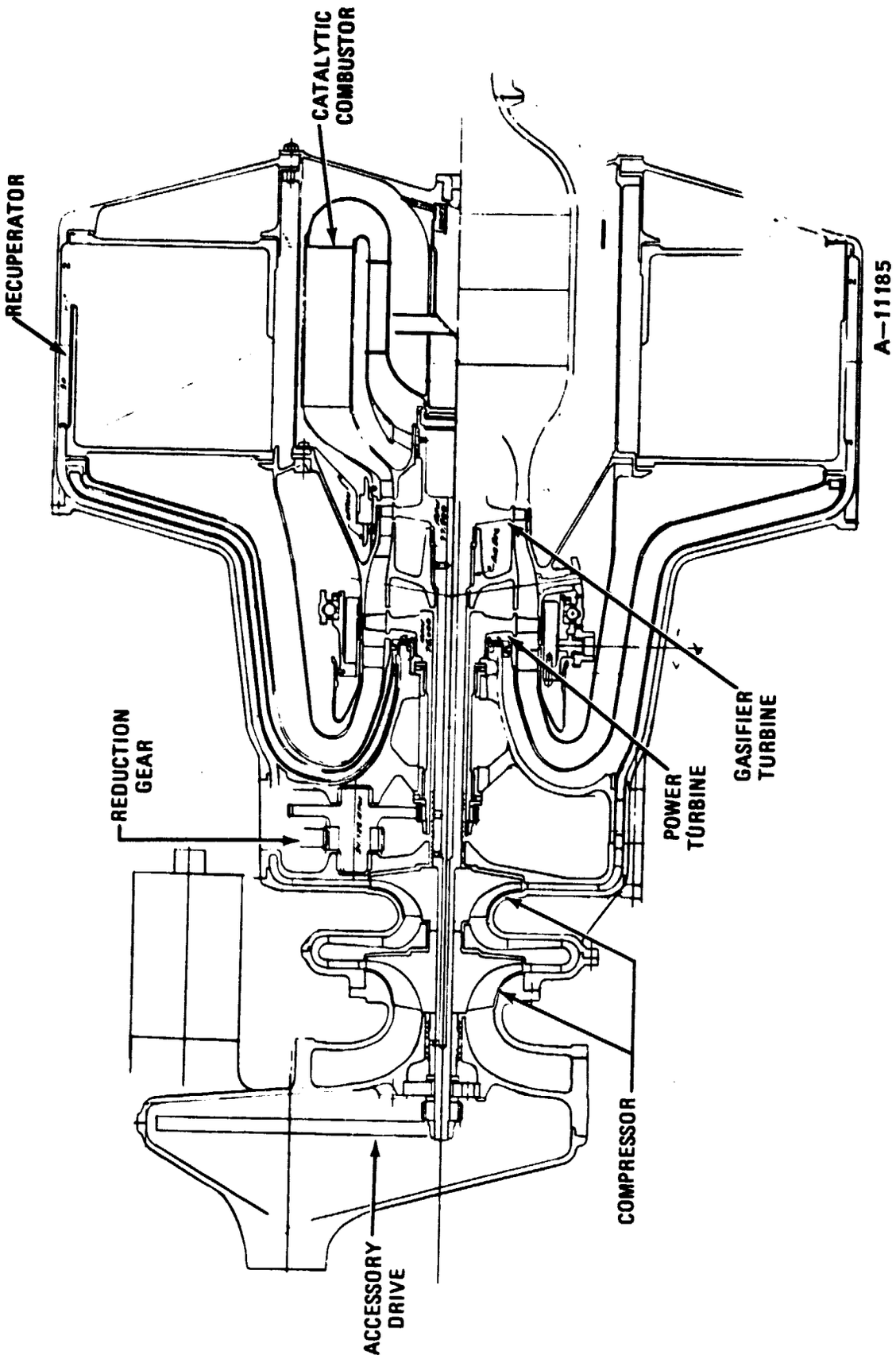

Figure 62. Component Arrangement for Selected Flowpath

Preliminary studies were made using the dual-rotor engine with four recuperator modules, Figure 56. The installation shown in Figure 63 meets most functional requirements. The air intake is located at the front of the engine compartment, with the exhaust ports at the rear to simplify both systems. The accessories are mounted at the front for good accessibility. The alternator and air conditioning compressor are driven from a power take-off from the power output drive to the transmission. The power steering pump is belt-driven from a separate accessory shaft. This drive requires the battery to supply all required current when idling and with transmission not in neutral.

Installation studies then continued on the dual-rotor engine arrangement of Figure 62 with the concentric annular recuperator and catalytic combustor. With the engine air inlet toward the rear, Figure 64, the engine fits into the compartment with direct connection to the transmission and drive line. The air intake duct for this configuration is long and complex and interferes with servicing the rear-mounted accessories. The exhaust is at the front of the engine, and routing the pipes to the rear of the vehicle also poses serious problems.

An alternate installation was studied, Figure 65, with the engine inlet at the front. This simplifies the intake and exhaust systems, and front-mounted accessories are easier to service. The output shaft must be moved outboard to pass the recuperator; reduction in recuperator diameter and relocation fore and aft eased this installation problem. An accessory drive gear train in the same gearcase as the output reduction gear was then considered for improving vehicle accessory location, drive, and servicing. This arrangement was selected and refined during Task III.

2.7 PRODUCTION COST COMPARISON

The IGT powertrain concepts, Table VIII, use essentially identical aerodynamic components, but have different drivetrains, accessory drives, and methods of turbine temperature control. The cost comparisons between the different concepts are as follows.

POWERTRAIN CONCEPT NO. 1 - DUAL-ROTOR ENGINE WITH VARIABLE POWER TURBINE NOZZLE

This powertrain concept is used as the base for comparing the other concepts. Powertrain concept Nos. 4 through 8 are similar in cost.

POWERTRAIN CONCEPT NO. 2 - DUAL-ROTOR ENGINE WITH SLIP CLUTCH POWER TRANSFER

This powertrain concept has the simpler fixed geometry power turbine nozzle, compared to the variable nozzle system for the base engine. In place of the nozzle mechanism, there is a clutch and shaft interconnecting the gasifier accessory drive and the power turbine drivetrain. This mechanism, along with its actuator and control functions, may cost slightly less than the variable nozzle system, but the difference is estimated as less than 5 percent of the powertrain cost.

POWERTRAIN CONCEPT NO. 3 - DUAL-ROTOR ENGINE WITH AXIAL-CENTRIFUGAL COMPRESSOR

This powertrain concept is the same as the base, concept No. 1, except for the axial-centrifugal compressor in place of the two-stage centrifugal compressor.

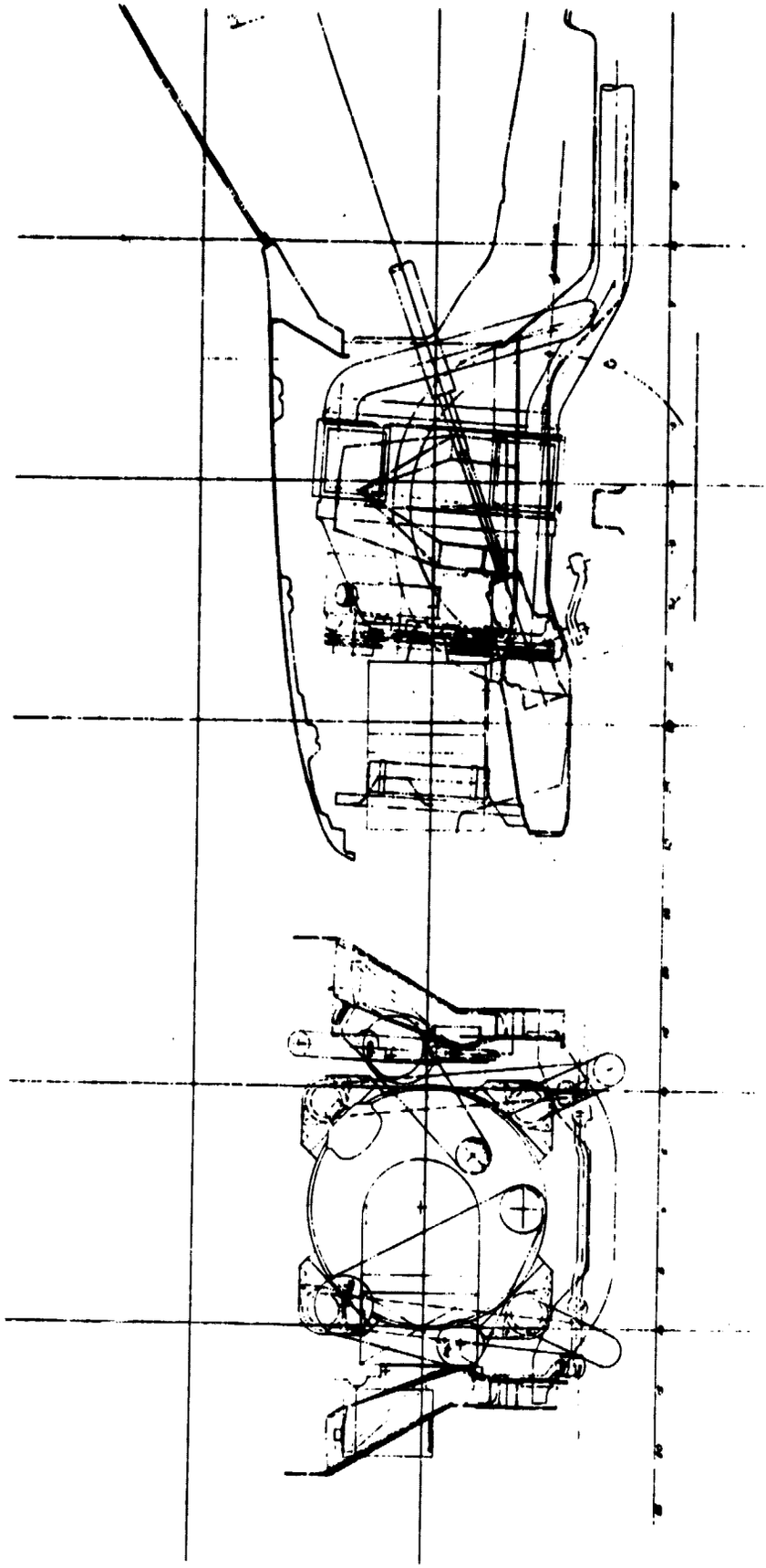

Figure 63. Preliminary Dual-Rotor Powertrain Installation Study

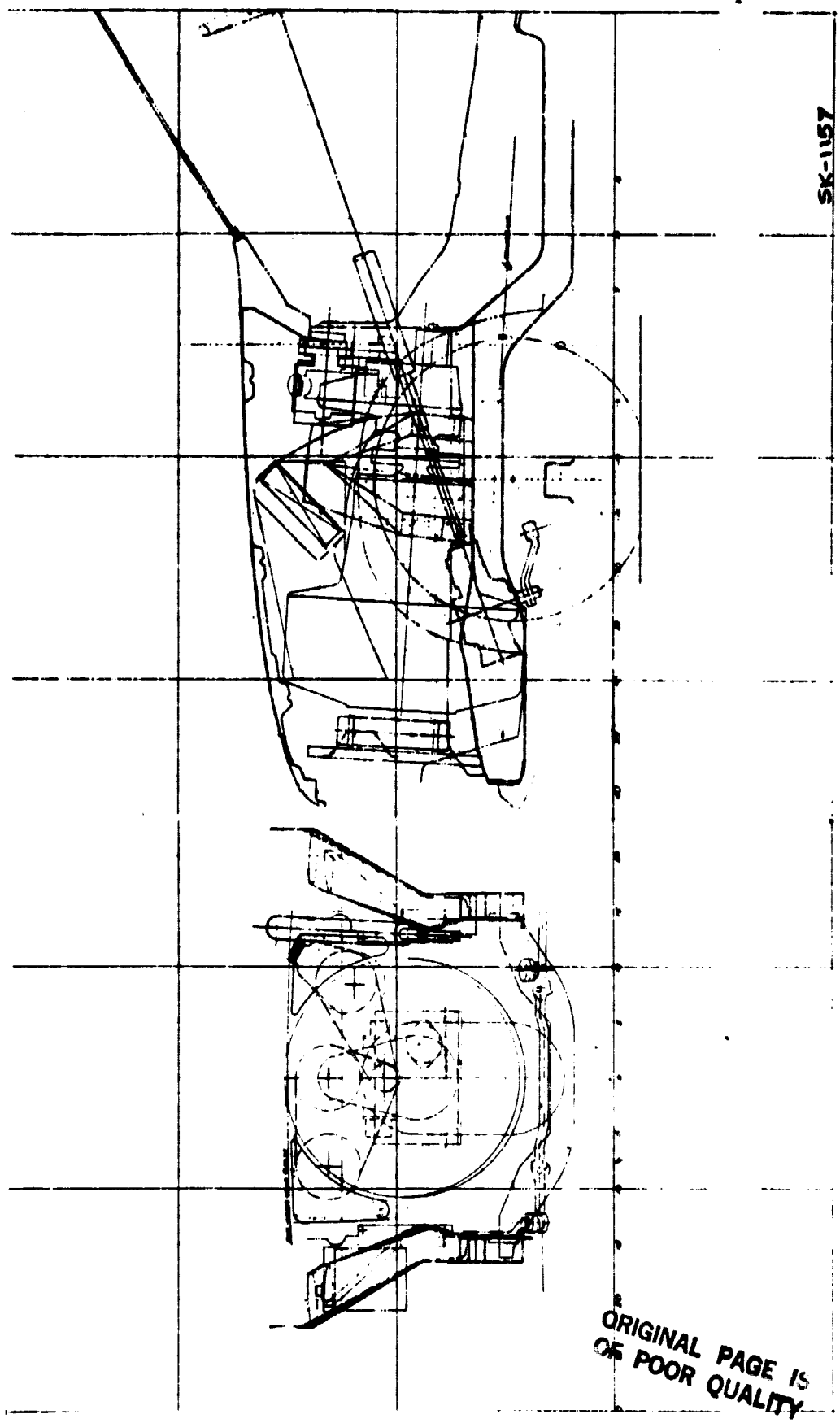

Figure 64. Installation of Dual-Rotor Powertrain, Rear Air Inlet

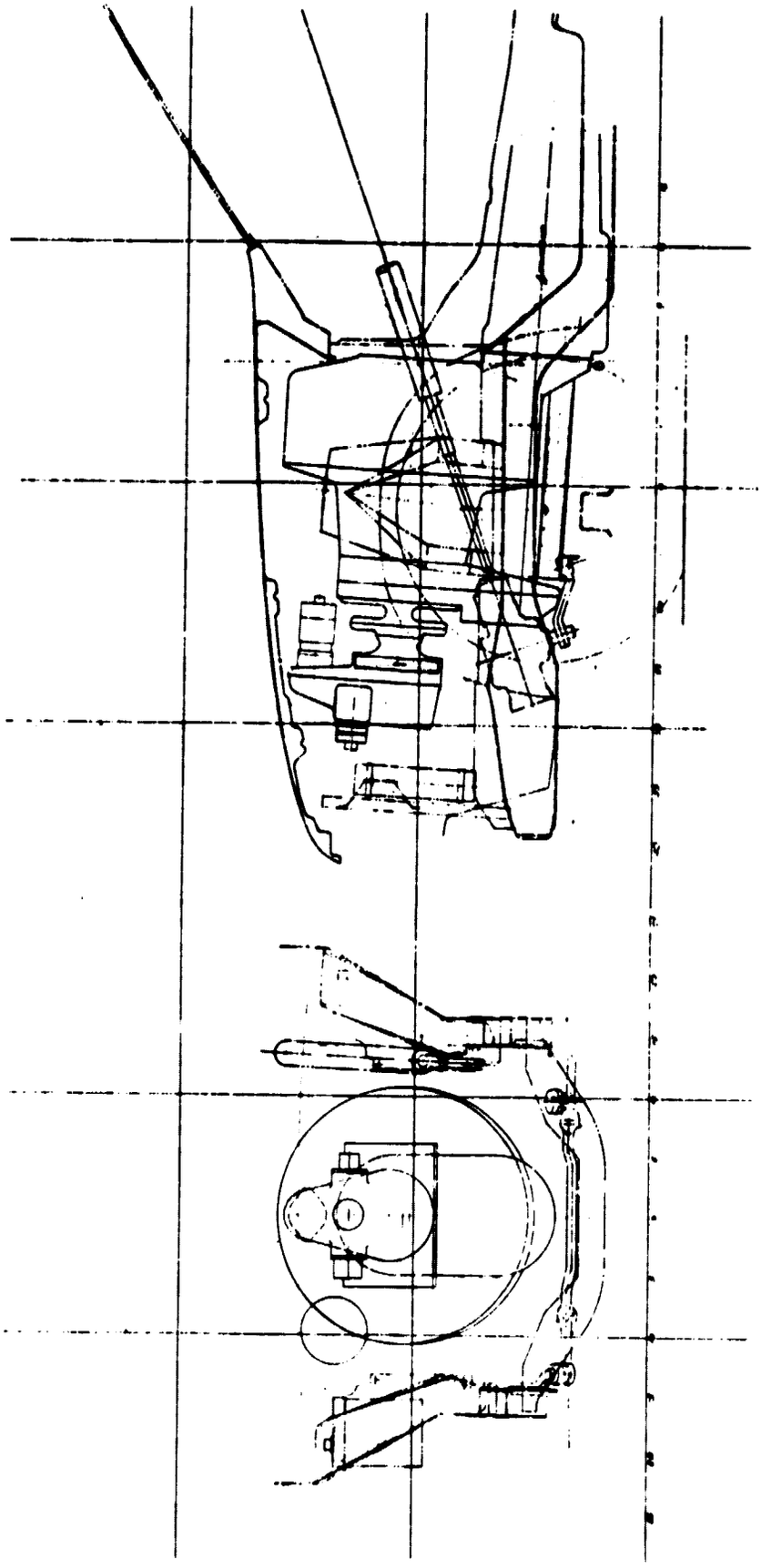

Figure 65. Installation of Dual-Rotor Powertrain, Front Air Inlet

Using the low-cost axial compressor fabrication techniques developed by WRC, the cost of the axial section should be on the same order as that of the centrifugal stage it replaces.

POWERTRAIN CONCEPT NO. 9 - SINGLE-ROTOR ENGINE

The single-rotor powertrain obviously has fewer bearings and gears.

	Dual-Rotor	Single-Rotor
Rotor System	2	1
Rotor Bearings	5	3
Rotor Thrust Bearings	2	1
Drivetrain Gears	5	5
Drivetrain Bearings	6	6
Accessory Gears	5	0
Accessory Bearings	6	0
Gear Case	1	1

The single-rotor engine also has the simpler fixed geometry power turbine nozzle, compared to the variable nozzle system for the base engine, complete with individual blades, actuating mechanism, actuator, and control functions.

The variable ratio transmission is expected to cost more than the three-speed automatic transmission. The Orshansky hydromechanical transmission used for this study has undergone production design studies to reduce cost, resulting in a relative cost 17 percent more than the three-speed automatic transmission with torque converter. Since the base engine omits the converter, the total cost penalty is about 35 percent.

Combining all these differences results in a cost savings for the single-rotor engine on the order of 10 percent.

POWERTRAIN CONCEPT NO. 10 - DUAL-ROTOR ENGINE WITH REGENERATOR

This powertrain concept is the same as the base, concept No. 1, except for the rotary ceramic regenerator in place of the ceramic recuperator. The ceramic regenerator core should cost less than the ceramic recuperator, but it requires rubbing seal assemblies and drive components, as well as a more complex engine housing with lateral ducts between the turbomachinery and the regenerator. The net effect is a cost penalty for the regenerator on the order of 10 percent of the powertrain cost.

2.8 POWERTRAIN SELECTION CRITERIA

The concept selection criteria were based on the capability of meeting the objectives of the IGT powertrain program. These objectives are summarized in Table XV, along with the criteria established by the contract. The approach used in this study is indicated and discussed below.

TABLE XV. POWERTRAIN CONCEPT SELECTION CRITERIA

Objective	Criteria	Approach
1. Fuel economy	CDC - 9.99 km/l (23.5 mpg)	Engine rating Part load SFC Idle fuel flow
2. Production engineering readiness	ASAP	1986
3. Reliability and life	Comparable	First turbine life = 160,000 km (100,000 miles)
4. Driveability	Acceptable	Variable PTN Gasifier inertia Electronic control
5. Emissions standards	0.25/2.11/0.25 g/km (0.4/3.4/0.4 g/mi)	Catalytic combustor
6. Noise Safety	Legislation Fail-safe	Inlet, gears Burst protection
7. Initial cost Life cycle cost	Competitive No greater than ICE	Simplified design Minimum fuel consumption

FUEL ECONOMY IMPROVEMENT

A 20 percent improvement powertrain thermal efficiency compared to a conventional 1976 powertrain is to be determined by at least a 20 percent improvement in the 1976 combined cycle fuel economy of 8.33 km/l (19.6 mpg). This study has optimized the cycle for best SFC at very low power. Further work was done in Task III on minimizing the power rating and idle fuel flow.

PRODUCTION ENGINEERING READINESS

The powertrain should be ready to enter the production engineering phase of development as soon as practicable. The development plan generated in Task IV indicated this could be as early as 1986.

RELIABILITY AND LIFE

These features were compared to powertrains currently on the market. This is a challenging objective, requiring rigorous design and extensive development activity. For the concepts being considered, the first-stage turbine rotor was the

primary determinant for life. The turbine design had to aim for at least 3000 hours or 160,000 km (100,000 miles) of severe vehicle operation, including 300 hours at maximum gasifier speed.

DRIVEABILITY

Acceptable driveability has been demonstrated using the variable power turbine nozzle for rapid control of output torque and a low-inertia gasifier rotor for fast response acceleration. The electronic control has the flexibility of combining all required control functions into a workable system.

EMISSIONS STANDARDS

The emissions standards of 0.25 g/km (0.4 gm/mi), 2.11 g/km (3.4 gm/mi), 0.25 g/km (0.4 gm/mi) for HC/CO/NO_x have been approached with several types of experimental gas turbine combustors. The catalytic combustor has been chosen for its unsurpassed potential for low emissions, but the engine arrangement can accommodate other combustion systems. This inherent flexibility is considered important.

NOISE AND SAFETY

Satisfactory noise control has been demonstrated in automotive turbines, and the basic principles are considered in this study. This includes inlet silencing, low velocity heat exchanger after the turbine exhaust, good quality gears, and well-developed rotor systems. Safety aspects will include fail-safe features, with any rotor failure being contained.

INITIAL COST AND LIFE CYCLE COST

Competitive initial cost and life cycle cost no greater than the conventionally powered vehicle will be difficult to meet. The basic engine design must be kept simple, with few parts, using low-cost materials wherever possible. Life cycle cost will be determined primarily by fuel consumption, since preliminary estimates indicate total fuel cost will be on the order of five times the initial powertrain cost. Maintenance costs are expected to be low compared to the piston engine, equivalent perhaps to half the initial powertrain cost. This indicates the importance of the objective of fuel economy improvement, and directs the major analysis, design and development effort toward that goal.

2.9 POWERTRAIN CONCEPT SELECTION

The dual-rotor turbine with the variable power turbine nozzle was selected for powertrain optimization during Task III. The comparison and elimination of the other powertrain concepts in Table IX are summarized below.

POWERTRAIN CONCEPT NO. 2 - DUAL-ROTOR ENGINE WITH SLIP CLUTCH POWER TRANSFER

Engine 2 with slip clutch power transfer was eliminated due to the higher SFC at part-load (18 percent at 10 percent power) compared to Engine 1, resulting in significantly lower fuel economy. The production cost saving of less than 5 percent is not enough to compensate for the higher fuel consumption.

POWERTRAIN CONCEPT NO. 3 - DUAL-ROTOR ENGINE WITH AXIAL-CENTRIFUGAL COMPRESSOR

The comparison of Engine 3 with the axial-centrifugal compressor to Engine 1 with the two-stage centrifugal compressor shows about the same fuel economy and cost. The two-stage centrifugal compressor was selected for powertrain optimization during Task III, but development of both types of compressors is proposed until detailed characteristics can be thoroughly defined and compared before making the final selection.

POWERTRAIN CONCEPT NO. 9 - SINGLE-ROTOR ENGINE

The single-rotor turbine Engine 9 was eliminated by fuel economy 5.3 percent below that of the dual-rotor Engine 8 with variable power turbine nozzle. A 25 percent lower production cost would be required to make life cycle cost comparable. This cost difference is not considered attainable with current and near-term technology.

In addition, extensive development is required for the variable ratio transmission, primarily noise and cost with the hydromechanical unit and durability with the mechanical variable ratio unit.

POWERTRAIN CONCEPT NO. 10 - DUAL-ROTOR ENGINE WITH REGENERATOR

Engine 10 with regenerator was estimated to have 8 percent lower fuel economy than Engine 8 with the ceramic recuperator. In addition, the recuperator has the potential for reliability and durability with no service or maintenance.

POWERTRAIN CONCEPTS WITH DUAL ROTOR ENGINE AND VARIABLE POWER TURBINE NOZZLE

Engines 1, 4, 5, 6, 7, and 8 are all dual-rotor engines with variable power turbine nozzle and a ceramic recuperator. Engines 1, 4, and 5 were used to select compressor pressure ratio, and Engines 4, 6, 7 and 8 compared TIT over the range of 1311°K (1900°F) to 1644°K (2500°F).

Engine 8 at 1422°K (2100°K) was selected for further powertrain optimization during Task III. This represents the highest practical TIT for an advanced nickel base alloy wheel, and exceeds the goal of 20 percent improved fuel economy. Higher TIT has potential for even better fuel economy, but requires the development of a ceramic turbine rotor considered too high a risk to accomplish in the specified time schedule.

3.0 TASK IIIA - POWERTRAIN OPTIMIZATION AND PERFORMANCE

3.1 PERFORMANCE ANALYSIS

COMPONENT CHARACTERISTICS

Compressor

The two-stage centrifugal compressor is the final ICT engine configuration. It was selected over the multiple-stage axial compressor coupled with a single-stage centrifugal compressor based on greater confidence in its ability to meet IGT performance requirements. This confidence arises in part from the greater centrifugal compressor data base at typical IGT airflow and pressure ratios. Both overall performance and stage range of operation and matching were considered in this decision.

Both the two-stage centrifugal and the axial-centrifugal compressor, because of their small geometric dimensions, are very sensitive to clearance between the stationary shroud and rotor. The centrifugal compressor clearance can be adjusted to minimize the part-to-part variation in production by adjusting the axial position of the impeller relative to the shroud. Because the radial clearance is, for the most part, unadjustable, the axial rotors will suffer performance irregularities in production of a much larger magnitude than for the two-stage centrifugal. This could result in not meeting minimum IGT engine performance. There are also more stages to match on the axial-centrifugal compressor which could adversely affect compressor performance due to part variation in production.

The flowpath for the two-stage centrifugal compressor is shown in Figure 66. The performance maps for each stage of the IGT compressor configuration are presented in Figures 67 and 68 with the overall map shown in Figure 69.

Turbine

The flowpath for the two-stage axial turbine with variable power turbine nozzle is shown in Figure 70. The first stage turbine performance characteristics are shown in Figure 71, and the second stage turbine performance is shown in Figure 72 with the variable nozzle losses included. The nozzle blades are set at the design angle for the nominal flow area. Performance was also estimated over a range of nozzle flow area to permit calculation of powertrain performance using the variable nozzle to control TIT.

Combustor

The flowpath through the precombustor and catalytic combustor is shown in the engine section views in Figure 73. The performance characteristics were based on the Powertrain Performance Analysis Assumptions used in Task II.

Recuperator

The flowpath through the recuperator is shown in Figures 74 and 75. The performance characteristics were calculated based on the procedure outlined in the Powertrain Performance Analysis Assumptions.

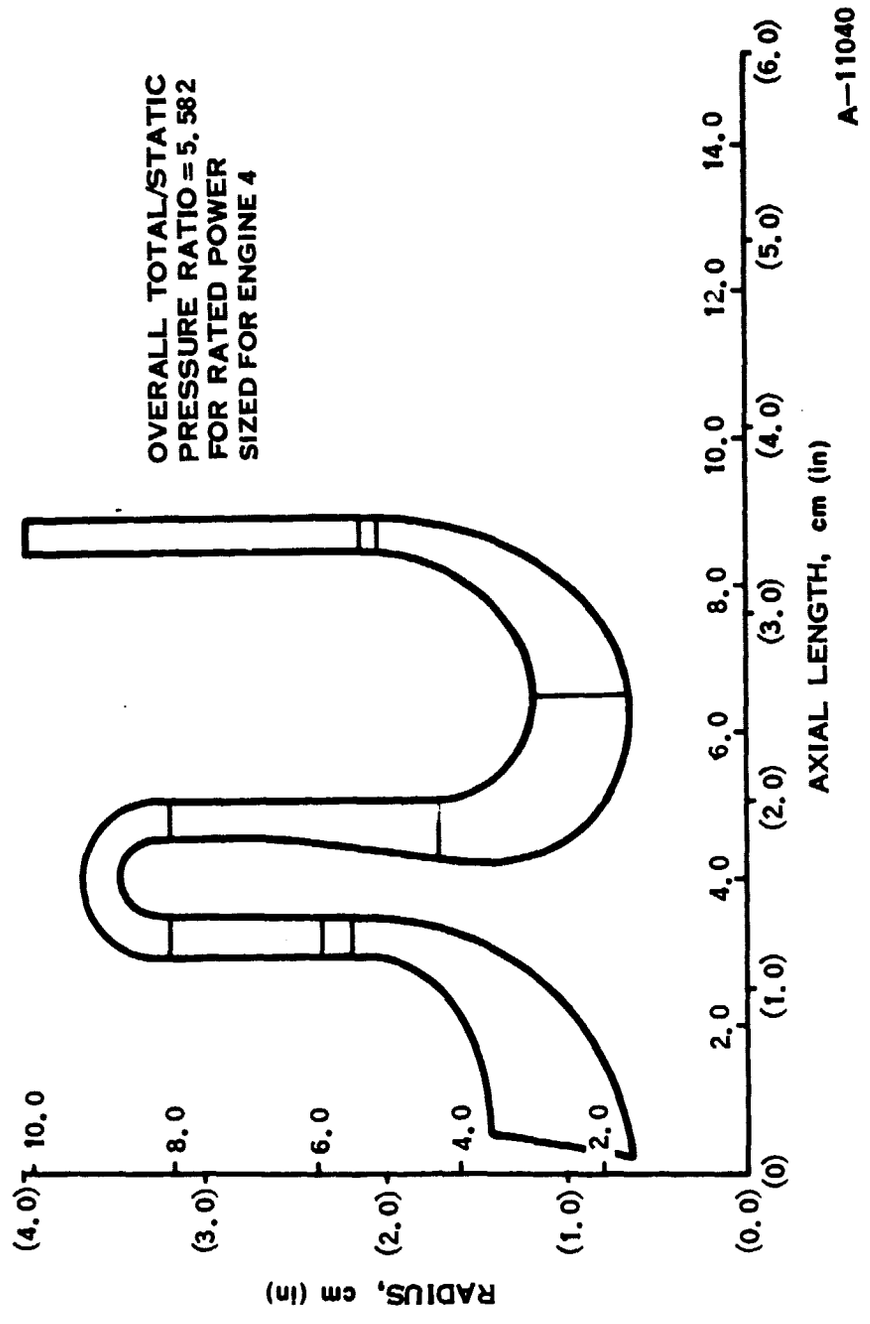

Figure 66. Two-Stage Centrifugal Compressor Flowpath

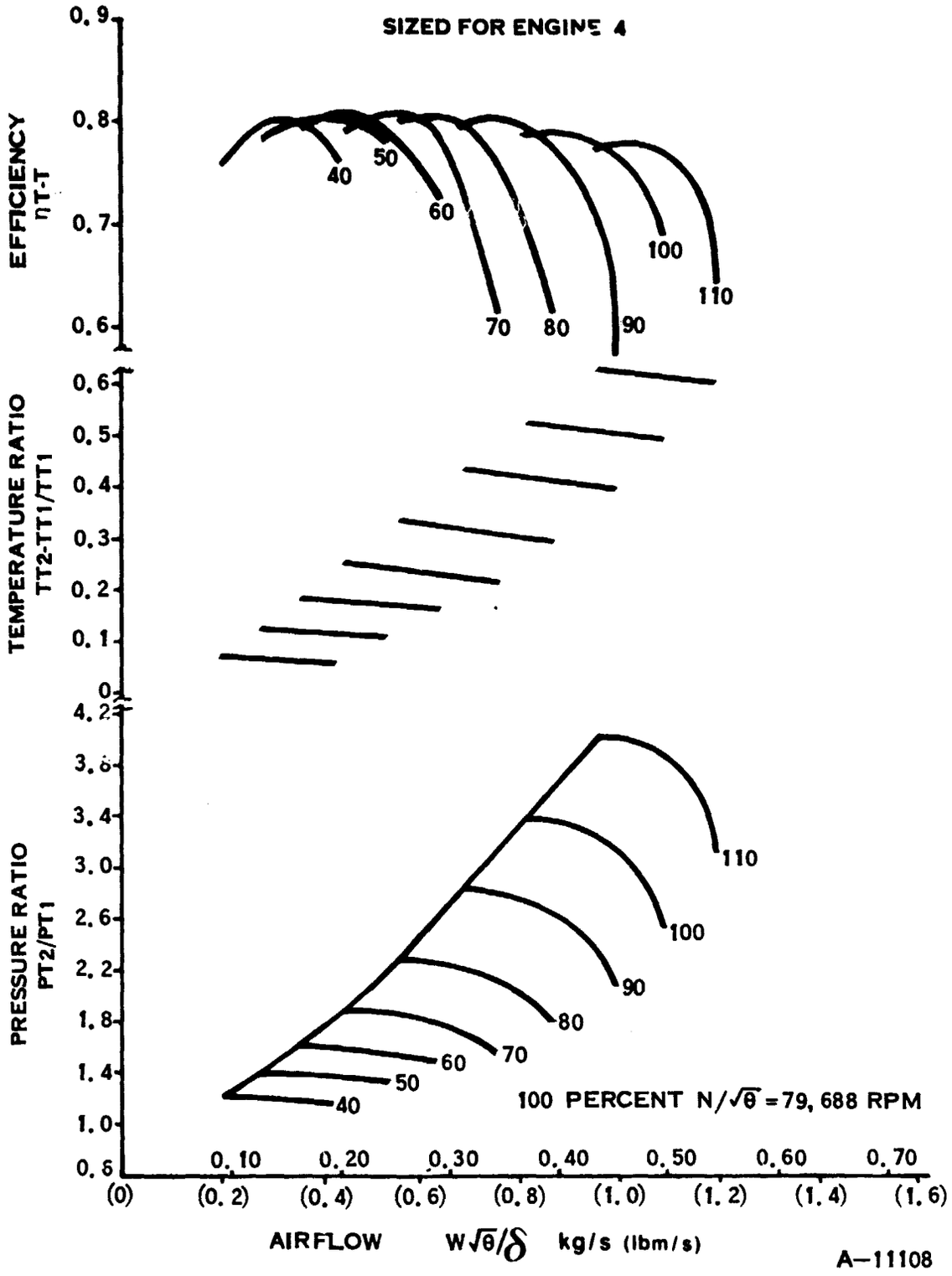

Figure 67. Two-Stage Centrifugal Compressor Performance, First Stage

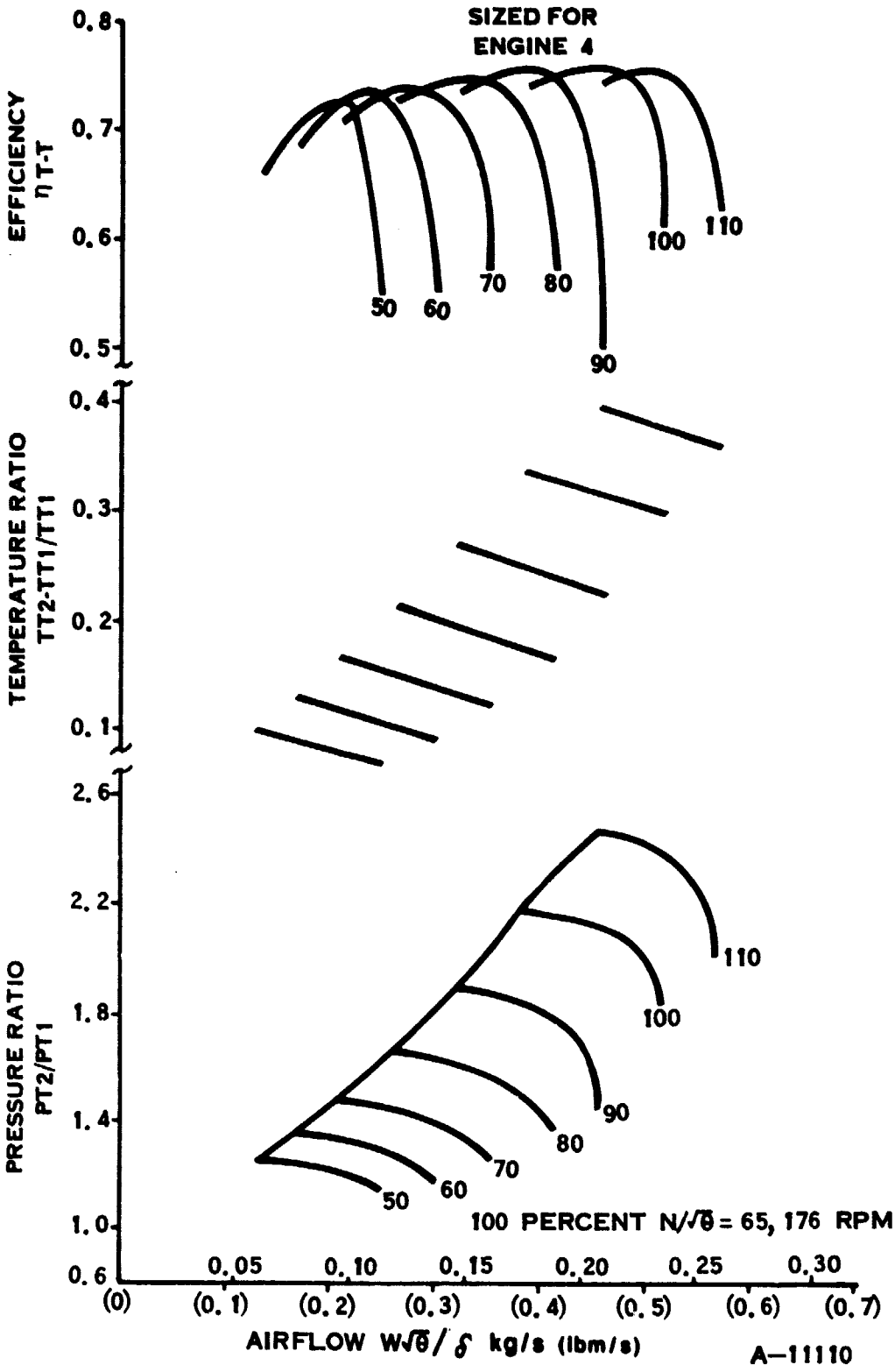

Figure 68. Two-Stage Centrifugal Compressor Performance, Second Stage

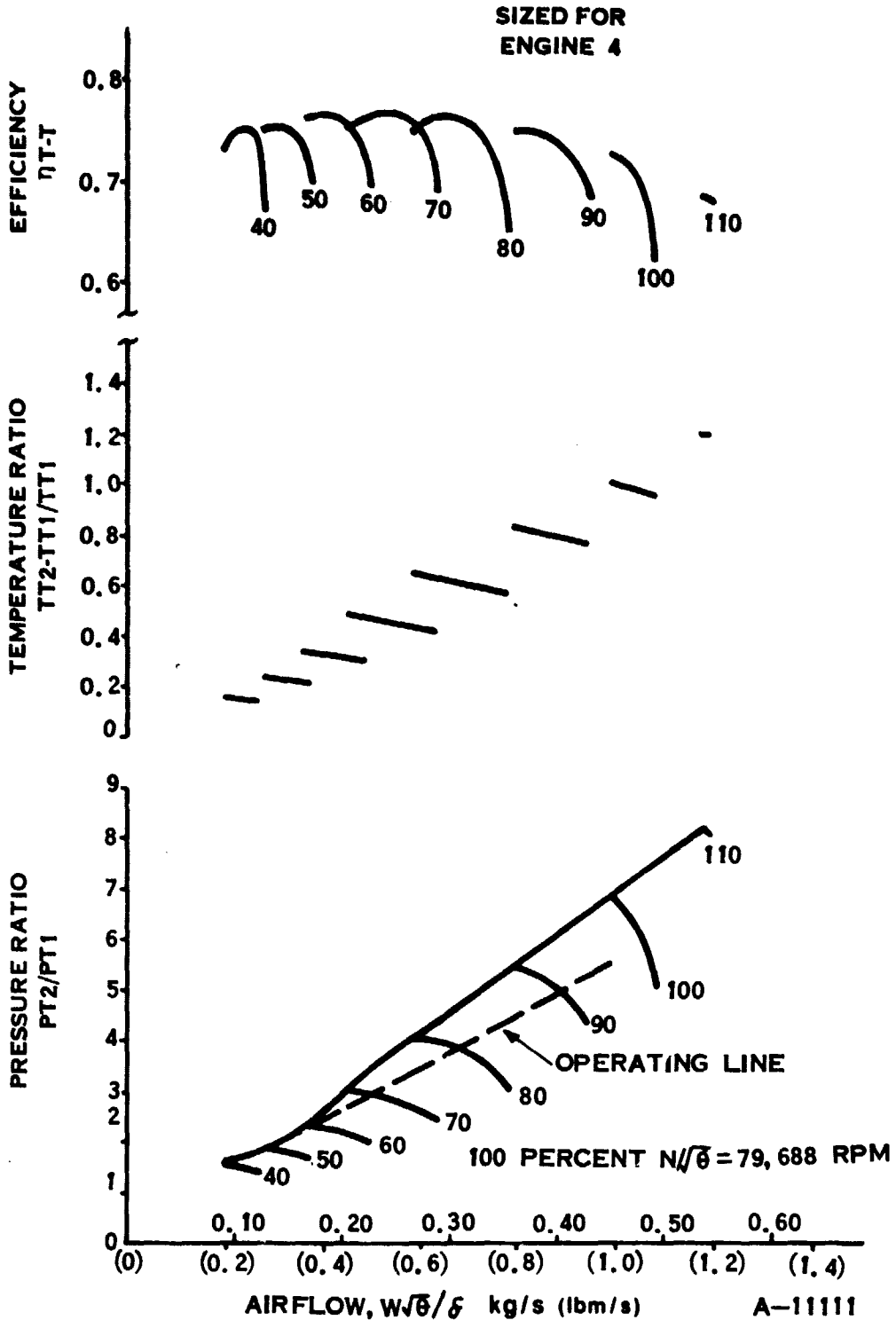

Figure 69. Two-Stage Centrifugal Compressor Performance, Overall

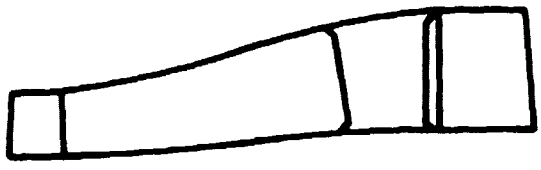

77500 RPM 75000 RPM

FULL SCALE

A-11295A

Figure 70. Axial Turbine Flowpath, Two-Shaft Engine

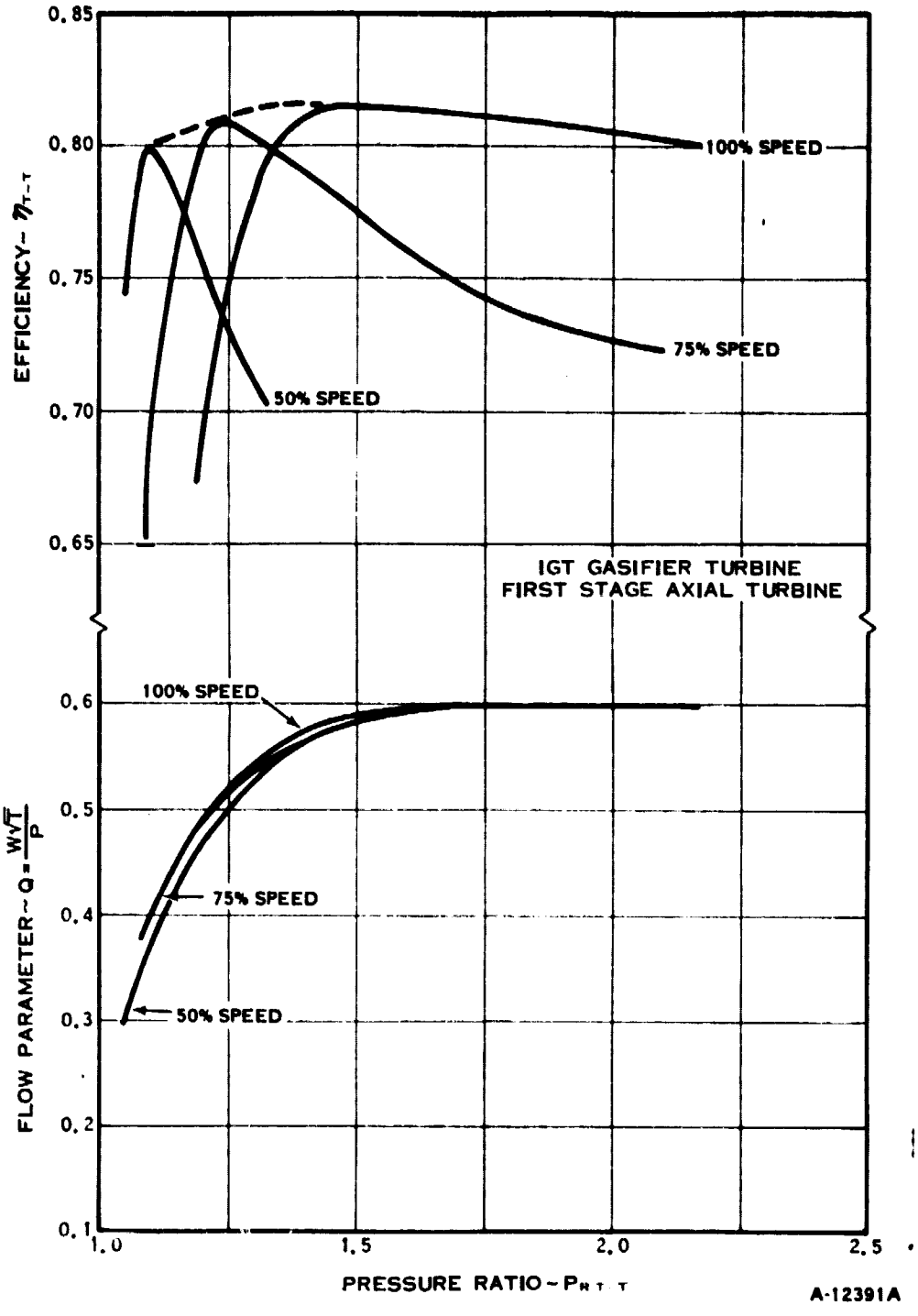

Figure 71. First Stage Axial Gasifier Turbine Performance

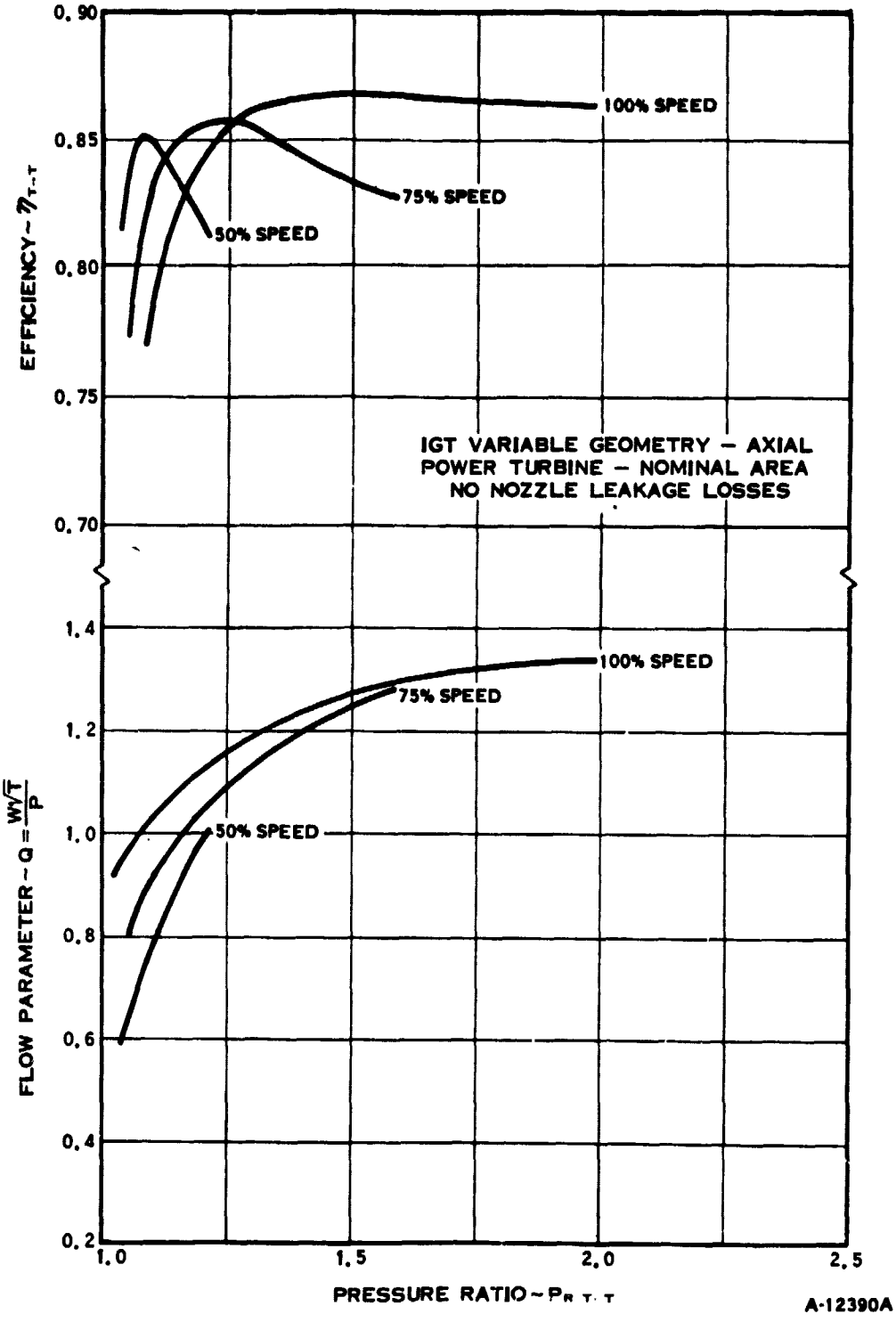

Figure 72. Variable Geometry Axial Power Turbine Performance

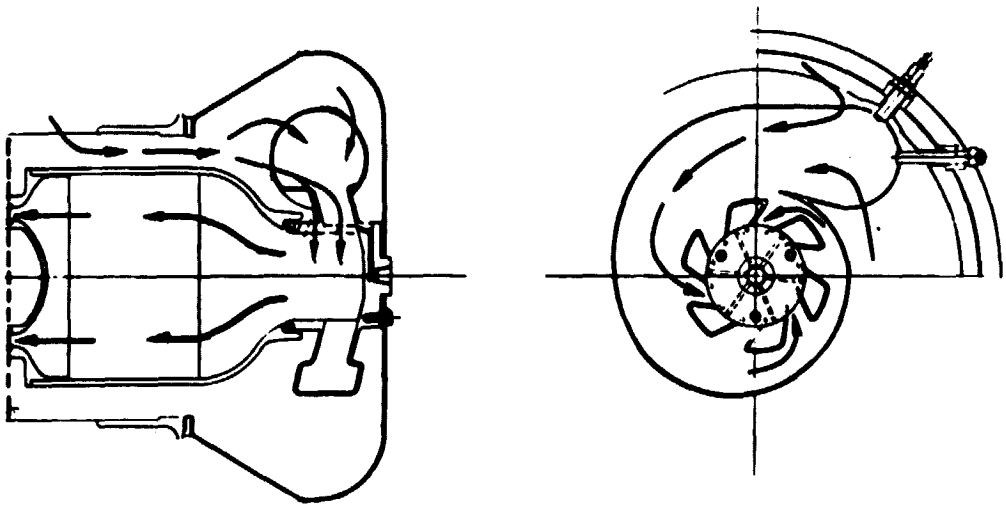

A-14010

Figure 73. Combustor Flowpath

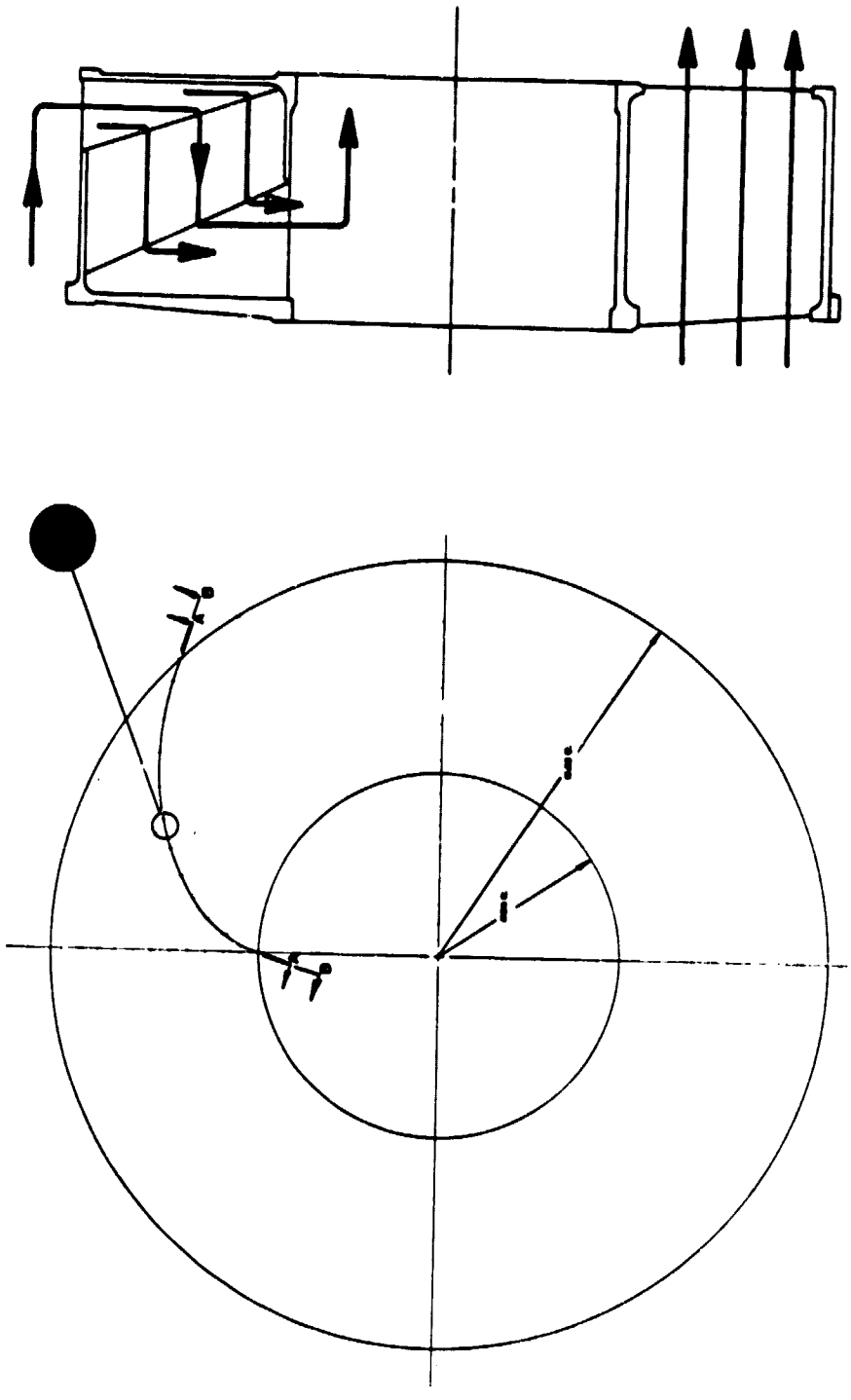

A-10853

Figure 74. Annular Recuperator

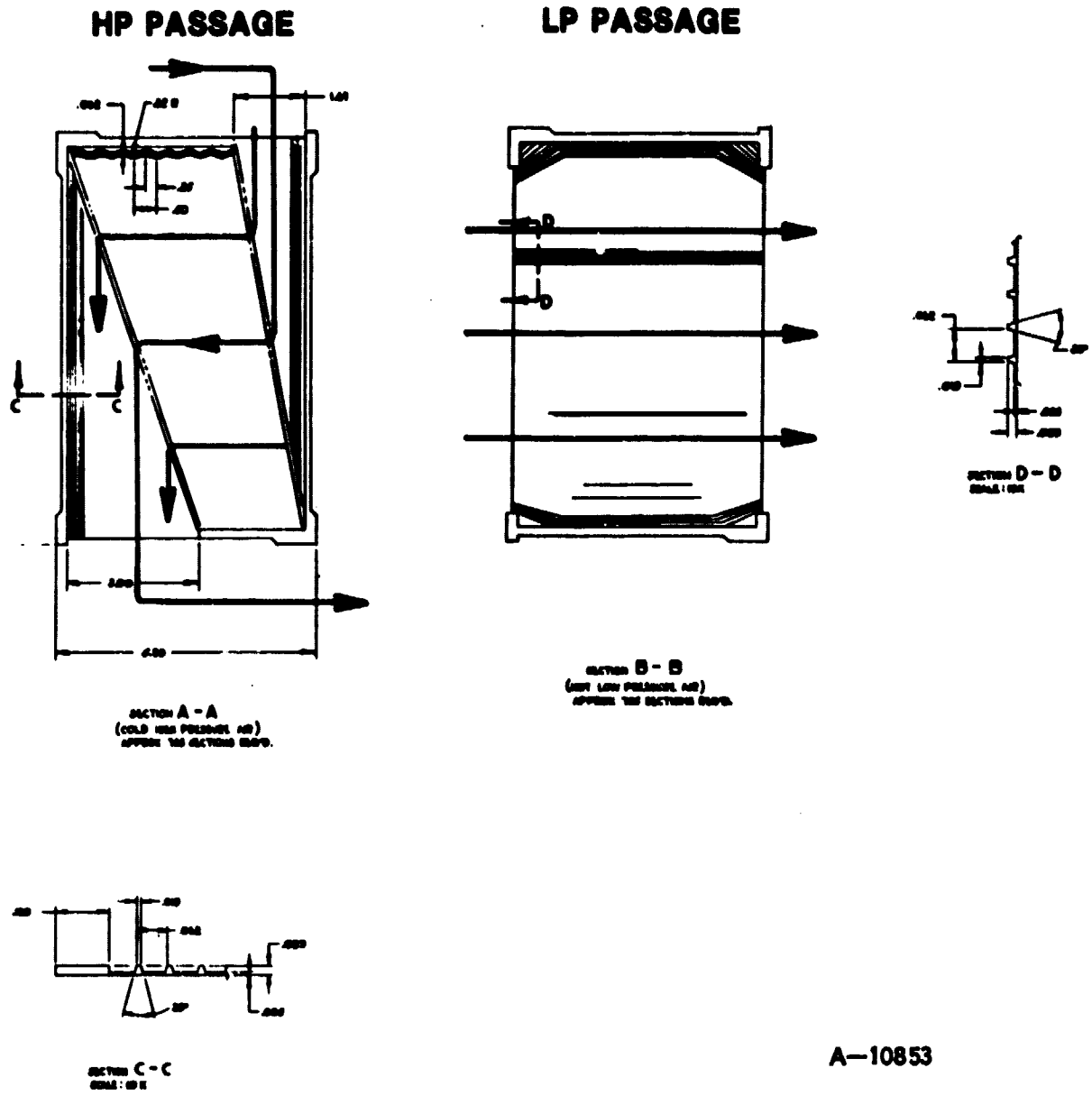

Figure 75. Recuperator Plates

POWERTRAIN PERFORMANCE

The cycle analysis for Engine 8 was refined in preparation for powertrain sizing to meet the acceleration requirement. A reduction gear loss of 2 percent was incorporated in the cycle analysis; on Engines 1 through 8, this loss was included in the driving cycle analysis. The alternator was loaded to half the nominal electrical load to simulate EPA driving cycle operation instead of the no-electrical load used previously on Engines 1 through 8. The engine was sized to deliver 74.6 kW (100 hp) at the output shaft (to transmission) at SAE standard conditions, 303°K (85°F) and 99.5 kPa (14.435 psia), equivalent to 152 m (500 ft) altitude. The performance characteristics with these modifications identified as Engine 8A are summarized in Table XXXVIII.

Engine 8B was also modeled, scaling Engine 8A down to 54.8 kW (73.5 hp) at SAE standard conditions but holding the same vehicle accessory power. The performance characteristics are summarized in Table XL, and the overall engine performance is shown in Figure 76. Minimum specific fuel consumption, Figure 77, is obtained at the rotor speeds shown in Figure 78, with turbine temperatures scheduled as shown in Figure 79 by the variable power turbine nozzle, Figure 80. The fuel flow and airflow are shown in Figure 81. The compressor operating lines are shown relative to the peak efficiency and surge lines in Figures 82 and 83, with surge margin in Figure 84. The component efficiencies for minimum SFC operation are shown in Figure 85, with pressure losses in Figure 86.

EFFECT OF AMBIENT TEMPERATURE

The effect of ambient temperature on engine performance is shown in Figure 87. For 1422°K (2100°F) TIT, the engine will develop 14 percent more power at 288°K (59°F) than at 303°K (85°F), and 31 percent more at 288°K (32°F). Noting that the driving cycle power requirement does not exceed 37.3 kW (50 hp), the engine can be reduced in size to improve fuel economy using water injection on warm days to meet the vehicle acceleration requirement of 0 to 96.6 km/h (60 mph) in 15 seconds. The engine size will be a compromise to maintain adequate steady-state power without water for normal driving, and provide for maximum acceleration with acceptable water usage.

WATER INJECTION ANALYSIS PROCEDURE

The part-load program was modified to simulate a water-injected engine. Since the detailed behavior of water injection is complex and relatively undocumented, a few simplifying assumptions were made in order to mathematically model the process. They were:

1. At any point, if liquid water were present, the gas had to be saturated.

2. For any point on the compressor map, the polytropic efficiency, the work or enthalpy rise, and the outlet flow parameter were all unaffected by water except if the inducer choked. If choke occurred, the inlet and outlet flow parameters stayed constant and the polytropic efficiency was reduced.

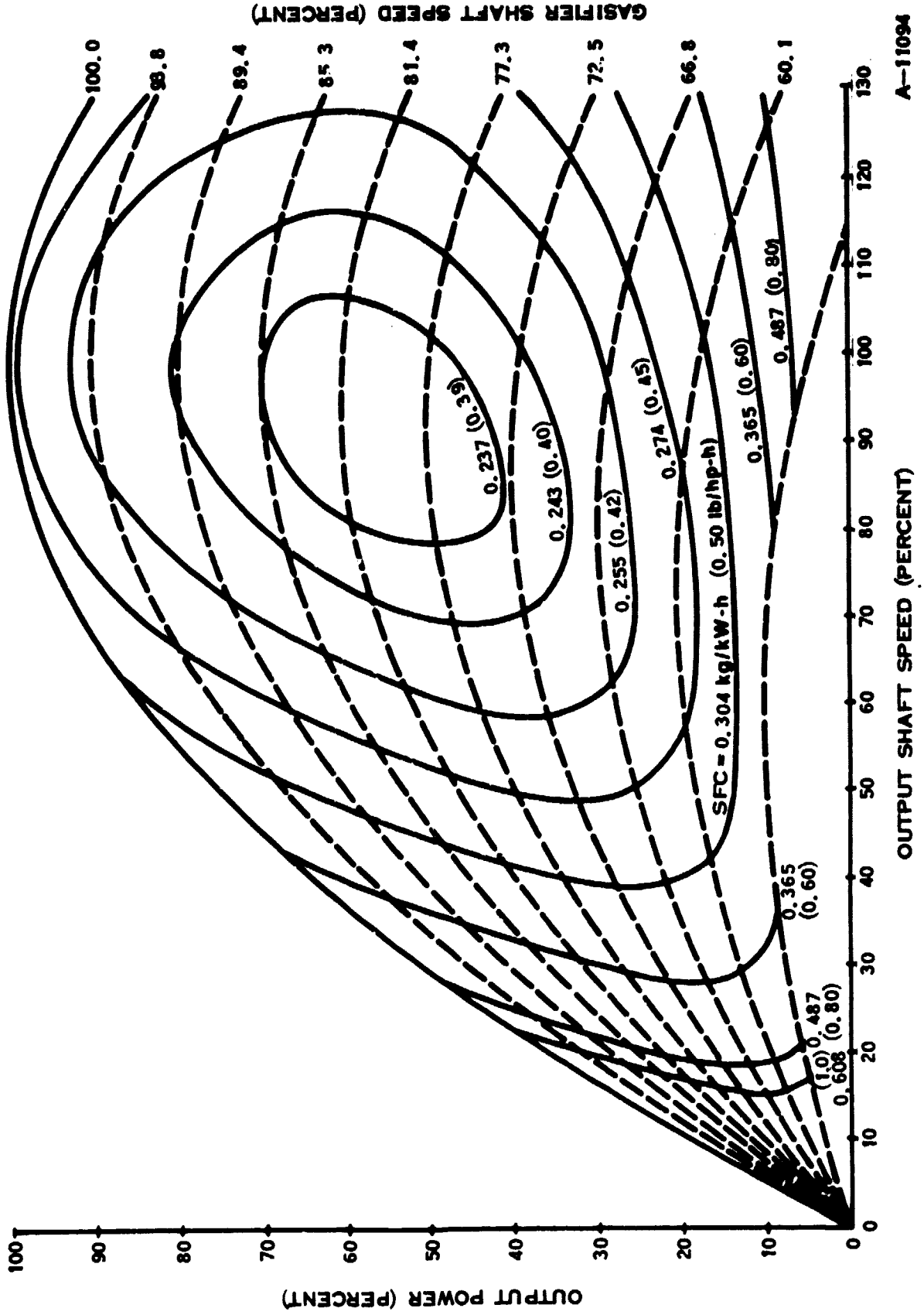

Figure 76. Overall Performance, Engine 8B

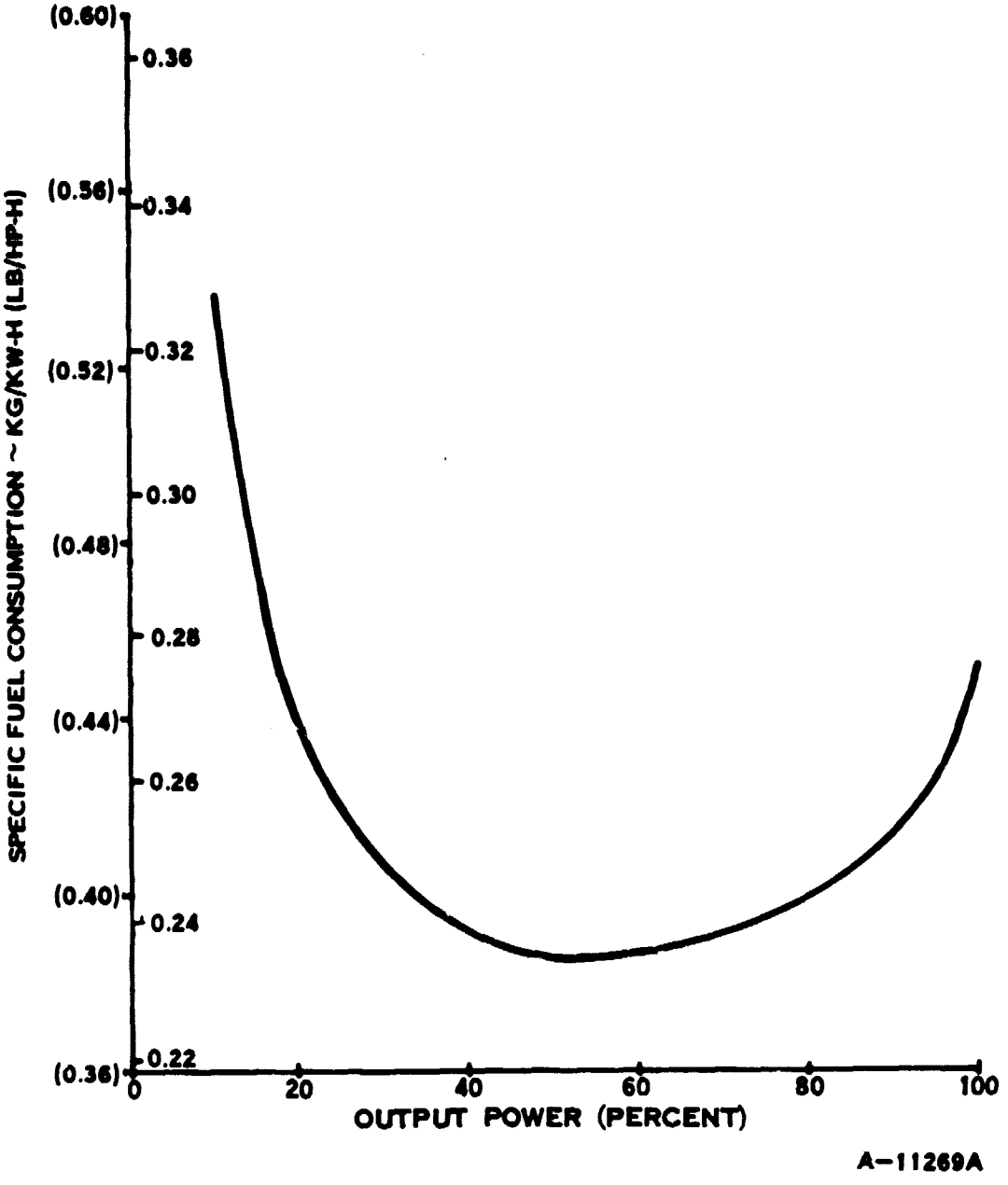

Figure 77. SFC versus Output Power, Engine 8B

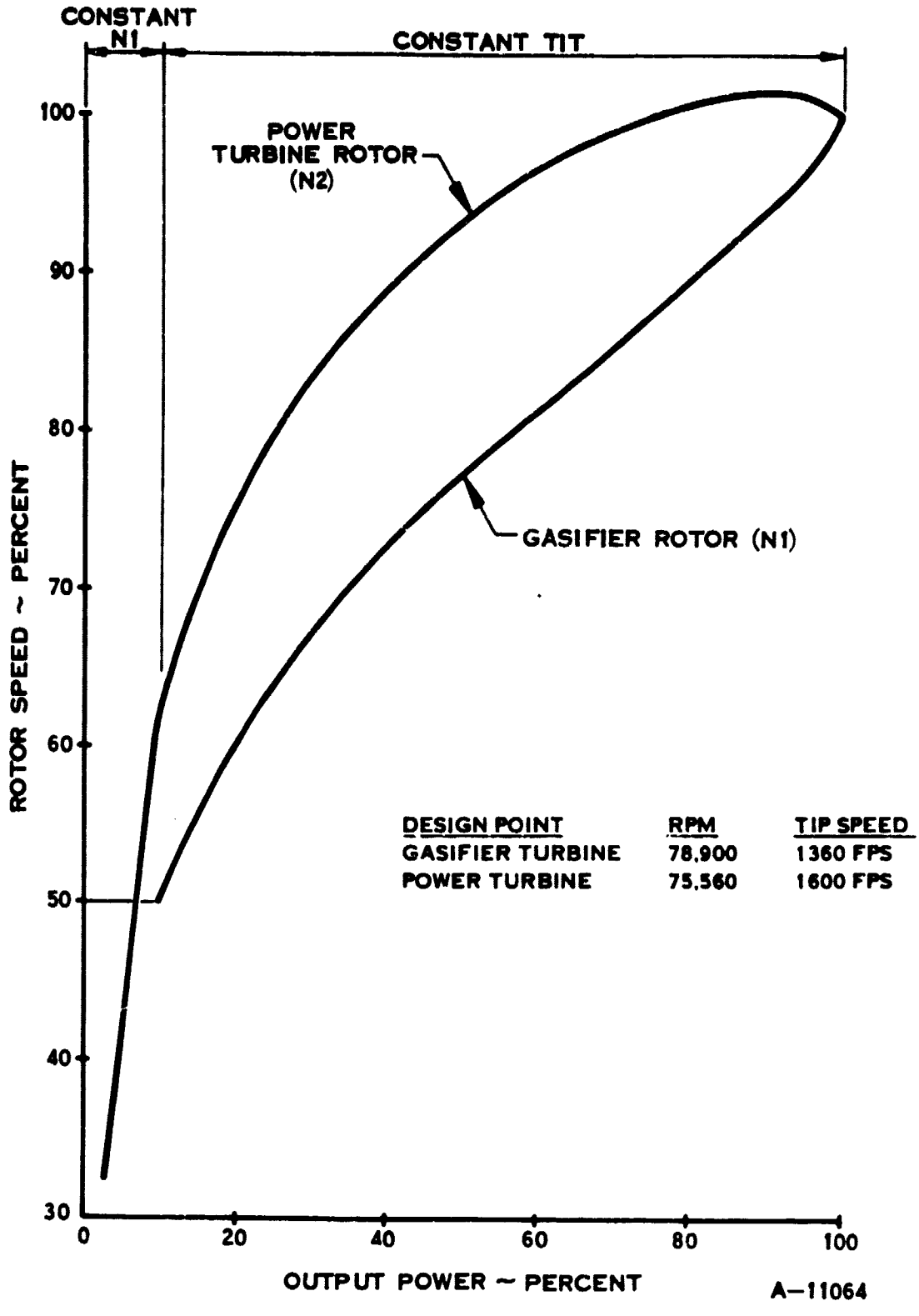

DESIGN POINT	RPM	TIP SPEED
GASIFIER TURBINE	78,900	1360 FPS
POWER TURBINE	75,560	1600 FPS

Figure 78. Rotor Speed versus Output Power, Engine 8B

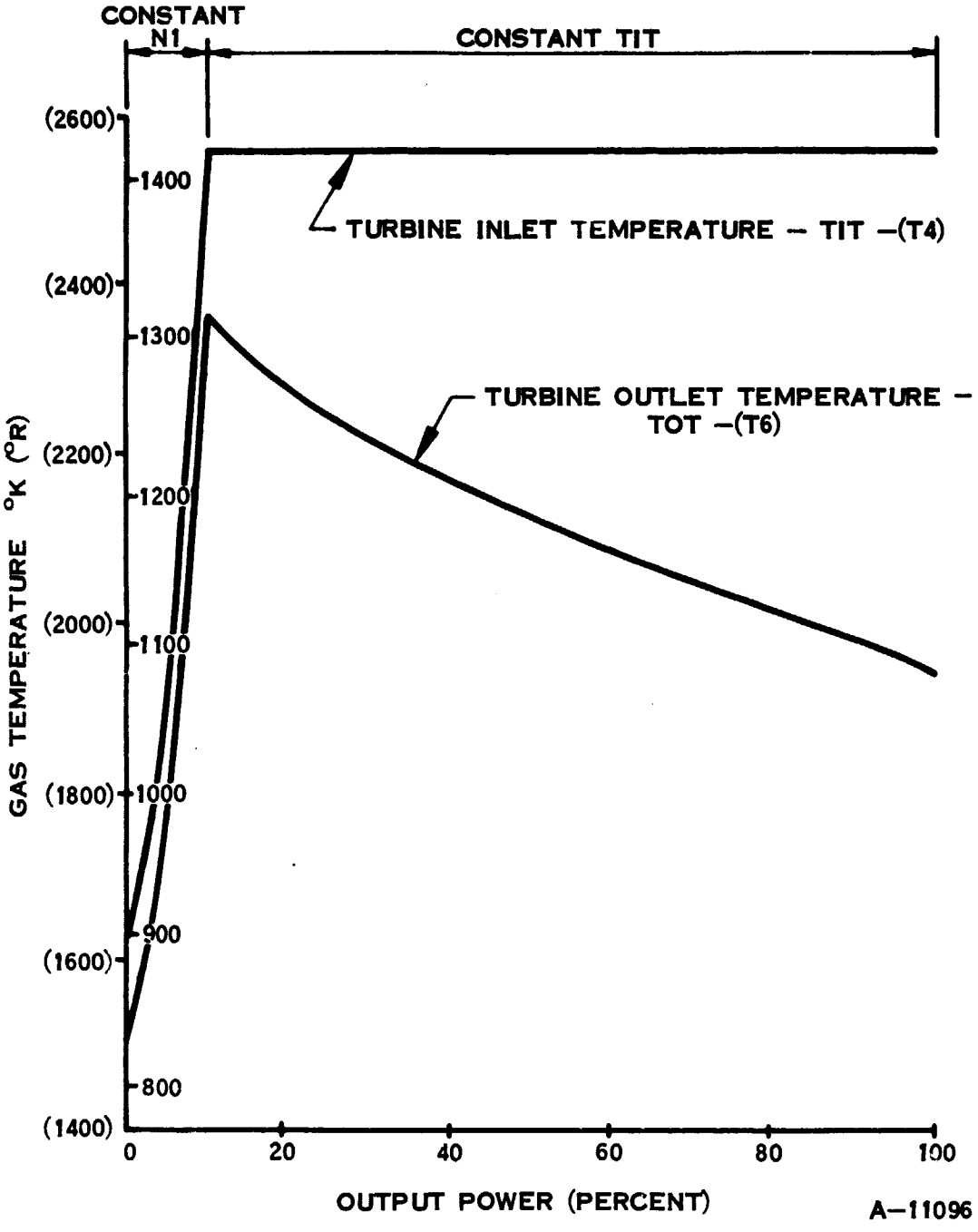

Figure 79. Gas Temperature versus Output Power, Engine 8B

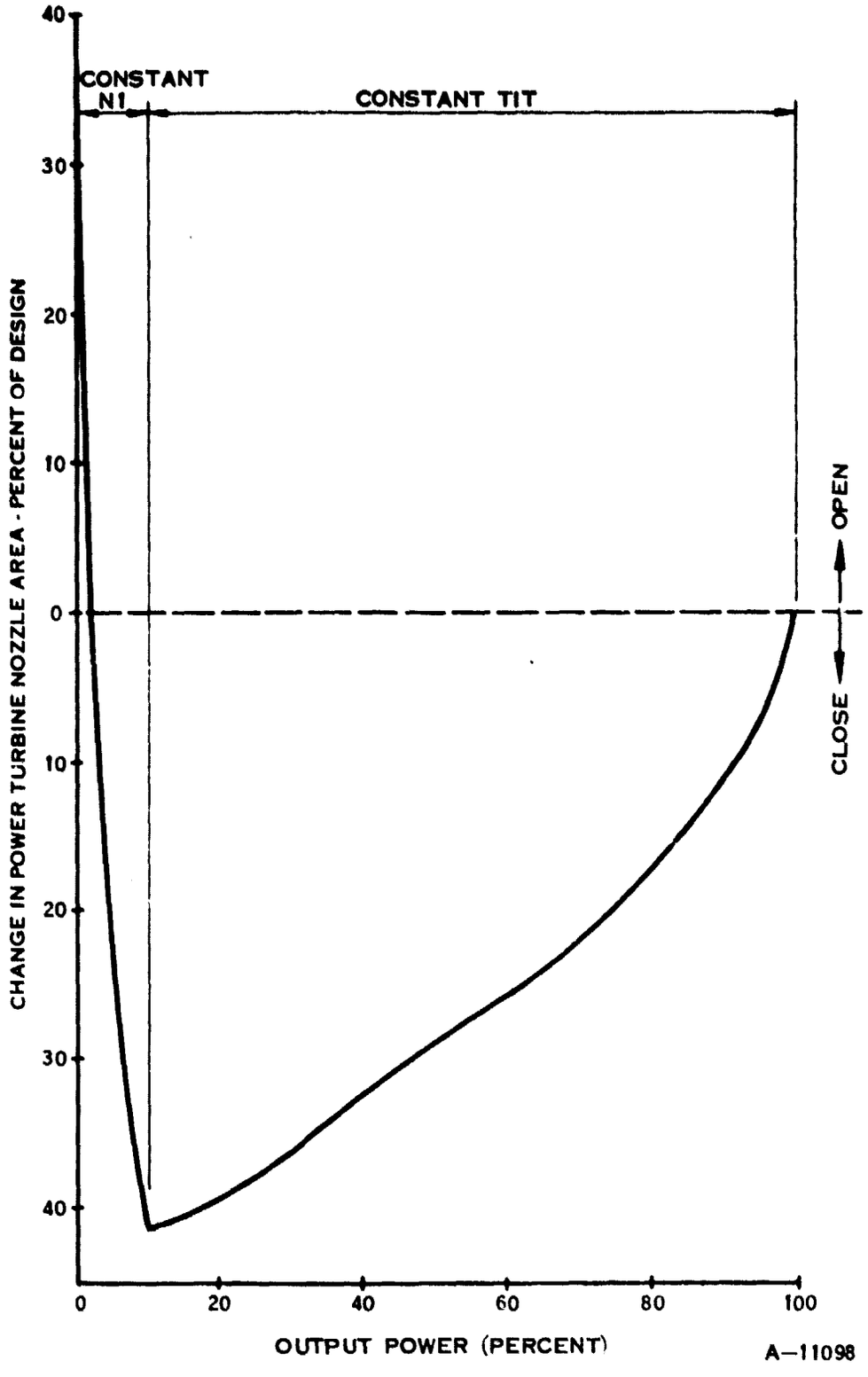

Figure 80. Turbine Nozzle Area versus Output Power, Engine 8B

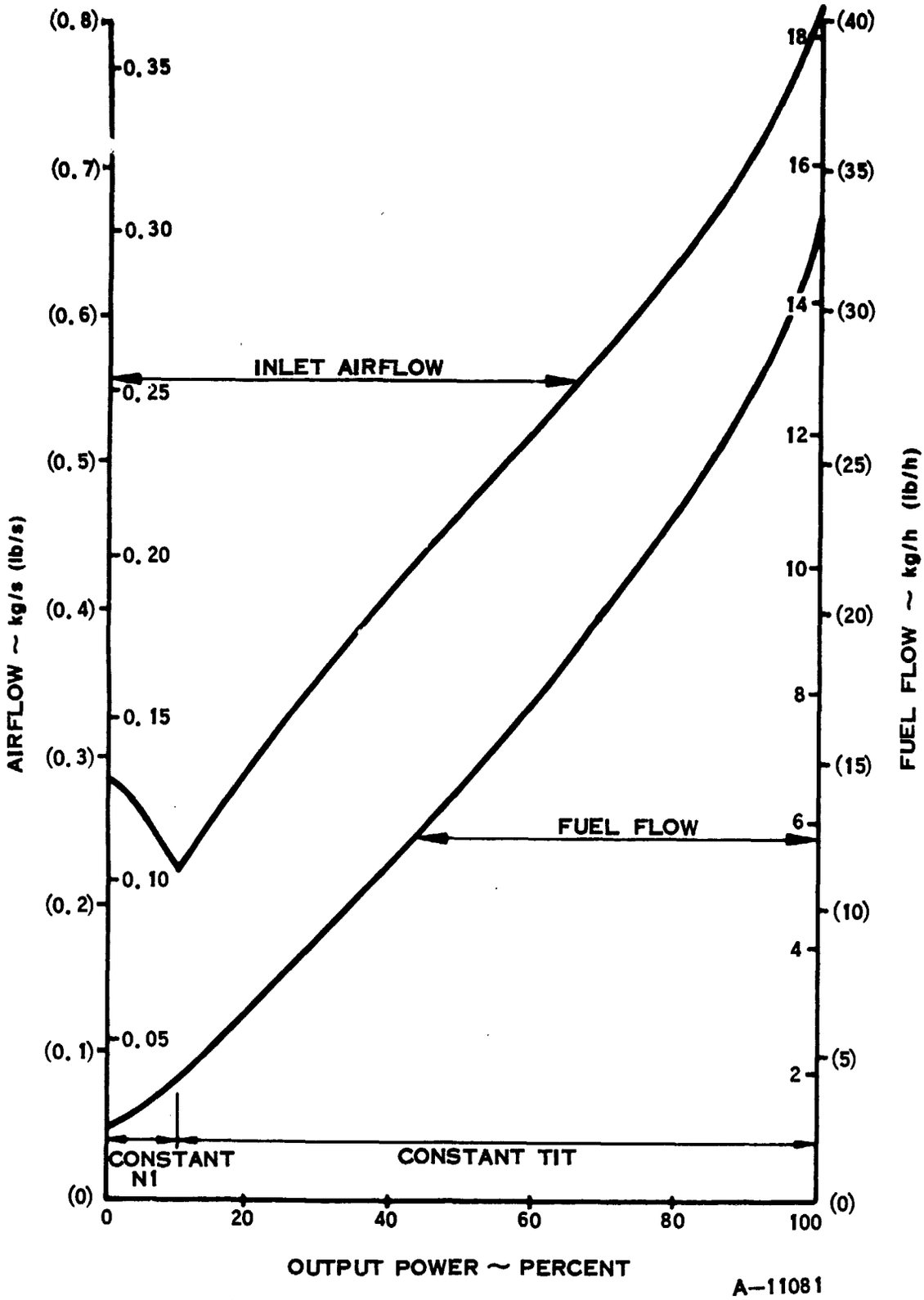

Figure 81. Airflow and Fuel Flow versus Output Power, Engine 8B

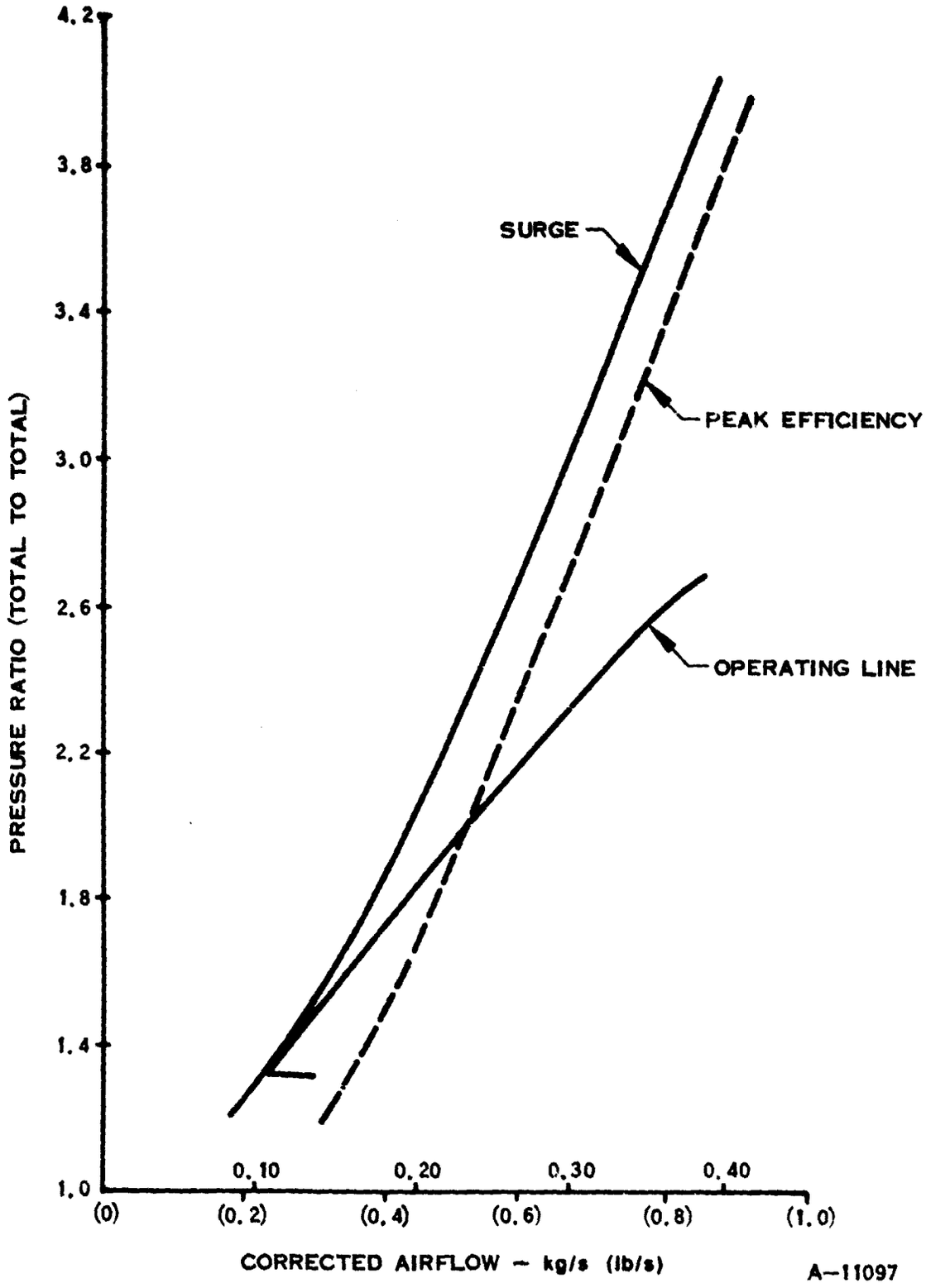

Figure 82. First Stage Compressor Pressure Ratio versus Corrected Airflow, Engine 8B

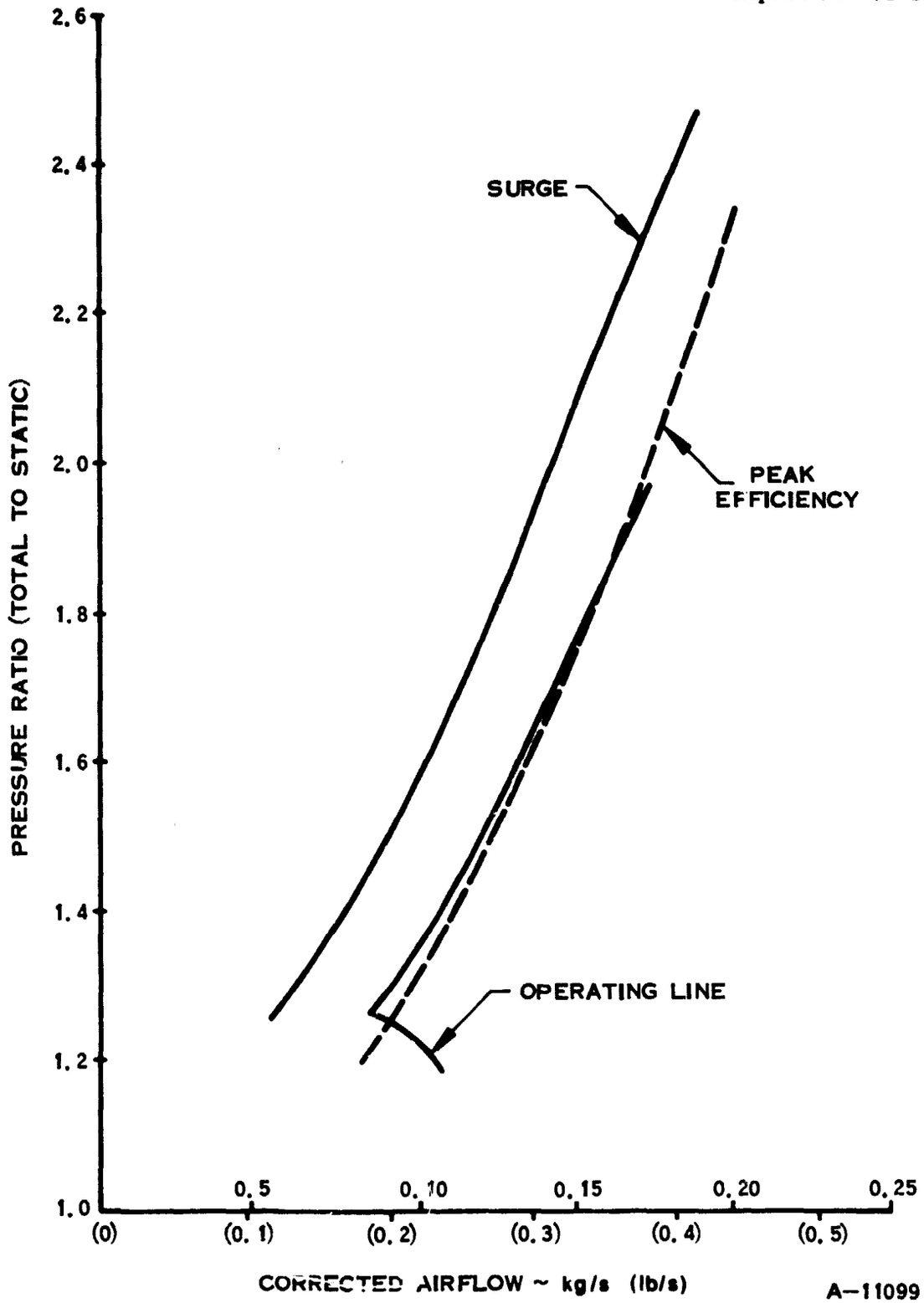

Figure 83. Second Stage Compressor Pressure Ratio versus Corrected Airflow, Engine 8B

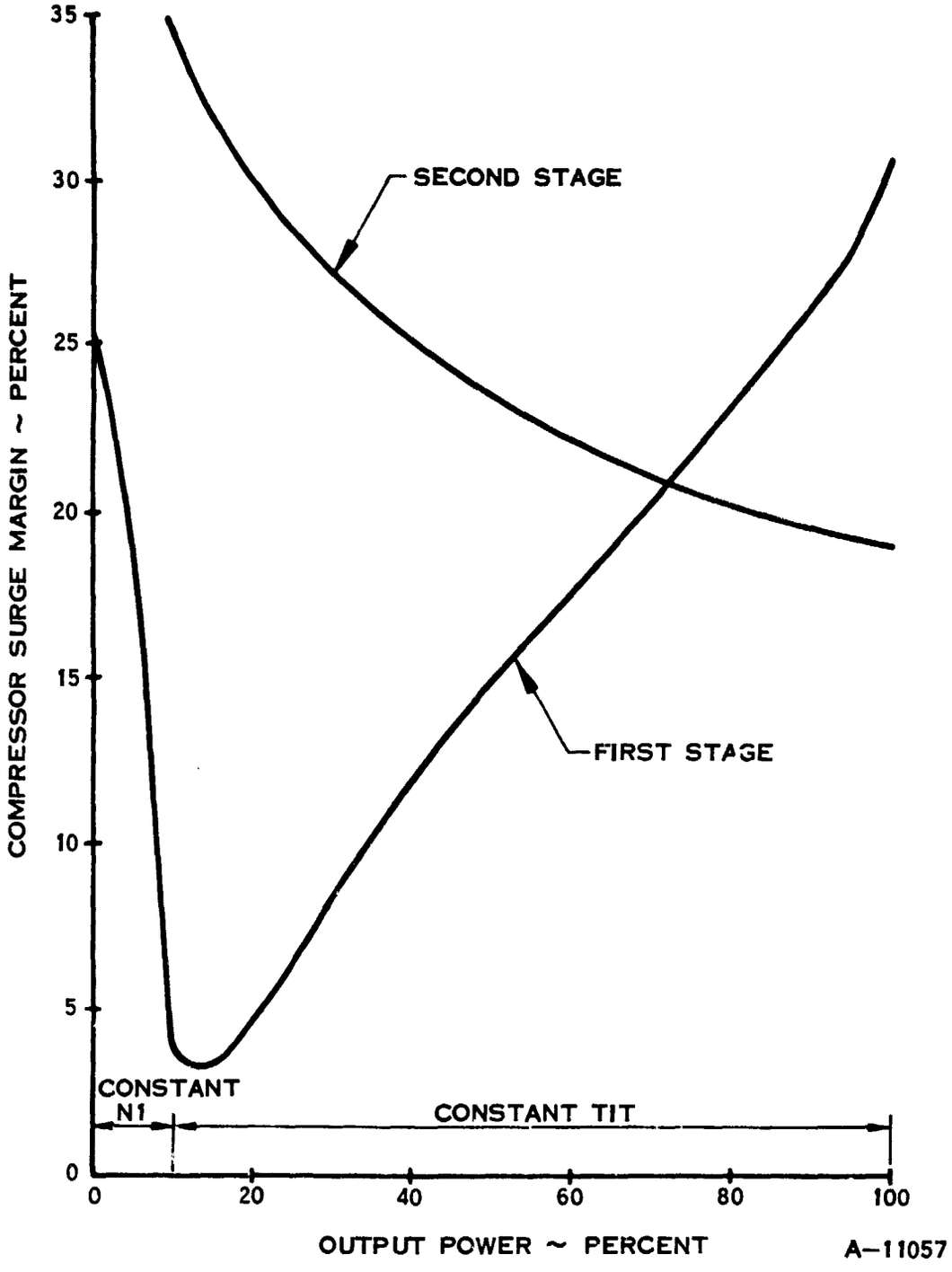

Figure 84. Compressor Surge Margin versus Output Power, Engine 8B

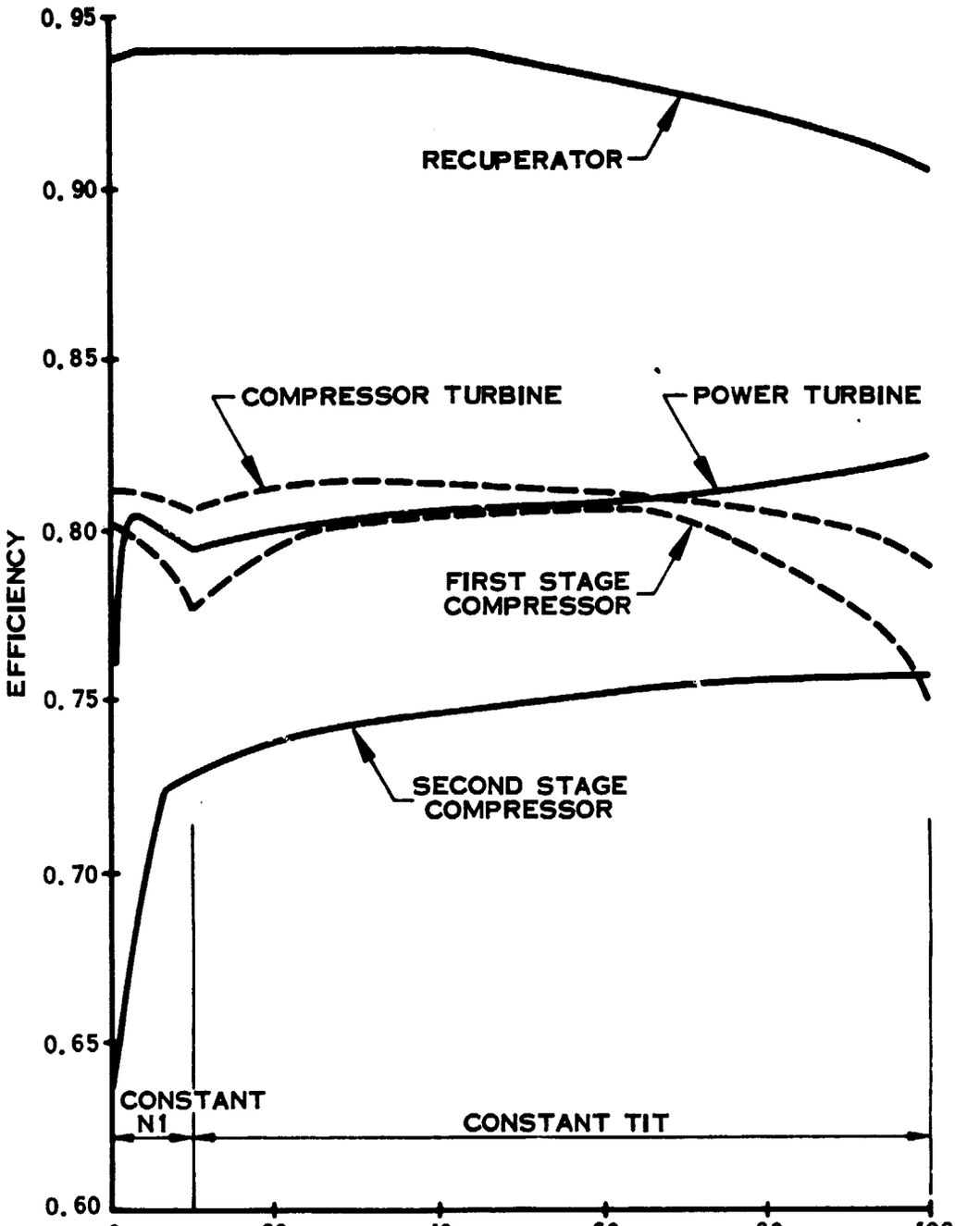

Figure 85. Component Efficiencies versus Output Power, Engine 8B

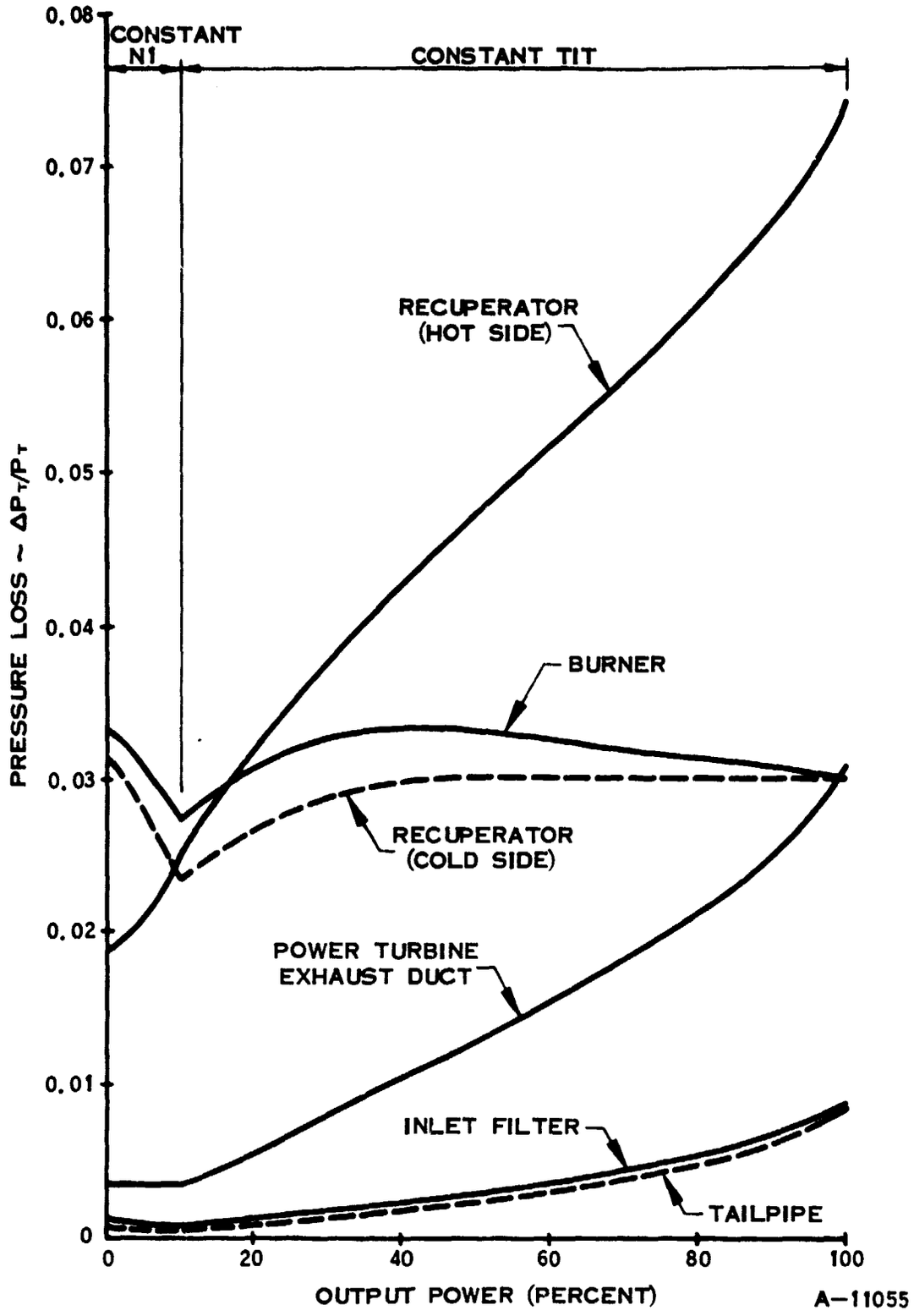

Figure 86. Pressure Loss versus Output Power, Engine 8B

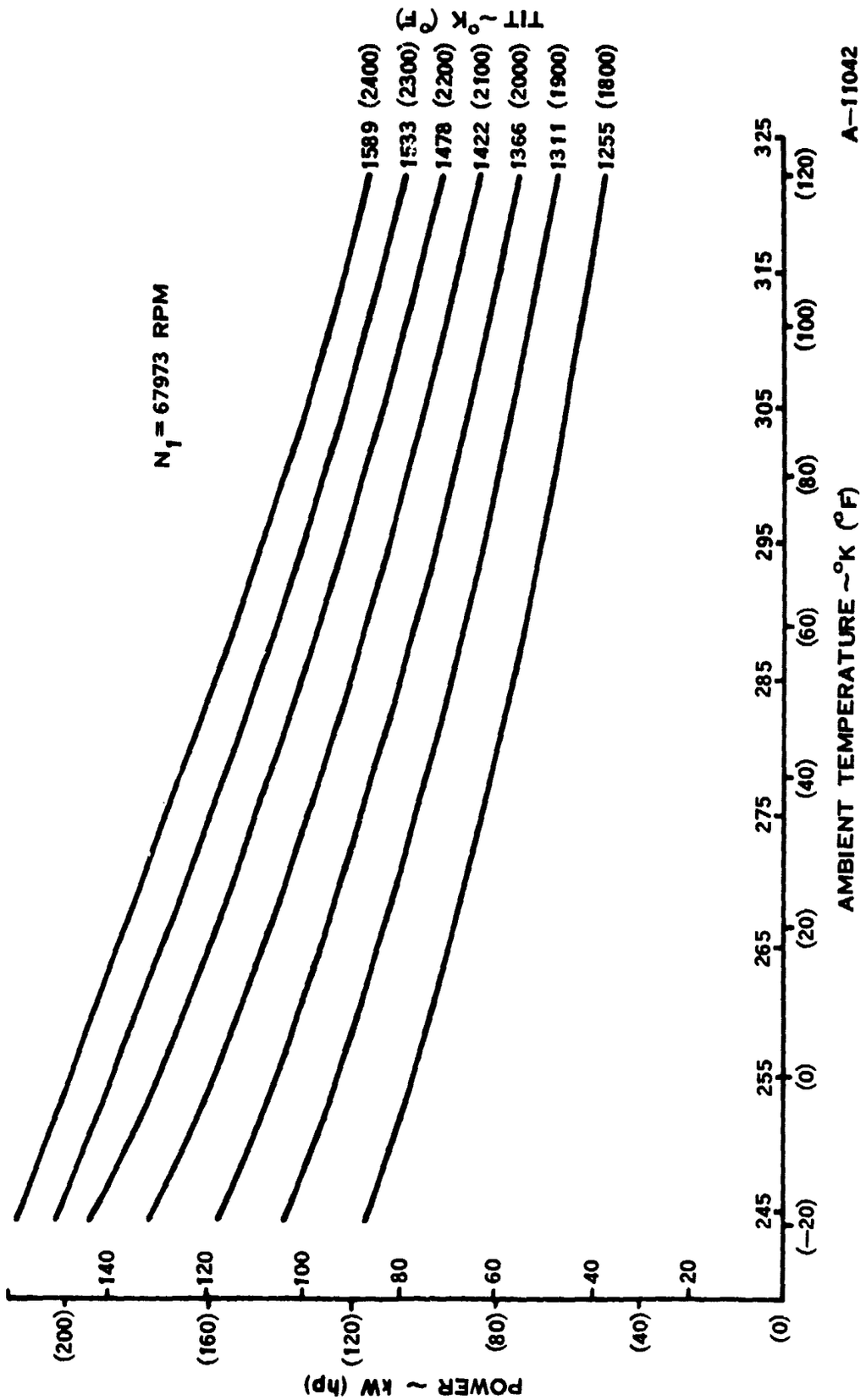

Figure 87. Effect of Ambient Temperature on Power, Engine 8

The workings of the part-load program were unchanged except for the modifications made to compressor performance.

The first effect of these assumptions was on compressor inlet conditions. If the air in the inlet was not saturated, then enough water was evaporated to bring it to saturation. This evaporation produced a precooling effect, lowering the inlet air temperature. If the air was saturated to begin with, that is, the ambient relative humidity was 100 percent, then no water evaporated.

The same assumption was made within the compressor. A representation of the process is shown in Figure 88 with the dry compressor performance described by the path from 1 to 2. After each increment, the liquid water present evaporated until saturation occurred, step 2 to 3. This process continued until all the water had been evaporated or until the enthalpy rise of the air and water vapor mixture equalled the enthalpy rise of the same compressor point run with dry air, shown by path B. If all the water evaporated before the latter condition was satisfied, the remainder of the enthalpy rise was used to calculate the remainder of the compressor temperature rise. This is shown by path C.

The overall compressor performance was then calculated. Pressure ratio was found using the assumption that polytropic efficiency was unaffected by the water. This assumption is not quite true since tests have shown an efficiency degradation due to the presence of water (Reference 22). However, this effect was looked at separate from the program. The mass flow was found using the assumption that the compressor outlet flow parameter was the same for both wet and dry operation unless the inducer choked.

WATER INJECTION STUDY

The engine part-load performance simulation program was modified to include the effects on compressor performance of water injection at the inlet. The rated power point of Engine 8B was run over a range of ambient temperature and water-air ratios, with dry and saturated (100 percent relative humidity) ambient air, as shown in Figures 89 and 90. A calculated 0.005 water-air ratio will deliver 62.3 kW (83.5 hp) up to 311°K (100°F), maintaining vehicle performance.

The analysis assumes no loss in compressor efficiency with water injection. This effect is illustrated in Figure 91. If the first stage compressor efficiency were reduced to 0.88 times the efficiency dry, Engine 8B would require 0.0075 water-air ratio to deliver 62.3 kW (83.5 hp) at 303°K (85°F) and 100 percent relative humidity. Figure 90 shows that with no loss in compressor efficiency, a water-air ratio of only 0.0025 is required for the same 62.3 kW (83.5 hp) output. The actual loss in compressor efficiency with water injection and the corresponding higher water requirement must be determined experimentally. Other possible effects of water injection, such as erosion and deposits, will also require experimental evaluation and development.

HEAT EXCHANGER STUDY

One major constraint on the powertrain installation in the automobile is the engine packaging, size, and shape. For the selected powertrain concept, both

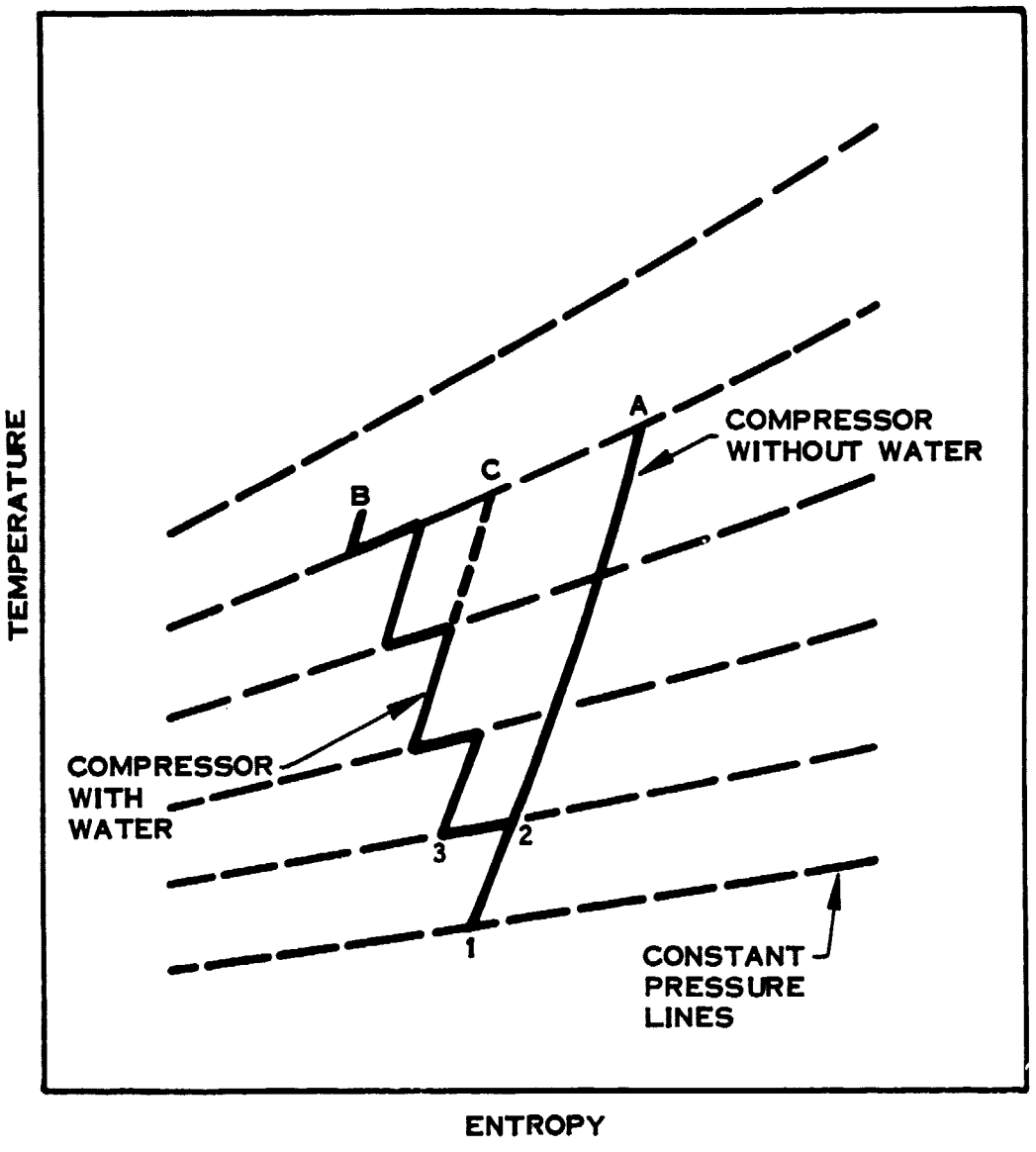

Figure 88. Water Injection Analysis

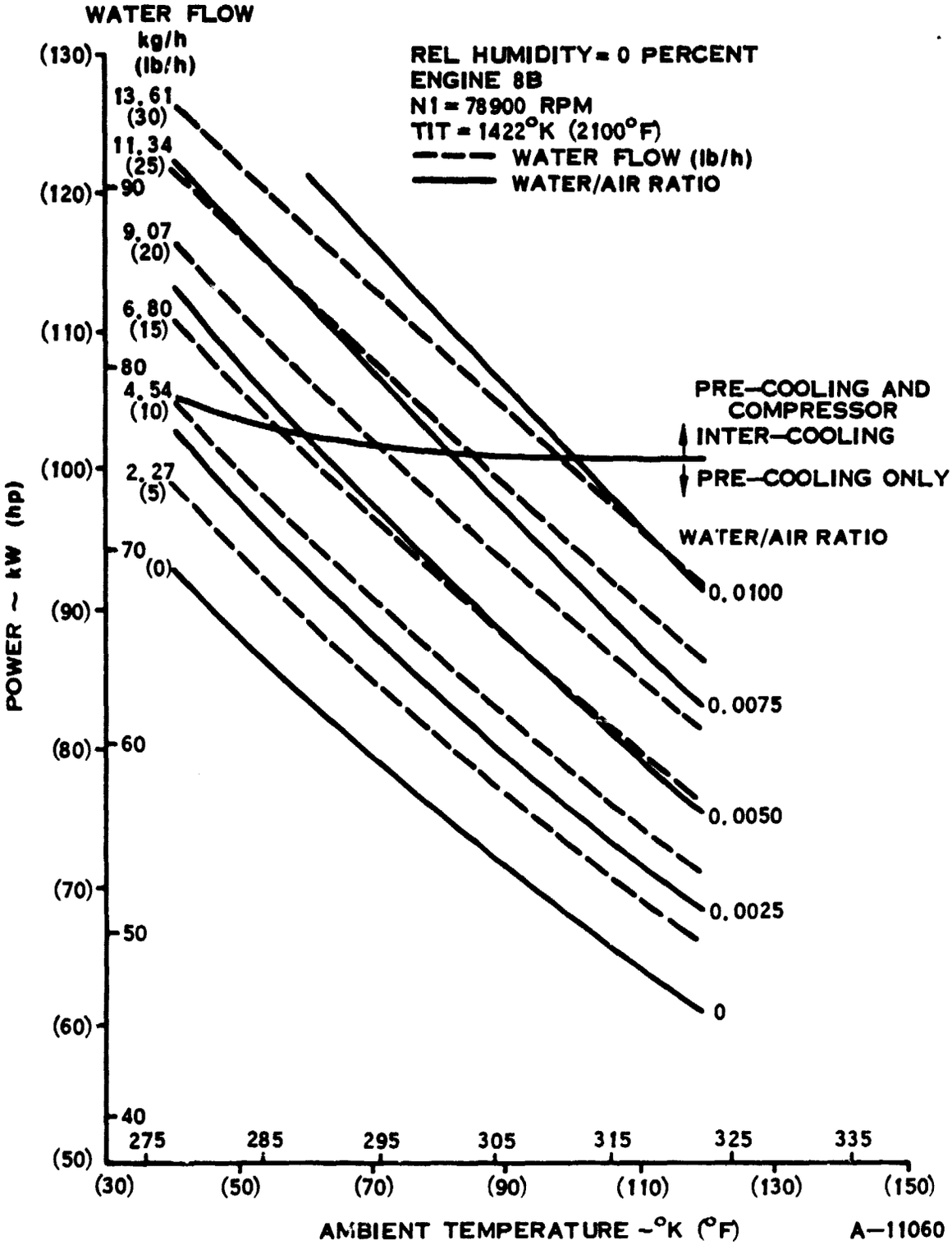

Figure 89. Effects of Water Injection on Compressor Performance, Relative Humidity = 0 Percent

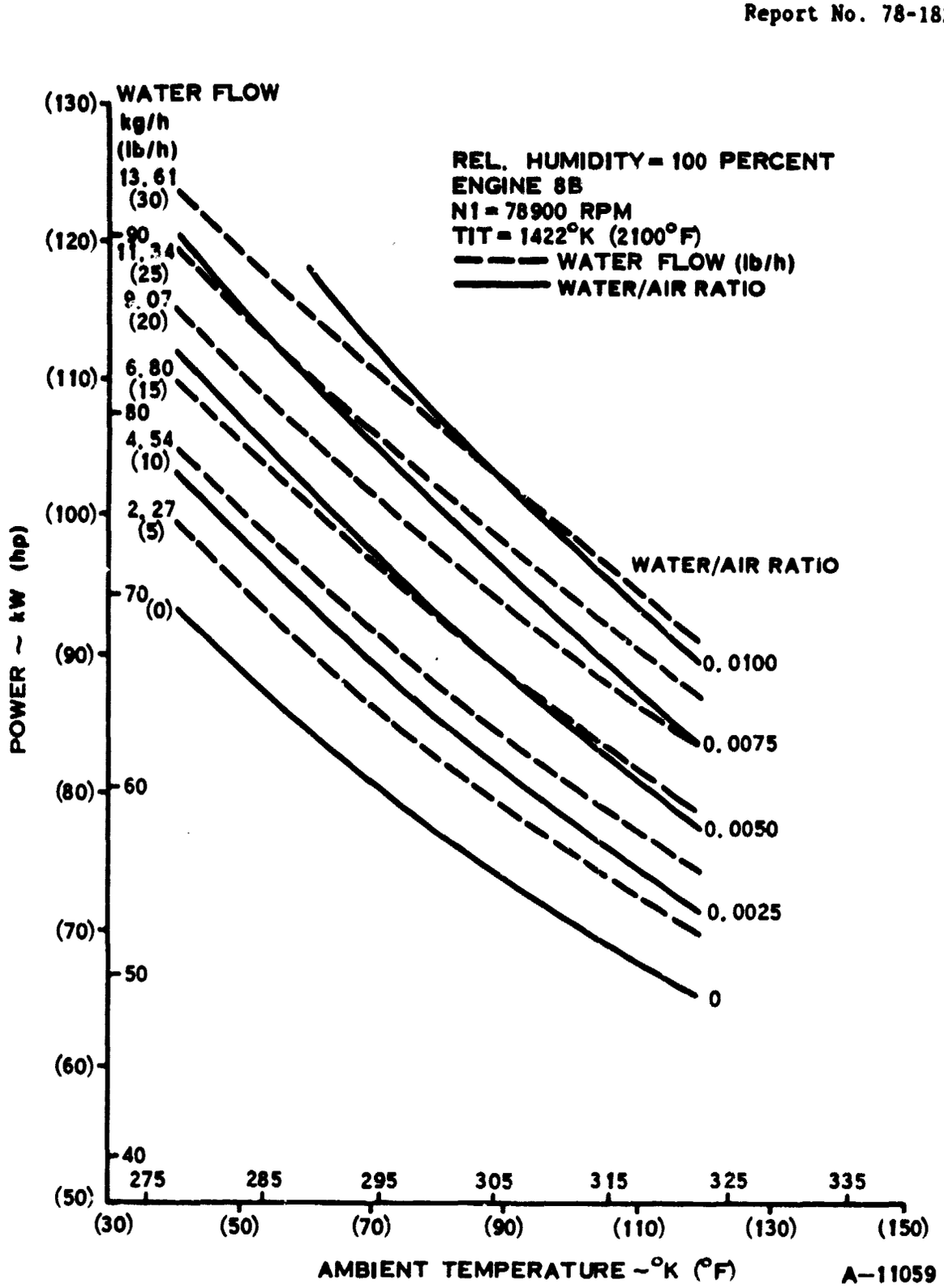

Figure 90. Effects of Water Injection on Compressor Performance, Relative Humidity = 100 Percent

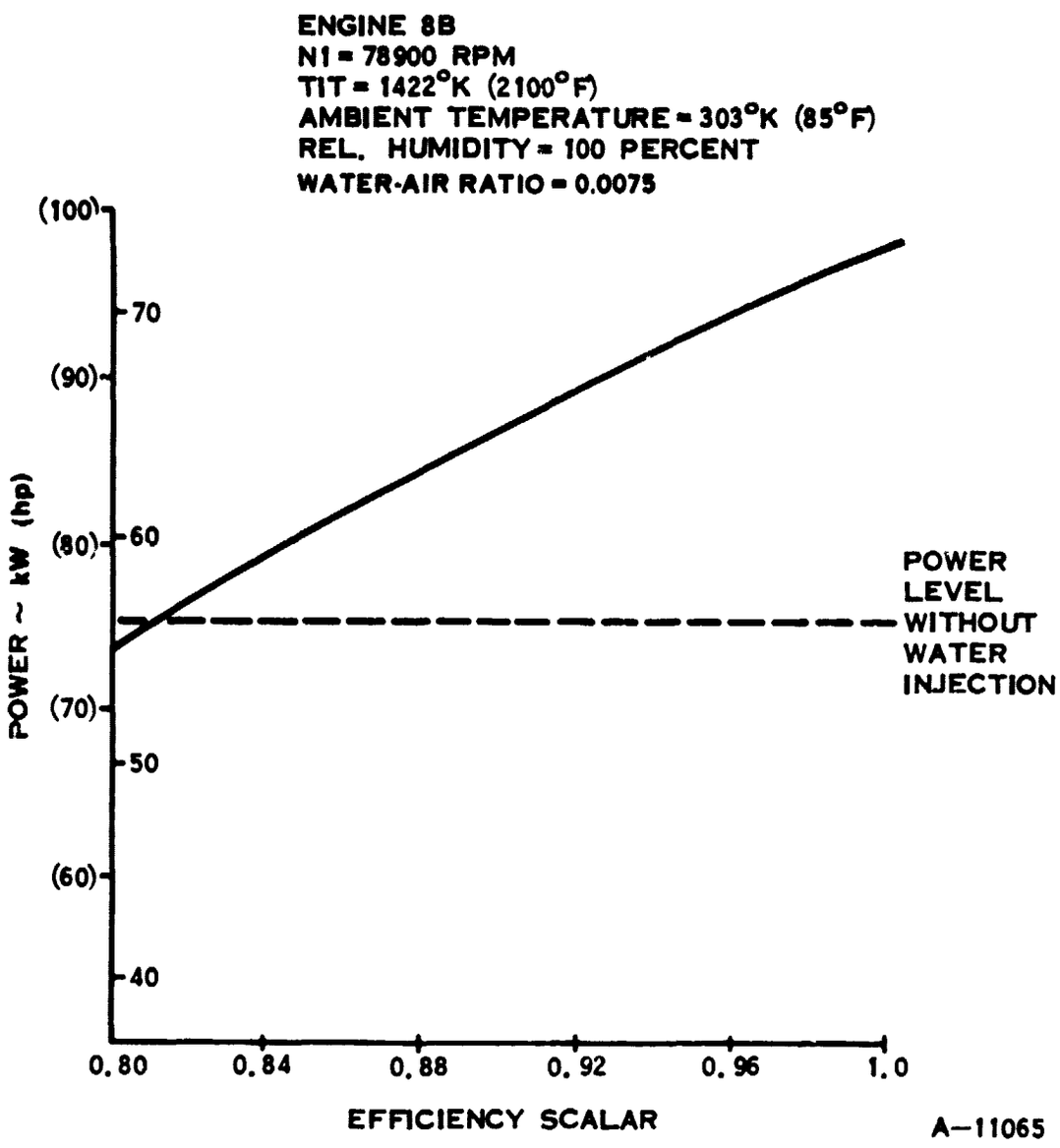

Figure 91. Effect of First Stage Compressor Efficiency Change with Water Injection

size and shape are set primarily by the outside diameter of the annular recuperator. This large circular shape must be accommodated in the engine compartment, with clearance to structure, sheet metal, and other vehicle components, and still provide room for intake and exhaust systems, drivetrain, and vehicle accessories.

Reducing the recuperator diameter facilitates vehicle installation and simultaneously forces a reduction in weight and cost, but with a trade-off in lower fuel economy. The recuperator pressure drop will increase and effectiveness will decrease in some combination, depending on the design optimization, but the result is higher SFC and reduced fuel economy.

This effect was calculated for two cases with Engine 8B by reducing the outside diameter by 2.54 cm and 5.08 cm (1.0 in. and 2.0 in.). The passage size was held constant on the high pressure side but was increased on the low pressure side to hold constant pressure drop at the design point. The SFC is shown in Figure 92 for the two cases; it is not affected at low power, since all three cases reach the arbitrary limit of 94 percent effectiveness. This limit has been used to allow for flow distribution effects on performance.

GASIFIER ACCELERATION

The power available for acceleration of the gasifier rotor is as shown in Figure 93. The estimated acceleration time from the nominal 50 percent idle speed to rated speed is calculated as 1.2 seconds with TIT limited to 1422°K (2100°F). This acceleration time should give acceptable vehicle response. Higher TIT during acceleration could reduce this time.

VEHICLE ACCELERATION

The driving cycle simulation program was modified to predict vehicle acceleration. Then the engine power rating required to accelerate the vehicle from 0 to 96.6 km/h (60 mph) in 13.5 seconds was calculated as a function of reduction gear ratio, as shown in Figure 94. (The 1.5 seconds difference is an allowance for gasifier acceleration effects.) The reduction gear ratio also affects fuel economy, and this was examined before selecting the final engine rating.

VEHICLE FUEL ECONOMY

The driving cycle fuel economy was calculated for Engine 8A [1422°K (2100°F) TIT] with 74.6 kW (100 hp) output at SAE standard conditions, 303°K (85°F) and 99.5 kPa (14.345 psia), equivalent to 152 m (500 ft) altitude. The driving cycle fuel economy is shown in Figure 95; optimum reduction gear ratio is 21.

The effect of engine size on fuel economy was next explored in two steps. Engine 8A was scaled down directly to 62.3 kW (83.5 hp) at SAE standard conditions. The driving cycle fuel economy is shown in Figure 96; optimum reduction gear ratio is 24.

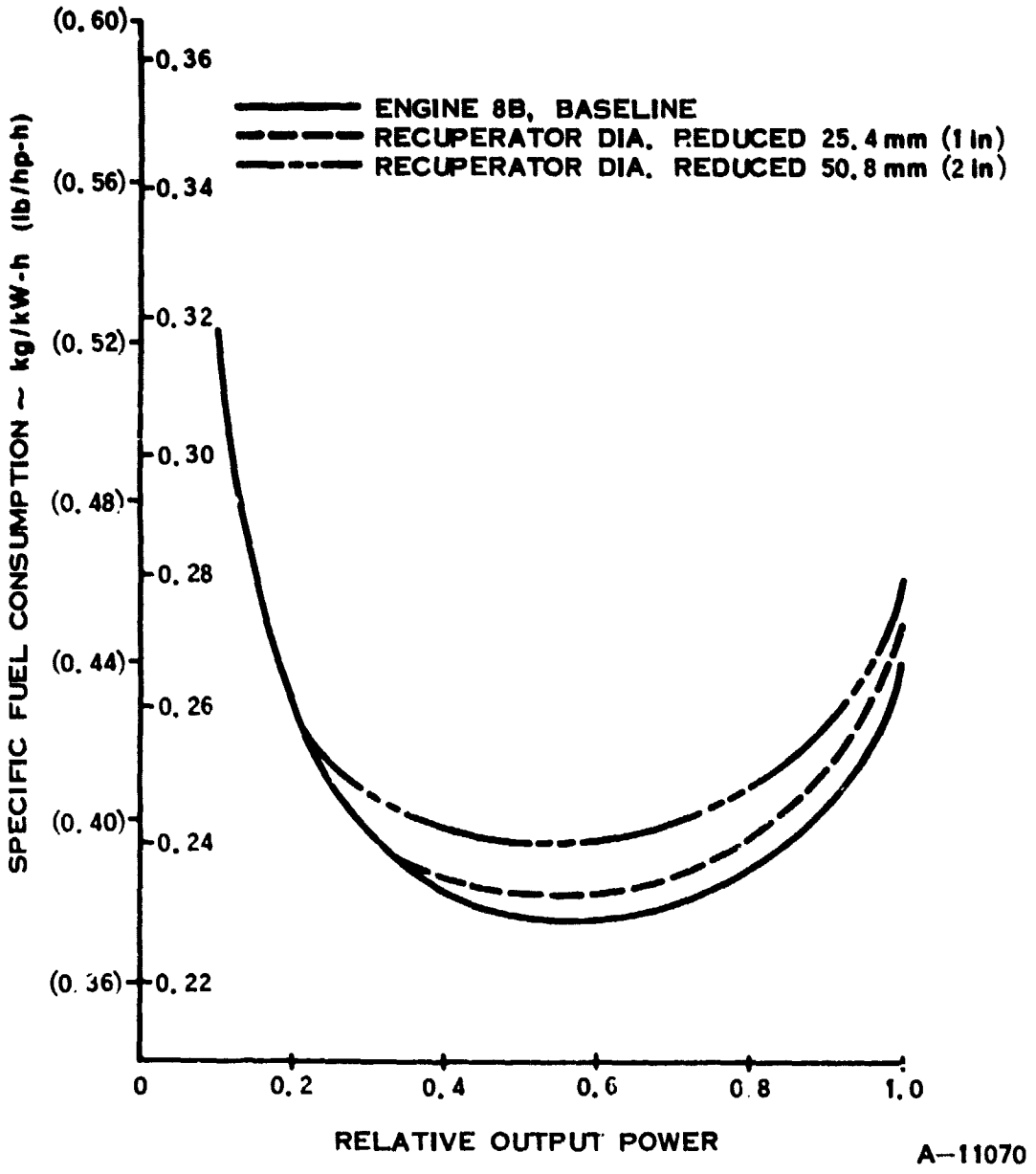

Figure 92. SFC at Reduced Recuperator Diameters

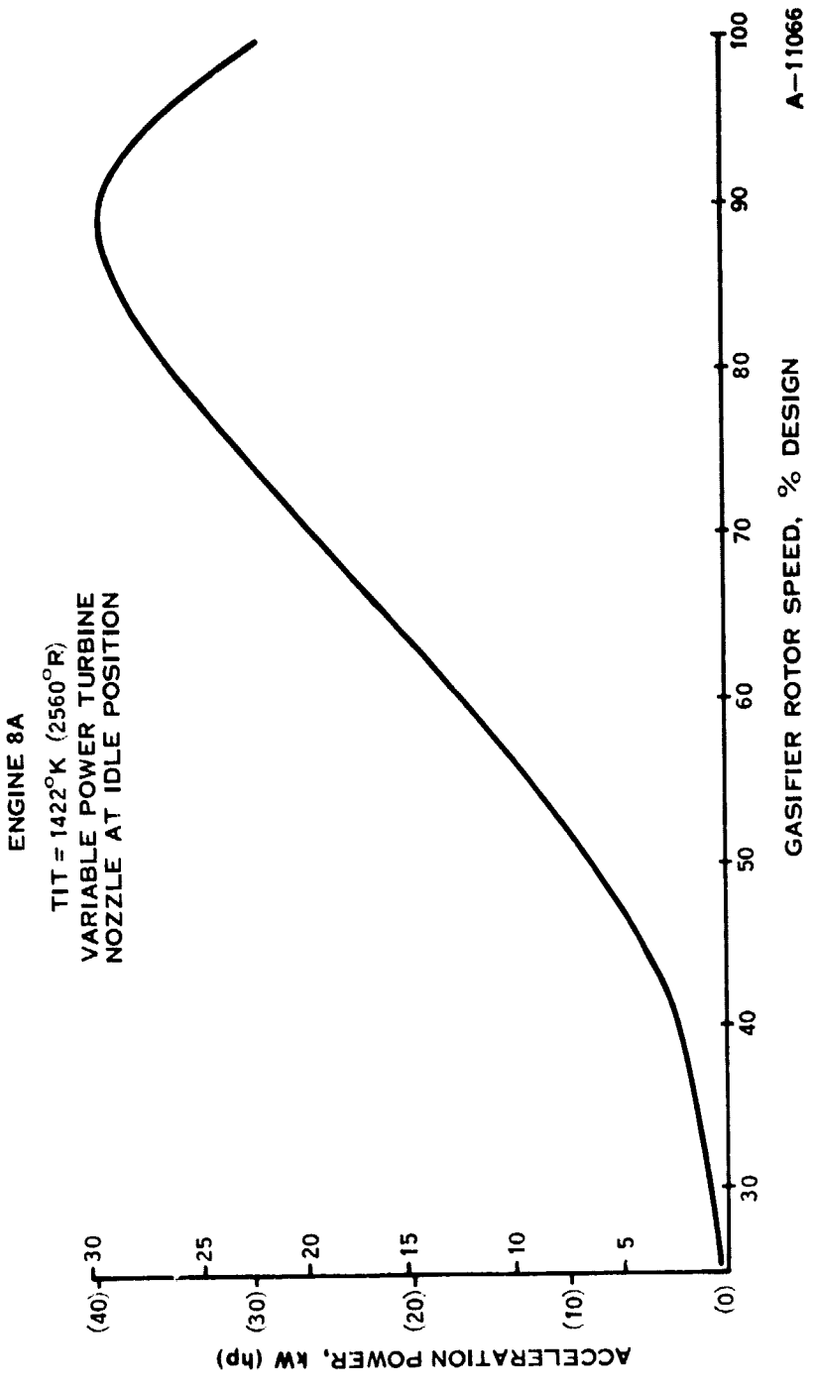

Figure 93. Acceleration Power versus Gasifier Rotor Speed

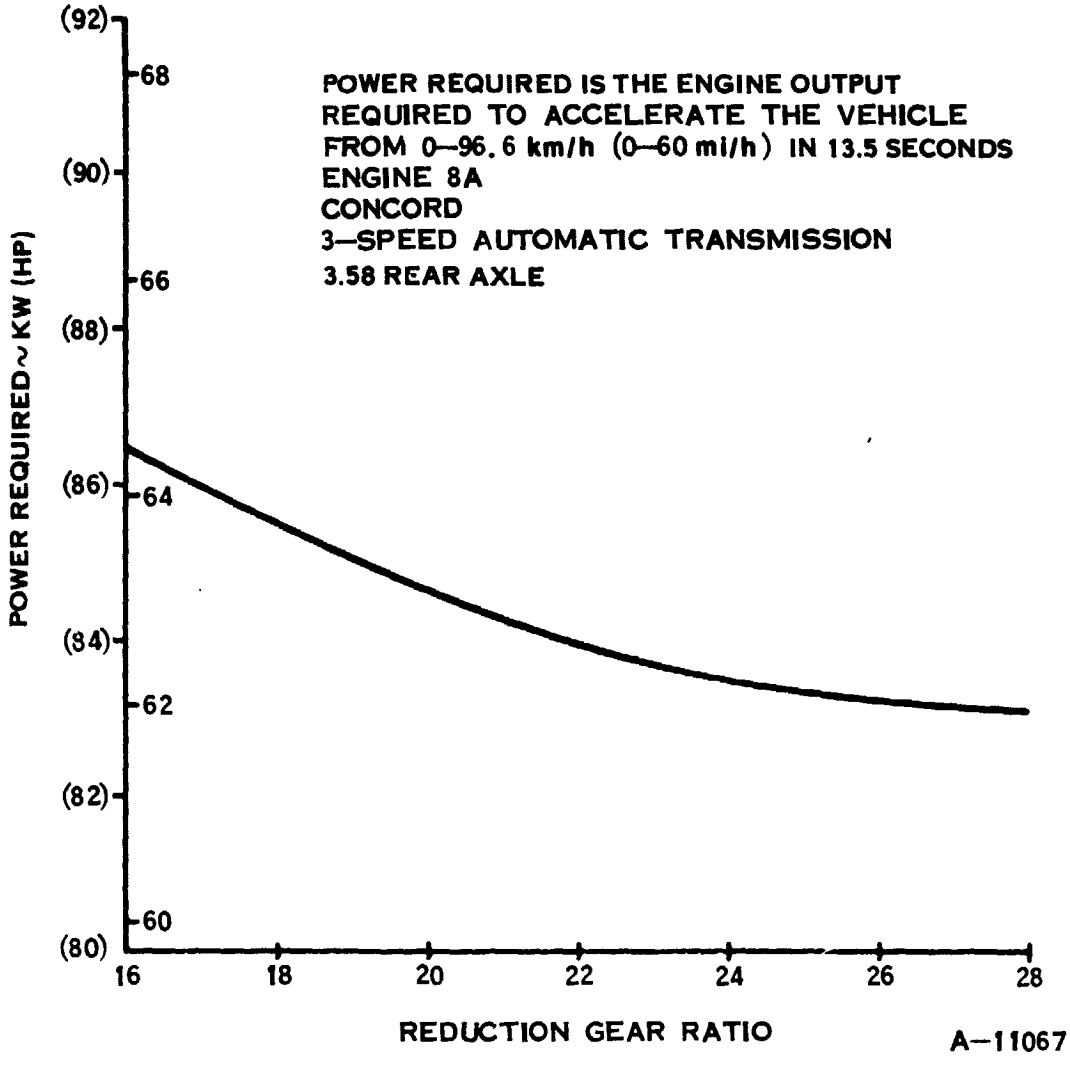

Figure 94. Power Required for Vehicle Acceleration

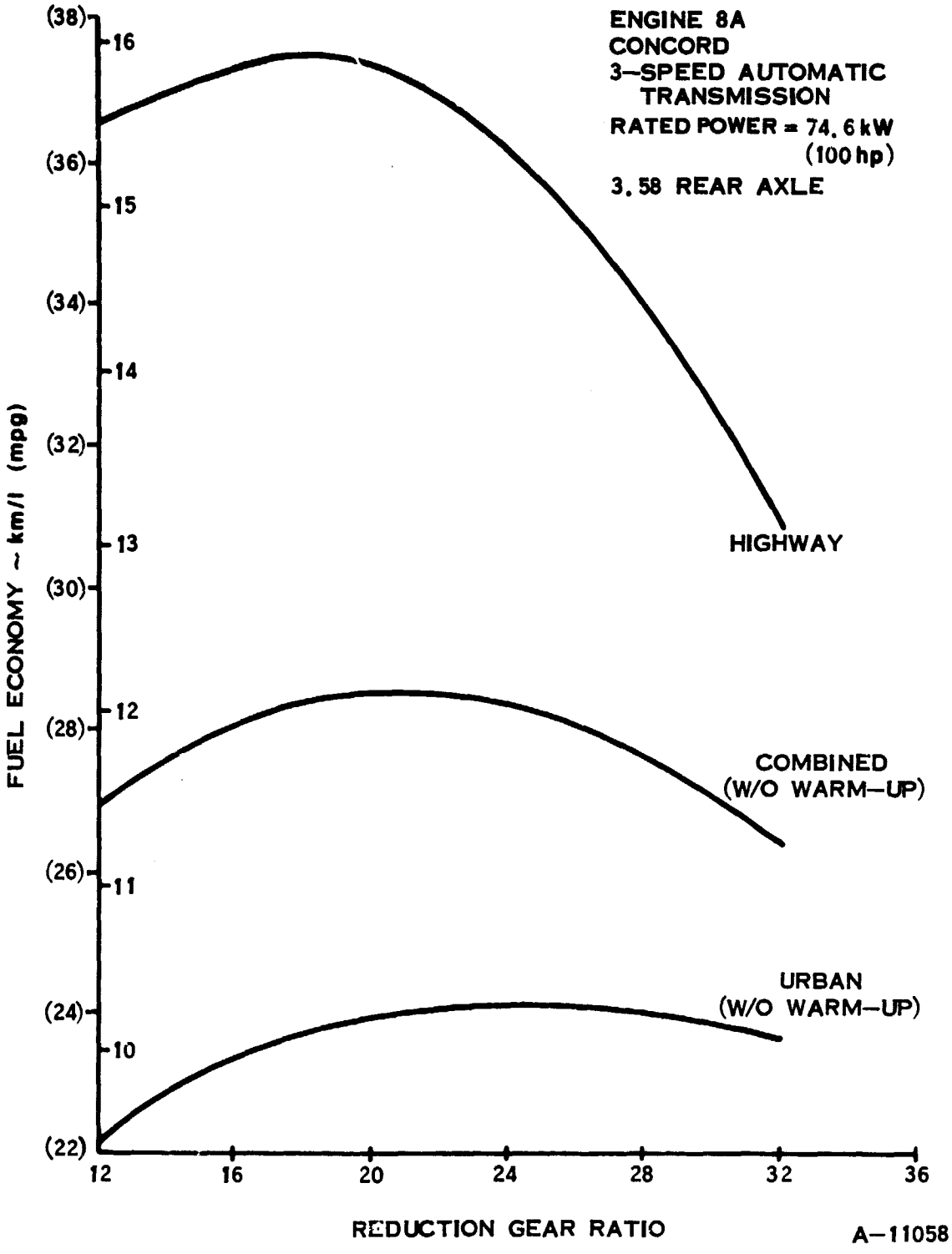

Figure 95. Fuel Economy, Engine 8A, Output = 74.6 kW

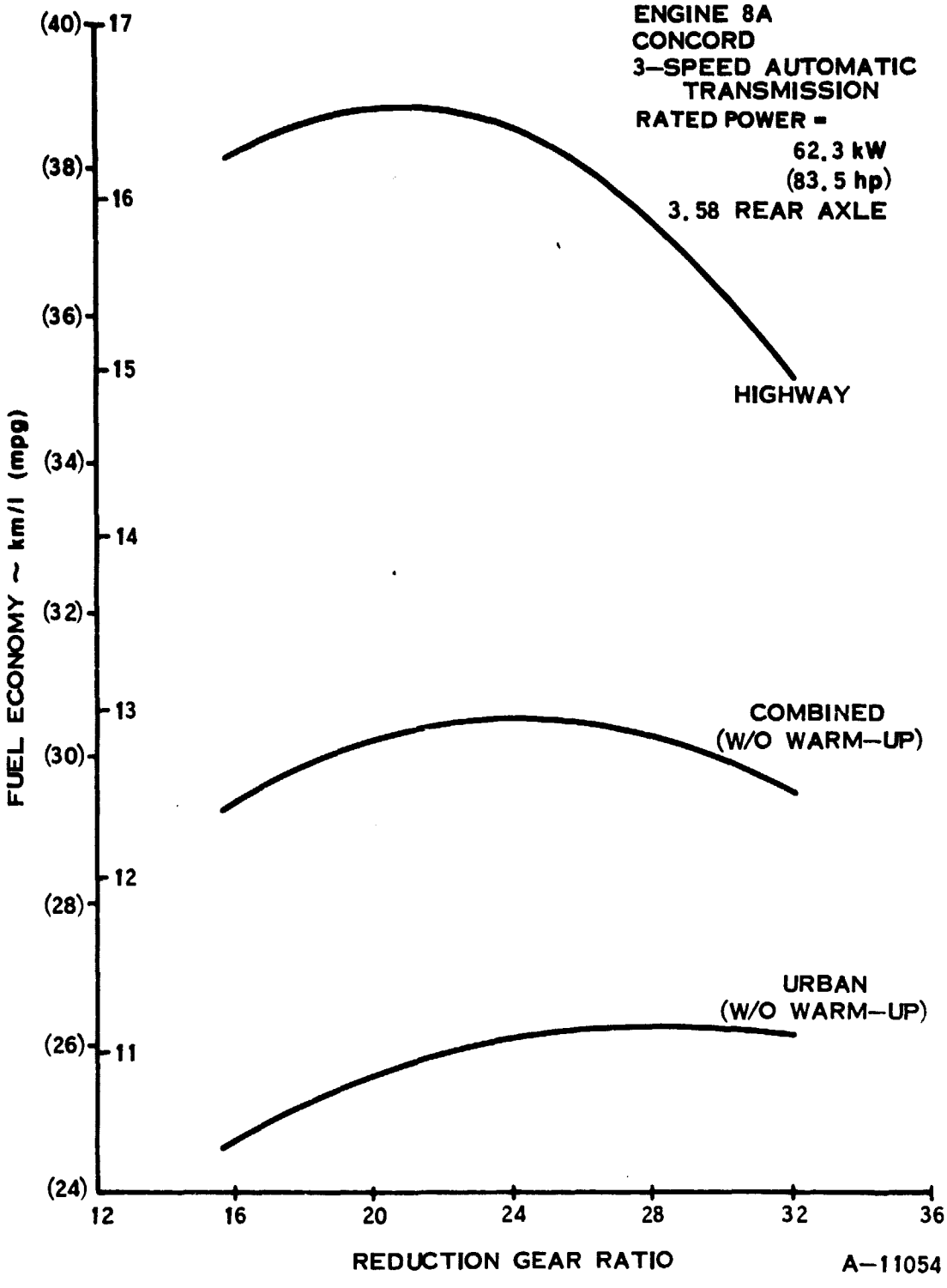

Figure 96. Fuel Economy, Engine 8A, Output = 62.3 kW

Engine 8B was then modeled, scaling Engine 8A [74.6 kW (100 hp)] down to 54.8 kW (73.5 hp) at SAE standard conditions but holding the vehicle accessory power. The driving cycle fuel economy is shown in Figure 97; optimum reduction gear ratio is 27.

The driving cycle fuel economy with the three engine sizes is summarized in Table XVI. Reducing engine size improves the fuel economy significantly; the 54.8 kW (73.5 hp) Engine 8B at 11.90 km/l (28.00 mpg) for the combined cycle fuel economy is 11.4 percent better than the 10.69 km/l (25.14 mpg) with Engine 8A at 74.6 kW (100 hp).

The effect on Engine 8B fuel economy of reducing the recuperator diameter by 5.08 cm (2.0 in.) was estimated as follows:

	Engine 8 Scaled to 54.9 kW (73.5 hp)	Recuperator Diameter Reduced 5.08 cm (2.0 in.)	Percent Change
Urban Cycle, km/l (mpg)	9.95 (23.40)	9.90 (23.28)	-0.5
Highway Cycle, km/l (mpg)	6.71 (39.31)	16.15 (37.99)	-3.4
Combined Cycle, km/l (mpg)	2.16 (28.60)	11.99 (28.19)	-3.4

The effect on the urban driving cycle is significantly less than on the highway cycle. The lower heat capacity of the smaller recuperator reduces the effect of the ambient temperature start on the first urban cycle.

POWERTRAIN SIZE

After the preceding studies, Engine 8B, rated at 54.8 kW (73.5 hp) at SAE standard conditions, 303°K (85°F) and 99.5 kPa (14.435 psia), was chosen as a good compromise for fuel economy, vehicle acceleration, and driveability. The combined driving cycle fuel economy is 11.4 percent better than Engine 8A at 74.6 kW (100 hp) while still meeting the vehicle acceleration requirement. The engine provides 62.3 kW (83.5 hp) dry (without water injection) below 288°K (59°F), and this power level will be maintained above 288°K (59°F), by the use of water injection, as shown in Figure 98. Water injection can also be used in the 273° to 288°K (32° to 59°F) range, providing margin for performance variation with production hardware and for deterioration with service. The power output dry is reduced to 50.7 kW (68 hp) at 311°K (100°F) and 47.7 kW (64 hp) at 317°K (110°F), adequate for normal driving. Attempting to size the engine even smaller than Engine 8B could run into marginal steady-state performance at altitude.

The recuperator diameter should also be reduced from the Engine 8B configuration to broaden the marketing base by permitting installation in a wider range of vehicles, passenger car, commercial, or military. The trade-off between production cost saving and fuel economy loss with the smaller recuperator should be restudied after the recuperator manufacturing process has been developed and production cost can be refined.

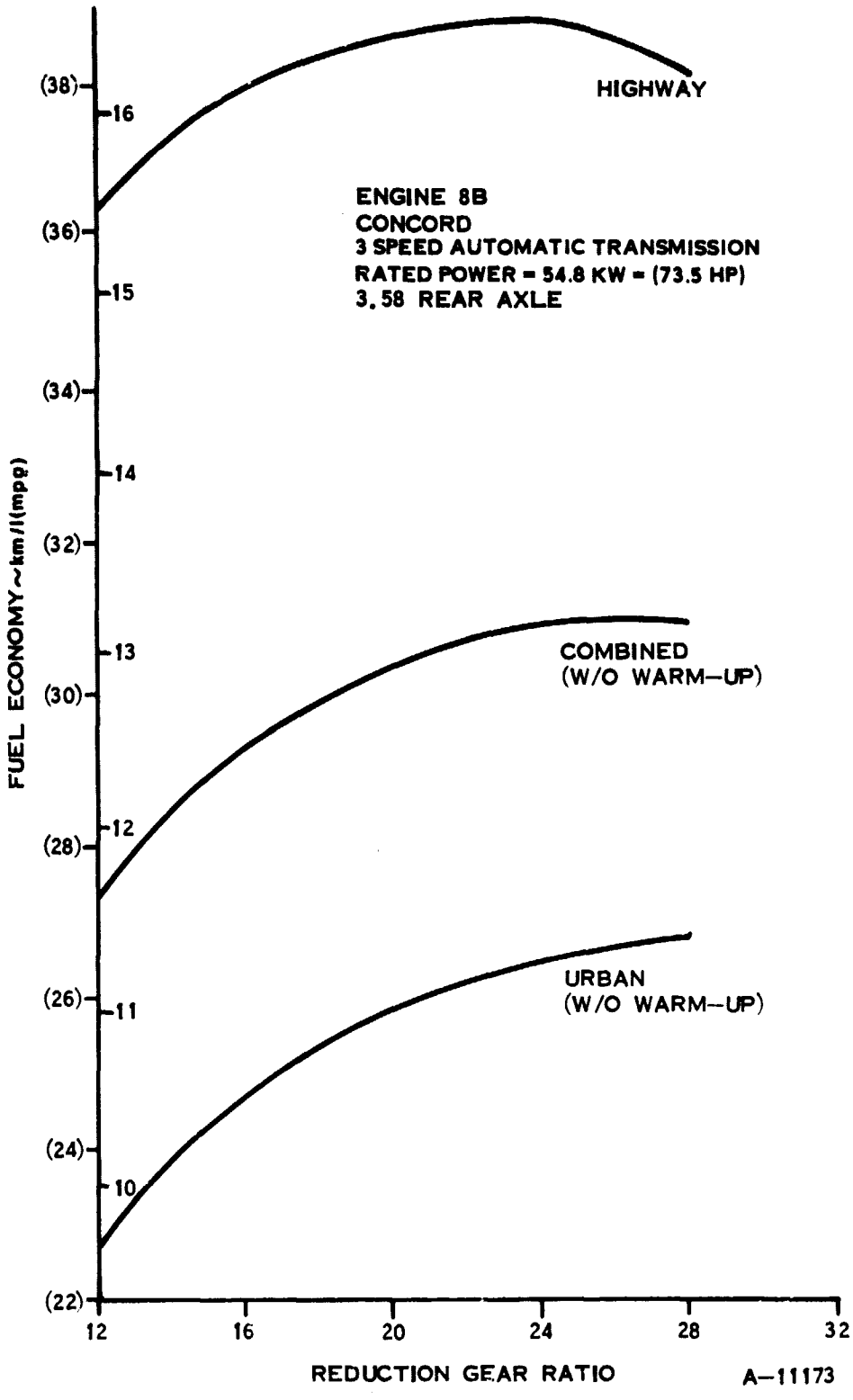

Figure 97. Fuel Economy, Engine 8B, Output = 54.8 kW

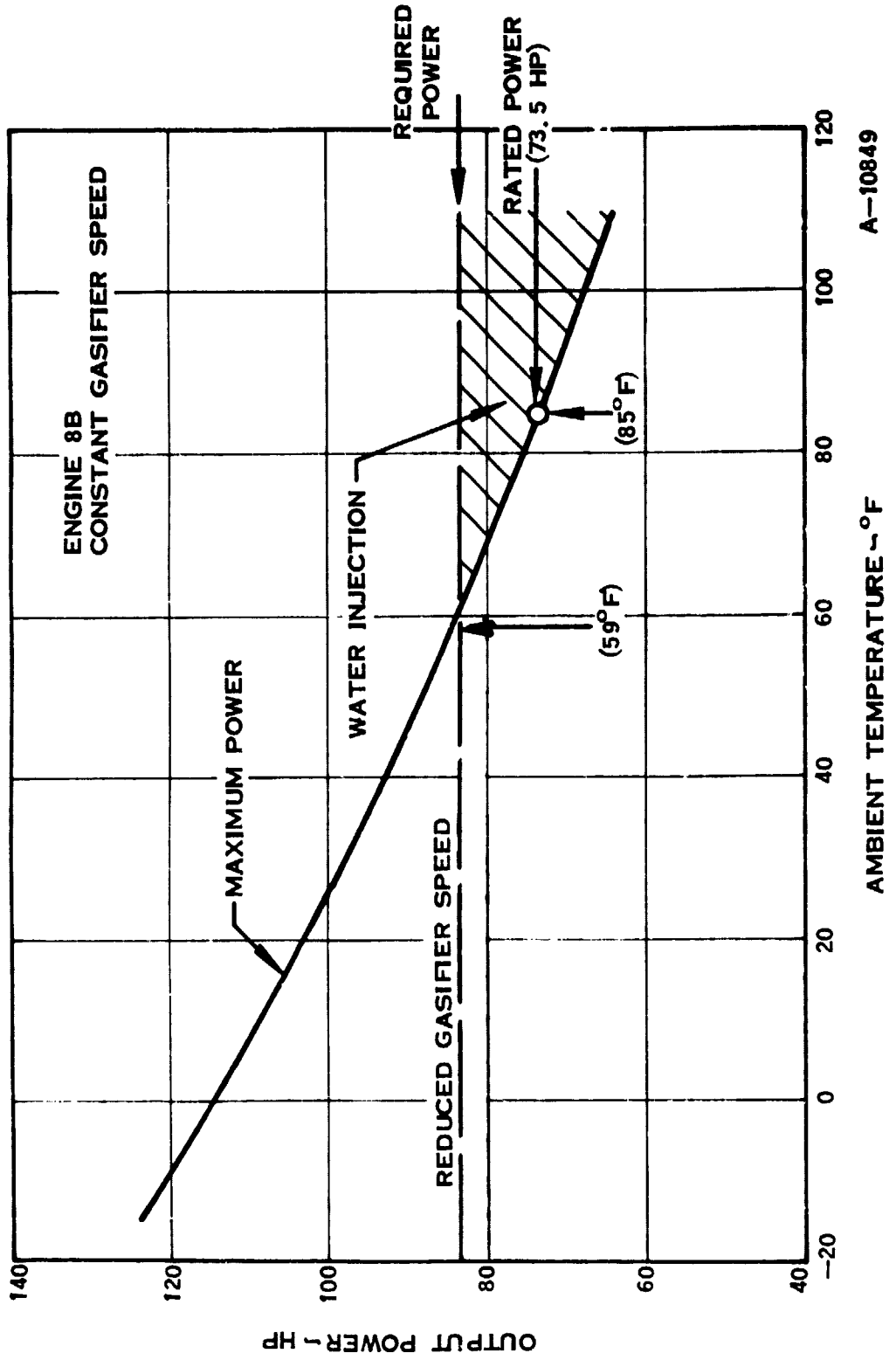

Figure 98. Engine 8B Output Power with Water Injection

TABLE XVI. DRIVING CYCLE FUEL ECONOMY COMPARISON

ENGINE NO.	8A	8 Scaled	8B
TIT ^{o}K (^{o}F)	1422 (2100)	1422 (2100)	1422 (2100)
RATED POWER, kW (hp)	74.6 (100)	62.35 (83.5)	54.8 (73.5)
URBAN CYCLE km/1 (mpg)	8.44 (19.85)	9.35 (21.98)	9.72 (22.87)
HIGHWAY CYCLE km/1 (mpg)	15.85 (37.27)	16.38 (38.52)	16.41 (38.59)
COMBINED CYCLE km/1 (mpg)	10.69 (25.14)	11.58 (27.24)	11.90 (28.00)
RATIO TO 8.33 km/1 (19.6 mpg)	1.28	1.39	1.43

NOTE: Concord at 1542 kg (3400 lb) test weight.
Ambient start on first urban cycle.

3.2 POWERTRAIN DESIGN

The final powertrain design is based on the components and the axisymmetric engine arrangement developed as part of Task II to best meet the turbine engine and vehicle system requirements.

POWERTRAIN ARRANGEMENT

The general arrangement of the IGT powertrain is shown by Figure 99. It is a dual-rotor arrangement, with the gasifier section consisting of a two-stage centrifugal compressor driven by the first stage axial flow turbine. The axial-centrifugal compressor that is the alternate design to the two-stage centrifugal compressor is shown in Figure 100. The second stage axial flow turbine drives the vehicle through a two-stage reduction gear and three-speed automatic transmission. A variable nozzle is used with the power turbine to control turbine temperature, output torque, and engine braking. An annular ceramic recuperator preheats the air on the way to the catalytic combustor, mounted coaxially at the inlet to the first stage turbine.

The air flowpath through the engine is shown by the arrows in Figure 101. Air enters the engine through the vehicle inlet system with air filtration and silencing. The air is compressed by the two-stage centrifugal compressor, then passed through an annular flow passage to the annular ceramic recuperator, Figures 74 and 75. The high-pressure passage through the recuperator has integral manifolds for the basic counterflow heat transfer surface, arranged in a Z-flow arrangement. High-pressure air from the compressor enters the outer rear manifold, flows inward, then forward through the counterflow section, then inward again to the combustion chamber. Air flows around the catalytic combustor to a swirler

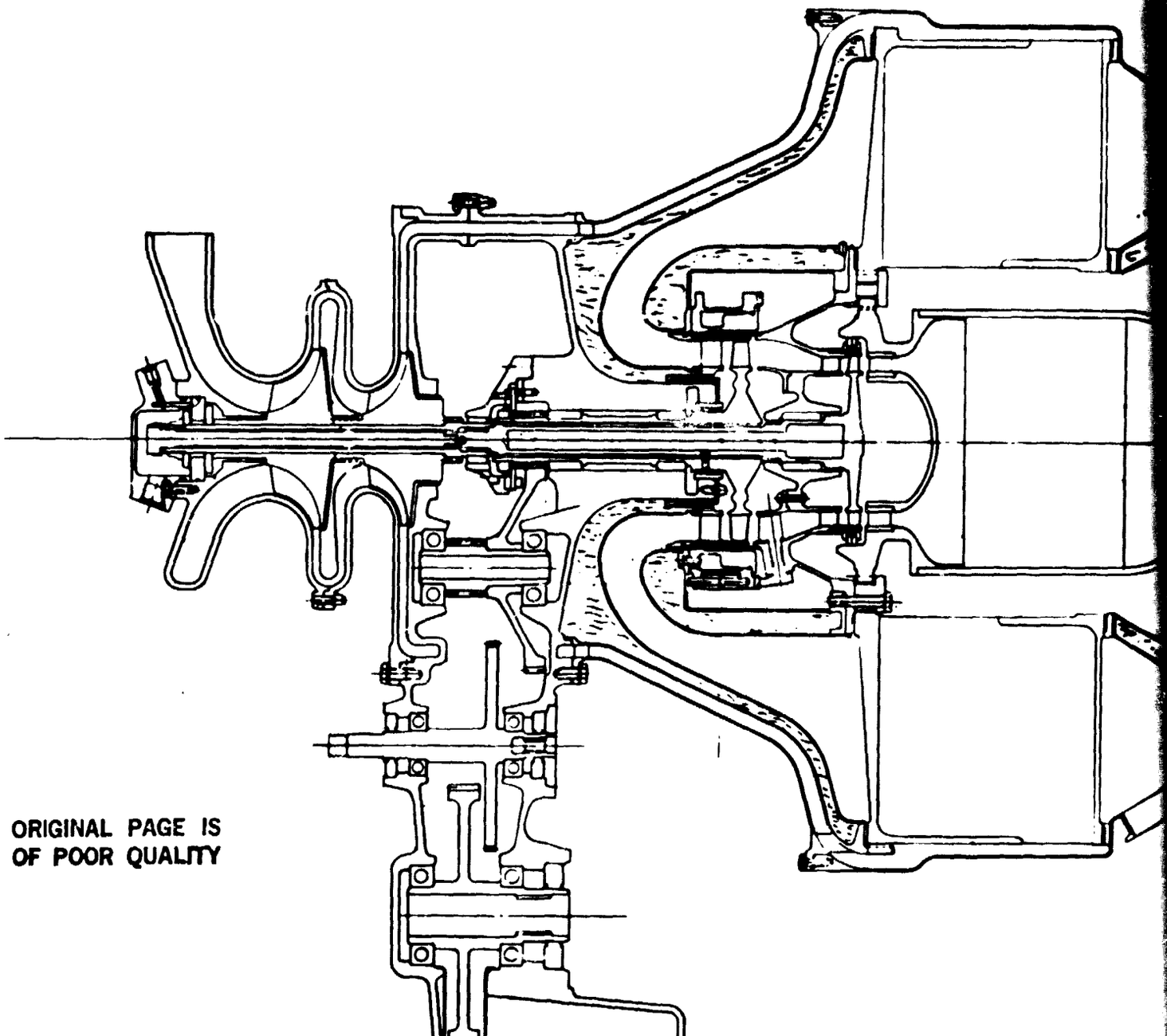

ORIGINAL PAGE IS
OF POOR QUALITY

FOLDOUT FRAME

PRECEDING PAGE BLANK NOT FILMED

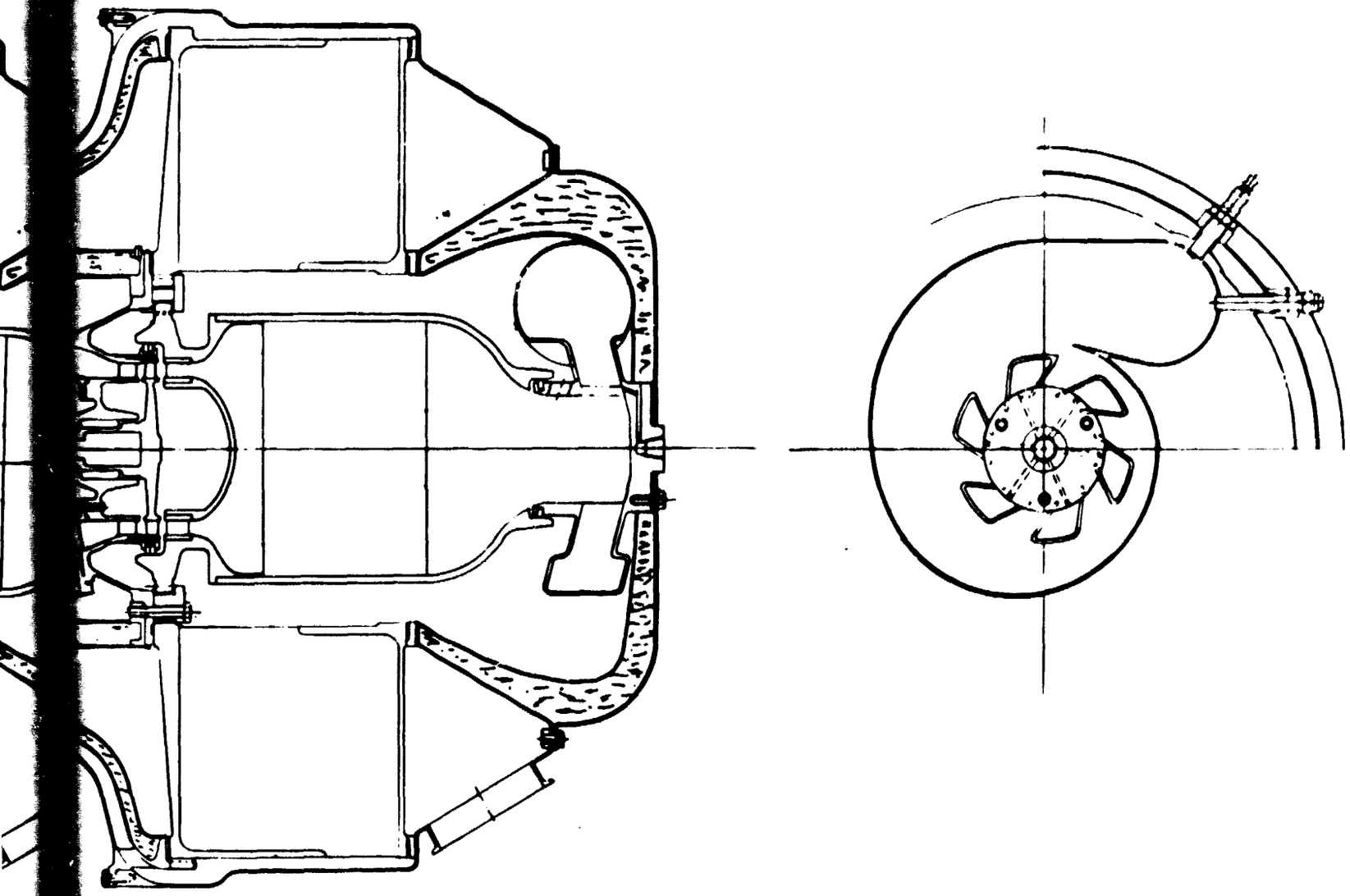

FOLDOUT FRAME 2

A-13262

Figure 99. Cross Section of IGT Powertrain

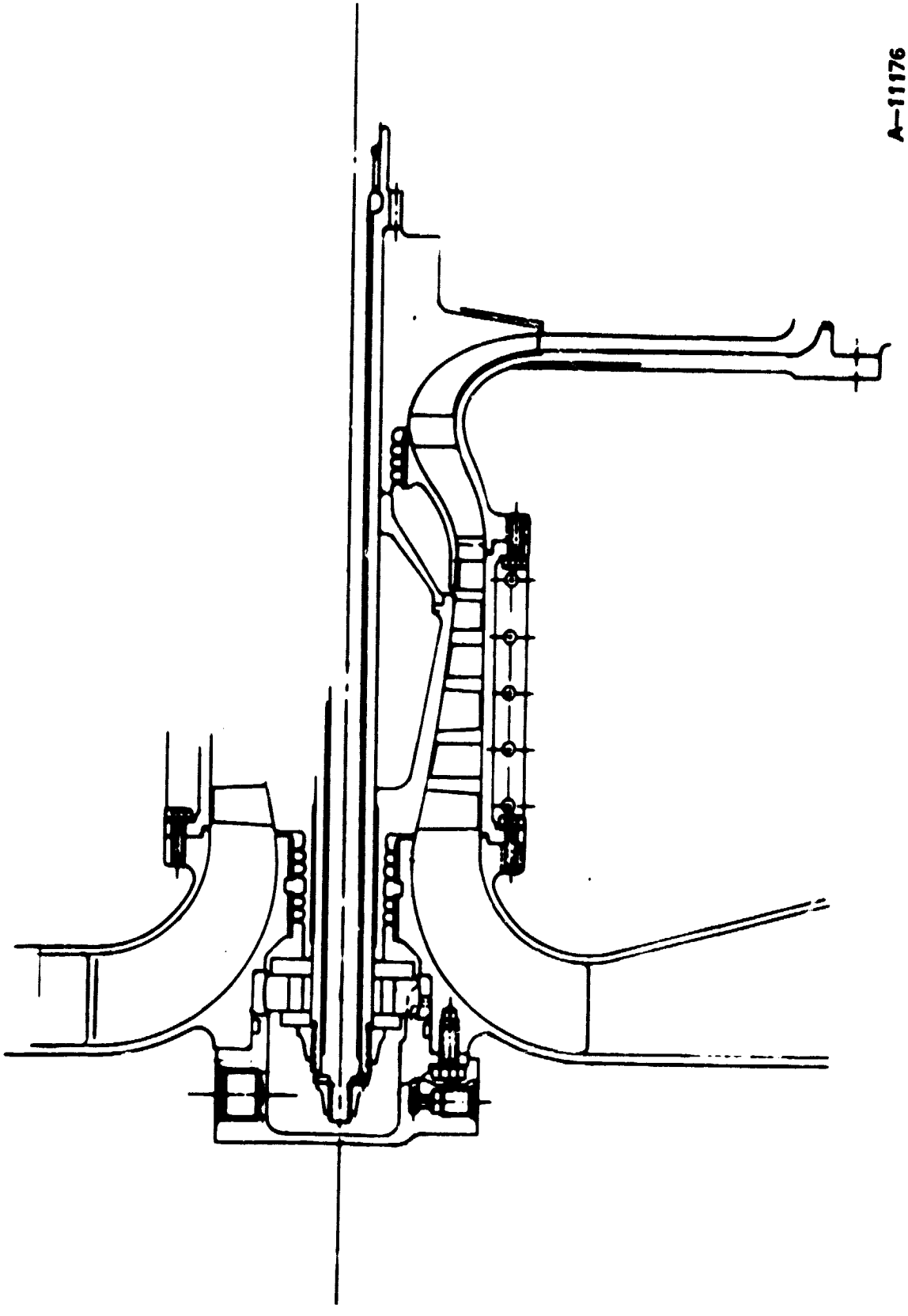

A-11176

Figure 100. Axial-Centrifugal Compressor

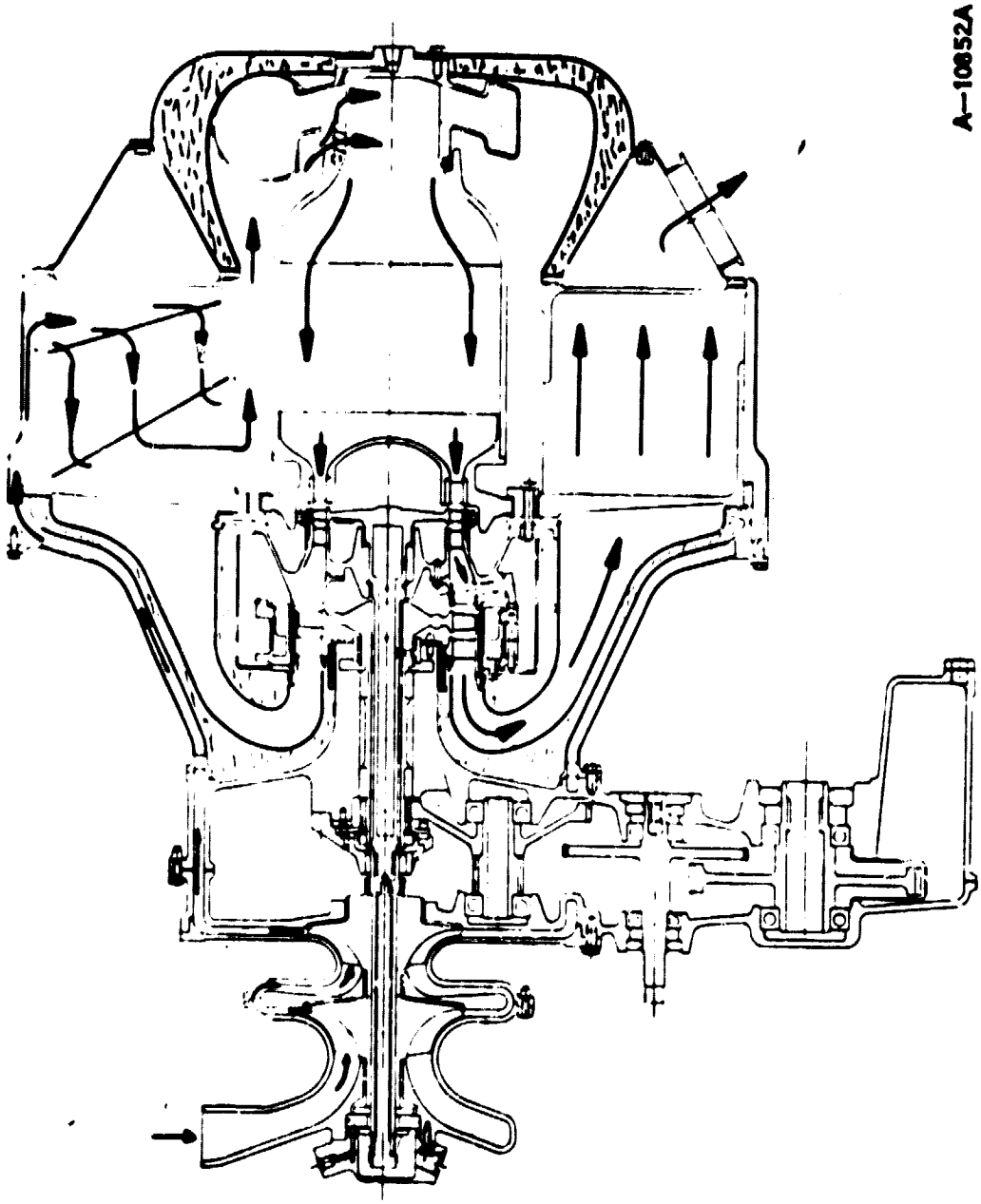

A-10852A

Figure 101. Powertrain Flowpath

which atomizes the fuel and guides the mixture into a high-energy vortex to ensure thorough mixing and vaporization prior to entering the catalyst bed. A precombustor heats some of the air, feeding alternate swirler passages through a volute to start combustion, warm up the catalyst bed, and maintain satisfactory combustion under idle and low-temperature conditions.

Combustion gases flow forward through the turbine stages, then are diffused and returned to the recuperator, passing to the rear through the low-pressure passages. Exhaust gas is collected at the rear of the engine and is discharged through the vehicle exhaust system.

This powertrain arrangement provides an efficient, axisymmetric structure. The turbomachinery is attached to the fore and aft ends of the gearcase, with shrouds and flow passages concentric to the bearing supports. A large double-walled sheet metal cone supports the recuperator housing. Radial keys are used from the housing to the recuperator, and from the recuperator to the turbine interstage structure, locating the flowpath relative to the rotors. Radial keys also locate the outlet end of the combustor; the inlet end is attached by the combustor cover to the recuperator housing.

This sheet metal cover is lightweight and efficient; the temperatures, pressure loads, and stresses are uniform around the axis for minimum distortion, maintaining flow passage alignment and permitting minimum running clearances. The external shell also has considerable load-carrying capacity to handle any external or inertia loads imposed by vehicle installation and operation.

The same axisymmetric structure provides ideal flowpaths between annular components and assures uniform circumferential flow distribution. Passage areas are generous for low velocity and low pressure drop. The short, annular flowpaths minimize surface area and heat loss, and at the same time permit simple insulating layers between passages. The flowpath also has cooler compressed air and engine exhaust behind most of the exterior surface, to minimize external heat loss and to ease engine compartment temperature problems. The flowpath arrangement also minimizes noise emission by isolating, with other flow passages and walls, the low velocity flows on the outside from the high velocity turbine section.

External views of the engine assembly are shown in Figures 102, 103 and 104.

ROTOR SYSTEMS

The gasifier rotor system is made up of two shaft assemblies mounted on three bearings. The two centrifugal compressor impellers are assembled to a steel shaft mounted on journal bearings at each end. The front bearing also has a tapered land thrust bearing and plain anti-thrust bearing. The pinion for the accessory drive gear train is integral with the shaft between the second stage impeller and the rear bearing.

The gasifier turbine wheel is welded to a shaft and located radially by a foil-type air bearing in the turbine interstage. The front end of the turbine shaft is splined into the compressor shaft, with a pilot to locate the shaft radially.

C-3

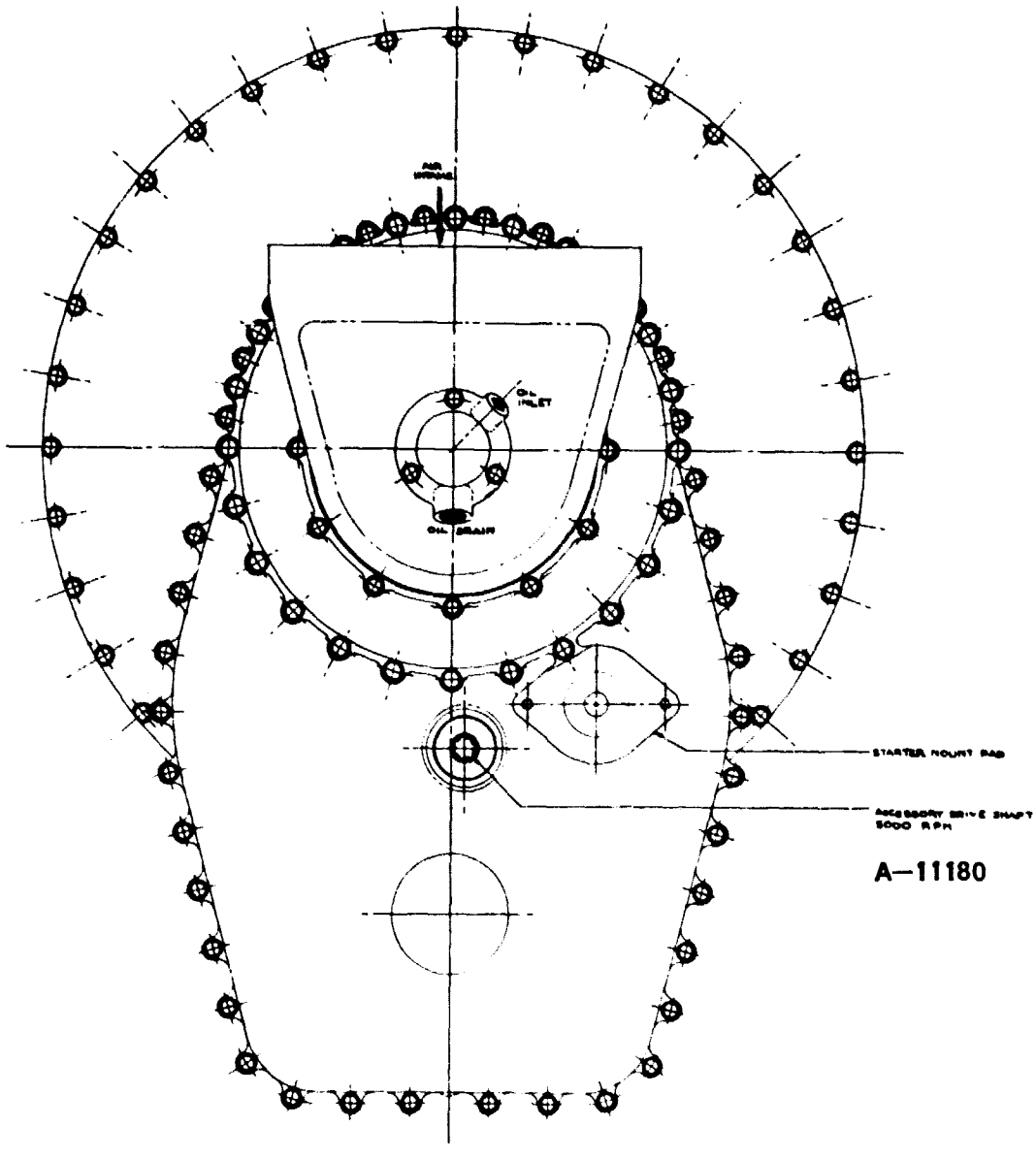

Figure 102. Engine Assembly, Front View

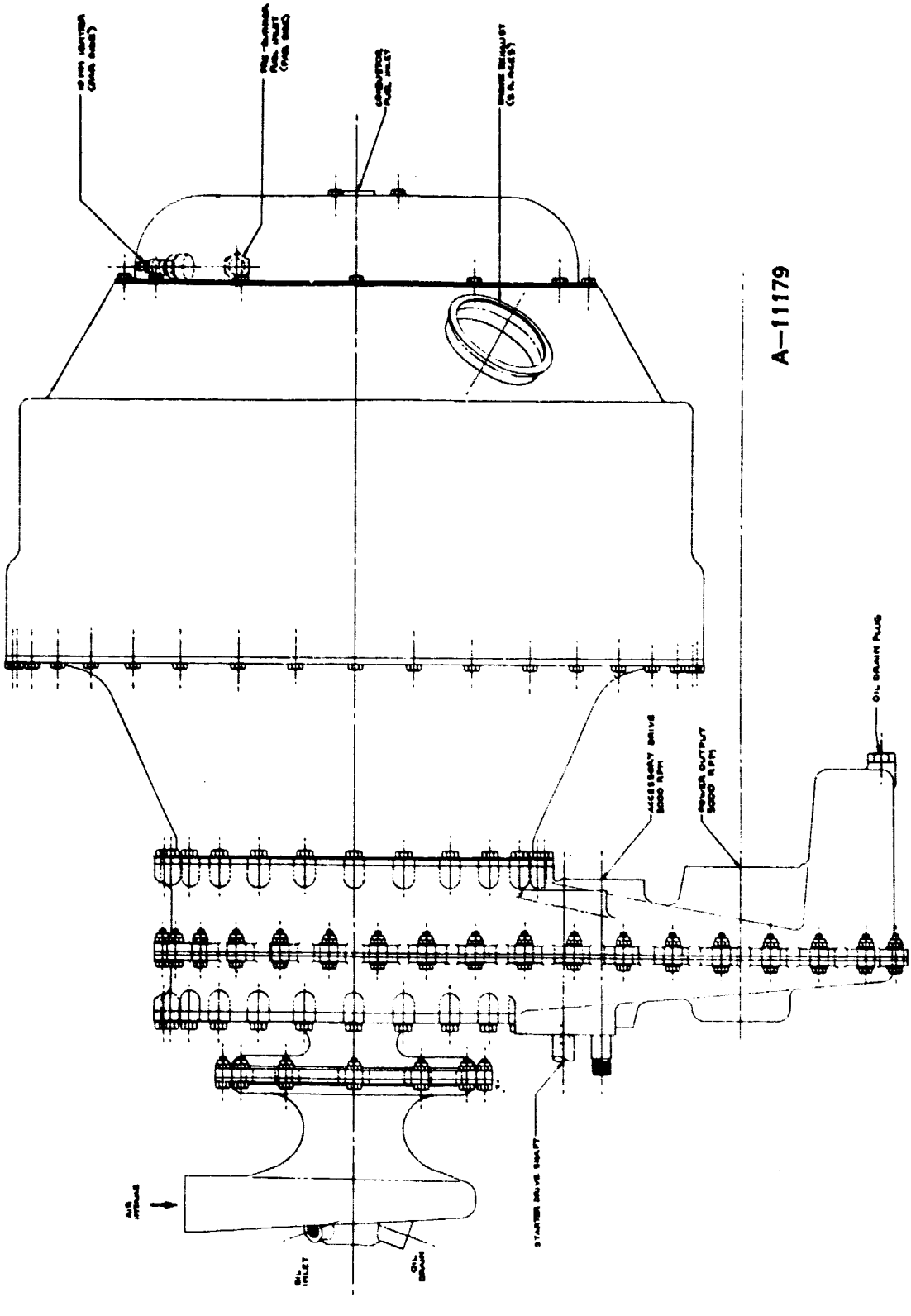

Figure 103. Engine Assembly, Side View

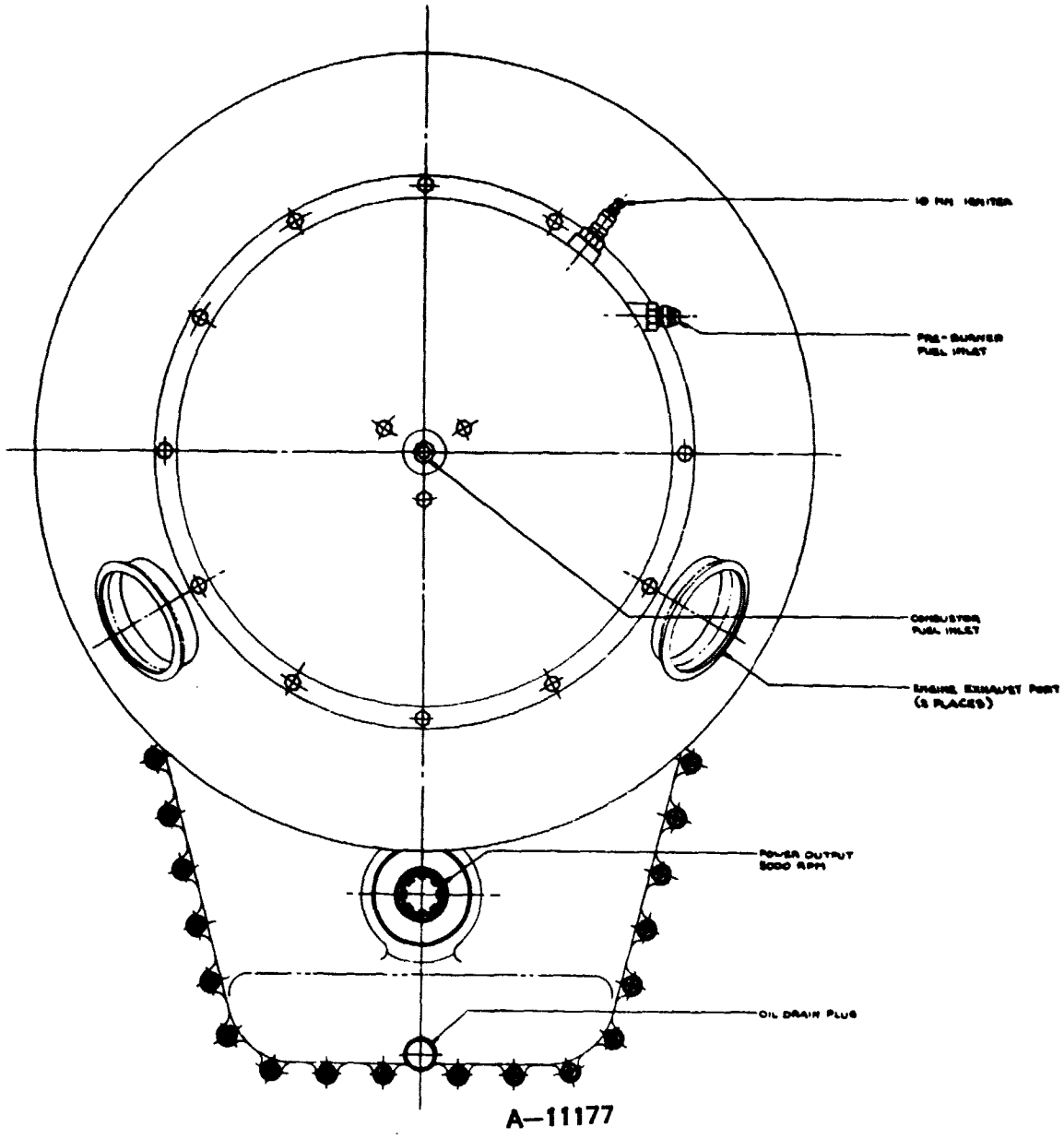

Figure 104. Engine Assembly, Rear View

The thrust load from the turbine wheel is carried by a shoulder to the compressor shaft. A shouldered tie bolt through the compressor shaft controls axial position with a small clearance to avoid clamping.

The power turbine wheel is also welded to the hollow drive shaft, concentric with the gasifier turbine shaft. The output reduction gear pinion is integral with the shaft, with two journals for segmented floating bushings. A thrust washer at one end of the pinion takes the thrust load through a tapered land thrust bearing, with a plain thrust washer to control axial clearance. The drive pinion helix angle is set to reduce the thrust load on the bearing.

DRIVE SYSTEM

The IGT powertrain has a single gearbox which houses two gear trains, one for vehicle propulsion, and the second for engine and vehicle accessories. This gearbox is integrated into the engine mid-section structure, with the gear trains and drives located below the engine centerline. The design and location of the gearbox provide good thermal isolation; the turbine exhaust passages are insulated and the combustor is located in the aft end of the engine, away from the gearbox. These features provide for cooler operation and longer life for gearbox components and the engine lubrication system.

The output gear train is driven from the front of the power turbine shaft by an overhung integral helical pinion. The output speed is reduced using two intermediate gearshafts and a final drive gear from 75,558 rpm to 3,780 rpm at rated power. The intermediate shaft is a two-gear cluster, one integral with the shaft and the other keyed to this shaft. Power takeoff from the gearbox is by means of a splined connection to a drive shaft which couples the engine gearbox to the automatic transmission.

The accessory drive train is driven by a pinion, integral with the compressor shaft, located between the second stage compressor impeller and the mid-gasifier shaft bearing. This drive pinion drives an idler gear which meshes with a gearshaft connected to both the electric starter and the engine/transmission oil pump. The electric starter is mounted on the front of the gearbox with the oil pump mounted on the back. The starter motor is disengaged during engine operation. The oil pump runs at approximately 12,600 rpm, reduced from the 78,900 rpm (at rated power) gasifier shaft. Next in the drive train is the fuel pump drive gear, which is on a common gearshaft with the vehicle accessories drive pulley. The fuel pump is mounted on the back of the gearbox, and the vehicle accessories are mounted to the front of the gearbox. Both the oil pump and fuel pump are mounted on pads integral to the gearbox casting. These engine accessories are coupled to the gearshafts with splines for high reliability and ease of maintenance. Vehicle accessories include the alternator, power steering pump, and air conditioning compressor, and are belt-driven from a multiple groove pulley operating at 5,000 rpm at rated power.

The gears will be manufactured to quality requirements and processed from alloys currently being used in automotive transmissions. All the gears will be of a helical type and will be case-hardened with shaved or ground tooth profiles for

long life and quiet operation. On the starter-oil pump gearshaft and on the intermediate gearshaft in the drive train, helixes will be established to provide a substantial thrust balance. Helix angles for each gear element will be optimized for long life, minimum noise, shaft thrust, and high efficiency.

All the gearshafts will be straddle-mounted on bushings or anti-friction bearings to provide long life, high efficiency, and low cost by 1) low-cost, automotive-type construction, 2) automotive quality requirements, and 3) a simplified lubrication system with minimum oil feed passages and other machining features. Gearbox splines will be case-hardened and mist-lubricated from the gearbox for long life and good reliability. Oil seals on the starter motor, fuel pump, and pulley gearshafts will be double-lipped, spring-reinforced types commonly used in the automotive industry.

LUBRICATION SYSTEM

The lubrication pump consists of one pressure element and one scavenge element. The pressure element supplies oil to the engine bearings, the transmission, and power turbine nozzle actuator. The scavenge element transfers oil from the transmission sump power turbine to the engine gearbox pump. Pump elements will be positive displacement, either gear, vane, or gerotor type, based on cost effectiveness.

A schematic of the lubrication system can be seen in Figure 105. The inlet to the high-pressure pump element is through a screened inlet in the gearbox sump. The exit of the pressure pump is regulated to a maximum of 1034 kPa (150 psi) by a spring-loaded regulator returning flow back to the pump inlet. The oil flow is then filtered in a 40-micron, spin-on, disposable oil filter. A bypass around the filter element is supplied in case of excessive pressure drop in the element itself. Filtered oil is then fed through restrictive orifices to the engine bearings and the gearbox. Bearings and gearbox are then gravity-scavenged to the gearbox oil sump.

Filtered high-pressure oil is also fed to the transmission to lubricate it and to supply the energy for shifting, which is initiated by electrical signals from the fuel control. As stated previously, the transmission is scavenged by a scavenge pump element back to the engine gearbox sump.

The major portion of the pressure pump output is available for the power turbine nozzle actuator. The nozzle actuator is controlled by an electrical signal from the fuel control. Valving in the actuator minimizes oil flow when the nozzles are being maintained in a steady-state condition. During an actuator transient, however, most of the oil is used to accelerate and move the actuator. Oil exiting from the actuator is returned to the gearbox sump.

The lubricant used in the engine will be a synthetic lubricant similar to MIL-L-23699 or MIL-L-7808.

FUEL SYSTEM

The fuel system will be capable of operating the engine on gasoline, diesel fuel, kerosene or similar liquid hydrocarbons. In order to keep the main fuel pump

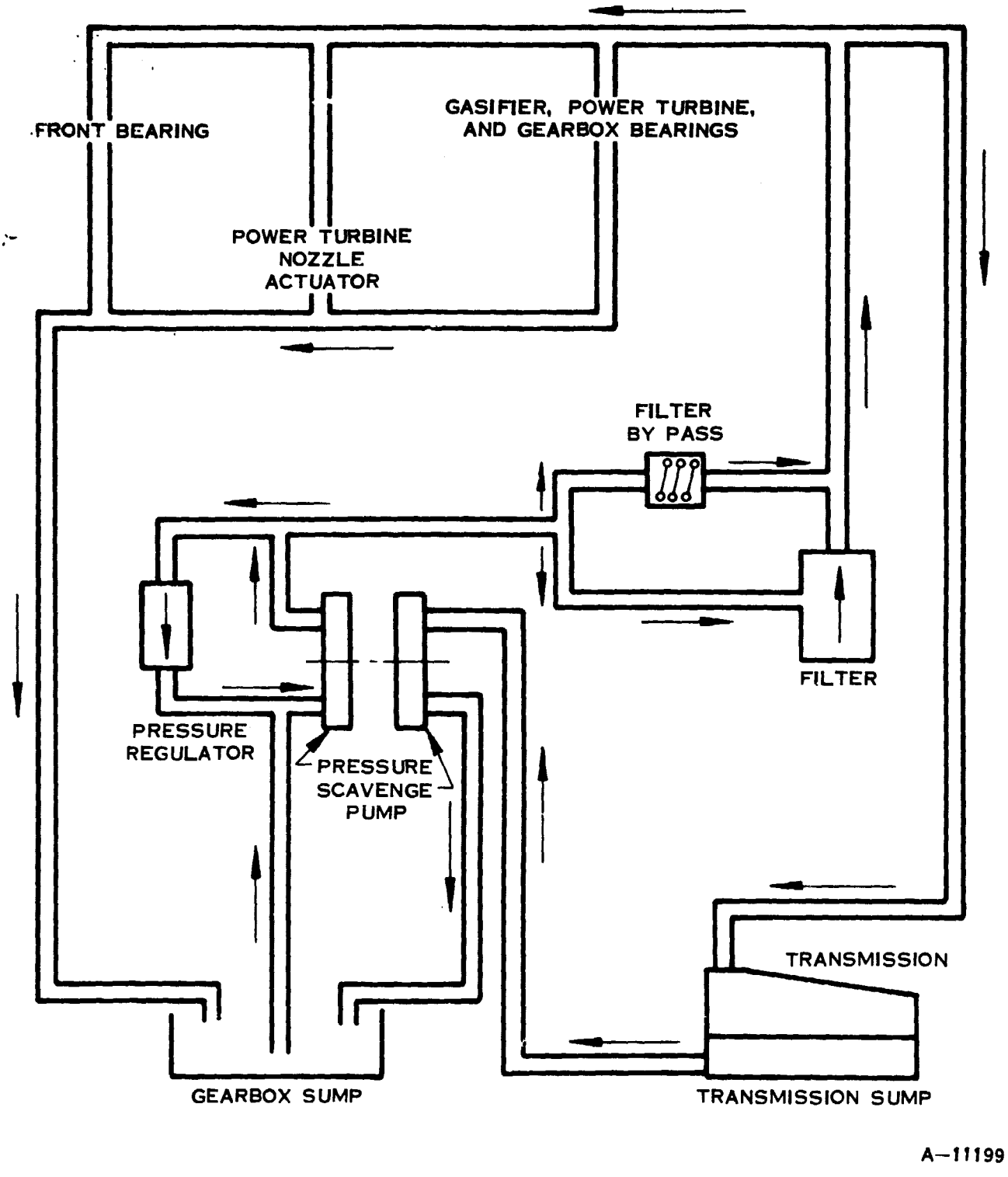

Figure 105. Lubrication System Schematic

from cavitating or vapor locking, a small pump will be tank mounted. The pump will supply enough pressure to overcome line resistance and fuel filter pressure drop, and keep the main pump from cavitating. The in-line fuel filter will filter the fuel to 10 microns prior to entering the main fu pump. The main fuel pump will be mounted on the gearbox pad and driven by the gasifier. It will be a positive displacement pump capable of supplying up to 1034 kPa (150 psig) to the fuel nozzles. If 1034 kPa (150 psig) is exceeded, the pump will be protected by a relief valve diverting flow back to the pump inlet. The outlet of the main fuel pump is fed to the fuel metering section of the control system. The fuel metering system returns any excess fuel supplied by the pump back to the fuel tank. Metered fuel is supplied to the engine fuel nozzle.

CONTROL SYSTEM

The control system establishes engine fuel flow for starting, accelerating, decelerating, and steady-state operation. The control also positions the power turbine nozzle vanes for optimum accelerating, decelerating, braking, and steady-state TIT control. In addition, the control system signals the transmission for gear changing for optimum acceleration and efficiency. Lastly, the control system has monitoring features to avoid catastrophic failures due to selected engine or fuel control malfunctions.

For starting, the control system supplies electrical power to the ignition system and start relay until the engine reaches 35 percent speed. For engine acceleration to idle, the control system supplies fuel flow according to a schedule of fuel flow versus corrected gasifier speed. This schedule is biased by the turbine temperature prior to engine startup so that the engine receives less fuel when it is being started while the recuperator is still hot from a previous run than when started cold. This start schedule stays in effect until the engine reaches idle.

The driver's power control setting (equivalent to the throttle for the piston engine) is converted to a power turbine nozzle position and gasifier speed demand in such a fashion that the power turbine output torque is approximately a linear function of power setting. This avoids the mushy feeling for the first part of the power range and the overly sensitive final portion. The power signal does not change gasifier speed for approximately the first 20 percent of the range. During this part of the demand variation, the power turbine nozzles are brought from the idle reference position to the normal temperature modulated power position. This reduces the backpressure on the gasifier with the foot off the throttle, thus improving fuel economy. It also allows power turbine torque to be taken smoothly from essentially zero torque up to operating torque levels. When the power demand exceeds 20 percent, the gasifier speed is increased in order to increase power turbine output torque. The gasifier speed control serves as the main source of control of output torque. The gasifier governor automatically compensates for the varying fuel requirements of the engine to maintain a constant gasifier speed.

At a given steady-state gasifier speed, maximum fuel economy is obtained by adjusting the power turbine nozzle to operate the engine at the highest TIT permissible under material or surge limitations. This temperature is maintained

at an optimum value by a schedule of turbine temperature (or corrected temperature below certain ambient temperature) versus corrected engine speed. This schedule causes the power turbine nozzle to position as required to maintain the temperature defined by the schedule.

If the gasifier speed is at maximum and the ambient temperature is higher than a predetermined value, water injection is used to maintain output power. The water will be modulated by the last 10 percent motion of the power setting, with the maximum water delivered being controlled to a schedule of water flow versus ambient temperature. By using water injection to boost the output of the engine at hot ambient conditions, it is possible to use a smaller engine and achieve better fuel economy. This is explained further in the performance section of this report.

If the gasifier-demanded speed is greater than the actual gasifier speed by a predetermined amount, the engine is considered to be in the acceleration mode. During accelerations, the turbine nozzle is biased open and the fuel flow is increased until the TIT is increased to a value determined by a schedule of temperature (or corrected temperature) versus corrected gasifier speed. With the nozzle biased in the open direction, the gasifier will accelerate more rapidly because of the lower back pressure on the gasifier.

Deceleration is treated differently depending upon the degree of deceleration, similar to the acceleration. Small or slow speed decreases are treated by the steady-state control system. When large and fast speed decreases are demanded, i.e., demanded speed is 10 percent less than the actual gasifier speed, the deceleration is handled differently; the power turbine nozzle is opened to the deceleration reference position. This reduces power turbine torque output while at the same time reducing the amount of fuel required to maintain gasifier speed, resulting in fuel saving. If the demanded speed is 10 percent less than gasifier speed and the driver's foot is off the throttle, the power turbine nozzle is moved to a reverse position to provide engine braking. During these decelerations, the fuel is cut back as required until a minimum fuel flow established by a corrected fuel flow versus corrected gasifier speed is reached, which prevents combustion flameout.

The control system supplies the signals to the transmission so that the proper gear is chosen for most efficient operation. This is accomplished by a schedule in the control system that is dependent upon gas generator speed, power turbine speed, and ambient temperature.

The safety and fail-safe features basically include overspeed protection, over-temperature protection and sensor failure protection. In the event that one or more of these failures occurs, the engine is put into a safe operating mode which will, in most cases, allow the vehicle to limp home. If the conditions are such that it cannot be tolerated at all, the engine is shut down.

The control system will be an electronic microprocessor-based control unit. This electronic control unit will be mounted inside the passenger compartment so that some benefit of environmental control is achieved. Fuel metering will be accomplished by one of the standard means of converting an electrical signal to fuel flow. The turbine nozzle actuator will be a piston-type actuator powered by oil from the lubrication pump, controlled by an electrically operated valve.

IGNITION SYSTEM

The ignition exciter will be a low-cost, inductive type of exciter which will result in a power dissipation at the igniter plug of at least four watts (average) with an input voltage range of 6 to 16 Vdc. The four watts average dissipation has been determined by test to be adequate for this type of engine. The output voltage capability of the exciter will be 12 kV minimum. This will be adequate to ionize the air gap type of igniter with a 2.54 mm (0.1 inch) gap.

The ignition leads for the output of the exciter will consist of an insulated standard wire cased with a tin-plated copper overbraid. The shield will be terminated at the exciter connection at one end and the igniter connection at the other end. The ignition lead connectors will be similar to the ARP 670 type 2.

The igniters themselves will be somewhat similar to present day jet engine igniters, except that the design will carefully consider high-volume production technique. The igniter will be positioned in the combustor to provide good starts and still keep igniter temperatures as low as possible.

STARTING SYSTEM

The signal to initiate a start will originally come from the driver's key. The control system will then engage the starter solenoid and ignition exciter until engine speed exceeds 35 percent, at which point the starter relay will be dropped out. The starter itself will be mounted on an engine gearbox pad driving the gasifier shaft. The starter will have a dog clutch or equivalent engagement mechanism. The starter relay will supply the required electrical power to the starter from the vehicle battery. The starter motor will be a 12-volt motor with approximately a 0.75 kW (1.0 hp) capability. Its speed-torque characteristics will be matched to the engine so that rapid starts can be achieved in less than 15 seconds to idle.

3.3 POWERTRAIN MECHANICAL ANALYSIS

ROTOR STRESS ANALYSIS

Preliminary structural analyses of the compressor and turbine rotors have been completed to evaluate the feasibility of the design. The design conditions used in this analysis are:

N_{gg} = 76,000 rpm
N_{pt} = 88,000 rpm
TIT = 1442°K (2100°F)
Stress Rupture Life = 400 hours half life
Low Cycle Fatigue = 10,000 cycles

The WRC plastic wheel computer program was used in evaluating all four rotors, including burst speeds. Metal temperatures were assumed by using past experience as a guide and are based on total relative temperature of the primary airflow and seal leakages that are normally used for cooling the disks. These assumed temperatures are usually within 10 percent of actual temperatures based on past experience and are suitable for preliminary design purposes.

Gasifier Turbine Rotor

Maximum turbine inlet temperature (TIT) is of primary concern when considering engine performance and specific fuel consumption (SFC). In order to meet the requirements for the IGT engine, an advanced high-temperature alloy made by the rapid solidification rate (RSR) process is proposed for the gas generator turbine rotor. Estimated properties are shown in Figure 106; extrapolation shows that the material is capable of operating at metal temperatures of 1422°K (2100°F) at stresses of 103400 kPa (15,000 psi) while maintaining a stress rupture life of 800 hours. It should be noted that the material properties data used in this analysis are preliminary and must be verified before final design.

The stress analysis of the gasifier turbine rotor blades, Figure 107, and disk, Figure 108, indicates a substantial increase in TIT capability using the RSR alloy versus conventional nickel alloys. The low shaft speed with the two-stage centrifugal compressor reduces turbine blade stress significantly; the analysis indicates that blade stress rupture life would be adequate at 111°C (200°F) higher metal temperatures. This means a TIT approaching 1533°K (2300°F) could be considered. Other factors such as turbine nozzle life, temperature gradient effects, power turbine nozzle and rotor life, and recuperator life must be carefully considered before increasing TIT above 1422°K (2100°F).

The turbine blade stress rupture life using an RSR alloy material at a TIT of 1422°K (2100°F) is 40,000 hours. TIT can be increased to 1533°K (2300°F) based on a stress rupture half life of 400 hours. The burst margin for this rotor is 23 percent based on a maximum design speed of 76,000 rpm. The critical area of the turbine rotor is in the neck area of the disk which is limited by low cycle fatigue (LCF) of 10,000 cycles. The effect on LCF in this area due to 367°K (200°F) increase in TIT has not been evaluated.

Power Turbine Rotor

Engine cycle limitations of TIT of 1422°K (2100°F) is based on the stress rupture life of 400 hours for the power turbine rotor, Figure 109, using a conventional nickel base cast alloy, IN-738. Improved stress rupture life with a resulting increase in TIT is possible using the RSR alloy for this turbine also.

The maximum speed capability is 20 percent over the 73,000 rpm at rated power, or 88,000 rpm. This is limited by an LCF life of 10,000 cycles. Burst speed for this rotor is 102,000 rpm for a burst margin of 40 percent over the 73,000 rpm rated and 16 percent over the 88,000 rpm maximum condition.

This turbine design is further limited by the physical size of the rotor hub that is required to support the turbine blades and dead rim load. The rotor hub must be sized as shown in Figure 110 to meet the burst speed of 102,000 rpm.

First Stage Compressor Rotor

The burst margin for the cast aluminum first stage compressor rotor exceeds 50 percent. There are no anticipated problems for this rotor.

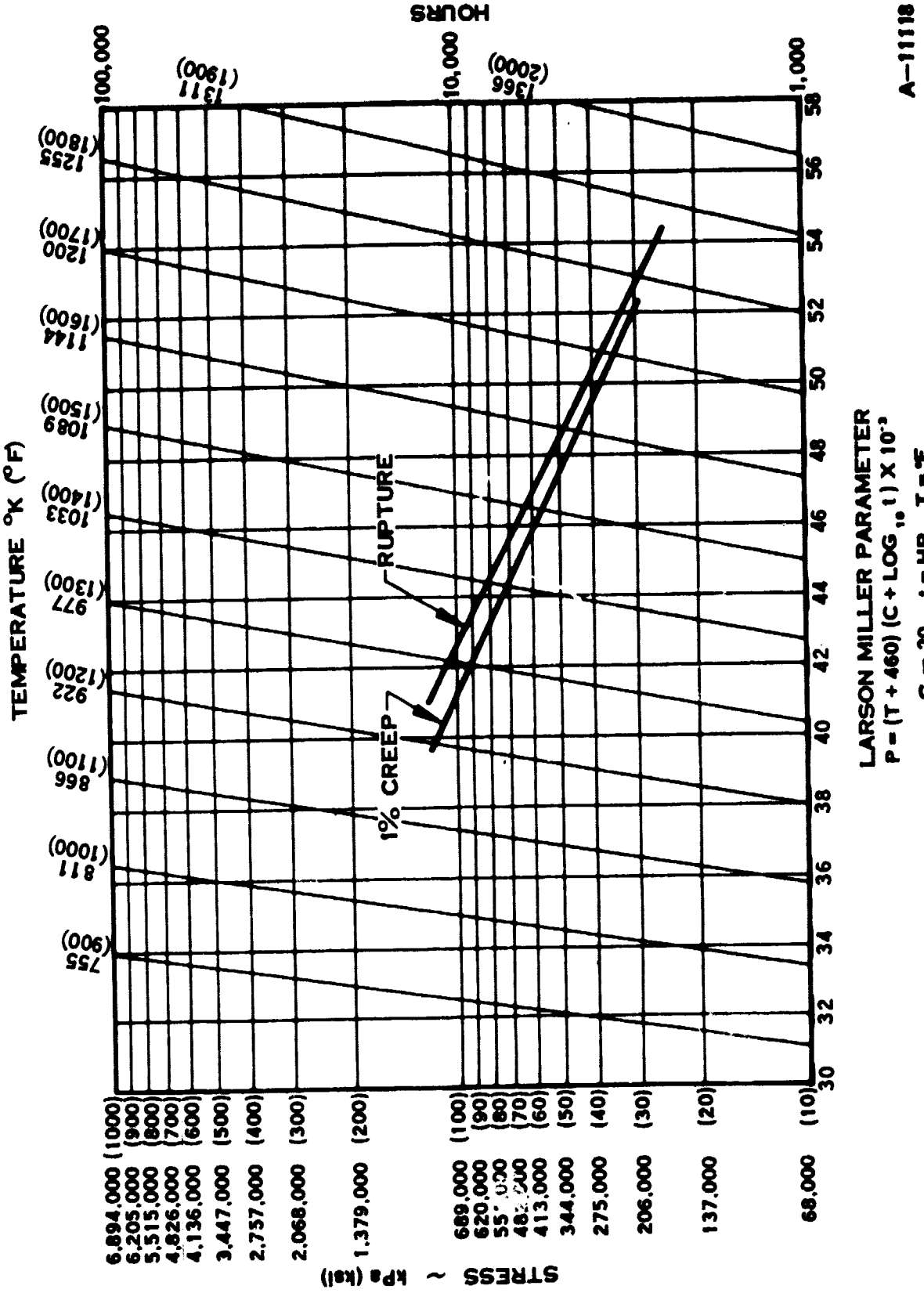

Figure 106. Estimated Characteristics of RSR Advanced High-Temperature Alloy

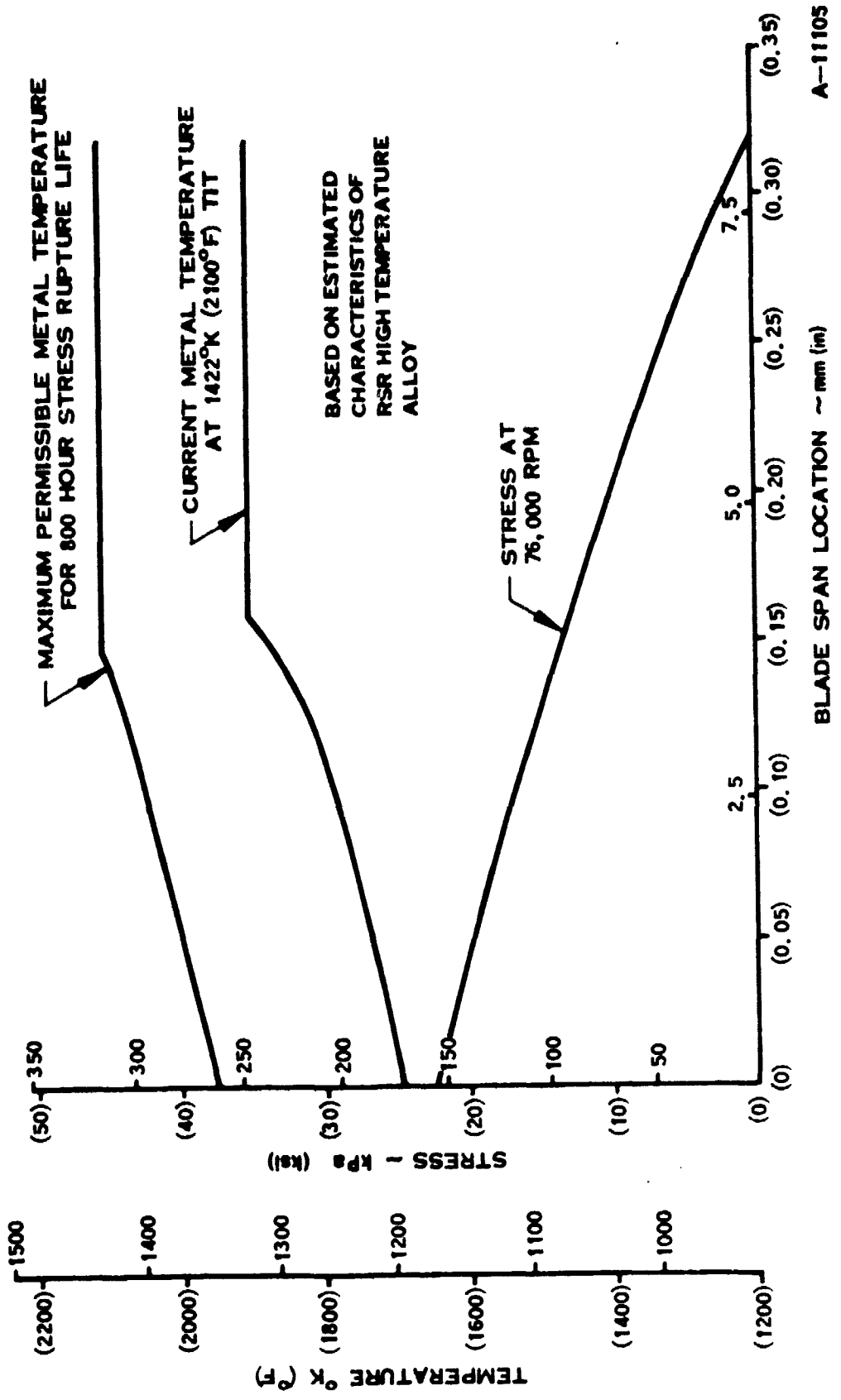

Figure 107. Gasifier Turbine Blade Stress

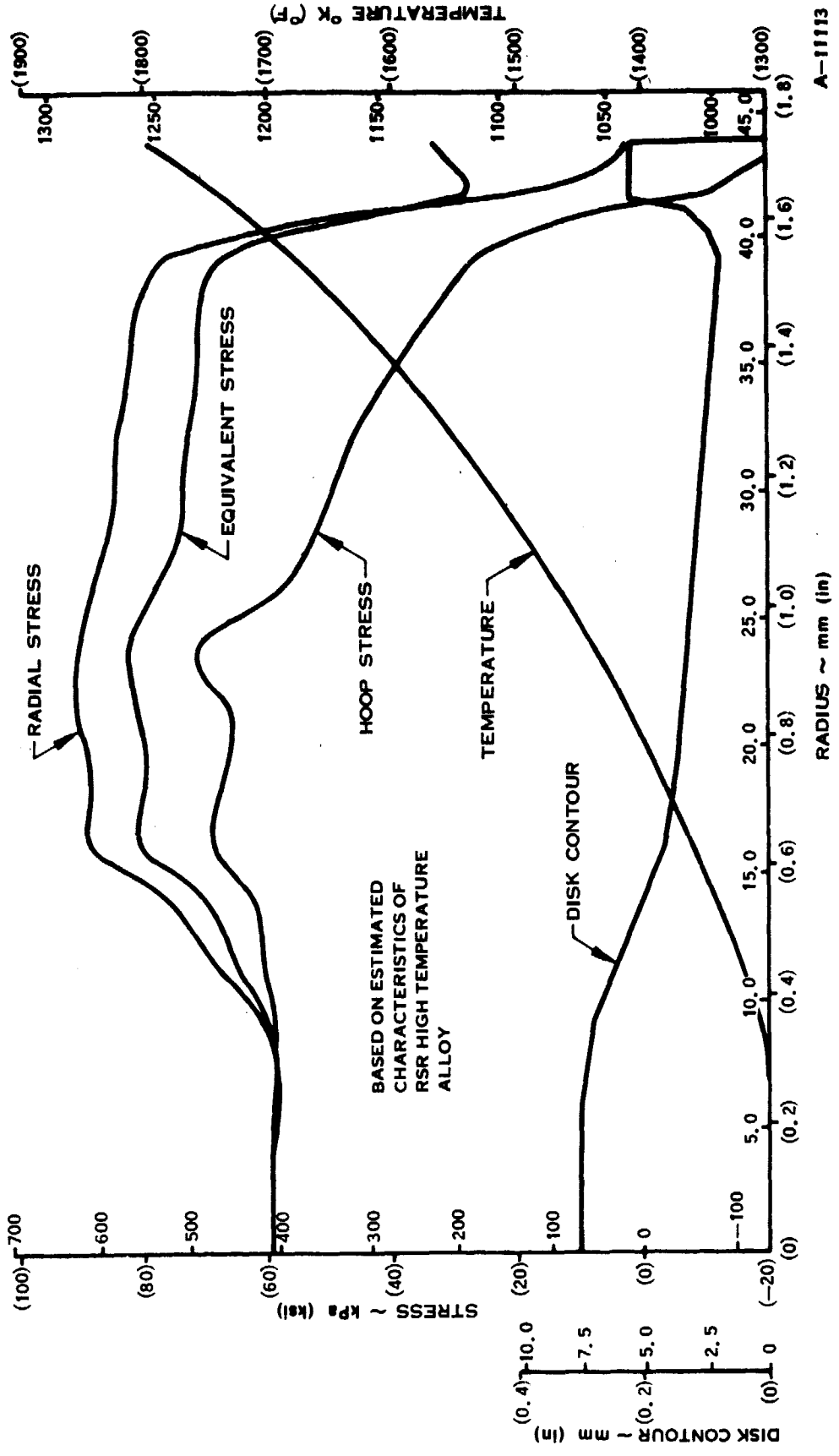

Figure 108. Gasifier Turbine Rotor Stress

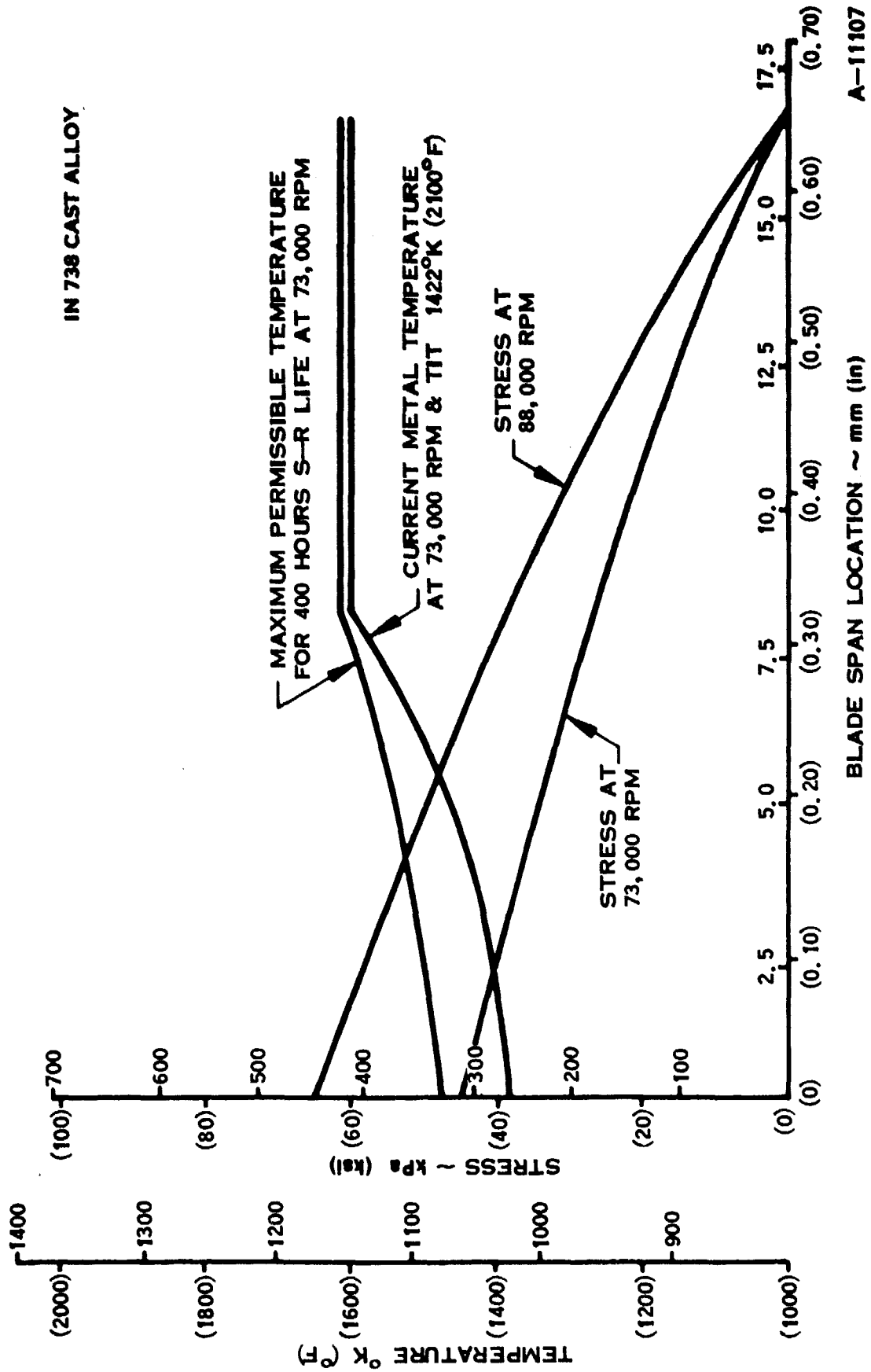

Figure 109. Power Turbine Blade Stress

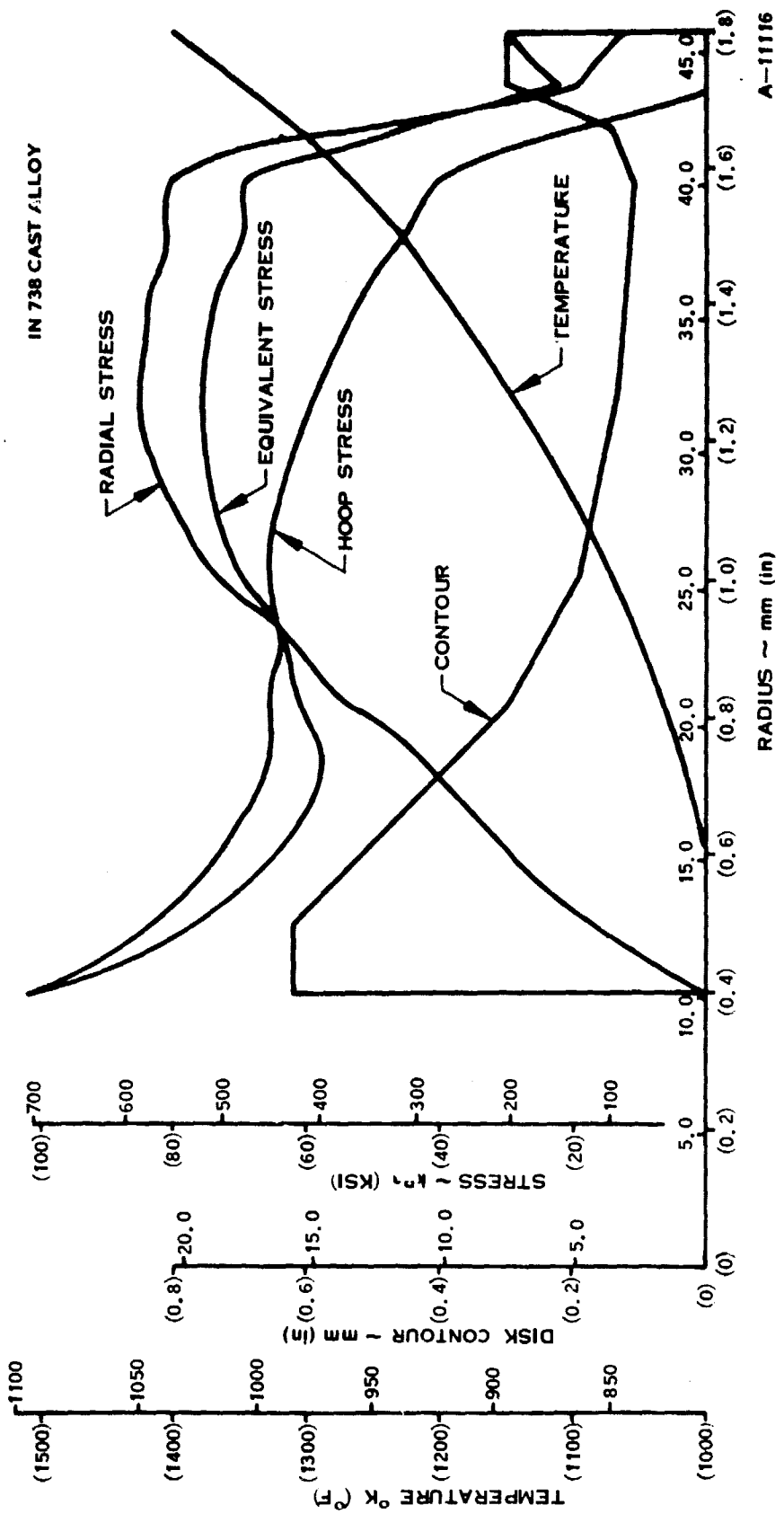

Figure 110. Power Turbine Rotor Stress

Second Stage Compressor Rotor

The burst margin for a titanium second stage compressor rotor is approximately 40 percent. An analysis was also made assuming an aluminum casting; stresses were too high at the estimated metal temperature for currently available alloys. There are no anticipated operational problems for the rotor using titanium, but it will have inertia and cost penalties compared to aluminum. Further study of advanced materials is recommended to eliminate or minimize these penalties.

ROTOR DYNAMICS

The WRC Shaft computer program was used to calculate the lateral critical speeds of both the gasifier and power turbine shafts. This program is an extension of the Prohl, or transfer matrix, method of calculation. Shear deformation, disk gyroscopic stiffening, and bearing support stiffnesses are all accounted for in the mathematical formulation. Fluid-film bearings are not simulated in the program. Further analyses would address shaft-bearing interaction and the design of the fluid-film bearings.

The design criterion for lateral critical speeds of a variable speed engine such as the IGT is that the shaft must be free of damaging lateral critical speeds between idle and 120 percent of maximum design speed. For the gasifier shaft, this operating window extends from idle at 39,450 rpm to 94,680 rpm, which is 120 percent of the maximum design speed of 78,900 rpm. The results of the lateral critical speed analysis of the gasifier shaft are presented in Figure 111, which shows the critical speed of the first four vibration modes and the corresponding mode shapes. As noted in Figure 111, these results are for the following bearing stiffnesses:

- No. 1 bearing (oil-film) - 35030 kN/m (200,000 lb/in)
- No. 2 bearing (oil-film) - 35030 kN/m (200,000 lb/in)
- No. 5 bearing (air-film) - 5250 kN/m (30,000 lb/in)

It can be seen that with these stiffnesses, the operating window from 39,450 rpm to 94,680 rpm is free of any lateral critical speeds. The first mode, at 22,395 rpm, is the turbine bounce mode, and the second mode, at 38,443 rpm, is the compressor bounce mode. Each of these rigid body modes exhibits considerable shaft flexibility. The third mode, which is the first shaft bending mode, occurs at 94,745 rpm, and the fourth mode, at 115,490 rpm, is the second shaft bending mode. This shaft design is suitable for the inherently "soft" foil bearing proposed for the hot end of the shaft.

Unlike the gasifier shaft, the power turbine shaft has no idle speed because it does not rotate at all when the vehicle is stopped. Therefore, the operating window of the power turbine shaft runs from 0 rpm to 108,800 rpm, which is 120 percent of the maximum design speed of 90,670 rpm. The following bearing stiffnesses were chosen for the power turbine shaft:

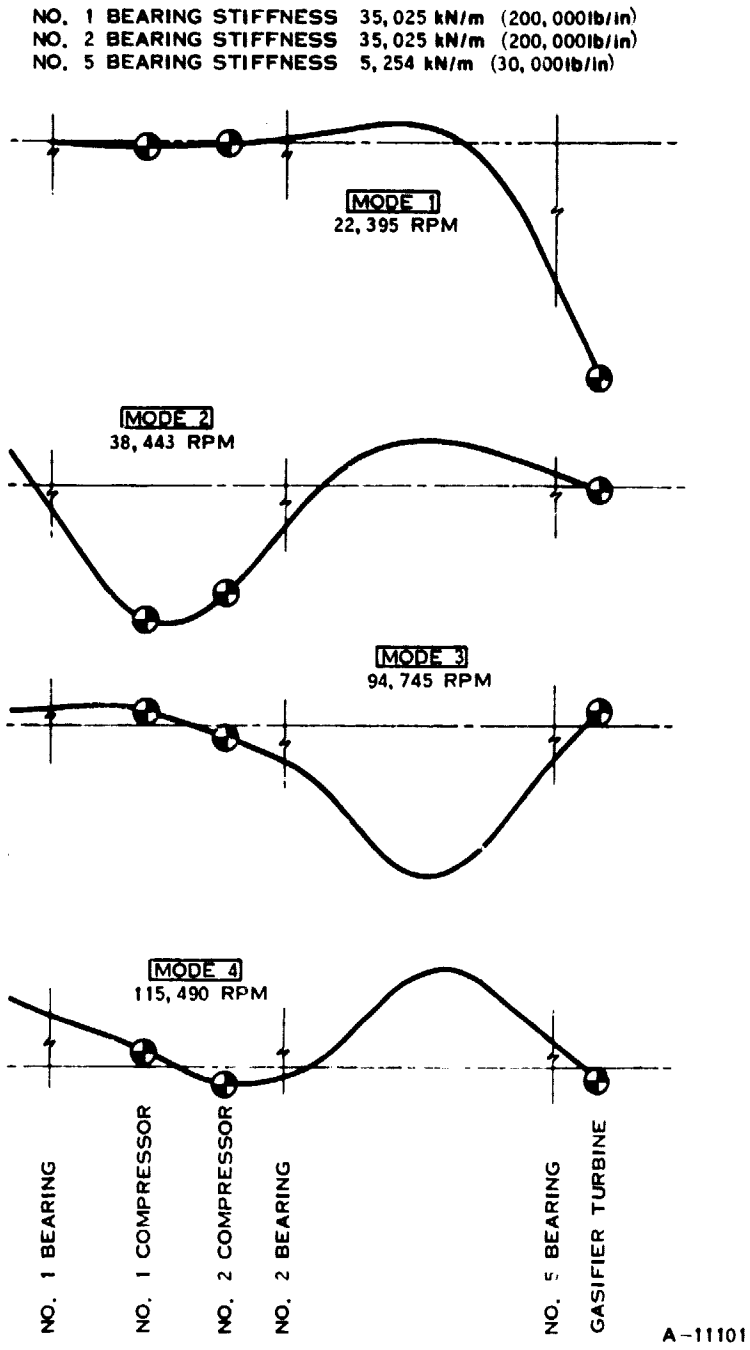

Figure 111. Lateral Critical Speed Analysis of Gasifier Shaft

- No. 3 bearing (oil-film) - 1750 kN/m (10,000 lb/in)
- No. 4 bearing (oil-film) - 1750 kN/m (10,000 lb/in)

Soft bearings were chosen to keep the critical speeds low and reduce the available excitation energy. Past experience has shown that the energy transmitted by rigid-body critical speeds at low shaft speeds and on soft bearings is so small that the vibration levels are not detectable in actual engine operation. As shown in Figure 112, the first two modes are rigid body modes with no shaft flexibility. The first mode, at 7786 rpm, is a rocking mode of the shaft. The second mode, at 25,257 rpm, consists primarily of motion of the drive gear. The first bending mode of the power turbine shaft occurs above 150,000 rpm, well out of the operating range, and is of no concern.

WEIGHT ANALYSIS

A detailed weight analysis was made of the engine. The base engine assembly is calculated as 193 lb. Oil, fuel, and control system (with fluids) increase this to about 240 lb.

3.4 POWERTRAIN/VEHICLE INTEGRATION

AM General made a complete design study of the front-engine, rear-drive installation of the selected IGT powertrain in the AMC Concord automobile, Figures 113 through 115. The alternate arrangement with the engine air inlet at the front simplifies intake and exhaust systems. The output shaft from the front-mounted reduction gear drives directly into the automatic transmission located in the normal (piston engine) location. The engine and transmission are mounted separately to minimize structural and vibration problems. The accessory drive gear train is located in the same gearcase as the drivetrain reduction gear to improve vehicle accessory location, drive, and servicing.

MOUNTING SYSTEM

The engine and the transmission are mounted separately with rubber isolation mounts. The engine is located from the two sides at the gearbox with the rear mount on the combuster cover flange. The transmission uses the conventional rear mount with two front mounts to an added frame crossmember.

INTAKE SYSTEM

The air intake for the IGT powertrain is a dual system with the intakes behind the front grille. The air ducts are on each side of the air conditioning condenser.

The packaged filter size is 13.67 cm by 33 cm (5.38 in. by 13.0 in.) and mounted at an angle to reduce the envelope of the ducts. The two air filters have an air restriction of 2.5 cm (1.0 in.) H_2O at 134 kg/s (0.75 lbm/s). Total filter area is approximately 903 cm^2 (140 $in.^2$). After the filters, the ducts taper down to provide for a gradual change in section to the turbine engine intakes. The air intake has been increased in size significantly over the initial packaging concepts to reduce restriction.

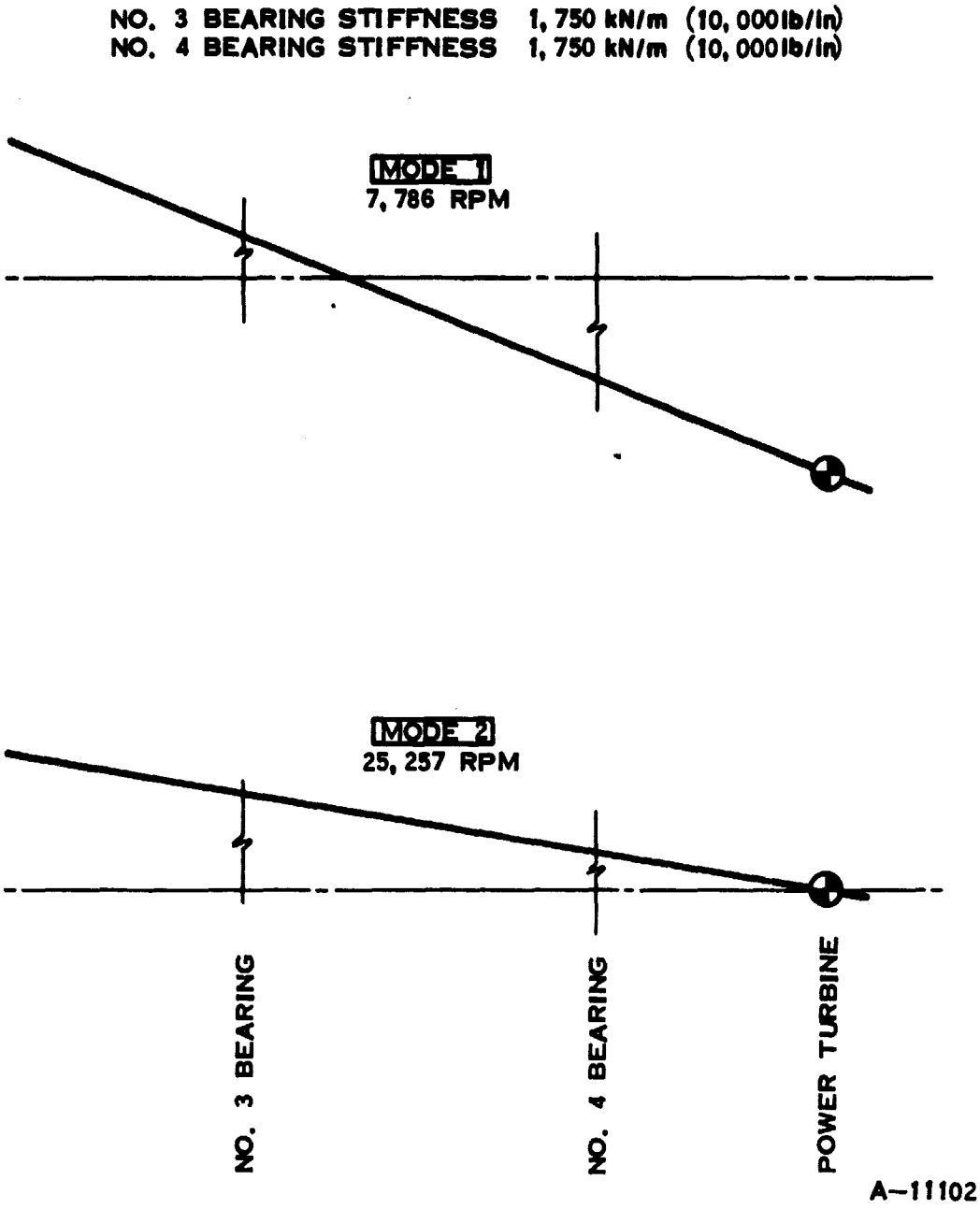

Figure 112. Lateral Critical Speed Analysis of Power Turbine Shaft

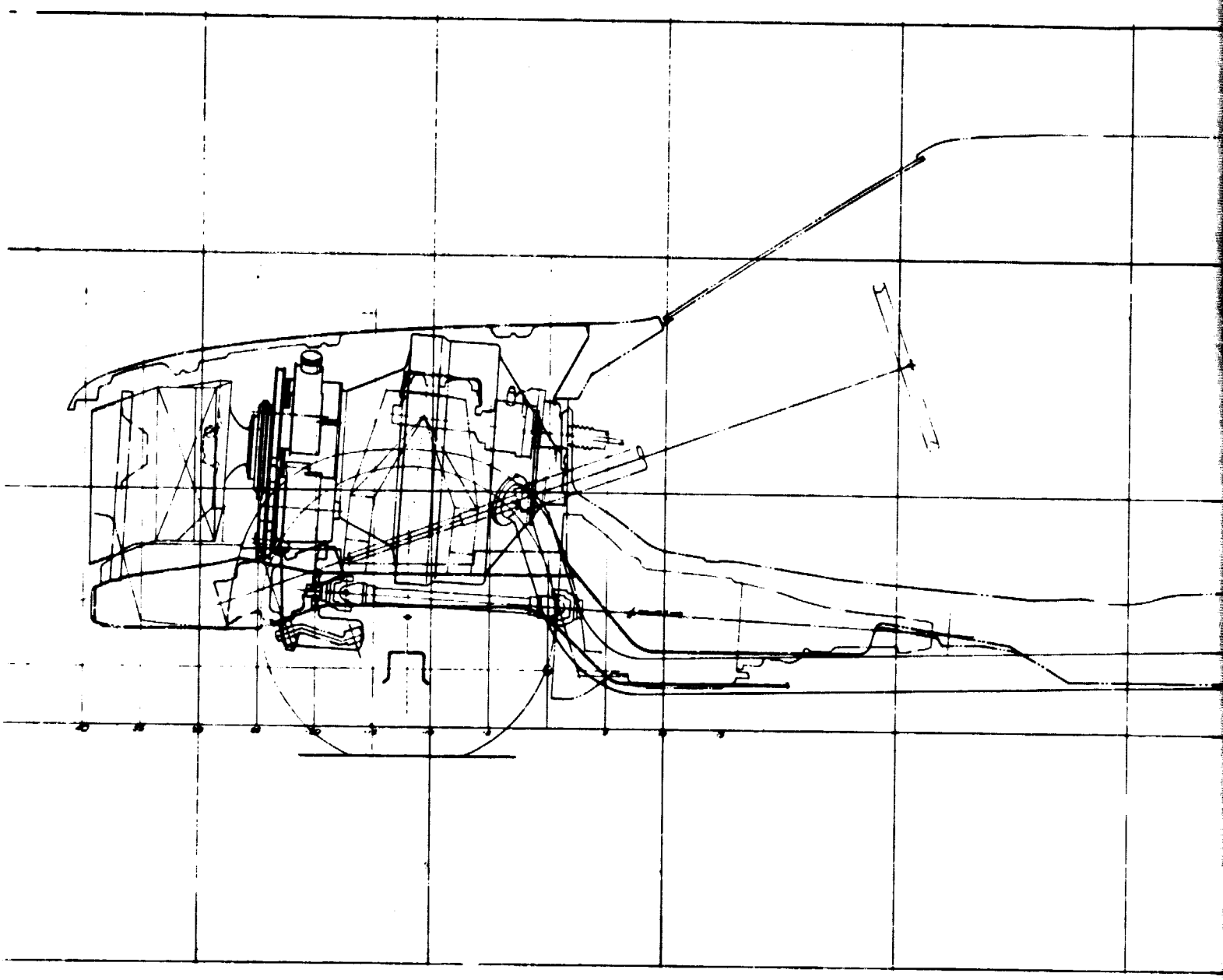

ORIGINAL PAGE IS
OF POOR QUALITY

FOLDOUT FRAME

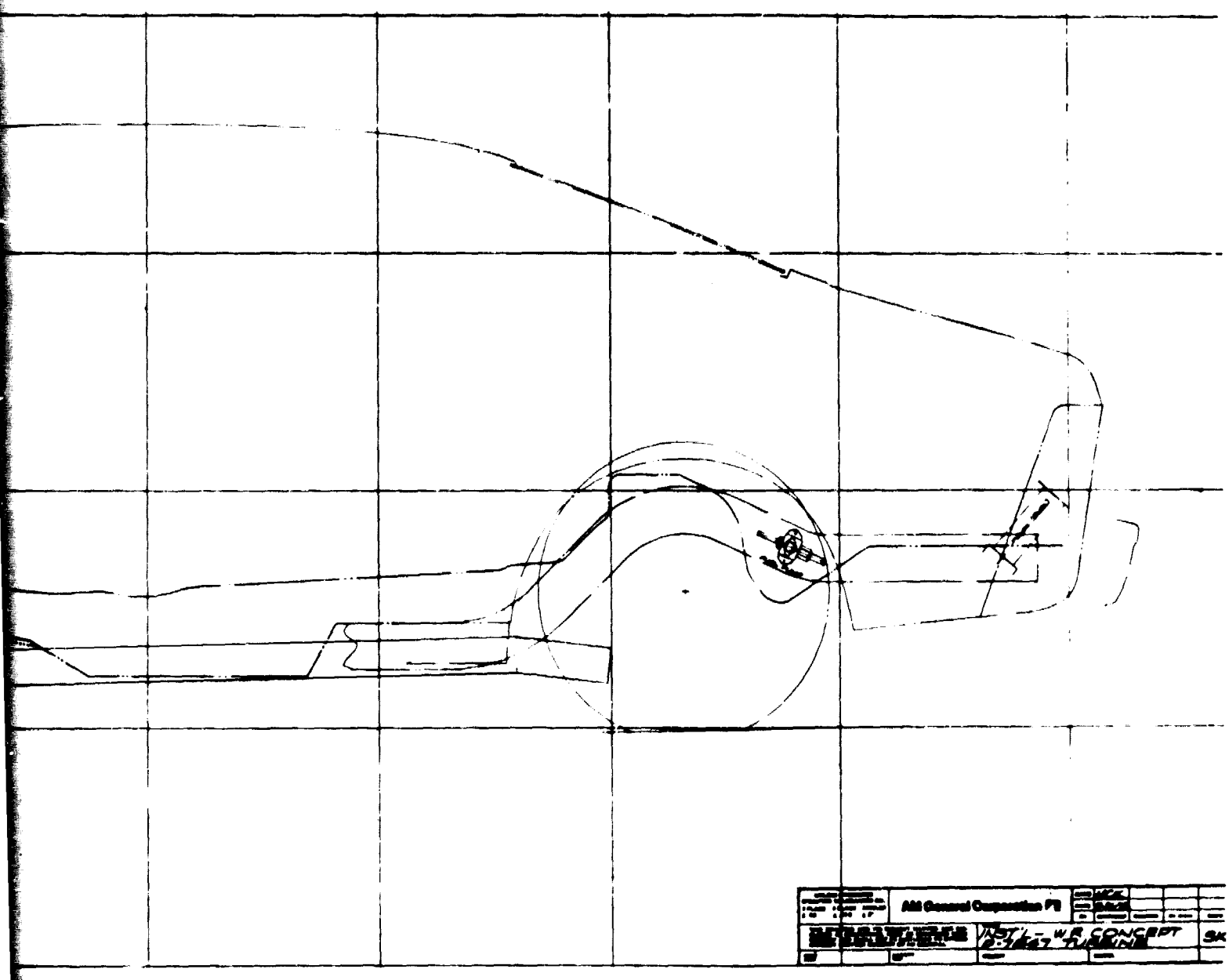

Figure 113. Powertrain Installation, Side View

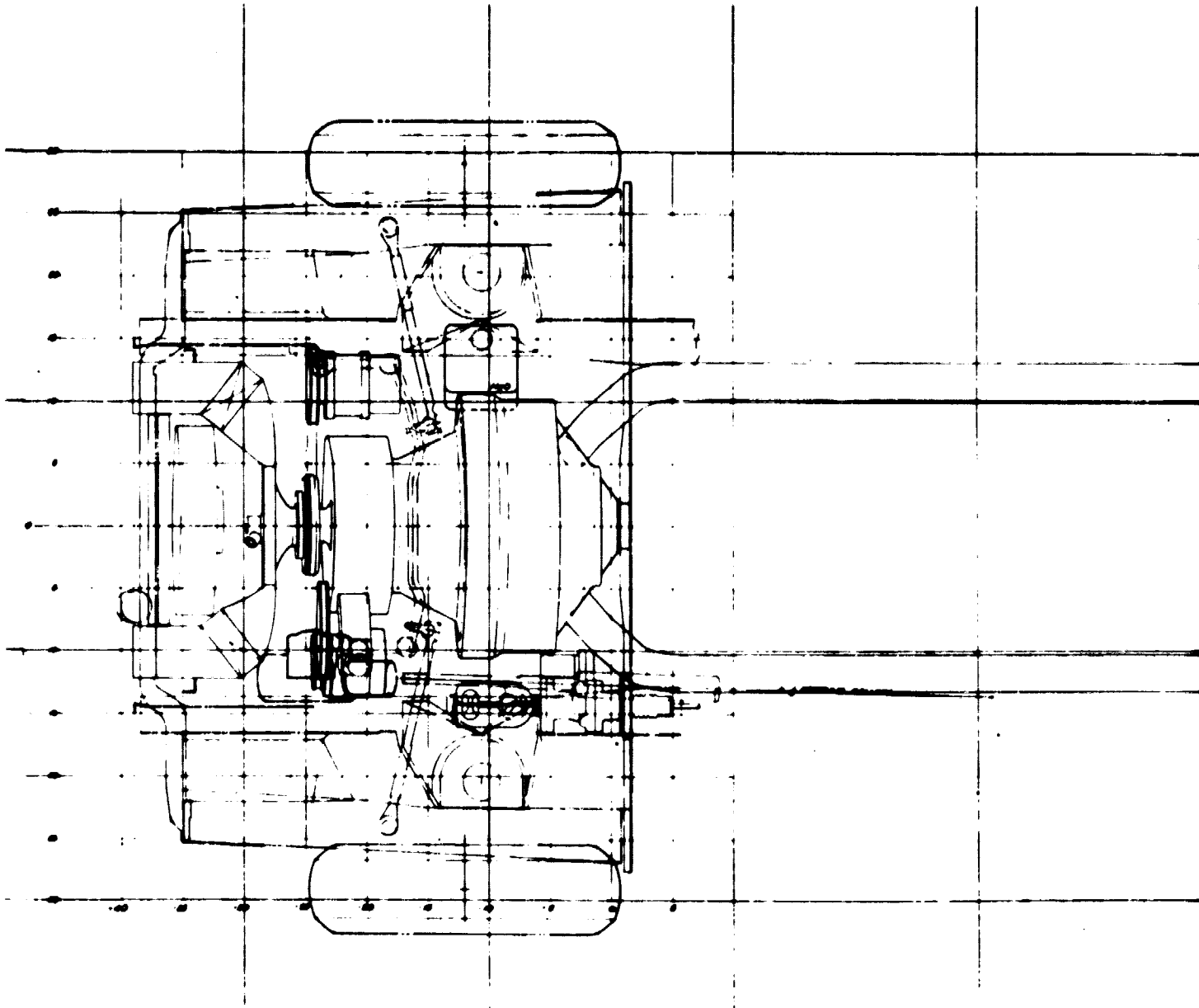

FOLDOUT FRAME

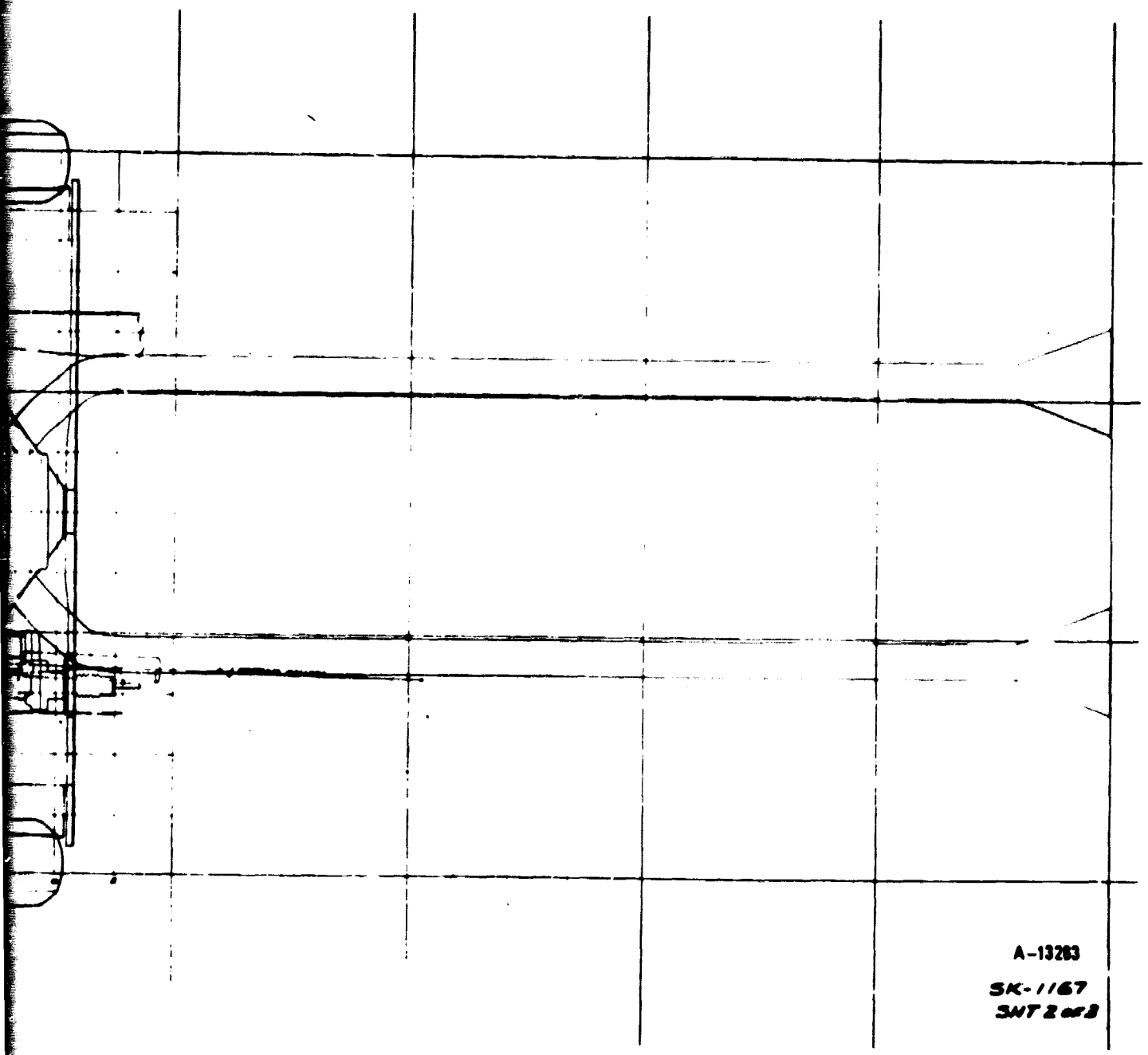

Figure 114. Powertrain Installation, Top View

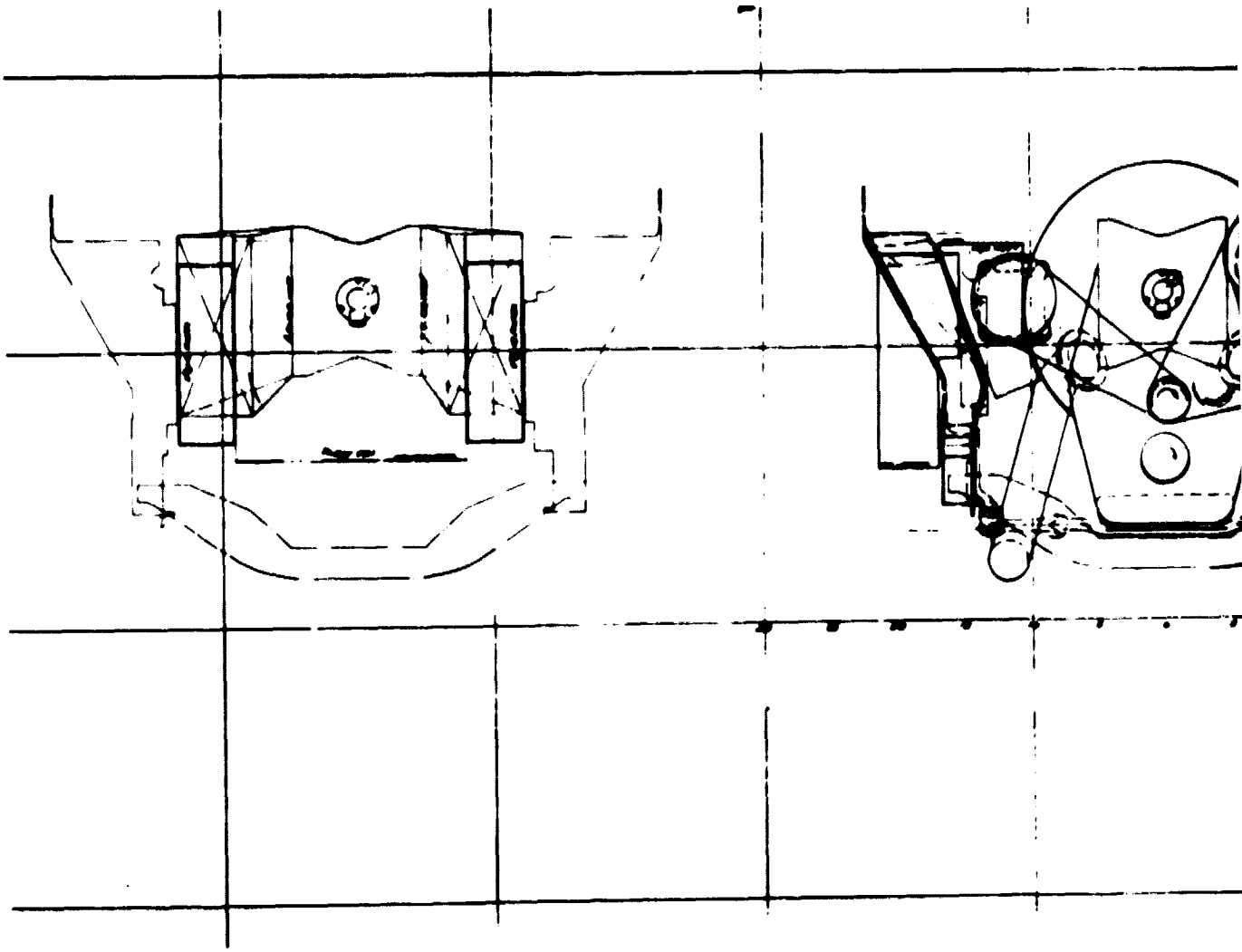

Figure 115. Po

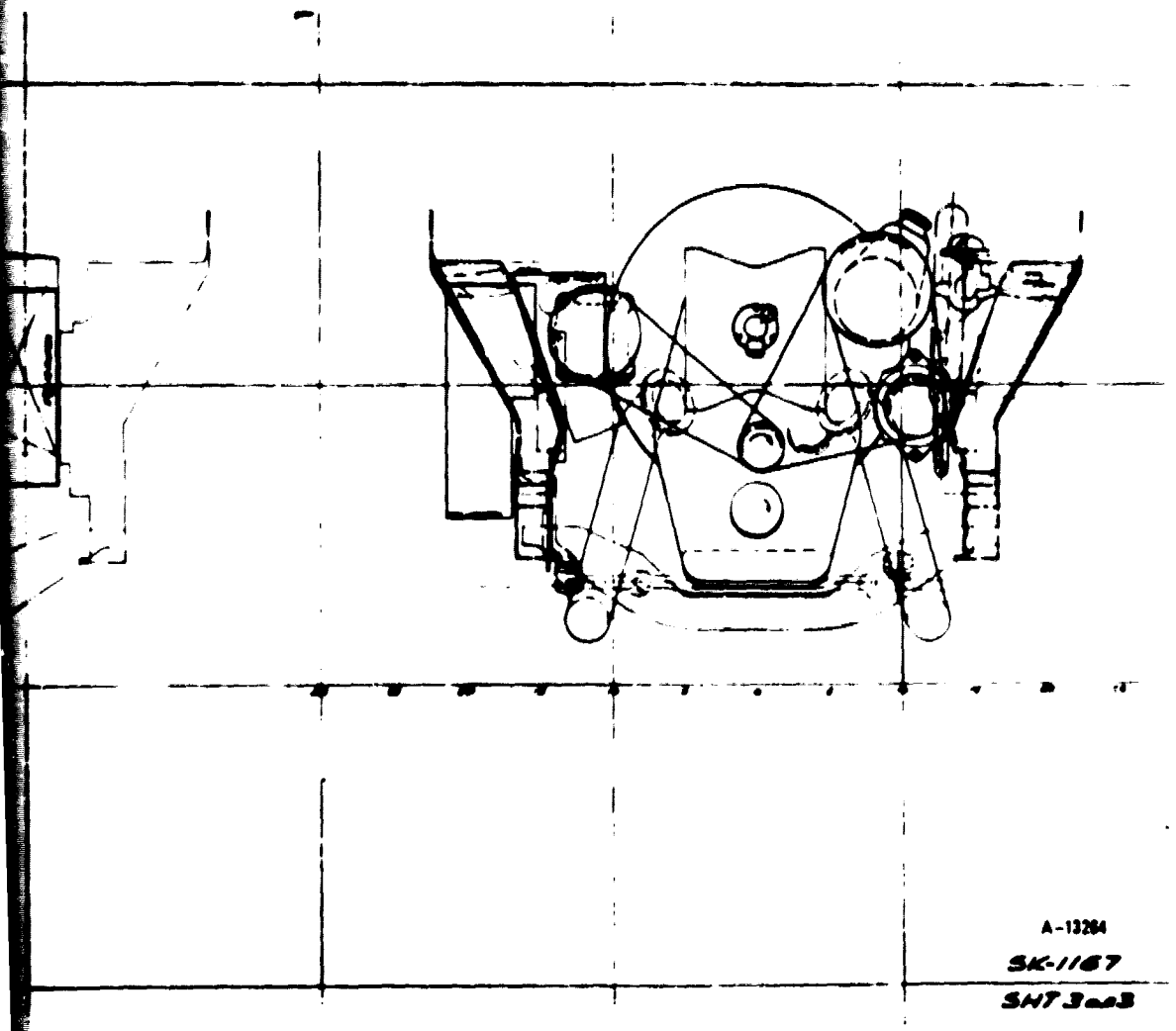

FOLDOUT FRAME 2

Figure 115. Powertrain Installation, Front View

EXHAUST SYSTEM

The exhaust system is also a dual system with 76.2 mm (3-inch) diameter tubing with no muffler. The final exhaust packaging has been simplified since the selected turbine engine powertrain has only two outlet ports. Each exhaust pipe required only one bend and flange for attachment to the engine. The pipe at the rear is flared to disperse gases more gradually to the atmosphere, thus reducing the noise. The system will have minimal back pressure but will have to be checked out for noise levels; if the noise levels exceed the requirements, sound absorption lining such as fiberglass can be added.

POWER STEERING

Power steering is an option on the Concord, and has been packaged into the turbine vehicle to comply with the "marketable" requirement. The production power steering pump is belt driven from the accessory output shaft. To minimize pump losses, the power steering pump pulley has been increased to reduce the maximum speed to 2,000 rpm for the pump, while the idle speed will be 1,000 rpm. This ratio should be adequate to provide the "dry park" requirement. The pump is basically unchanged except for a provision of the Bendix Hydro-Boost power brake system return line discussed under the brake section.

POWER BRAKES

Power brakes are packaged to comply with the marketable requirement for the IGT vehicle. The original power brakes on the Concord require vacuum from the engine for assist, but comparable vacuum is not available on a turbine engine. Compressor pressure is available, adequate even at idle, and a pressure booster could be designed for this function.

An alternate way to power the brakes is to utilize the power steering pump to reduce the brake pedal effort. The Hydro-Boost system utilizes this method and has been on the market for several years. The Hydro-Boost also provides two or more reserve power-assisted brake applications in the event of a pressure supply loss (i.e., engine quits, belt failure, etc.). The number of reserve stops varies with the severity and duration of the applications. The Hydro-Boost does require an additional return port in the power steering pump reservoir and will require minor rerouting of the power steering gear plumbing.

ALTERNATOR

The turbine car will have additional electrical loads due to the electrically driven condenser fan, water pump, and fuel pump. Based on this additional load, a 72-amp alternator was recommended in place of the 55-amp alternator (with air conditioning). However, to minimize losses, a 55-amp alternator can be used but will have to be checked out for adequacy. The alternator pulley ratio was reduced to minimize the losses. The alternator will run at an idle speed of 1,800 rpm and a maximum speed of 3,600 rpm.

AIR CONDITIONING

Air conditioning is also an option of the Concord, but is packaged to comply with the marketable requirement. For simplified packaging, a rotary type compressor was packaged, with the pulley ratios revised to reduce the speed and minimize losses. The AC compressor will have a 1,200 rpm idle speed and a 2,400 rpm maximum speed. Power requirements for these two speeds are 1.34 kW and 2.24 kW (1.8 and 3.0 hp).

The condenser has been revised to provide room for the dual air intake ducts. However, total frontal area will be the same as the current model Concord. The condenser cooling fan will be electrically driven. This type of design will add to the electrical load requirement, but will save fuel since it will only rotate when required. Cooling fans are primarily required during idling and/or low speeds. The controls will have to be solenoid or air-operated to replace the vacuum controls.

HEATING

Initial plans were to divert hot gases from the turbine engine through a heat exchanger, heating water which would be circulated by a water pump to the heater core in the passenger car compartment for the interior heating.

Due to time limitation, it was decided to package a complete heater assembly which has been produced for many years. This Stewart Warner unit features a gasoline-fired burner, blower, electrically driven water and fuel pump, and an igniter. This unit, if switched "ON," will ignite a gasoline burner. The combustion gases are blown through a heat exchanger while the water pump, driven by the same motor as the fuel pump, circulates the heated water.

This unit has been packaged with the current heater assembly, an 11.36 liter (3-gallon) water container and 6.8 liter (1.8 gallon) gas tank. The capacity of this unit is advertised by the supplier to be 52753 kJ/h (50,000 Btu/h), which should be more than adequate.

TRANSMISSION

The selected automatic transmission is a Chrysler Model 904. The ratios are 2.45, 1.45 and 1.00 (with 2.22 reverse). The transmission will be used without torque converter, pump, and cooling core. The oil pressure needed for control and lubrication will be supplied by the engine oil pump.

REAR AXLE

The recommended axle ratio is 3.58:1.0 and does not require any tooling. Higher ratios can be used but will require new tooling. The maximum torque with a 3.58 ratio rear axle without torque converter is still below the allowable level of 490 kN/m (28,000 in. lb).

TIRES

The available radial tire on the Concord is a DR78-14 for 1978, which is adequate for its weight. Specifications require an ER78-14, which is no major problem but will add weight and cost.

4.0 TASK IIIB - VEHICLE COST ANALYSIS

POWERTRAIN PRODUCTION COST ANALYSIS

A detailed estimate was made of the production cost of the powertrain at an automotive volume of 1,000,000 units per year. Part callouts were made on an early version of the engine cross section, Figure 116, and a parts list was generated by engine section, Appendix C. The differences between this engine design and the final design in Figure 99 were not considered significant for overall production cost. Types of material were also specified for each part on the list. Supplemental lists were made of lubrication, fuel, ignition, and control system components that did not show on the drawing.

A production cost estimate was made by Manufacturing for each part on the list; assembly labor was also estimated. Several manufacturing approaches were considered for major parts, and the lowest cost approach with engineering concurrence was used, although the drawing was not changed to reflect this selection.

Quotations were obtained from several suppliers for lubrication, fuel, ignition, and control system components. The costs for these parts as purchased were then converted to an equivalent direct labor and material cost, assuming these parts were integrated by the automobile manufacturer.

This production cost analysis followed the same general procedure and guidelines as those used previously in WRC Report No. WR-ER11, Automotive Gas Turbine Economic Analysis. The results of the IGT powertrain analysis are comparable to the previous, more detailed analysis, with allowance for escalation.

The total direct labor hours and material cost were then transmitted to AM General for generating cost and price differences from the baseline piston engine, using automotive practice.

VEHICLE PRODUCTION COST ANALYSIS

AM General estimated the production cost difference between the IGT vehicle and the conventional piston engine vehicle, including the IGT engine production cost input from WRC. The vehicle component cost data was based on quotations from automotive suppliers. In several cases, such as the transmission and heating system, the cost was based on the adaptation of available components to the baseline vehicle, resulting in a significant cost penalty. With continued design and development, every effort would be made to reduce these penalties by redesign and/or by using other approaches. Just the commitment to several years of automotive production would permit tooling for new designs more suitable to the IGT powertrain.

To provide a more realistic production cost estimate, alternate approaches were used for several systems on a judgment basis as follows:

Intake System - The dual system was replaced by a single filter element and duct.

Power Brakes - The Hydro-Boost system, using the power steering pump, was replaced by a diaphragm unit operating on compressor outlet pressure.

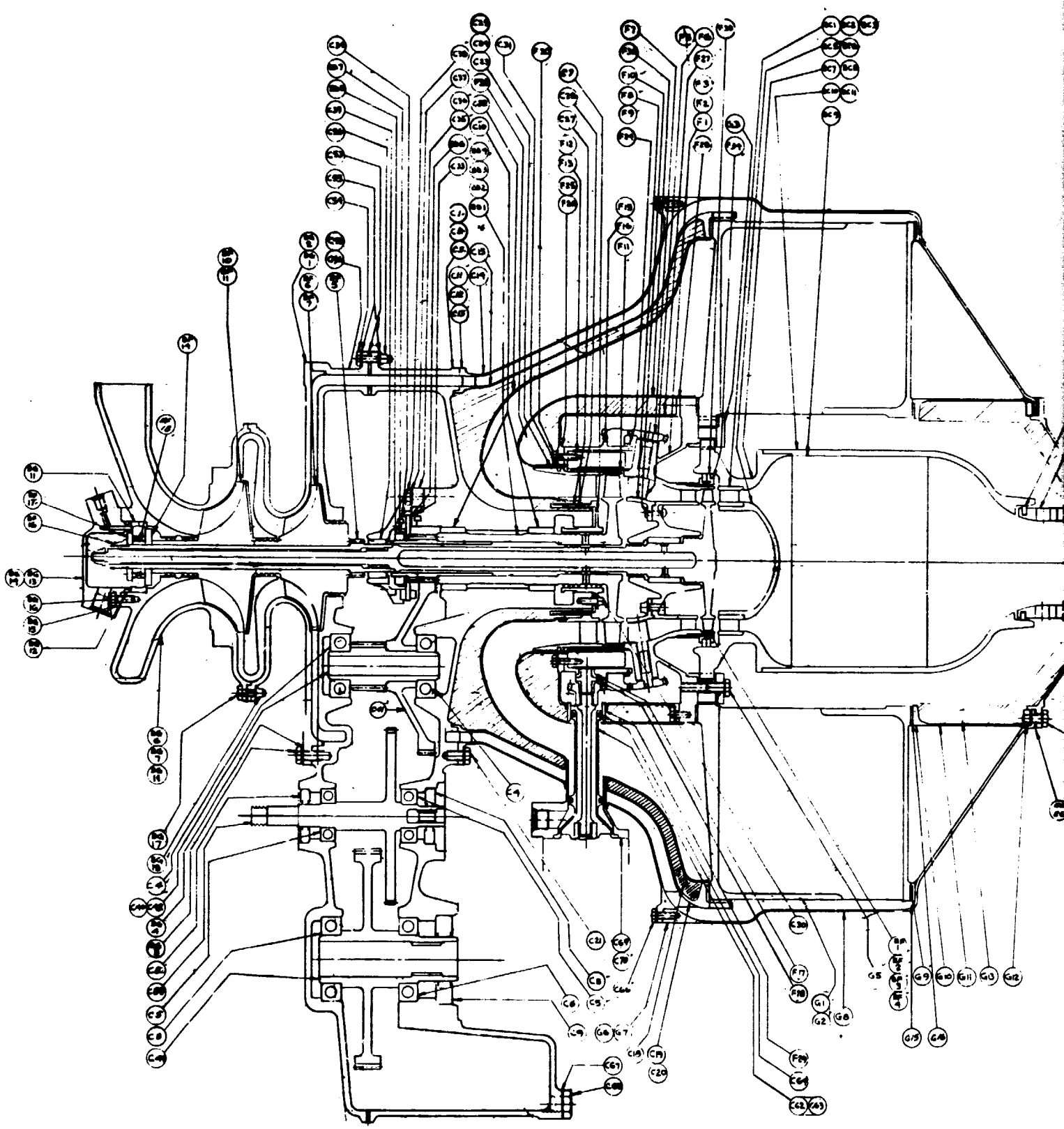

PRECEDING PAGE BLANK NOT FILMED

FOLDOUT FRAME

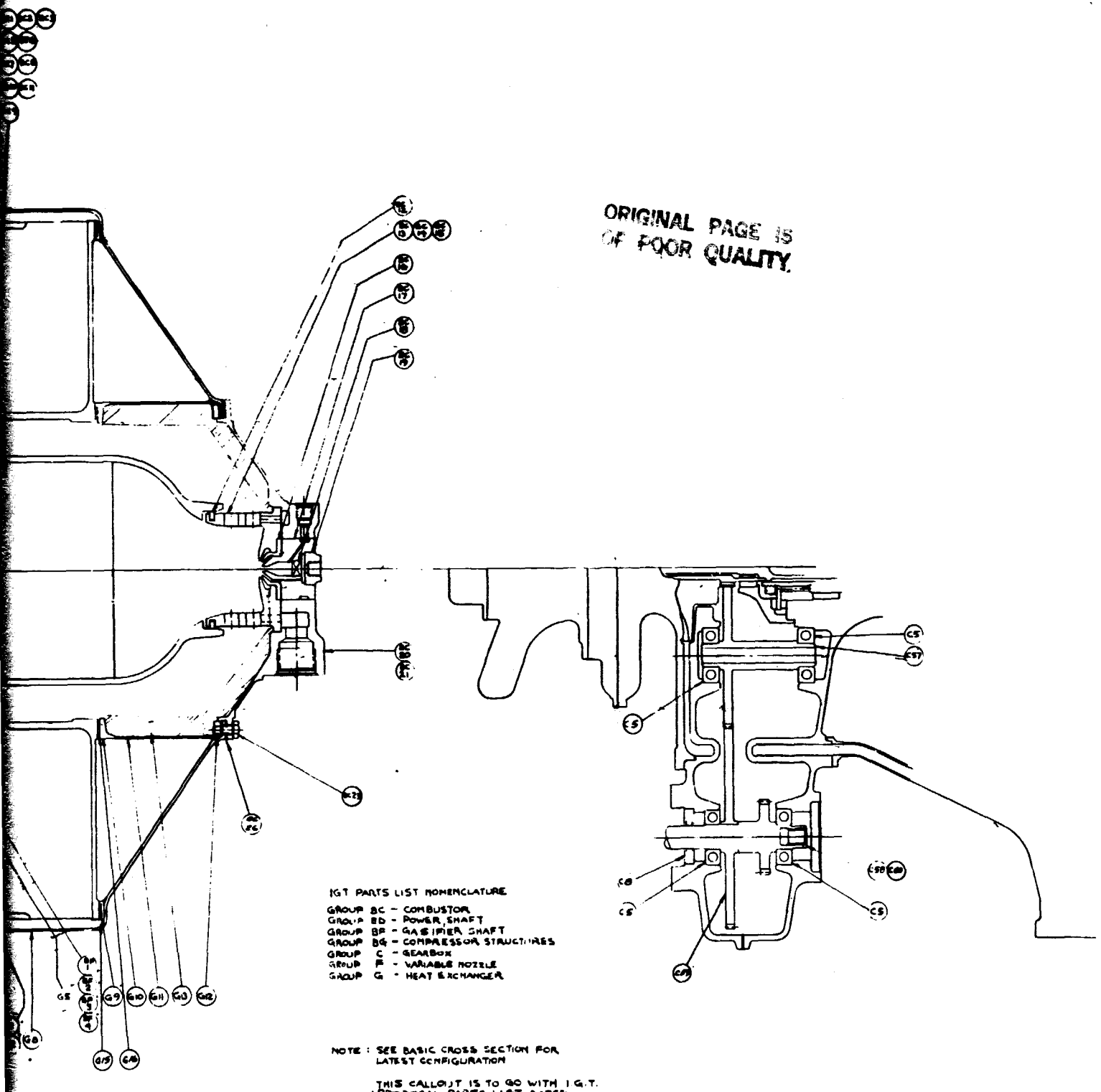

A-12563

Figure 116. Preliminary Powertrain Cross Section with Parts Callouts

FOLDOUT FRAME 2

Alternator - The 72-amp alternator (with air conditioning) was replaced by a 55-amp alternator.

Air Conditioning - The rotary type compressor was replaced by the current two-cylinder compressor to avoid the cost penalty.

Heating - The Stewart Warner gasoline-fired heater was replaced by a hot water system heated by hot gas diverted from the power turbine discharge.

Fuel System - The electric pump was removed from the fuel tank, using the engine-mounted fuel pump only.

LIFE CYCLE COST ANALYSIS

AM General supplied a life cycle cost summary for the baseline piston engine vehicle, assuming a total mileage of 90,000 miles over 6 years. This cost included initial purchase cost, taxes, financing, registration, license, insurance, fuel, maintenance and repair.

Maintenance, Table XVII, includes scheduled maintenance following the manufacturer's recommendations, and normal repair and replacement, including major and minor engine repair based on fleet test experience. An equivalent maintenance estimate, Table XVIII, was generated for the IGT compact car on a judgment basis, since no hard data exists.

From the differences in initial vehicle cost, fuel consumption, and maintenance and repair cost, comparative life cycle costs were calculated for both the baseline piston engine vehicle and the IGT vehicle, as summarized in Table XIX. The initial purchase cost penalty of $471.56 for the IGT vehicle is more than made up by the $703.18 fuel saving, based on a combined driving cycle fuel economy of 11.9 km/l (28.0 mpg) compared to 8.75 km/l (20.6 mpg) for the piston engine car. The additional saving of $851.00 in estimated maintenance and repair cost results in a net saving of $1,221.40 (10 percent) for the IGT vehicle over the 6-year period.

TABLE XVII. MAINTENANCE AND REPAIR SCHEDULE, PISTON ENGINE VEHICLE (Sheet 1 of 2)

		Interval I 0 - 15,000	Interval II 15,001- 30,000	Interval III 30,001- 45,000	Interval IV 45,001- 60,000	Interval V 60,001- 75,000	Interval VI 75,001- 90,000	TOTAL
Maintenance:								
Eng. Oil & Oil Filter	Every 5,000 Miles	$ 30	$ 30	$ 30	$ 30	$ 30	$ 30	$ 180
Body Lube & Brake Inspec.	Every 15,000 Miles	10	10	10	10	10	10	60
Chassis Lubrication	Every 30,000 Miles	-	10	-	10	-	10	30
Major Tune Up	Every 30,000 Miles	-	100	-	100	-	-	200
Replace Fuel Filter	Every 15,000 Miles	5	5	5	5	5	5	30
Inspect Drive Belts	At 5, 15, 45, 75	20	-	10	-	10	-	40
Emissions System Check	Every 5,000 Miles	30	30	30	30	30	30	180
Minor Tune Up		50	-	50	-	50	-	150
Front End Alignment		12	12	12	12	12	12	72
A/C System Check Up (Check hoses & Freon - Add Freon if required)		20	20	20	20	20	20	120
Cooling System Flush (4-Way Flush w/pressurized air and water - 2 Gal. anti-freeze; flushing compound, cooling system conditioner, stop leak and complete cooling system check.)		-	30	-	30	-	30	90
Sub-Total Maintenance		$ 177	$ 247	$ 167	$ 247	$ 167	$ 147	$ 1,152

TABLE XVII. MAINTENANCE AND REPAIR SCHEDULE, PISTON ENGINE VEHICLE (Sheet 2 of 2)

	Interval I 0 - 15,000	Interval II 15,001- 30,000	Interval III 30,001- 45,000	Interval IV 45,001- 60,000	Interval V 60,001- 75,000	Interval VI 75,001- 90,000	TOTAL
Repair & Replace:							
Exhaust System (Replace Muffler & Pipes)	--	-	100	-	50	-	$ 150
Shock Absorbers (Replace All 4 Shocks)	--	-	60	-	-	60	120
Brakes (Rebuild wheel cylinders; resurface brake drums - repack wheel bearings; inspect master cylinder; install new seals & return springs; inspect brake hoses; bleed system and road test)	--	-	-	120	-	-	120
Tires (Replace original tires with 4 steel-belted radials)	--	-	-	200	-	-	200
Paint - Rust	--	-	-	100	-	-	100
Lights - Interior & Exterior (Replace & Adjust Headlights, Taillights, Dome Lights)	--	10	-	10	-	10	$ 30
A/C / Heat / Vent (Repair & Replace Components in A/C and heating system)	--	-	50	-	50	-	100
Battery (Replace Original Battery with a maintenance-free battery)	--	-	-	55	-	-	55
Suspension (Replace ball joints and seals)	--	-	-	50	-	-	50
Transmission (Replace Trans Filter; Pan Gasket; Clean & inspect oil reservoir; Add fluid & road test)	--	25	-	25	-	25	75
Alternator (Rebuilt)	--	-	-	70	-	-	70
Starter Motor (Rebuilt)	--	-	-	55	-	-	55
Carburetor (Rebuilt)	--	-	55	-	-	-	55
Water Pump (Rebuilt)	--	-	-	46	-	-	46
Sub-Total Repair & Replacement	$ -0-	$ 35	$ 265	$ 731	$ 100	$ 95	$ 1,226
Major & Minor Eng. Repair (Includes rebuild or replacement of the block or any components of the block)	--	--	--	--	--	--	$ 110
TOTAL MAINTENANCE, REPAIR & REPLACEMENT	$ 177	$ 282	$ 432	$ 978	$ 267	$ 242	$ 2,488

$2,488.00 ; 90,000 Miles = .0276/Mile

Report No. 78-182

TABLE XVIII. MAINTENANCE AND REPAIR SCHEDULE, TURBINE ENGINE VEHICLE (Sheet 1 of 2)

Maintenance:		Interval I 0-15,000	Interval II 15001-30,000	Interval III 30,001 45,000	Interval IV 45,001 60,000	Interval V 60,001 75,000	Interval VI 75,001-90,000	Total
Eng. Oil & Oil Filter	Every 15,000 Miles	$ 10	$ 10	$ 10	$ 10	$ 10	$ 10	$ 60
Body Lube & Brake Inspec	Every 15,000 Miles	10	10	10	10	10	10	60
Chassis Lubrication	Every 30,000 Miles	--	10	--	10	--	10	30
Replace Fuel Filter	Every 15,000 Miles	5	5	5	5	5	5	30
Inspect Drive Belts	At 5, 15, 45, 75	20	--	10	--	10	--	40
Minor Tune Up		50		50		50		150
Front End Alignment		12	12	12	12	12	12	72
A/C System Check Up (Check hoses & Freon-Add Freon if required)		20	20	20	20	20	20	120
Sub-Total Maintenance		$ 127	$ 67	$ 117	$ 67	$ 117	$ 67	$ 562

TABLE XVIII. MAINTENANCE AND REPAIR SCHEDULE, TURBINE ENGINE VEHICLE (Sheet 2 of 2)

Repair & Replace:	Interval I 0-15,000	Interval II 15001-30,000	Interval III 30,001 45,000	Interval IV 45,001 60,000	Interval V 60,001 75,000	Interval VI 75,001-90,000	Total
Exhaust System (Replace Pipes)			$ 50		$ 50		$ 100
Shock Absorbers (Replace All 4 Shocks)	--	--	60	--		60	120
Brakes (Rebuild wheel cylinders; resurface brake drums - repack wheel bearings; inspect master cylinder; install new seals & return springs; inspect brake hoses; bleed system and road test)				120			120
Tires (Replace original tires with 4 steel-belted radials)				200			200
Paint - Rust				100			100
Lights - Interior & Exterior (Replace & Adjust Headlights, Taillights, Dome Lights)		10		10		10	30
A/C/Heat/Vent (Repair & Replace Components in A/C and heating system)			50		50		100
Battery (Replace Original with a maintenance-free battery)				55			55
Suspension (Replace ball joints and seals)				50			50
Transmission (Replace Trans Filter; Pan Gasket; Clean & inspect oil reservoir); add fluid & road test		25		25		25	75
Alternator (Rebuilt)				70			70
Starter Motor (Rebuilt)				55			55
Sub-Total Repair & Replacement	0	35	160	685	100	95	1075
Total Maintenance, Repair & Replacment	$127	$102	$277	$752	$217	$162	$1637

TABLE XIX. IMPROVED GAS TURBINE COMPACT CAR LIFE CYCLE COST ANALYSIS

	1977 Hornet Base Car	IGT Compact Car
Purchase Cost	$ 4,779.00	$ 5,250.56
Sales Tax	191.16	210.02
Interest --- (@ 10% Compound Interest for 3 Years)	1,002.00	1,100.87
Insurance	1,500.00	1,586.99
Registration, License	153.00	153.00
Fuel --- 15,000 Miles Per Year Piston -- 20.6 mpg @ 0.609 per gallon Turbine -- 28.0 mpg @ 0.609 per gallon	2,660.68	1,957.50
Maintenance & Repair	2,488.00	1,637.00
TOTAL:	$ 13,117.34	$ 11,895.94

5.0 TASK IV - POWERTRAIN DEVELOPMENT PLAN

5.1 OVERALL DEVELOPMENT PLAN

Task IV is the overall development plan for the IGT automotive powertrain, summarizing the development effort required to bring the IGT powertrain from the Phase I Conceptual Design Study through vehicle testing of prototype powertrains. The complete development plan was submitted in August 1978 as WRC Report No. 78-152.

Phase I of the plan is the Conceptual Design Study as accomplished by Williams Research Corporation and AM General Corporation.

Phase II, Preliminary Design and Concept Component Verification, identifies the component work required to verify the concept and component selections and demonstrate performance characteristics. Development will proceed to bring each component to a level adequate for powertrain evaluation and development.

Phase III, Component and System Development, starts powertrain design and development; component development will also continue on a parallel path, diminishing or phasing out on each component as powertrain development takes over. Vehicle system test and development will start within a year after start of powertrain development, so that the experimental system can be demonstrated in fiscal year 1983. Powertrain and vehicle system development will continue after this to further improve performance, durability, and reliability.

The next phase of the development plan is a large-scale fleet test to demonstrate that the powertrain is indeed suited for production and application. A minimum of 50 vehicles is suggested for this test, to provide data over a wide range of operating conditions. These vehicles could be production automobiles, modified to incorporate the IGT powertrain, or could be specially designed vehicles for commercial, governmental or military use. The special vehicle application can provide a natural transition from the development phase to the higher production levels required to make the IGT powertrain a commercial success.

The vehicle fleet test program would be supported by accelerated durability testing on a minimum of 20 powertrains, set up to simulate vehicle operation. One year of rigorous vehicle fleet test can indicate that the powertrain has adequate durability and reliability to consider production and marketing, but the program should continue for several years to provide longer term durability and maintenance information and to minimize the chances of unpleasant surprises during the early production phase.

The overall schedule for the IGT powertrain plan is shown in Figure 117, showing the correlation of the development phases.

5.2 PHASE II – PRELIMINARY DESIGN AND CONCEPT/COMPONENT VERIFICATION

COMPRESSOR COMPONENT PROGRAM (Figure 118)

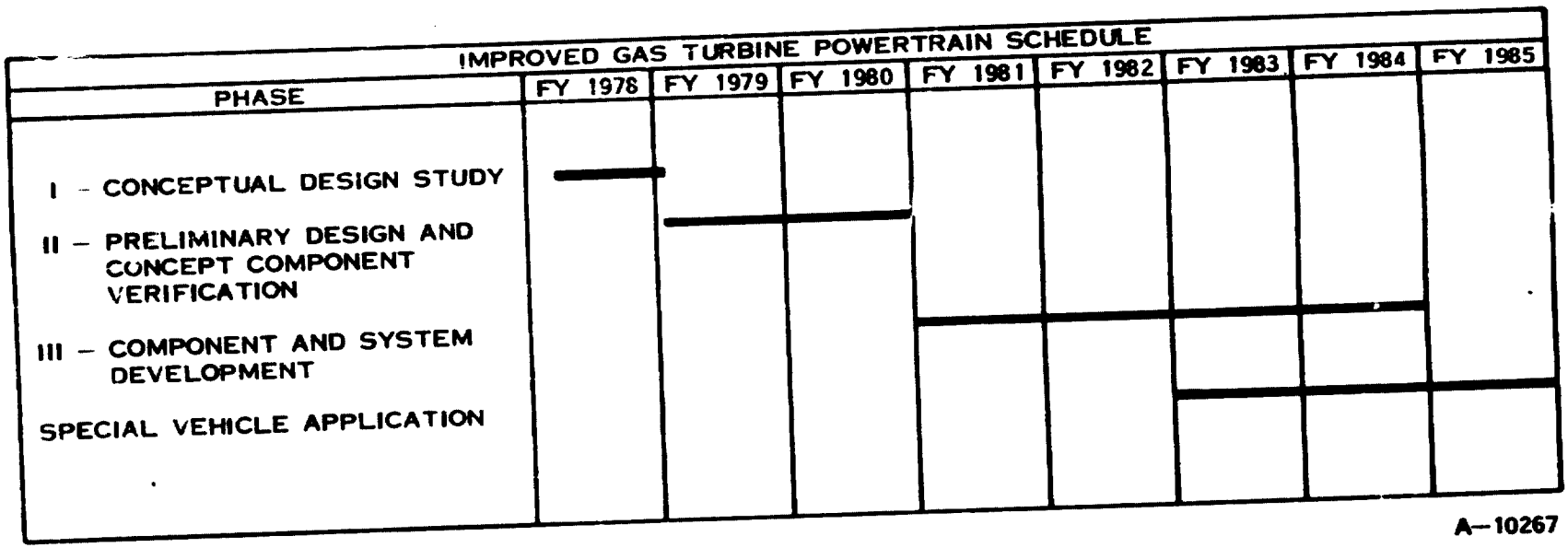

Figure 117. Improved Gas Turbine Powertrain Schedule

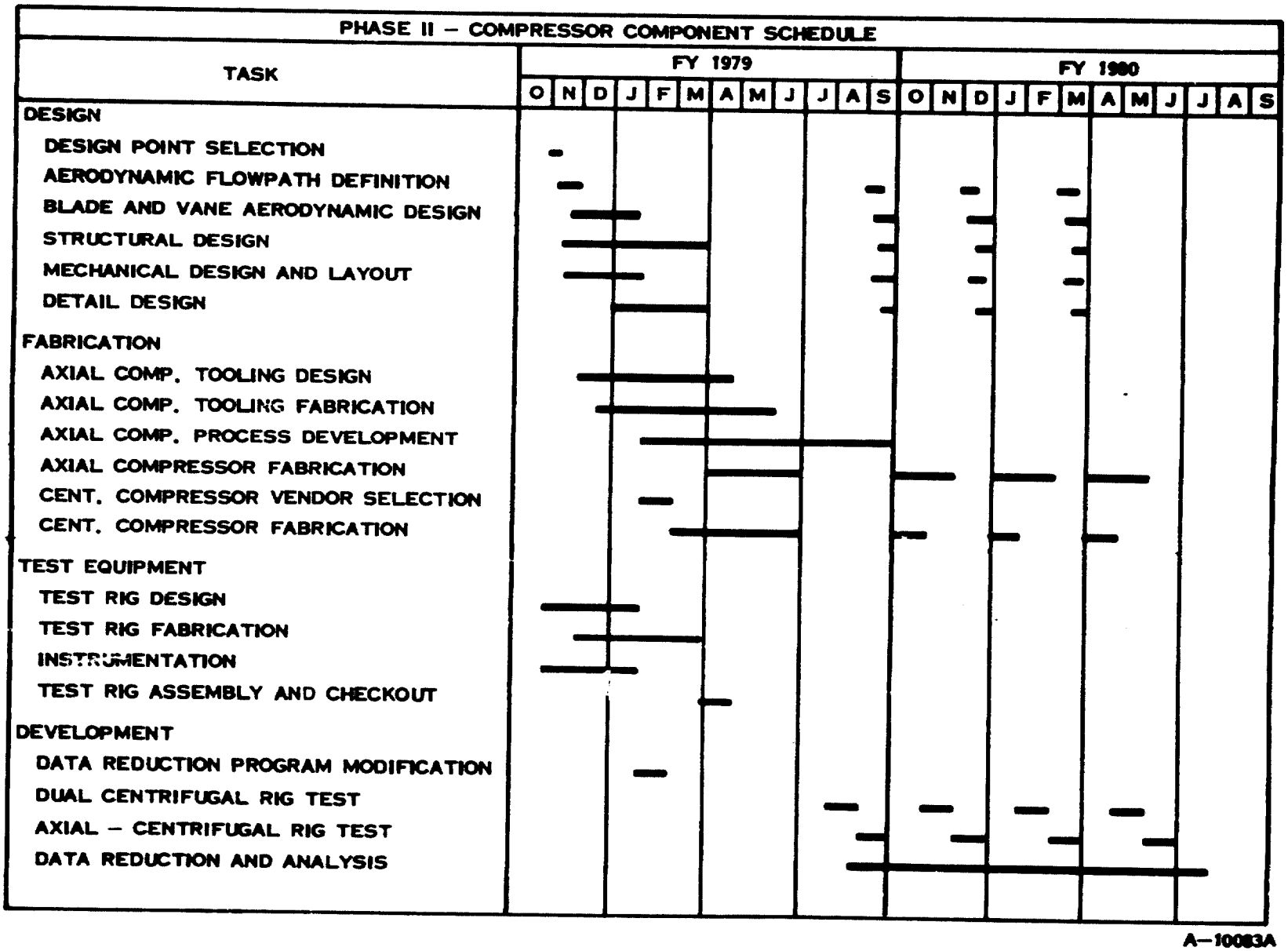

Figure 118. Phase II - Compressor Component Schedule

Compressor Design

A design point for both the dual centrifugal and axial-centrifugal compressors will be selected with regard to stage matching, relative inlet Mach numbers, choking flow limits and range of operation.

The first design phase will be a one-dimensional flowpath sizing of the dual centrifugal compressor followed by a similar exercise on the backup axial compressor design. The next phase will involve the two-dimensional design of the dual centrifugal compressor. The axisymmetric streamline curvature design of the axial compressor will then be initiated.

The blade design of the dual centrifugal compressor rotors will be carried out using a modified version of the NASA Vanco (Reference 23) program. The vane design of the dual centrifugal compressor diffuser also will be finalized at this time. The blade and vane design for the axial compressor will be conducted using options of the Hearsey (Reference 24) axial compressor design program.

Complete stress, thermal, and dynamic analysis will be made of the compressor structure to ensure a practical, reliable mechanical design, suited for automotive use.

Compressor Fabrication

Axial compressor components will be fabricated by WRC using low-cost casting techniques. Selected vendors will fabricate the centrifugal compressor hardware in accordance with detail drawing specifications. Final machining, flame spraying, polishing, and subassembly will be carried out by WRC or by designated vendors.

Test Equipment

The WRC small compressor test rig will be modified to operate with either the axial-centrifugal or dual centrifugal compressors. Design modifications will be required for the gearbox and inlet systems, including a new step-up helical gear set to accommodate the high speed required by this design.

Compressor Development

Four major test periods are planned for the dual centrifugal compressor. The major tests are the overall performance assessments of the prime and alternate compressor configurations. Each configuration will be tested with two diffusers to investigate rotor-diffuser match and ensure adequate surge margin for engine operation.

Succeeding tests will be aimed at optimizing rotor and diffuser performance through modifications to inducer and diffuser blade and vane angles, cross sections, number, and location. Final tests will be devoted to sensitivity testing where clearance, surface finish, and leakage rates can be investigated.

Four major test periods are planned for the axial-centrifugal compressor. The first major axial-centrifugal test period is staggered to follow the first major

dual centrifugal test. This has been done so data on the second stage centrifugal compressor will be available to aid in axial-centrifugal compressor matching. The first major test period will be principally devoted to obtaining overall performance and stage matching data with variant designs of the axial compressor.

Succeeding major test periods will deal with optimizing the compressor from an interstage point of view. One major redesign to the axial compressor has been considered for the third major test period. Final tests will be devoted to sensitivity studies where clearance, leakages, and surface finish can be systematically varied.

TURBINE COMPONENT PROGRAM (Figure 119)

Turbine Design

The turbine design process consists of flow path preliminary definition, velocity triangle design and analysis, blade and vane shape definition, and surface velocity analysis. Preliminary flowpath and blade chord definition are obtained by simultaneous considerations of the maximum hub loading coefficient, desired nozzle exit Mach number, stage flow and work requirement, stage efficiency objective as compared to the Smith (Ref. 25) plot, and the acceptable maximum Zweifel loading coefficient. WRC utilizes a velocity triangle computer program which is based on mass, momentum, and energy conservation principles, and can be operated in either the design or analysis mode. The program is first operated in the design mode to obtain preliminary throat sizes and other basic parameters. Following this initial step, the program is switched to the analysis mode, and a series of small changes are analyzed to optimize the design. The optimization typically involves consideration of efficiency, flow matching, work and pressure ratio requirements, exit velocity swirl and profile, static pressure reaction, and numerous other parameters. When a satisfactory configuation is obtained, the preliminary geometry estimates are translated into blade and vane shapes intended to provide the specified velocity triangles.

WRC utilizes a computer program to define a three-dimensional blade shape, starting with airfoil shapes constructed on cylindrical surfaces. During shape development, the designer considers the fabrication effects of minimum leading and trailing edge radii, minimum thicknesses, and other blade geometry parameters. Additionally, various stress parameters, such as hub-tip cross-section area ratio and blade weight, are set according to design requirements. Other geometric requirements, such as smoothness of the stackup, must also be met. Finally, the surface velocity profiles are checked for excessive velocity diffusion. Usually this step will require shape change iterations to eliminate areas of undesirably high diffusion. Upon completion of this step, the new blade geometry parameters are placed in the velocity triangle analysis program and the final triangle definition is obtained.

Structural design analysis will be conducted to provide structurally adequate turbine rotor and nozzle assemblies for the design life and operating requirements. This effort, which includes heat transfer, stress, and dynamic analyses, will analyze the nozzles and support structure, the rotor blades, rotor, and blade/rotor combination to ensure that no harmful operating stresses and resonant frequencies are present to cause premature failure. In addition, analysis of rotor shaft stresses and critical speeds will be made.

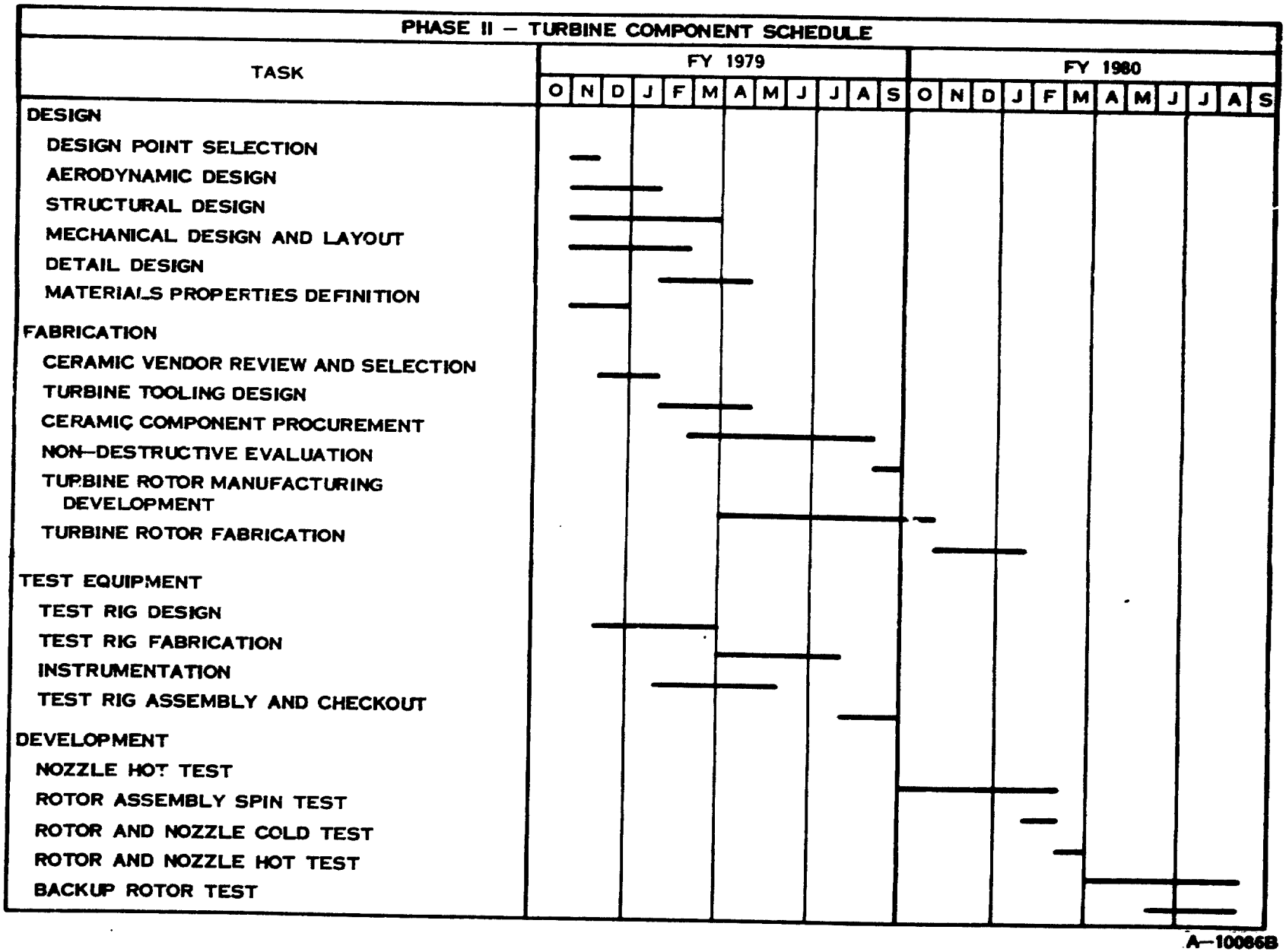

Figure 119. Phase II - Turbine Component Schedule

Turbine Fabrication

The methodology of manufacturing the first stage turbine rotor will be developed to assure a consistent and reliable, yet economical, means of producing the rotor. Alternate methods of manufacture will be investigated and one selected from these candidates. The selected method of manufacture will then be refined until sufficient assurances are present that the resulting rotor will satisfy all the prescribed requirements on a consistent basis. Ceramic static parts will be supplied by selected vendors.

Turbine Test Equipment

The turbine test rig will be designed to operate in two modes; first, in the usual cold flow performance test mode and second, in a high-temperature durability and performance test mode.

Turbine Development

The turbine rotor and nozzle will be cold flow tested, i.e., operated at much reduced temperatures, etc., to check out its performance. This permits evaluation of some of the turbine and rig performance before imposing design operating temperatures which may cause premature failure before data can be obtained.

Hot flow tests of the nozzle assembly will be performed to monitor nozzle aerodynamic performance and to identify potential structural anomalies before a rotor is introduced to the system. The initial hot test of the nozzle will provide an opportunity to obtain preliminary aerodynamic performance data from the nozzle cascade. Primary items of interest will be nozzle exit flow direction, flow velocity, and total pressure profiles as compared with analytical predictions. This test will give an early diagnosis of possible ceramic nozzle aerodynamic problems, such as flow separation, shock losses or excessive losses from rough surfaces or trailing edge effects. These data can also be used to refine the analytical prediction of overall stage efficiency.

The turbine assembly will then be tested hot, simulating engine operation. While the primary objective of the hot test is to verify structural integrity of the high pressure turbine stage, overall stage performance, work output, flow capacity, and exit swirl angles will be measured. Local pressure and temperature traverses will also be made to determine radial distributions of work and losses.

Following performance evaluation, the test rig will be used to evaluate the durability of the first stage turbine. This includes endurance running at maximum speed and temperature, and simulation of engine starting, stopping, and other transient operations.

COMBUSTOR COMPONENT PROGRAM (Figure 120)

Combustor Design

The premixer prevaporizer must be capable of delivering a uniformly mixed and vaporized fuel air mixture to the catalyst bed and preventing autoignition or

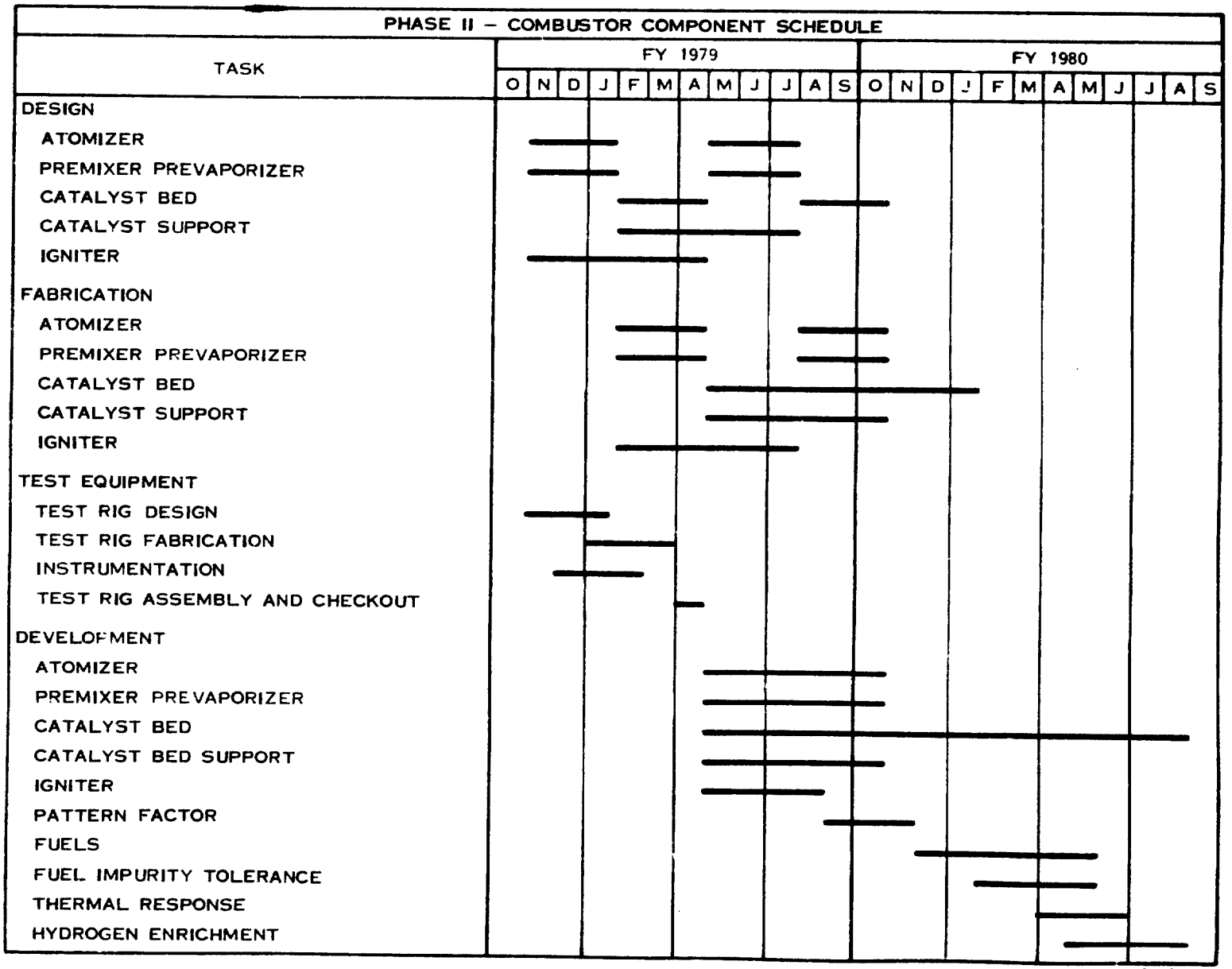

Figure 120. Phase II - Combustor Component Schedule

flashback from occurring. The optimization of mixing length will require aerodynamic analysis of mixing processes and analysis of vaporization and chemical reaction rates.

The catalyst bed will be a purchased item. WRC will work with one or more catalytic bed manufacturers to obtain the optimum design for the ceramic catalyst substrate and catalyst material. The design of the structure which will support the catalyst bed is important for mechanical durability and combustion efficiency reasons. The support structure must protect the catalyst substrate from mechanical damage and provide a seal around the catalyst bed.

Combustor Fabrication

The catalyst bed will be made by the selected vendor(s). The substrate may be a ceramic material with a thin layer of noble metal catalyst applied over the substrate. The catalyst bed support will probably be a ceramic material.

Combustor Test Equipment

A test rig will be designed to house the experimental combustor hardware. The WRC laboratory air system will be used to supply air to the rig, preheated to engine conditions without vitiation by a commercial high-temperature heat exchanger.

Combustor Development

The atomizer development will consist of establishing the proper droplet size distribution and diffusion pattern to obtain a uniform fuel/air ratio at the combustor inlet. The premixer prevaporizer will serve to complete the mixing and vaporization process started at the atomizer. The mixing length and cross-sectional area will be developed to give the optimum mixture distribution with control over flashback and autoignition.

The development of the catalyst bed will optimize the design of the substrate material and cell configuration, the washcoat and catalyst material, combustor inlet area, bed length and reference velocity to be used in the final combustor.

Testing on a variety of fuels, such as unleaded gasoline, diesel fuel, kerosene, and first-cut low octane gasoline, will be conducted to determine the alternate fuel capabilities and low-cost fuel potential of the combustor.

RECUPERATOR COMPONENT PROGRAM (Figure 121)

Recuperator Design

A complete analytical investigation will be made of alternative recuperator geometries to obtain a configuration which satisfies the thermal efficiency and pressure drop requirements. Heat transfer analyses are also used to develop temperature gradients used in subsequent structural analyses.

Detailed structural analysis will ensure that the recuperator will not fail prematurely when subjected to operating thermal gradients and pressure loads. This

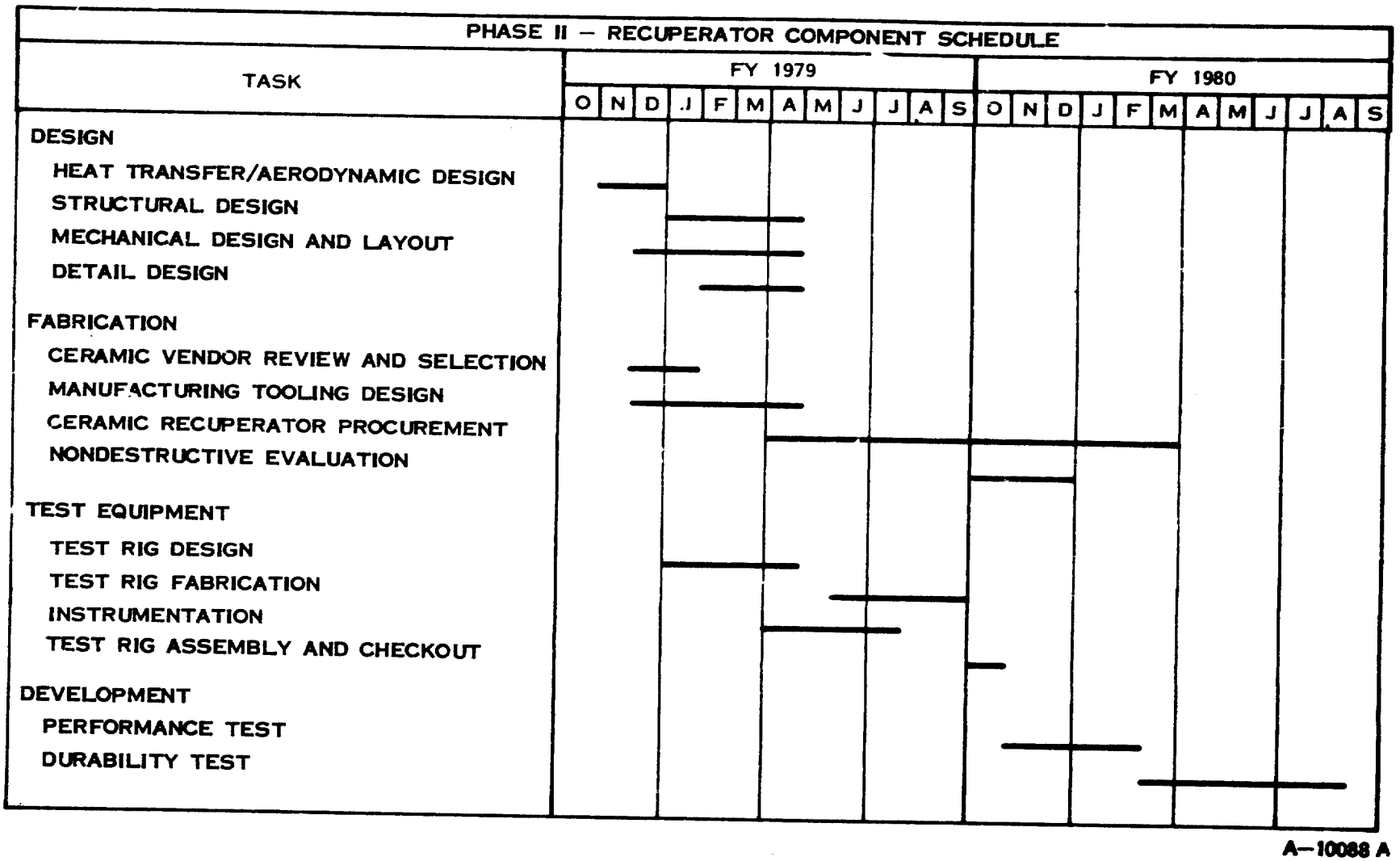

Figure 121. Phase II - Recuperator Component Schedule

analysis will include finite-element stress analyses which can incorporate the complex temperature distribution. This is necessitated by the inherent brittle nature of the ceramic recuperator material.

Recuperator Fabrication

The capabilities of the different vendors will be evaluated for their ability to provide a satisfactory configuration from an aerodynamic, structural and geometric point of view while also providing the best cost and delivery potential.

Production of the ceramic recuperator requires a design concept suitable for high-volume production on automatic equipment. The design concept has this potential, but methods of forming, assembly, and bonding must be considered as part of the original design. Experimental tooling will be designed for the fabrication of prototypes, compatible with proposed production processing. The selected vendor will provide tooling and materials and develop the manufacturing process to supply recuperators which satisfy the prescribed requirements.

Recuperator Test Equipment

The recuperator test rig will house the recuperator assembly and provide air ducts and seals to simulate the engine. The WRC laboratory air system and the turbine test rig combustion heater will handle the high pressure side of the recuperator. A low pressure blower and a second combustion heater will be required for the low pressure side.

Recuperator Development

Performance testing must be accomplished to determine the adequacy of the recuperator design for the intended application. This testing will include operating over a range of temperatures, flows and pressures to measure recuperator effectiveness. Various performance monitoring parameters will be measured and these data will be compiled, reduced and combined to yield data which gives an indication of the recuperator acceptability.

Performance tests will start at low pressure and temperature levels and with minimum transients to evaluate performance characteristics and refine analytical techniques. Sections of recuperators and large-scale models may be used to further define heat transfer and pressure drop characteristics and explore flow distribution effects. Then pressure and temperature will be stepped up to engine conditions, followed by simulated transient operation, including starts and shutdown.

Durability testing will be done to ensure that the recuperator is capable of satisfying the expected operational and life requirements. Accelerated cycling tests will be run as well as steady-state testing. Structural operating parameters will be measured and these data reduced to provide an indication of the structural ability of the recuperator to meet the operating life requirements. Test data and analysis will guide design changes if needed to improve durability.

POWERTRAIN SYSTEM INTEGRATION (Figure 122)

Design

There will be continuing interface activity between WRC, AM General, and American Motors, with interchange of information on powertrain and vehicle characteristics and requirements. Proposed changes will be studied and agreed to before incorporation to make sure they can be accommodated and will improve the overall system performance. This will include preliminary studies of proposed production automobiles, including front drive arrangements.

The powertrain layout developed as part of the Phase I Conceptual Design Study will be reviewed and additional design work performed where needed to define and control the component design envelope and interfaces.

Performance Analysis

As component test data becomes available, the powertrain performance analysis will continue to evaluate the effect of component changes and to guide the component development program rationally toward achieving the system performance goals.

Driving cycle fuel economy and vehicle response characteristics will be calculated for selected powertrain configurations to show the relative effects and to guide the selection of the best configuration.

5.3 PHASE III – COMPONENT AND SYSTEM DEVELOPMENT (FIGURE 123)

COMPONENT DEVELOPMENT

The component development started during Phase II will continue on all major components. It is expected that this work will continue until powertrain testing is well under way, although the level of activity will be reduced as performance goals are reached. The combustor and HP turbine require extensive durability development and demonstration, which can continue in the test rigs until engine testing can take over this function.

One additional area requiring component test and development is the control system. Programmable electronic controls will be used to start the powertrain development program, permitting rapid and easy changes with great flexibility. The remaining hardware in the control system such as transducers and actuators will be designed to meet the system requirements. Each component will be bench tested, and then a complete system will be set up to simulate engine operation. This will permit demonstration and development of system characteristics, preparing for initial powertrain tests.

POWERTRAIN DESIGN

The powertrain will be designed and detailed for the development phase. The design will be based on the concept selected in the Phase I Conceptual Design Study and refined during the Phase II Preliminary Design and Concept/Component Verification. The powertrain design will be sized to meet the vehicle class

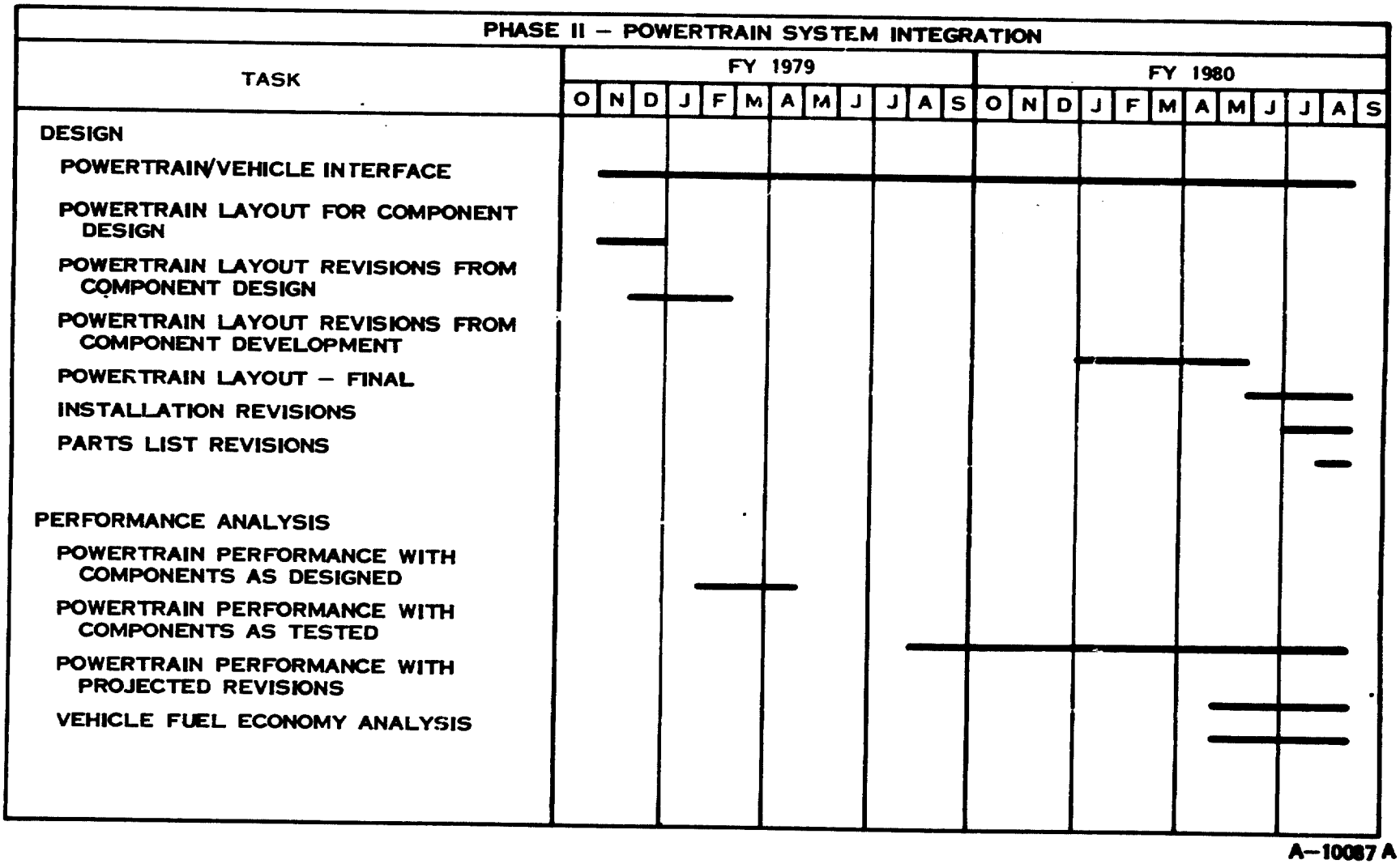

Figure 122. Phase II - Powertrain System Integration

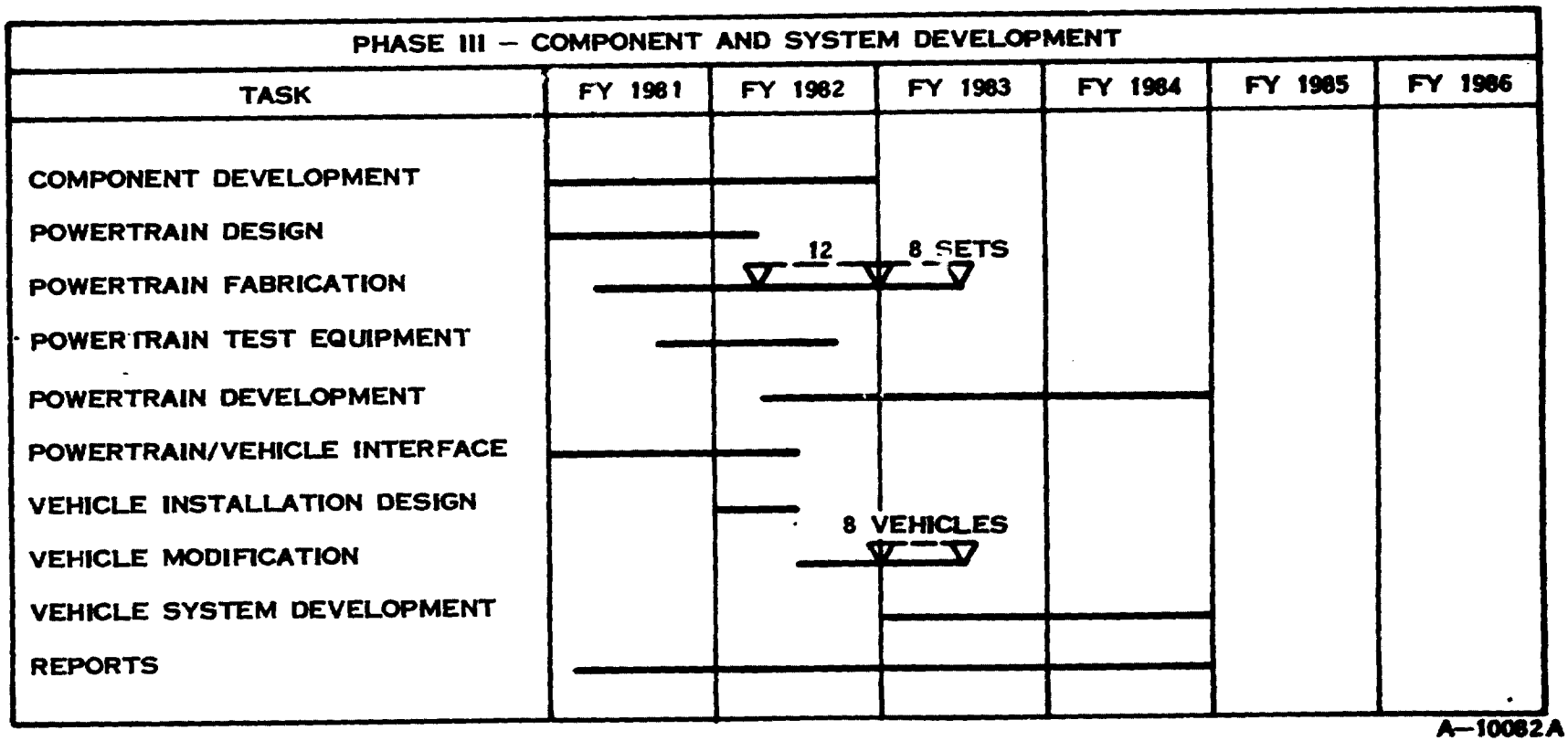

Figure 123. Phase III - Component and System Development

selected for market introduction. The sensitivity and risk analysis will influence the final sizing to ensure that the powertrain design is adequate for meeting development and marketing goals.

The powertrain and vehicle performance analysis will be reviewed and updated with newly acquired component data and analytical techniques. The powertrain design will be reviewed for producibility with manufacturing engineering and vendors. Their thinking and suggestions will be incorporated into the detail design to make sure that the parts and assemblies are suitable for volume production.

A final layout will be made of the powertrain assembly, with separate layouts of sections, subassemblies, and components. Final analyses of aerodynamics, stress, temperature, vibration, etc., will be concurrent with the design layouts. These layouts must be approved by all engineering and manufacturing disciplines before detail drawings are completed and checked. A similar engineering and manufacturing review and approval of each detail part or assembly drawing is required before it is released for fabrication.

POWERTRAIN FABRICATION

All parts released for development will be procured or fabricated in the quantities specified by project engineering. In general, tooling, fixtures, gaging, etc., will be tailored to the development quantity and schedule requirements. The finished parts will, however, be as close to production parts as practical in terms of material, heat treatment, surface finish, tolerances, and other physical specifications that may affect the evaluation and development of performance and durability characteristics.

Compressor

When the centrifugal compressor rotor design is finalized during the development program, casting tooling and castings will be procured for engine test to permit evaluation of hardware suitable for production.

Turbine

Turbine hardware will continue to be fabricated with the prototype tooling used during the Phase II component program.

Combustor

Ceramic components including the catalyst bed will be procured from the same vendors as in Phase II. Metal parts will continue to be fabricated by WRC and vendors using the prototype tooling.

Recuperator

Ceramic recuperator assemblies will be fabricated using the processes developed and the vendors selected on the Phase II component program.

Structure

Structural parts of the engine such as housing, shrouds, supports, etc., will be fabricated from sheet metal or castings as in a production design. Initial hardware or revised designs may be machined to simulate sheet metal or castings to permit development until specified hardware is available.

Transmission

The 3-speed automatic transmission in then current production will be adapted to the IGT powertrain, without the torque convertor and oil pumps, and with modifications for mounting, input drive shaft, and shift pattern.

Control System

Initial powertrain development will use programmable electronic controls to evaluate a wide range of control system concepts and parameters. After the desired control characteristics have been thereby established, a production prototype control will be supplied on a contract basis by a selected vendor. This will include design, fabrication, and bench engineering verification tests to demonstrate that the control meets all design specifications.

POWERTRAIN TEST EQUIPMENT

Two test stands will be set up for powertrain performance and mechanical development. These will each be equipped with a dynamometer and full instrumentation for pressures, temperatures, airflow and fuel flow to assure overall performance characteristics and provide additional information to correlate with and supplement the component performance tests.

In addition to the performance test stands, six endurance test stands will be used for steady-state and cyclic durability development. General performance instrumentation will be provided, with additional instrumentation to monitor critical areas and detect changes in performance or impending failure. These will be set up for eventual automatic operation to minimize manpower requirements.

POWERTRAIN DEVELOPMENT

Powertrain assembly and test will start as soon as sufficient parts are available, although component development will be continuing and changes are in process or planned. Powertrain test will be required to evaluate overall performance, define transient characteristics and requirements, and indicate durability and reliability problems. Testing will start with the gasifier assembly, with the addition of the combustor, recuperator, and power sections as development progresses.

A total of 12 powertrain assemblies will be used for development, with enough spare parts and optional designs to pursue a vigorous development program. Two engines will be assigned for performance development, two for mechanical development, and eight for endurance testing, with extensive transient and cyclic operation.

The goal of powertrain development is to demonstrate satisfactory operation at all conditions predicted for the vehicle. Endurance development should reach the capability of several hundred hours in typical vehicle operation. Problem areas should be identified, with sufficient data to guide component development, analysis, and redesign.

POWERTRAIN/VEHICLE INTERFACE

There will be continuing interface activity between WRC, AM General, and American Motors, with interchange of information on powertrain and vehicle characteristics and requirements. Proposed changes will be studied and agreed to before incorporation, to make sure they can be accommodated and will improve the overall system.

This will include preliminary studies of proposed production automobiles, including front drive arrangements. Special vehicle applications may be considered, and feasibility studies will be conducted.

VEHICLE INSTALLATION DESIGN

For vehicle development, powertrains will be installed and tested in current production vehicles of the selected vehicle class. A preliminary design of this installation will be done concurrent with the powertrain layout work, and then updated and completed based on the final detail and assembly drawings as released.

VEHICLE MODIFICATION

The production vehicle will be modified to accommodate the powertrain. Parts will be removed, reworked, and/or replaced as required.

VEHICLE DEVELOPMENT

As soon as the powertrain has demonstrated adequate performance and durability, it will be installed in vehicles for development test and evaluation. A total of eight vehicles will be used, with two concentrating on development changes, four for endurance running, and the final two available for demonstration.

The goal of vehicle development is to demonstrate satisfactory powertrain operation at all vehicle conditions, with capability of at least 10,000 miles of vehicle operation. Problem areas should be identified, with sufficient data to guide powertrain development, analysis, and redesign.

5.4 SPECIAL VEHICLE APPLICATION (FIGURE 124)

VEHICLE SYSTEM INTEGRATION

The vehicle for fleet test and possible market introduction may not be a conventional production automobile, but the basic IGT powertrain will be adaptable to the installation. The gas turbine components and flow path will not change, but external changes may be required to integrate the powertrain and vehicle.

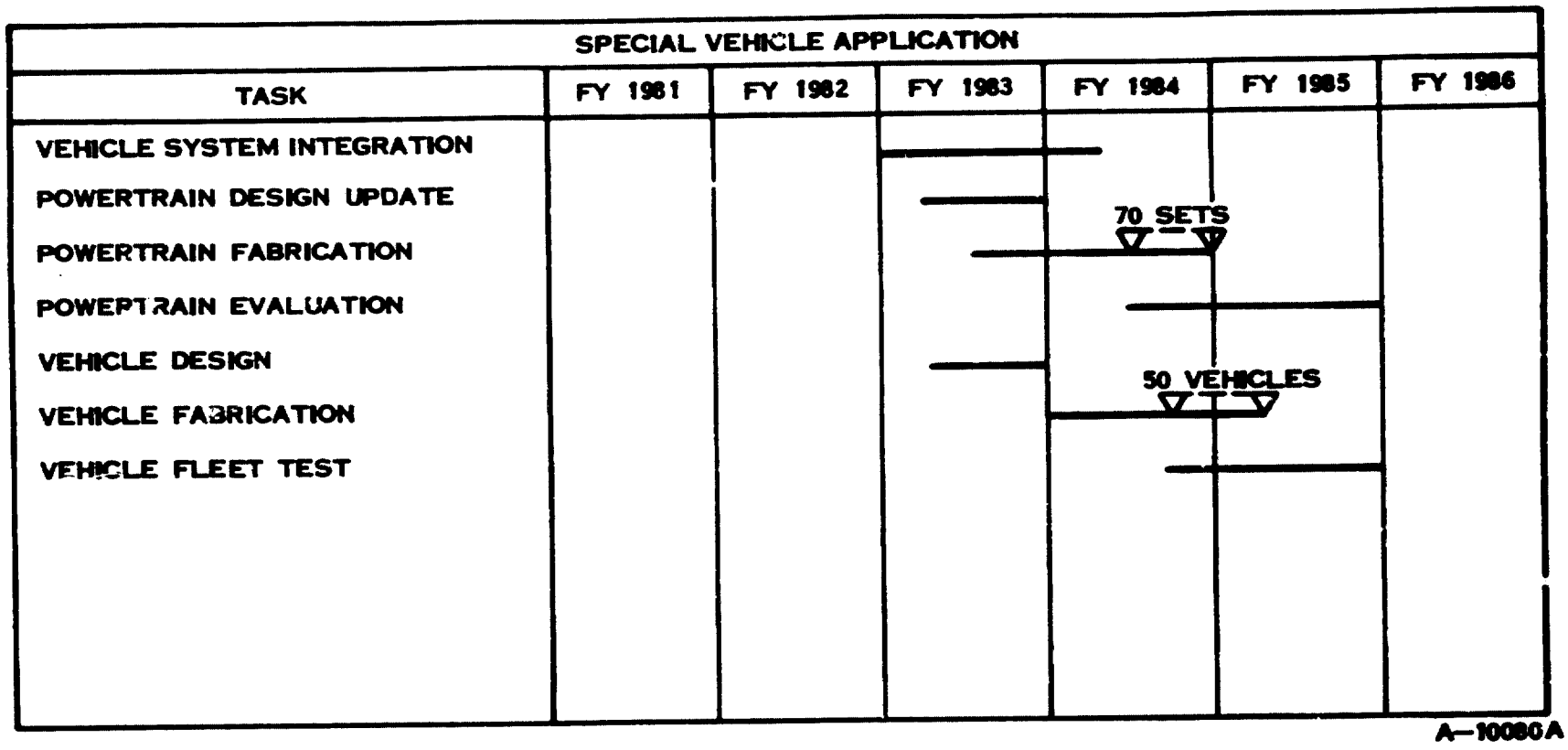

Figure 124. Special Vehicle Application

These changes may include the output shaft speed and location, accessory drive speed and location, intake and exhaust locations, and mounting arrangement. The transmission and drivetrain may be entirely different from the IGT automotive design, but must meet all system requirements, including coordination of functions with the powertrain control system.

System integration design work will start with installation studies, trying different engine positions and drivetrain arrangements in the vehicle, followed by vehicle accessory locations and drives. High load accessories may require a separate drive from the output shaft. The intake system must include adequate filtration, possibly an inertial type separator, for acceptable service life in dusty environments. The exhaust system requires acceptable pressure drop and exit location from the vehicle. The mounting system must handle all loads imposed by the vehicle, including any off-road requirements.

The vehicle electrical and fuel systems must provide for the powertrain requirements. The vehicle heating system may extract hot air from the turbine, or a self-contained fuel-fired system may be used.

The powertrain electronic control system can be easily tailored to meet the vehicle system requirements. The programmable electronic control will be used to develop unique system characteristics and requirements before finalizing the prototype control design.

This integration work will provide input for the powertrain and vehicle design work. It will continue through the design effort to coordinate the activity and resolve any problems as they occur.

POWERTRAIN DESIGN UPDATE

After extensive component and powertrain development have demonstrated product capability during Phase III, the powertrain design will be reviewed and updated. The basic design concept will not be changed, but only improvements that have been identified and proven as a result of development will be incorporated. These will include component refinement such as blade settings and matching adjustments, mechanical changes to correct durability and reliability problems, and manufacturing and processing changes to reduce cost.

This review will start with powertrain and component performance analysis and proceed through a complete review of the powertrain assembly, subassemblies, components, and details. Material changes will be made where required or permitted based on development experience. Design revisions will include adaptation of the powertrain to the vehicle application, as defined by the vehicle system integration studies.

Drawings will be revised as required to specify the improvements, and the updated design will be released with engineering and manufacturing approval for procurement and fabrication of prototype powertrain assemblies.

POWERTRAIN FABRICATION

Sufficient components will be fabricated for 70 powertrain assemblies plus spare parts to support prototype powertrain evaluation and the vehicle fleet test program. This requires hardware production at approximately four assemblies per week to get prototype powertrains and vehicles on test quickly.

Additional effort will be required on tooling, gaging, and processing, not only to handle this hardware but also to simulate production hardware as closely as practical.

POWERTRAIN EVALUATION

Prototype powertrain assemblies will be tested under conditions representing the special vehicle application, including cyclic endurance operation over a range of ambient conditions.

The first group of four powertrains will be carefully evaluated after initial testing to make sure the projected improvements have been achieved, and no new problems have been discovered or generated.

Powertrains will be disassembled and inspected on a scheduled basis as part of the evaluation to ensure that all components and details are adequate for production. Where deficiencies are noted, engineering and manufacturing review, analysis, and redesign will be implemented. Modified or redesigned parts will be retrofitted as required to support the evaluation program.

VEHICLE DESIGN

The vehicle design or adaptation for the IGT powertrain will use the input from the system integration studies. Layouts will be made of the installation to cover all interface requirements, which will then be incorporated as an integral part of the vehicle design.

VEHICLE FABRICATION

Vehicles will be fabricated or current production vehicles will be reworked to accommodate the powertrain installation. A total of 50 vehicles is proposed, scheduled for two per week after the initial installation to get prototype vehicles on test as rapidly as possible.

VEHICLE FLEET TEST

Prototype vehicles will be evaluated by fleet test of a group of 50 vehicles. The initial group of 10 vehicles will be tested by the contractor under accelerated, controlled conditions with continuous surveillance to provide early, hard data on performance, durability and reliability.

The remaining 40 vehicles will be distributed to users across the 48-state area to cover a wide range of operating conditions, although users will be grouped geographically to simplify service requirements. Users would be selected to achieve high mileage in a short time to generate a data base of operational experience over the range of usage and environment rapidly and efficiently. Powertrains will be exchanged, performance checked, inspected, and evaluated at scheduled intervals to obtain the maximum information from the fleet test program.

DISCUSSION OF RESULTS

The initial evaluation of the basic thermodynamic cycle parameters in Task I, Powertrain Identification and Description, showed conclusively that a regenerative cycle is required to achieve good automotive fuel economy. The TIT must be as high as practical with the available materials, and the compressor pressure ratio should be higher than optimum at rated power to improve SFC at low power.

The turbomachinery components were then chosen to attain the high TIT and suitable pressure ratio using current and near-term technology. A two-stage centrifugal compressor was chosen for its pressure ratio capability and wide operating range with good efficiency. The two-stage rotor also operates at a much lower shaft speed than an equivalent single-stage compressor rotor, permitting a higher TIT for a given turbine wheel material. A single stage axial gasifier turbine was chosen to match the compressor requirements with good efficiency and the low inertia necessary for good driveabiiity. The use of the two-stage compressor permits this turbine to operate at a TIT of 1422°K (2100°F) or higher with advanced high-temperature alloys.

The two static flow components, the combustor and heat exchanger, were chosen based on superior performance capabilities considered attainable with the development of near-term technology. The catalytic combustor is already under development on other programs and has the potential for high efficiency with very low emissions using a wide variety of fuels.

The ceramic recuperator has not had the years of extensive development that have successfully brought the ceramic regenerator to its current advanced state, but the materials and manufacturing processes that have evolved for the regenerator provide a sound basis for the development of a ceramic recuperator. The ceramic annular recuperator with axisymmetric flow passages has the potential for good flow distribution and very high effectiveness with minimum leakage and no drive power requirement, resulting in improved vehicle fuel economy. In addition, the recuperator is an ideal component for automotive production, because it is an integral assembly with projected low initial cost and no moving, wearing parts or service requirements.

The detailed analysis in Task II, Powertrain Analysis, explored the range of cycle parameters and rotor systems with these components. The 1422°K (2100°F) TIT engine exceeds the vehicle fuel economy and response requirements. This permits a practical development program targeted for production engineering in the near future without the very high risk of a ceramic turbine rotor.

Comparison of TIT control systems led to the choice of the dual-rotor engine with the variable power turbine nozzle. This system combines good driveability with good SFC at part load and requires only a conventional automatic transmission with high efficiency and low cost.

Although a single-rotor engine has inherent advantages over the dual-rotor engine with regard to simplicity, cost, and mechanical and leakage losses, the lack of a fully developed and proven continuously variable transmission (CVT) produces a

significant risk factor. The hydromechanical CVT is the only unit that has demonstrated power and wide ratio drive capability, but low efficiency, noise and high cost are still major concerns. A CVT that overcomes all these problems will provide a major impetus toward the development of a single-rotor automotive gas turbine engine.

The approach used in Task IIIA, Powertrain Optimization and Performance, was to make the basic engine as small as practical, increasing the percentage of rated power at any given power requirement to improve SFC at low power. This was enhanced by sizing the engine so it developed satisfactory performance at all ambient temperatures below 288°K (59°F). Water injection is used to maintain adequate vehicle acceleration at higher ambient temperatures.

Task IIIB, Vehicle Cost Analysis, shows that a moderate penalty in initial (sticker) price can be overcome by reduced fuel and maintenance costs. Ever-increasing fuel cost will make this factor much more significant in the future, further emphasizing the need for improved vehicle fuel economy. The lower maintenance cost has not been demonstrated, but experience in the aircraft industry has been excellent, indicating that a very low level of scheduled and nonscheduled maintenance should also be possible in the automotive application.

The use of the two-stage compressor and the advanced high-temperature alloy turbine rotor is the key to the demonstration and evaluation of the IGT powertrain by FY1984 as shown by the Task IV Powertrain Development Plan. This tight schedule is possible only by forgoing the development of a very high risk ceramic turbine rotor. This demonstration is followed immediately by a large-scale fleet test program to support a production engineering decision by FY1985.

SUMMARY OF RESULTS

A dual-rotor gas turbine engine was selected for the IGT powertrain, and optimized for good fuel economy. A two-stage centrifugal compressor is used with a design pressure ratio of 5.28 to achieve good efficiency and broad surge margin over the operating range. The lower shaft speed with this compressor makes it possible to operate an advanced high temperature alloy integral first stage gasifier turbine wheel at a TIT of 1422°K (2100°F). The integral metal second stage power turbine wheel uses a variable nozzle for turbine temperature and output torque control. A catalytic combustor is used for very low emissions and high efficiency, with the combustion air preheated by an annular ceramic recuperator. Component characteristics and matching are directed toward reducing SFC at low power to achieve good vehicle fuel economy.

The engine is sized as small as practical for steady-state operation with a 1406 kg (3100 lb) car, rated at 54.8 kW (73.5 hp) at 303°K (85°F) and 152.4 m (500 ft). This engine rating meets the vehicle acceleration requirement of 0 to 96.6 km/h (0 to 60 mph) in 15.0 seconds at ambient temperatures below 288°K (59°F). Water injection is used at higher ambient temperatures to maintain the power and acceleration. This optimized IGT powertrain is estimated to achieve a vehicle fuel economy of 11.9 km/l (28.0 mpg) on the combined driving cycle, 43 percent more than the 1976 compact automobile.

The IGT powertrain is packaged into a compact, axisymmetric arrangement made possible by the annular recuperator. A concentric rotor arrangement is used with a common gearcase for the power turbine reduction gear and gasifier-driven accessory drive train. The powertrain is packaged into an American Motors Concord 2-door sedan, using a 3-speed automatic transmission and conventional rear drive.

The production cost estimate of the IGT vehicle shows a 10 percent cost penalty over the piston engine vehicle. Less than half of the cost penalty is in the turbine engine; the remainder is due to the adaptation of the current production vehicle and systems. The fuel economy improvement and reduced maintenance and repair result in an overall life cycle cost saving of 9 percent for the IGT vehicle.

APPENDIX A

IGT DATA TABLES *

TABLE XX. ENGINE 1 PERFORMANCE SUMMARY (SI UNITS)

Engine	1			
Compressor Configuration	R - R			
TIT @ 100 Percent Power, ^{o}K	1505			
TIT Control	VPT			
Nominal Compressor Pressure Ratio @ 100 Percent Power	5.0			
Ta, ^{o}K	303	303	303	303
Pa, kPa	99.519	99.519	99.519	99.519
Power, kW	74.6	37.3	7.5	-0-
SFC, kg/kW-h	0.253	0.363	0.300	1.298
T4 (TIT), ^{o}K	2710	2710	2564	1633.0
G.G. Shaft Speed, rpm	71890	55052	36300	35945
P.T. Shaft Speed (Optimum), rpm	69640	64496	42050	-0-
Inlet Airflow, kg/s	0.435	0.256	0.127	0.158
P1/PA - Inlet Filter Pressure Ratio	0.99	0.997	0.999	0.998
P2/P1 - First Compressor Pressure Ratio	2.504	1.878	1.318	1.304
P3/P2 - Second Compressor Pressure Ratio	1.989	1.563	1.255	1.162
P3A/P2 - Regenerator Cold Side Pressure Ratio	0.970	0.970	0.977	0.969
P4/P3A - Burner Pressure Ratio	0.970	0.967	0.974	0.968
P4/P5 - Compressor Turbine Pressure Ratio	2.218	1.561	1.239	1.348
P5/P6 - Power Turbine Pressure Ratio	1.840	1.639	1.231	1.028
P7/P6 - Exhaust Duct Pressure Ratio	0.965	0.985	0.996	0.996
P8/P7 - Regenerator Hot Side Pressure Ratio	0.921	0.949	0.973	0.980
P9/P8 - Tailpipe Pressure Ratio	0.990	0.997	0.999	0.999
T2, ^{o}K	426.0	377.0	334.0	332.0
T3, ^{o}K	545.0	444.0	365.0	357.0
T3A, ^{o}K	1096.0	1206.0	1258.0	819.0
T5, ^{o}K	1301.0	1384.0	1257.0	853.0
T6, ^{o}K	1156.0	1261.0	1311.0	853.0
T8, ^{o}K	631.0	526.0	445.0	397.0
Q1 - (kg/s)($\sqrt{^{o}K}$/kPa)	0.0768	0.0449	0.0222	0.0278
Q2 - (kg/s)($\sqrt{^{o}K}$/kPa)	0.0364	0.0267	0.0177	0.0223
Q4 - (kg/s)($\sqrt{^{o}K}$/kPa)	0.0366	0.0363	0.0305	0.0335
Q5 - (kg/s)($\sqrt{^{o}K}$/kPa)	0.0755	0.0544	0.0369	0.0438
EC1 - First Compressor Efficiency (Total-to-Total)	0.732	0.807	0.787	0.806
EC2 - Second Compressor Efficiency (Total-to-Static)	0.760	0.751	0.733	0.581
ET1 - Compressor Turbine Efficiency (Total-to-Total)	0.798	0.814	0.806	0.812
ET2 - Power Turbine Efficiency (Total-to-Total)	0.822	0.808	0.796	-0-
EB - Burner Efficiency	0.999	0.998	0.999	0.999
ER - Regenerator Effectiveness	0.900	0.933	0.940	0.940
WL1/W1 - Labyrinth Seal Leakage	0.010	0.010	0.010	0.010
HP1ext - G.G. Shaft Bearing Friction Loss, kW	0.796	0.514	0.269	0.265
HP2ext - Accessory Load Requirement (from G.G. Shaft), kW	1.242	0.915	0.599	0.593
HP3ext - Gearbox Frictional (Bearing) Loss, kW	1.193	1.051	0.530	-0-
HP4ext - Gearbox Gear Loss, kW				

*REFER TO FIGURE 33 FOR STATION IDENTIFICATION

TABLE XXI. ENGINE 1 PERFORMANCE SUMMARY (ENGLISH UNITS)

Engine	1
Compressor Configuration	R - R
TIT @ 100 Percent Power, ^{o}F	2250
TIT Control	VPT
Nominal Compressor Pressure Ratio @ 100 Percent Power	5.0

Ta, ^{o}R	545	545	545	545
Pa, psia	14.434	14.434	14.434	14.434
Power, hp	100.0	50.0	10.0	-0-
SFC, lb/hp hr (W_f, lb/hr)	0.416	0.363	0.493	2.862
T4 (TIT), ^{o}R	2710	2710	2564	1633
G.G. Shaft Speed, rpm	71890	55052	36300	35945
P.T. Shaft Speed (Optimum), rpm	69640	64496	42050	-0-
Inlet Airflow, lb/sec	0.958	0.565	0.279	0.349
P1/PA - Inlet Filter Pressure Ratio	0.99	0.997	0.999	0.998
P2/P1 - First Compressor Pressure Ratio	2.504	1.878	1.318	1.304
P3/P2 - Second Compressor Pressure Ratio	1.989	1.563	1.255	1.162
P3A/P2 - Regenerator Cold Side Pressure Ratio	0.970	0.970	0.977	0.969
P4/P3A - Burner Pressure Ratio	0.970	0.967	0.974	0.968
P4/P5 - Compressor Turbine Pressure Ratio	2.218	1.561	1.239	1.348
P5/P6 - Power Turbine Pressure Ratio	1.840	1.639	1.231	1.028
P7/P6 - Exhaust Duct Pressure Ratio	0.965	0.985	0.996	0.996
P8/P7 - Regenerator Hot Side Pressure Ratio	0.921	0.949	0.973	0.980
P9/P8 - Tailpipe Pressure Ratio	0.990	0.997	0.999	0.999
T2, ^{o}R	767.0	678.0	602.0	598.0
T3, ^{o}R	981.0	800.0	657.0	643.0
T3A, ^{o}R	1972.0	2170.0	2264.0	1475.0
T5, ^{o}R	2348.0	2491.0	2262.0	1536.0
T6, ^{o}R	2081.0	2269.0	2360.0	1536.0
T8, ^{o}R	1135.0	947.0	801.0	715.0
Q1 - lb/sec$\sqrt{^{o}R}$/psia	1.566	0.9164	0.453	0.566
Q2 - lb/sec$\sqrt{^{o}R}$/psia	0.7418	0.5442	0.361	0.454
Q4 - lb/sec$\sqrt{^{o}R}$/psia	0.7465	0.7409	0.621	0.683
Q5 - lb/sec$\sqrt{^{o}R}$/psia	1.539	0.1088	0.753	0.892
EC1 - First Compressor Efficiency (Total-to-Total)	0.732	0.807	0.787	0.806
EC2 - Second Compressor Efficiency (Total-to-Static)	0.760	0.751	0.733	0.581
ET1 - Compressor Turbine Efficiency (Total-to-Total)	0.798	0.814	0.806	0.812
ET2 - Power Turbine Efficiency (Total-to-Total)	0.822	0.808	0.796	-0-
EB - Burner Efficiency	0.999	0.998	0.999	0.999
ER - Regenerator Effectiveness	0.900	0.933	0.940	0.940
WL1/W1 - Labyrinth Seal Leakage	0.010	0.010	0.010	0.010
HP1ext - G.G. Shaft Bearing Friction Loss, hp	1.067	0.689	0.361	0.355
HP2ext - Accessory Load Requirement (from G.G. Shaft), hp	1.665	1.227	0.803	0.795
HP3ext - Gearbox Frictional (Bearing) Loss, hp	1.601	1.410	0.711	-0-
HP4ext - Gearbox Gear Loss, hp				

TABLE XXIII. ENGINE 2 PERFORMANCE SUMMARY (ENGLISH UNITS)

Engine	2			
Compressor Configuration	R - R			
TIT @ 100 Percent Power, ^{o}F	2250			
TIT Control	SC**			
Nominal Compressor Pressure Ratio @ 100 Percent Power	5.0			
Ta, ^{o}R	545	545	545	545
Pa, psia	14.434	14.434	14.434	14.434
Power, hp	100.0	50.0	10.0	-0-
SFC, lb/hp$_{o}$hr (W_f, lb/hr)	0.412	0.399	0.583	2.849
T4 (TIT), ^{o}R	2710	2710	2568	1652
G.G. Shaft Speed, rpm	72618	57575	38709	36309
P.T. Shaft Speed (Optimum), rpm	69747	52006	30090	-0-
Inlet Airflow, lb/sec	0.939	0.595	0.320	0.343
P1/PA - Inlet Filter Pressure Ratio	0.99	0.996	0.999	0.998
P2/P1 - First Compressor Pressure Ratio	2.504	1.948	1.364	1.304
P3/P2 - Second Compressor Pressure Ratio	1.999	1.619	1.266	1.179
P3A/P2 - Regenerator Cold Side Pressure Ratio	0.97	0.970	0.971	0.969
P4/P3A - Burner Pressure Ratio	0.97	0.967	0.967	0.968
P4/P5 - Compressor Turbine Pressure Ratio	2.287	2.007	1.411	1.347
P5/P6 - Power Turbine Pressure Ratio	1.794	1.360	1.106	1.043
P7/P6 - Exhaust Duct Pressure Ratio	0.965	0.984	0.994	0.996
P8/P7 - Regenerator Hot Side Pressure Ratio	0.921	0.945	0.969	0.980
P9/P8 - Tailpipe Pressure Ratio	0.990	0.997	0.999	0.999
T2, ^{o}R	767.0	687	608.0	598.0
T3, ^{o}R	983.0	820	666.0	644.0
T3A, ^{o}R	1965.0	2144	2260.0	1492.0
T5, ^{o}R	2330.0	2387	2409	1554
T6, ^{o}R	2074.0	2244	2360	1554
T8, ^{o}R	1135.0	969	809	717.0
Q1 - lb/sec$\sqrt{^{o}R}$/psia	1.533	0.9658	0.518	0.556
Q2 - lb/sec$\sqrt{^{o}R}$/psia	0.7263	0.5565	0.401	0.446
Q4 - lb/sec$\sqrt{^{o}R}$/psia	0.7275	0.7275	0.689	0.665
Q5 - lb/sec$\sqrt{^{o}R}$/psia	1.543	1.3704	0.942	0.869
EC1 - First Compressor Efficiency (Total-to-Total)	0.732	0.805	0.798	0.806
EC2 - Second Compressor Efficiency (Total-to-Static)	0.759	0.753	0.734	0.624
ET1 - Compressor Turbine Efficiency (Total-to-Total)	0.798	0.790	0.788	0.813
ET2 - Power Turbine Efficiency (Total-to-Total)	0.846	0.845	0.832	-0-
EB - Burner Efficiency	0.999	0.998	0.999	0.999
ER - Regenerator Effectiveness	0.900	0.930	0.940	0.940
WL1/W1 - Labyrinth Seal Leakage	0.010	0.010	0.010	0.010
HP1ext - G.G. Shaft Bearing Friction Loss, hp	1.067	0.729	0.392	0.356
HP2ext - Accessory Load Requirement (from G.G. Shaft), hp	1.665	1.274	0.849	0.795
HP3ext - Gearbox Frictional (Bearing) Loss, hp	1.602	0.992	0.429	-0-
HP4ext - Gearbox Gear Loss, hp				

**Bypass Valve Open at Idle

TABLE XXIV. ENGINE 3 PERFORMANCE SUMMARY (SI UNITS)

Engine	3			
Compressor Configuration	R - R			
TIT @ 100 Percent Power, ^{o}K	1505			
TIT Control	VPT			
Nominal Compressor Pressure Ratio @ 100 Percent Power	5.0			
Ta, ^{o}K	303	303	303	303
Pa, kPa	99.519	99.519	99.519	99.519
Power, kW	74.6	37.3	7.5	-0-
SFC, kg/kW-h	0.234	0.353	0.293	1.285
T4 (TIT), ^{o}K	2710	2710	2505	1580
G.G. Shaft Speed, rpm	73124	56410	36562	36562
P.T. Shaft Speed (Optimum), rpm	74786	68046	43786	-0-
Inlet Airflow, kg/s	0.397	0.243	0.123	0.155
P1/PA - Inlet Filter Pressure Ratio	0.990	0.996	0.999	0.999
P2/P1 - First Compressor Pressure Ratio	2.513	1.980	1.383	1.367
P3/P2 - Second Compressor Pressure Ratio	1.989	1.541	1.232	1.147
P3A/P2 - Regenerator Cold Side Pressure Ratio	0.970	0.970	0.976	0.968
P4/P3A - Burner Pressure Ratio	0.970	0.968	0.973	0.967
P4/P5 - Compressor Turbine Pressure Ratio	2.107	1.572	1.259	1.384
P5/P6 - Power Turbine Pressure Ratio	1.944	1.685	1.243	1.033
P7/P6 - Exhaust Duct Pressure Ratio	0.965	0.984	0.996	0.996
P8/P7 - Regenerator Hot Side Pressure Ratio	0.921	0.947	0.972	0.980
P9/P8 - Tailpipe Pressure Ratio	0.990	0.997	0.999	0.999
T2, ^{o}K	415	380	338	336
T3, ^{o}K	531	446	367	360
T3A, ^{o}K	1092	1197	1223	788
T5, ^{o}K	1312	1383	1332	821
T6, ^{o}K	1154	1252	1278	821
T8, ^{o}K	619	528	443	398
Q1 - (kg/s)($\sqrt{^{o}K}$/kPa)	0.0702	0.0426	0.0216	0.0271
Q2 - (kg/s)($\sqrt{^{o}K}$/kPa)	0.0327	0.0241	0.0165	0.0208
Q4 - (kg/s)($\sqrt{^{o}K}$/kPa)	0.0334	0.0332	0.0284	0.0312
Q5 - (kg/s)($\sqrt{^{o}K}$/kPa)	0.0667	0.0500	0.0351	0.0418
EC1 - First Compressor Efficiency (Total-to-Total)	0.808	0.843	0.825	0.858
EC2 - Second Compressor Efficiency (Total-to-Static)	0.760	0.749	0.726	0.551
ET1 - Compressor Turbine Efficiency (Total-to-Total)	0.802	0.813	0.801	0.808
ET2 - Power Turbine Efficiency (Total-to-Total)	0.822	0.811	0.801	-0-
EB - Burner Efficiency	0.999	0.998	0.999	0.999
ER - Regenerator Effectiveness	0.900	0.932	0.940	0.940
WL1/W1 - Labyrinth Seal Leakage	0.010	0.010	0.010	0.010
HP1ext - G.G. Shaft Bearing Friction Loss, kW	0.796	0.520	0.265	0.265
HP2ext - Accessory Load Requirement (from G.G. Shaft), kW	1.242	0.922	0.593	0.593
HP3ext - Gearbox Frictional (Bearing) Loss, kW	1.193	1.022	0.506	-0-
HP4ext - Gearbox Gear Loss, kW				

TABLE XXV. ENGINE 3 PERFORMANCE SUMMARY (ENGLISH UNITS)

Engine	3
Compressor Configuration	R - R
TIT @ 100 Percent Power, ^{o}F	2250
TIT Control	VPT
Nominal Compressor Pressure Ratio @ 100 Percent Power	5.0

Ta, ^{o}R	545	545	545	545
Pa, psia	14.434	14.434	14.434	14.434
Power, hp	100.0	50.0	10.0	-0-
SFC, lb/hp$_{o}$hr (W_f, lb/hr)	0.384	0.353	0.481	2.832
T4 (TIT), ^{o}R	2710	2710	2505	1580
G.G. Shaft Speed, rpm	73124	56410	36562	36562
P.T. Shaft Speed (Optimum), rpm	74786	68046	43786	-0-
Inlet Airflow, lb/sec	0.876	0.535	0.272	0.342
P1/PA - Inlet Filter Pressure Ratio	0.990	0.996	0.999	0.999
P2/P1 - First Compressor Pressure Ratio	2.513	1.980	1.383	1.367
P3/P2 - Second Compressor Pressure Ratio	1.989	1.541	1.232	1.147
P3A/P2 - Regenerator Cold Side Pressure Ratio	0.970	0.970	0.976	0.968
P4/P3A - Burner Pressure Ratio	0.970	0.968	0.973	0.967
P4/P5 - Compressor Turbine Pressure Ratio	2.107	1.572	1.259	1.384
P5/P6 - Power Turbine Pressure Ratio	1.944	1.685	1.243	1.033
P7/P6 - Exhaust Duct Pressure Ratio	0.965	0.984	0.996	0.996
P8/P7 - Regenerator Hot Side Pressure Ratio	0.921	0.947	0.972	0 980
P9/P8 - Tailpipe Pressure Ratio	0.990	0.997	0.999	0.999
T2, ^{o}R	747.0	684	609	604.0
T3, ^{o}R	956.0	803	660	648.0
T3A, ^{o}R	1966.0	2155	2202	1418.0
T5, ^{o}R	2362.0	2489	2398	1477.0
T6, ^{o}R	2078.0	2254	2300	1477.0
T8, ^{o}R	1114.0	951	798.0	717.0
Q1 - lb/sec$\sqrt{^{o}R}$/psia	1.432	0.8686	0.440	0.553
Q2 - lb/sec$\sqrt{^{o}R}$/psia	0.667	0.4915	0.337	0.425
Q4 - lb/sec$\sqrt{^{o}R}$/psia	0.681	0.6763	0.580	0.636
Q5 - lb/sec$\sqrt{^{o}R}$/psia	1.339	1.0187	0.715	0.851
EC1 - First Compressor Efficiency (Total-to-Total)	0.808	0.843	0.825	0.858
EC2 - Second Compressor Efficiency (Total-to-Static)	0.760	0.749	0.726	0.551
ET1 - Compressor Turbine Efficiency (Total-to-Total)	0.802	0.813	0.801	0.808
ET2 - Power Turbine Efficiency (Total-to-Total)	0.822	0.811	0.801	-0-
EB - Burner Efficiency	0.999	0.998	0.999	0.999
ER - Regenerator Effectiveness	0.900	0.932	0.940	0.940
WL1/W1 - Labyrinth Seal Leakage	0.010	0.010	0.010	0.010
HP1ext - G.G. Shaft Bearing Friction Loss, hp	1.068	0.698	0.356	0.356
HP2ext - Accessory Load Requirement (from G.G. Shaft), hp	1.665	1.237	0.795	0.795
HP3ext - Gearbox Frictional (Bearing) Loss, hp	1.601	1.370	0.679	-0-
HP4ext - Gearbox Gear Loss, hp				

TABLE XXVI. ENGINE 4 PERFORMANCE SUMMARY (SI UNITS)

Engine	4
Compressor Configuration	R - R
TIT @ 100 Percent Power, °K	1505
TIT Control	VPT
Nominal Compressor Pressure Ratio @ 100 Percent Power	5.58

Ta, °K	303	303	303	303
Pa, kPa	99.519	99.519	99.519	99.519
Power, kW	74.6	37.3	7.5	-0-
SFC, kg/kW-h	0.256	0.356	0.293	1.242
T4 (TIT), °K	2710	2710	2571	1560
G.G. Shaft Speed, rpm	77935	59518	38967	38970
P.T. Shaft Speed (Optimum), rpm	70728	66543	43880	-0-
Inlet Airflow, kg/s	0.424	0.241	0.117	0.151
P1/PA - Inlet Filter Pressure Ratio	0.991	0.997	0.999	0.998
P2/P1 - First Compressor Pressure Ratio	2.754	1.987	1.347	1.341
P3/P2 - Second Compressor Pressure Ratio	2.027	1.594	1.274	1.178
P3A/P2 - Regenerator Cold Side Pressure Ratio	0.97	0.970	0.977	0.968
P4/P3A - Burner Pressure Ratio	0.97	0.967	0.972	0.968
P4/P5 - Compressor Turbine Pressure Ratio	2.437	1.623	1.262	1.408
P5/P6 - Power Turbine Pressure Ratio	1.899	1.715	1.256	1.025
P7/P6 - Exhaust Duct Pressure Ratio	0.969	0.988	0.997	0.996
P8/P7 - Regenerator Hot Side Pressure Ratio	0.926	0.953	0.976	0.983
P9/P8 - Tailpipe Pressure Ratio	0.991	0.998	0.999	0.999
T2, °K	442	384	337	336
T3, °K	568	456	370	363
T3A, °K	1079	1193	1253	778
T5, °K	1281	1374	1367	807
T6, °K	1133	1242	1311	807
T8, °K	644	531	450	397
Q1 - (kg/s)($\sqrt{°K}$/kPa)	0.0747	0.0423	0.0205	0.0264
Q2 - (kg/s)($\sqrt{°K}$/kPa)	0.0388	0.0240	0.0161	0.0207
Q4 - (kg/s)($\sqrt{°K}$/kPa)	0.03180	0.0317	0.0272	0.0301
Q5 - (kg/s)($\sqrt{°K}$/kPa)	0.0715	0.0492	0.0336	0.0408
EC1 - First Compressor Efficiency (Total-to-Total)	0.729	0.807	0.780	0.803
EC2 - Second Compressor Efficiency (Total-to-Static)	0.758	0.749	0.729	0.589
ET1 - Compressor Turbine Efficiency (Total-to-Total)	0.790	0.813	0.807	0.813
ET2 - Power Turbine Efficiency (Total-to-Total)	0.817	0.796	0.793	-0-
EB - Burner Efficiency	0.999	0.998	0.999	0.999
ER - Regenerator Effectiveness	0.905	0.938	0.940	0.940
WL1/W1 - Labyrinth Seal Leakage	0.010	0.010	0.010	0.010
HP1ext - G.G. Shaft Bearing Friction Loss, kW	0.736	0.475	0.248	0.248
HP2ext - Accessory Load Requirement (from G.G. Shaft), kW	1.181	0.868	0.569	0.569
HP3ext - Gearbox Frictional (Bearing) Loss, kW	1.268	1.145	0.585	-0-
HP4ext - Gearbox Gear Loss, kW				

TABLE XXVII. ENGINE 4 PERFORMANCE SUMMARY (ENGLISH UNITS)

Engine	4
Compressor Configuration	R - R
TIT @ 100 Percent Power, °F	2250
TIT Control	VPT
Nominal Compressor Pressure Ratio @ 100 Percent Power	5.58

Ta, °R	545	545	545	545
Pa, psia	14.434	14.434	14.434	14.434
Power, h	100.0	50.0	10.0	-0-
SFC, lb/hp hr (W_f, lb/hr)	0.421	0.356	0.481	2.739
T4 (TIT), °R	2710	2710	2571	1560
G.G. Shaft Speed, rpm	77935	59518	38967	38970
P.T. Shaft Speed (Optimum), rpm	70728	66543	43880	-0-
Inlet Airflow, lb/sec	0.934	0.532	0.258	0.333
P1/PA - Inlet Filter Pressure Ratio	0.991	0.997	0.999	0.998
P2/P1 - First Compressor Pressure Ratio	2.754	1.987	1.347	1.341
P3/P2 - Second Compressor Pressure Ratio	2.027	1.594	1.274	1.178
P3A/P2 - Regenerator Cold Side Pressure Ratio	0.97	0.970	0.977	0.968
P4/P3A - Burner Pressure Ratio	0.97	0.967	0.972	0.968
P4/P5 - Compressor Turbine Pressure Ratio	2.437	1.623	1.262	1.408
P5/P6 - Power Turbine Pressure Ratio	1.899	1.715	1.256	1.025
P7/P6 - Exhaust Duct Pressure Ratio	0.969	0.988	0.997	0.996
P8/P7 - Regenerator Hot Side Pressure Ratio	0.926	0.953	0.976	0.983
P9/P8 - Tailpipe Pressure Ratio	0.991	0.998	0.999	0.999
T2, °R	795.0	691	607.0	604.0
T3, °R	1023.0	821	666.0	653.0
T3A, °R	1943.0	2148	2255.0	1400.0
T5, °R	2306.0	2473	2460.0	1453.0
T6, °R	2039.0	2236	2360.0	1453.0
T8, °R	1159.0	956	810.0	715.0
Q1 - lb/sec$\sqrt{°R}$/psia	1.524	0.8630	0.418	0.539
Q2 - lb/sec$\sqrt{°R}$/psia	0.6679	0.4891	0.328	0.423
Q4 - lb/sec$\sqrt{°R}$/psia	0.6486	0.6472	0.555	0.613
Q5 - lb/sec$\sqrt{°R}$/psia	1.458	1 0036	0.685	0.833
EC1 - First Compressor Efficiency (Total-to-Total)	0.729	0.807	0.780	0 803
EC2 - Second Compressor Efficiency (Total-to-Static)	0.758	0.749	0.729	0.589
ET1 - Compressor Turbine Efficiency (Total-to-Total)	0.790	0.813	0.807	0.813
ET2 - Power Turbine Efficiency (Total-to-Total)	0.817	0.796	0.793	-0-
EB - Burner Efficiency	0.999	0.998	0.999	0.999
ER - Regenerator Effectiveness	0.905	0.938	0.940	0.940
WL1/W1 - Labyrinth Seal Leakage	0.010	0.010	0.010	0.010
HP1ext - G.G. Shaft Bearing Friction Loss, hp	0.987	0.637	0.332	0.332
HP2ext - Accessory Load Requirement (from G.G. Shaft), hp	1.584	1.164	0.763	0.763
HP3ext - Gearbox Frictional (Bearing) Loss, hp	1.701	1.535	0.784	-0-
HP4ext - Gearbox Gear Loss, hp				

TABLE XXVIII. ENGINE 4A PERFORMANCE SUMMARY (SI UNITS)

Engine	**4A**			
Compressor Configuration	**R - R**			
TIT @ 100 Percent Power, ^{o}K	**1505**			
TIT Control	**VPT**			
Nominal Compressor Pressure Ratio @ 100 Percent Power	**5.5**			
Ta, ^{o}K	303	303	303	303
Pa, kPa	99.519	99.519	99.519	99.519
Power, kW	74.6	37.3	7.5	-0-
SFC, kg/kW-h (W_f, kg/h)	0.272	0.230	0.332	(1.44)
T4 (TIT), ^{o}K	1505	1505	1401	897
G.G. Shaft Speed, rpm	75180	56782	37590	37590
P.T. Shaft Speed (Optimum), rpm	65685	62319	40439	-0-
Inlet Airflow, kg/s	0.458	0.258	0.130	0.162
P1/PA - Inlet Filter Pressure Ratio	0.991	0.997	0.999	0.999
P2/P1 - First Compressor Pressure Ratio	2.727	1.953	1.346	1.341
P3/P2 - Second Compressor Pressure Ratio	2.019	1.577	1.269	1.177
P3A/P2 - Regenerator Cold Side Pressure Ratio	0.970	0.971	0.976	0.968
P4/P3A - Burner Pressure Ratio	0.970	0.967	0.972	0.966
P4/P5 - Compressor Turbine Pressure Ratio	2.510	1.625	1.272	1.405
P5/P6 - Power Turbine Pressure Ratio	1.815	1.666	1.239	1.025
P7/P6 - Exhaust Duct Pressure Ratio	0.969	0.988	0.997	0.996
P8/P7 - Regenerator Hot Side Pressure Ratio	0.924	0.953	0.976	0.982
P9/P8 - Tailpipe Pressure Ratio	0.991	0.998	0.999	0.999
T2, ^{o}K	794	687	607	604
T3, ^{o}K	1021	813	665	653
T3A, ^{o}K	1941	2137	2186	1440
T5, ^{o}K	2276	2445	2378	1490
T6, ^{o}K	2028	2222	2284	1490
T8, ^{o}K	1166	972	835	729
Q1 - (kg/s)($\sqrt{^{o}K}$/kPa)	1.648	0.920	0.464	0.580
Q2 - (kg/s)($\sqrt{^{o}K}$/kPa)	0.730	0.529	0.364	0.456
Q4 - (kg/s)($\sqrt{^{o}K}$/kPa)	0.697	0.696	0.601	0.658
Q5 - (kg/s)($\sqrt{^{o}K}$/kPa)	1.636	1.095	0.757	0.907
EC1 - First Compressor Efficiency (Total-to-Total)	0.722	0.807	0.783	0.803
EC2 - Second Compressor Efficiency (Total-to-Static)	0.758	0.748	0.731	0.586
ET1 - Compressor Turbine Efficiency (Total-to-Total)	0.780	0.805	0.799	0.804
ET2 - Power Turbine Efficiency (Total-to-Total)	0.820	0.799	0.792	-0-
EB - Burner Efficiency	0.998	0.998	0.998	0.998
ER - Regenerator Effectiveness	0.913	0.940	0.940	0.940
WL1/W1 - Labyrinth Seal Leakage	0.010	0.010	0.010	0.010
HP1ext - G.G. Shaft Bearing Friction Loss, kW	0.790	0.500	0.268	0.268
HP2ext - Accessory Load Requirement (from G.G. Shaft), kW	1.268	0.925	0.611	0.611
HP3ext - Gearbox Frictional (Bearing) Loss, kW	1.283	1.171	0.589	-0-
HP4ext - Gearbox Gear Loss, kW				

TABLE XXIX. ENGINE 4A PERFORMANCE SUMMARY (ENGLISH UNITS)

Engine	4A
Compressor Configuration	R - R
TIT @ 100 Percent Power, ^{o}F	2250
TIT Control	VPT
Nominal Compressor Pressure Ratio @ 100 Percent Power	5.5

Ta, ^{o}R	545	545	545	545
Pa, psia	14.434	14.434	14.434	14.434
Power, hp	100	50	10	-0-
SFC, lb/hp hr (W_f, lb/hr)	0.447	0.378	0.546	(3.18)
T4 (TIT), ^{o}R	2710	2710	2522	1615
G.G. Shaft Speed, rpm	75180	56782	37590	37590
P.T. Shaft Speed (Optimum), rpm	65685	62319	40439	-0-
Inlet Airflow, lb/sec	1.010	0.568	0.287	0.358
P1/PA - Inlet Filter Pressure Ratio	0.991	0.997	0.999	0.999
P2/P1 - First Compressor Pressure Ratio	2.727	1.953	1.346	1.341
P3/P2 - Second Compressor Pressure Ratio	2.019	1.577	1.269	1.177
P3A/P2 - Regenerator Cold Side Pressure Ratio	0.970	0.971	0.976	0.968
P4/P3A - Burner Pressure Ratio	0.970	0.967	0.972	0.966
P4/P5 - Compressor Turbine Pressure Ratio	2.510	1.625	1.272	1.405
P5/P6 - Power Turbine Pressure Ratio	1.815	1.666	1.239	1.025
P7/P6 - Exhaust Duct Pressure Ratio	0.969	0.988	0.997	0.996
P8/P7 - Regenerator Hot Side Pressure Ratio	0.924	0.953	0.976	0.982
P9/P8 - Tailpipe Pressure Ratio	0.991	0.998	0.999	0.999
T2, ^{o}R	794	687	607	604
T3, ^{o}R	1021	813	665	653
T3A, ^{o}R	1941	2137	2186	1440
T5, ^{o}R	2276	2445	2378	1490
T6, ^{o}R	2028	2222	2284	1490
T8, ^{o}R	1166	972	835	729
Q1 - lb/sec$\sqrt{^{o}R}$/psia	1.648	0.920	0.464	0.580
Q2 - lb/sec$\sqrt{^{o}R}$/psia	0.730	0.529	0.364	0.456
Q4 - lb/sec$\sqrt{^{o}R}$/psia	0.697	0.696	0.601	0.658
Q5 - lb/sec$\sqrt{^{o}R}$/psia	1.636	1.095	0.757	0.907
EC1 - First Compressor Efficiency (Total-to-Total)	0.722	0.807	0.783	0.803
EC2 - Second Compressor Efficiency (Total-to-Static)	0.758	0.748	0.731	0.586
ET1 - Compressor Turbine Efficiency (Total-to-Total)	0.780	0.805	0.799	0.804
ET2 - Power Turbine Efficiency (Total-to-Total)	0.820	0.799	0.792	-0-
EB - Burner Efficiency	0.998	0.998	0.998	0.998
ER - Regenerator Effectiveness	0.913	0.940	0.940	0.940
WL1/W1 - Labyrinth Seal Leakage	0.01	0.01	0.01	0.01
HP1ext - G.G. Shaft Bearing Friction Loss, hp	1.06	0.67	0.36	0.36
HP2ext - Accessory Load Requirement (from G.G. Shaft), hp	1.70	1.24	0.82	0.82
HP3ext - Gearbox Frictional (Bearing) Loss, hp	1.72	1.57	0.79	-0-
HP4ext - Gearbox Gear Loss, hp				

TABLE XXX. ENGINE 5 PERFORMANCE SUMMARY (SI UNITS)

Engine	5
Compressor Configuration	R - R
TIT @ 100 Percent Power, °K	1505
TIT Control	VPT
Nominal Compressor Pressure Ratio @ 100 Percent Power	6.21

Ta, °K	303	303	303	303
Pa, kPa	99.519	99.519	99.519	99.519
Power, kW	74.6	37.3	7.5	-0-
SFC, kg/kW-h	0.266	0.361	0.304	1.238
T4 (TIT), °K	2710	2710	2298	1432
G.G. Shaft Speed, rpm	74972	57562	39827	37486
P.T. Shaft Speed (Optimum), rpm	72329	69200	42930	-0-
Inlet Airflow, kg/s	0.424	0.235	0.130	0.143
P1/PA - Inlet Filter Pressure Ratio	0.99	0.997	0.999	0.998
P2/P1 - First Compressor Pressure Ratio	3.036	2.100	1.434	1.371
P3/P2 - Second Compressor Pressure Ratio	2.047	1.624	1.303	1.195
P3A/P2 - Regenerator Cold Side Pressure Ratio	0.970	0.970	0.973	0.966
P4/P3A - Burner Pressure Ratio	0.970	0.967	0.969	0.965
P4/P5 - Compressor Turbine Pressure Ratio	2.672	1.707	1.356	1.455
P5/P6 - Power Turbine Pressure Ratio	1.905	1.749	1.259	1.027
P7/P6 - Exhaust Duct Pressure Ratio	0.965	0.987	0.996	0.996
P8/P7 - Regenerator Hot Side Pressure Ratio	0.921	0.951	0.976	0.983
P9/P8 - Tailpipe Pressure Ratio	0.990	0.998	0.999	0.999
T2, °K	453	392	345	339
T3, °K	589	471	382	368
T3A, °K	1063	1178	1105	767
T5, °K	1264	1362	1203	796
T6, °K	1116	1226	1151	796
T8, °K	663	544	447	402
Q1 - (kg/s)($\sqrt{°K}$/kPa)	0.0748	0.0411	0.0227	0.0252
Q2 - (kg/s)($\sqrt{°K}$/kPa)	0.0302	0.0223	0.0169	0.0194
Q4 - (kg/s)($\sqrt{°K}$/kPa)	0.0286	0.0286	0.0260	0.0275
Q5 - (kg/s)($\sqrt{°K}$/kPa)	0.0701	0.0465	0.0347	0.0385
EC1 - First Compressor Efficiency (Total-to-Total)	0.745	0.800	0.781	0.795
EC2 - Second Compressor Efficiency (Total-to-Static)	0.735	0.726	0.712	0.594
ET1 - Compressor Turbine Efficiency (Total-to-Total)	0.781	0.812	0.812	0.813
ET2 - Power Turbine Efficiency (Total-to-Total)	0.822	0.800	0.796	-0-
EB - Burner Efficiency	0.999	0.998	0.999	0.999
ER - Regenerator Effectiveness	0.900	0.936	0.940	0.940
WL1/W1 - Labyrinth Seal Leakage	0.010	0.010	0.010	0.010
HP1ext - G.G. Shaft Bearing Friction Loss, kW	0.730	0.474	0.266	0.243
HP2ext - Accessory Load Requirement (from G.G. Shaft), kW	1.138	0.841	0.578	0.544
HP3ext - Gearbox Frictional (Bearing) Loss, kW	1.095	1.017	0.474	-0-
HP4ext - Gearbox Gear Loss, kW				

TABLE XXXI. ENGINE 5 PERFORMANCE SUMMARY (ENGLISH UNITS)

Engine	5			
Compressor Configuration	R - R			
TIT @ 100 Percent Power, °F	2250			
TIT Control	VPT			
Nominal Compressor Pressure Ratio @ 100 Percent Power	6.21			
Ta, °R	545	545	545	545
Pa, psia	14.434	14.434	14.434	14.434
Power, hp	100.0	50.0	10.0	-0-
SFC, lb/hp hr (W_f, lb/hr)	0.437	0.361	0.500	2.73
T4 (TIT), °R	2710	2710	2298.0	1432.0
G.G. Shaft Speed, rpm	74972	57562	39827	37486
P.T. Shaft Speed (Optimum), rpm	72329	69200	42930	-0-
Inlet Airflow, lb/sec	0.935	0.517	0.286	0.316
P1/PA - Inlet Filter Pressure Ratio	0.99	0.997	0.999	0.998
P2/P1 - First Compressor Pressure Ratio	3.036	2.100	1.434	1.371
P3/P2 - Second Compressor Pressure Ratio	2.047	1.624	1.303	1.195
P3A/P2 - Regenerator Cold Side Pressure Ratio	0.970	0.970	0.973	0.966
P4/P3A - Burner Pressure Ratio	0.970	0.967	0.969	0.965
P4/P5 - Compressor Turbine Pressure Ratio	2.672	1.707	1.356	1.455
P5/P6 - Power Turbine Pressure Ratio	1.905	1.749	1.259	1.027
P7/P6 - Exhaust Duct Pressure Ratio	0 965	0.987	0.996	0.996
P8/P7 - Regenerator Hot Side Pressure Ratio	0.921	0.951	0.976	0.983
P9/P8 - Tailpipe Pressure Ratio	0.990	0.998	0.999	0.999
T2, °R	816.0	705	621.0	610.0
T3, °R	1061.0	848	688.0	663.0
T3A, °R	1913.0	2121	1989.0	1380.0
T5, °R	2275.0	2451	2166.0	1432.0
T6, °R	2008.0	2207	2072.0	1432.0
T8, °R	1194.0	980	804.0	723.0
Q1 - lb/sec$\sqrt{°R}$/psia	1.526	0.8376	0.463	0.513
Q2 - lb/sec$\sqrt{°R}$/psia	0.6154	0.4538	0.344	0.395
Q4 - lb/sec$\sqrt{°R}$/psia	0.5839	0.5840	0.530	0.561
Q5 - lb/sec$\sqrt{°R}$/psia	1.430	0.9477	0.707	0.785
EC1 - First Compressor Efficiency (Total-to-Total)	0.745	0.800	0.781	0.795
EC2 - Second Compressor Efficiency (Total-to-Static)	0.735	0.726	0.712	0.594
ET1 - Compressor Turbine Efficiency (Total-to-Total)	0.781	0.812	0.812	0.813
ET2 - Power Turbine Efficiency (Total-to-Total)	0.822	0.800	0.796	-0-
EB - Burner Efficiency	0.999	0.998	0.999	0.999
ER - Regenerator Effectiveness	0.900	0.936	0.940	0.940
WL1/W1 - Labyrinth Seal Leakage	0.010	0.010	0.010	0.010
HP1ext - G.G. Shaft Bearing Friction Loss, hp	0.979	0.635	0.357	0.326
HP2ext - Accessory Load Requirement (from G.G. Shaft), hp	1.527	1.128	0.775	0.729
HP3ext - Gearbox Frictional (Bearing) Loss, hp	1.468	1.364	0.635	-0-
HP4ext - Gearbox Gear Loss, hp				

TABLE XXXII. ENGINE 6 PERFORMANCE SUMMARY (SI UNITS)

Engine	**6**
Compressor Configuration	**R - R**
TIT @ 100 Percent Power, °K	**1311**
TIT Control	**VPT**
Nominal Compressor Pressure Ratio @ 100 Percent Power	**4.74**

Ta, °K	303	303	303	303
Pa, kPa	99.519	99.519	99.519	99.519
Power, kW	74.6	37.3	7.5	-0-
SFC, kg/kW-h	0.4461	0.389	0.327	1.478
T4 (TIT), °K	2360	2360	2304	1499
G.G. Shaft Speed, rpm	56640	44140	28320	28320
P.T. Shaft Speed (Optimum), rpm	57850	53353	34921	-0-
Inlet Airflow, kg/s	0.577	0.342	0.167	0.212
P1/PA - Inlet Filter Pressure Ratio	0.994	0.998	0.999	0.999
P2/P1 - First Compressor Pressure Ratio	2.539	1.834	1.279	1.275
P3/P2 - Second Compressor Pressure Ratio	1.865	1.525	1.240	1.170
P3A/P2 - Regenerator Cold Side Pressure Ratio	0.970	0.971	0.978	0.971
P4/P3A - Burner Pressure Ratio	0.969	0.967	0.974	0.968
P4/P5 - Compressor Turbine Pressure Ratio	2.359	1.625	1.239	1.350
P5/P6 - Power Turbine Pressure Ratio	1.704	1.527	1.189	1.017
P7/P6 - Exhaust Duct Pressure Ratio	0.976	0.990	0.997	0.998
P8/P7 - Regenerator Hot Side Pressure Ratio	0.936	0.959	0.978	0.983
P9/P8 - Tailpipe Pressure Ratio	0.994	0.998	0.999	0.999
T2, °K	421	374	331	330
T3, °K	528	437	360	354
T3A, °K	965	1058	1138	755
T5, °K	1118	1194	1228	781
T6, °K	1006	1098	1187	781
T8, °K	583	495	427	383
Q1 - (kg/s)($\sqrt{°K}$/kPa)	0.1016	0.0598	0.0292	0.0371
Q2 - (kg/s)($\sqrt{°K}$/kPa)	0.0471	0.0363	0.0239	0.0304
Q4 - (kg/s)($\sqrt{°K}$/kPa)	0.0474	0.0473	0.0395	0.0435
Q5 - (kg/s)($\sqrt{°K}$/kPa)	0.1033	0.0734	0.0479	0.0568
EC1 - First Compressor Efficiency (Total-to-Total)	0.775	0.804	0.773	0.799
EC2 - Second Compressor Efficiency (Total-to-Static)	0.757	0.746	0.725	0.619
ET1 - Compressor Turbine Efficiency (Total-to-Total)	0.793	0.813	0.807	0.813
ET2 - Power Turbine Efficiency (Total-to-Total)	0.822	0.820	0.811	-0-
EB - Burner Efficiency	0.999	0.998	0.999	0.999
ER - Regenerator Effectiveness	0.916	0.940	0.940	0.940
WL1/W1 - Labyrinth Seal Leakage	0.010	0.010	0.010	0.010
HP1ext - G.G. Shaft Bearing Friction Loss, kW	0.641	0.430	0.218	0.218
HP2ext - Accessory Load Requirement (from G.G. Shaft), kW	1.075	0.812	0.529	0.530
HP3ext - Gearbox Frictional (Bearing) Loss, kW	1.367	1.193	0.601	-0-
HP4ext - Gearbox Gear Loss, kW				

TABLE XXXIII. ENGINE 6 PERFORMANCE SUMMARY (ENGLISH UNITS)

Engine	**6**			
Compressor Configuration	**R - R**			
TIT @ 100 Percent Power, ^{o}F	**1900**			
TIT Control	**VPT**			
Nominal Compressor Pressure Ratio @ 100 Percent Power	**4.74**			
Ta, ^{o}R	545	545	545	545
Pa, psia	14.434	14.434	14.434	14.434
Power, hp	100.0	50.0	10.0	-0-
SFC, lb/hp hr (W_f, lb/hr)	0.4461	0.389	0.538	3.259
T4 (TIT), ^{o}R	2360	2360	2304	1499
G.G. Shaft Speed, rpm	56640	44140	28320	28320
P.T. Shaft Speed (Optimum), rpm	57850	53353	34921	-0-
Inlet Airflow, lb/sec	1.273	0.753	0.3681	0.467
P1/PA - Inlet Filter Pressure Ratio	0.994	0.998	0.999	0.999
P2/P1 - First Compressor Pressure Ratio	2.539	1.834	1.279	1.275
P3/P2 - Second Compressor Pressure Ratio	1.865	1.525	1.240	1.170
P3A/P2 - Regenerator Cold Side Pressure Ratio	0.970	0.971	0.978	0.971
P4/P3A - Burner Pressure Ratio	0.969	0.967	0.974	0.968
P4/P5 - Compressor Turbine Pressure Ratio	2.359	1.625	1.239	1.350
P5/P6 - Power Turbine Pressure Ratio	1.704	1.527	1.189	1.017
P7/P6 - Exhaust Duct Pressure Ratio	0.976	0.990	0.997	0.998
P8/P7 - Regenerator Hot Side Pressure Ratio	0.936	0.959	0.978	0.983
P9/P8 - Tailpipe Pressure Ratio	0.994	0.998	0.999	0.999
T2, ^{o}R	758.0	673	596	594
T3, ^{o}R	950.0	787	648	638
T3A, ^{o}R	1737.0	1905	2048	1359
T5, ^{o}R	2012.0	2149	2211	1405
T6, ^{o}R	1810.0	1977	2137	1405
T8, ^{o}R	1049.0	891	768	690
Q1 - lb/sec$\sqrt{^{o}R}$/psia	2.071	1.2205	0.595	0.756
Q2 - lb/sec$\sqrt{^{o}R}$/psia	0.962	0.7396	0.487	0.619
Q4 - lb/sec$\sqrt{^{o}R}$/psia	0.967	0.9654	0.805	0.887
Q5 - lb/sec$\sqrt{^{o}R}$/psia	2.107	1.4970	0.976	1.159
EC1 - First Compressor Efficiency (Total-to-Total)	0.775	0.804	0.773	0.799
EC2 - Second Compressor Efficiency (Total-to-Static)	0.757	0.746	0.725	0.619
ET1 - Compressor Turbine Efficiency (Total-to-Total)	0.793	0.813	0.807	0.813
ET2 - Power Turbine Efficiency (Total-to-Total)	0.822	0.820	0.811	-0-
EB - Burner Efficiency	0.999	0.998	0.999	0.999
ER - Regenerator Effectiveness	0.916	0.940	0.940	0.940
WL1/W1 - Labyrinth Seal Leakage	0.010	0.010	0.010	0.010
HP1ext - G.G. Shaft Bearing Friction Loss, hp	0.860	0.576	0.292	0.292
HP2ext - Accessory Load Requirement (from G.G. Shaft), hp	1.442	1.089	0.710	0.711
HP3ext - Gearbox Frictional (Bearing) Loss, hp	1.833	1.600	0.806	-0-
HP4ext - Gearbox Gear Loss, hp				

TABLE XXXIV. ENGINE 7 PERFORMANCE SUMMARY (SI UNITS)

Engine	7
Compressor Configuration	R - R
TIT @ 100 Percent Power, ^{o}K	1644
TIT Control	VPT
Nominal Compressor Pressure Ratio @ 100 Percent Power	6.0

Ta, ^{o}K	303	303	303	303
Pa, kPa	99.519	99.519	99.519	99.519
Power, kW	74.6	37.3	7.5	-0-
SFC, kg/kW-h	0.246	0.338		1.151
T4 (TIT), ^{o}K	2960	2960		1609
G.G. Shaft Speed, rpm	92982	69528		46491
P.T. Shaft Speed (Optimum), rpm	79857	75935		-0-
Inlet Airflow, kg/s	0.351	0.197		0.126
P1/PA - Inlet Filter Pressure Ratio	0.99	0.997		0.999
P2/P1 - First Compressor Pressure Ratio	2.824	2.059		1.380
P3/P2 - Second Compressor Pressure Ratio	2.125	1.627		1.180
P3A/P2 - Regenerator Cold Side Pressure Ratio	0.97	0.970		0.966
P4/P3A - Burner Pressure Ratio	0.97	0.967		0.965
P4/P5 - Compressor Turbine Pressure Ratio	2.428	1.600		1.441
P5/P6 - Power Turbine Pressure Ratio	2.025	1.833		1.029
P7/P6 - Exhaust Duct Pressure Ratio	0.965	0.986		0.996
P8/P7 - Regenerator Hot Side Pressure Ratio	0.921	0.951		0.983
P9/P8 - Tailpipe Pressure Ratio	0.990	0.997		0.999
T2, ^{o}K	453	388		339
T3, ^{o}K	591	464		368
T3A, ^{o}K	1164	1291		795
T5, ^{o}K	1404	1507		829
T6, ^{o}K	1228	1348		829
T8, ^{o}K	683	556		407
Q1 - (kg/s)($\sqrt{^{o}K}$/kPa)	0.0619	0.0345		0.0220
Q2 - (kg/s)($\sqrt{^{o}K}$/kPa)	0.0268	0.0190		0.0169
Q4 - (kg/s)($\sqrt{^{o}K}$/kPa)	0.0257	0.0256		0.0247
Q5 - (kg/s)($\sqrt{^{o}K}$/kPa)	0.0577	0.0392		0.0343
EC1 - First Compressor Efficiency (Total-to-Total)	0.693	0.808		0.806
EC2 - Second Compressor Efficiency (Total-to-Static)	0.760	0.750		0.568
ET1 - Compressor Turbine Efficiency (Total-to-Total)	0.791	0.813		0.813
ET2 - Power Turbine Efficiency (Total-to-Total)	0.821	0.799		-0-
EB - Burner Efficiency	0.999	0.998		0.999
ER - Regenerator Effectiveness	0.900	0.935		0.940
WL1/W1 - Labyrinth Seal Leakage	0.010	0.010		0.010
HP1ext - G.G. Shaft Bearing Friction Loss, kW	0.796	0.495		0.265
HP2ext - Accessory Load Requirement (from G.G. Shaft), kW	1.242	0.893		0.594
HP3ext - Gearbox Frictional (Bearing) Loss, kW	1.195	1.099		-0-
HP4ext - Gearbox Gear Loss, kW				

TABLE XXXV. ENGINE 7 PERFORMANCE SUMMARY (ENGLISH UNITS)

Engine		**7**		
Compressor Configuration		**R - R**		
TIT @ 100 Percent Power, ^{o}F		**2500**		
TIT Control		**VPT**		
Nominal Compressor Pressure Ratio @ 100 Percent Power		**6.0**		
Ta, ^{o}R	545	545	545	545
Pa, psia	14.434	14.434	14.434	14.434
Power, hp	100.0	50.0	10.0	-0-
SFC, lb/hp hr (W_f, lb/hr)	0.405	0.338		2.538
T4 (TIT), ^{o}R	2960	2960		1609
G.G. Shaft Speed, rpm	92982	69528		46491
P.T. Shaft Speed (Optimum), rpm	79857	75935		-0-
Inlet Airflow, lb/sec	0.773	0.434		0.277
P1/PA - Inlet Filter Pressure Ratio	0.99	0.997		0.999
P2/P1 - First Compressor Pressure Ratio	2.824	2.059		1.380
P3/P2 - Second Compressor Pressure Ratio	2.125	1.627		1.180
P3A/P2 - Regenerator Cold Side Pressure Ratio	0.97	0.970		0.966
P4/P3A - Burner Pressure Ratio	0.97	0.967		0.965
P4/P5 - Compressor Turbine Pressure Ratio	2.428	1.600		1.441
P5/P6 - Power Turbine Pressure Ratio	2.025	1.833		1.029
P7/P6 - Exhaust Duct Pressure Ratio	0.965	0.986		0.996
P8/P7 - Regenerator Hot Side Pressure Ratio	0.921	0.951		0.983
P9/P8 - Tailpipe Pressure Ratio	0.990	0.997		0.999
T2, ^{o}R	814.7	699		610
T3, ^{o}R	1064.5	836		662
T3A, ^{o}R	2095.2	2323		1431
T5, ^{o}R	2527.1	2712		1492
T6, ^{o}R	2209.8	2426		1492
T8, ^{o}R	1229.2	1000		732
Q1 - lb/sec$\sqrt{^{o}R}$/psia	1.263	0.7030		0.449
Q2 - lb/sec$\sqrt{^{o}R}$/psia	0.547	0.3868		0.344
Q4 - lb/sec$\sqrt{^{o}R}$/psia	0.524	0.5218		0.504
Q5 - lb/sec$\sqrt{^{o}R}$/psia	1.176	0.7990		0.700
EC1 - First Compressor Efficiency (Total-to-Total)	0.693	0.808		0.806
EC2 - Second Compressor Efficiency (Total-to-Static)	0.760	0.750		0.568
ET1 - Compressor Turbine Efficiency (Total-to-Total)	0.791	0.813		0.813
ET2 - Power Turbine Efficiency (Total-to-Total)	0.821	0.799		-0-
EB - Burner Efficiency	0.999	0.998		0.999
ER - Regenerator Effectiveness	0.900	0.935		0.940
WL1/W1 - Labyrinth Seal Leakage	0.010	0.010		0.010
HP1ext - G.G. Shaft Bearing Friction Loss, hp	1.068	0.664		0.356
HP2ext - Accessory Load Requirement (from G.G. Shaft), hp	1.666	1.197		0.796
HP3ext - Gearbox Frictional (Bearing) Loss, hp	1.602	1.474		-0-
HP4ext - Gearbox Gear Loss, hp				

TABLE XXXVI. ENGINE 8 PERFORMANCE SUMMARY (SI UNITS)

Engine	**8**			
Compressor Configuration	**R - R**			
TIT @ 100 Percent Power, °K	**1422**			
TIT Control	**VPT**			
Nominal Compressor Pressure Ratio @ 100 Percent Power	**5.28**			
Ta, °K	303	303	303	303
Pa, kPa	99.519	99.519	99.519	99.519
Power, kW	74.6	37.3	7.5	-0-
SFC, kg/kW-h (W_f, kg/h)	0.265	0.255	0.308	(1.34)
T4 (TIT), °K	2100	2100	2014	1087
G.G. Shaft Speed, rpm	68873	53115	34436	34436
P.T. Shaft Speed (Optimum), rpm	66305	62091	40706	-0-
Inlet Airflow, kg/s	0.482	0.278	0.135	0.172
P1/PA - Inlet Filter Pressure Ratio	0.991	0.997	0.996	0.999
P2/P1 - First Compressor Pressure Ratio	2.687	1.927	1.321	1.316
P3/P2 - Second Compressor Pressure Ratio	1.964	1.571	1.261	1.178
P3A/P2 - Regenerator Cold Side Pressure Ratio	0.970	0.970	0.977	0.969
P4/P3A - Burner Pressure Ratio	0.970	0.967	0.973	0.967
P4/P5 - Compressor Turbine Pressure Ratio	2.426	1.630	1.254	1.382
P5/P6 - Power Turbine Pressure Ratio	1.805	1.631	1.225	1.027
P7/P6 - Exhaust Duct Pressure Ratio	0.969	0.988	0.996	0.997
P8/P7 - Regenerator Hot Side Pressure Ratio	0.926	0.953	0.976	0.982
P9/P8 - Tailpipe Pressure Ratio	0.992	0.998	0.999	0.999
T2, °K	434	380	335	333
T3, °K	553	449	367	360
T3A, °K	1028	1134	1212	775
T5, °K	1209	1269	1316	803
T6, °K	1078	1180	1267	803
T8, °K	622	517	442	393
Q1 - (kg/s)($\sqrt{°K}$/kPa)	0.0850	0.0487	0.0236	0.0301
Q2 - (kg/s)($\sqrt{°K}$/kPa)	0.0389	0.0283	0.0188	0.0240
Q4 - (kg/s)($\sqrt{°K}$/kPa)	0.0372	0.0371	0.0316	0.0347
Q5 - (kg/s)($\sqrt{°K}$/kPa)	0.0832	0.0577	0.0387	0.0463
EC1 - First Compressor Efficiency (Total-to-Total)	0.750	0.805	0.777	0.801
EC2 - Second Compressor Efficiency (Total-to-Static)	0.757	0.748	0.727	0.610
ET1 - Compressor Turbine Efficiency (Total-to-Total)	0.791	0.813	0.807	0.813
ET2 - Power Turbine Efficiency (Total-to-Total)	0.822	0.806	0.794	-0-
EB - Burner Efficiency	0.999	0.999	0.999	0.999
ER - Regenerator Effectiveness	0.905	0.937	0.940	0.936
WL1/W1 - Labyrinth Seal Leakage	0.010	0.010	0.010	0.010
HP1ext - G.G. Shaft Bearing Friction Loss, kW	0.697	0.459	0.236	0.236
HP2ext - Accessory Load Requirement (from G.G. Shaft), kW	1.133	0.848	0.553	0.553
HP3ext - Gearbox Frictional (Bearing) Loss, kW	1.193	1.069	0.544	-0-
HP4ext - Gearbox Gear Loss, kW				

TABLE XXXVII. ENGINE 8 PERFORMANCE SUMMARY (ENGLISH UNITS)

Engine	8
Compressor Configuration	R - R
TIT @ 100 Percent Power, ^{o}F	2100
TIT Control	VPT
Nominal Compressor Pressure Ratio @ 100 Percent Power	5.28

Ta, ^{o}R	545	545	545	545
Pa, psia	14.434	14.434	14.434	14.434
Power, hp	100	50	10	-0-
SFC, lb/hp hr (W_f, lb/hr)	0.435	0.369	0.506	(2.95)
T4 (TIT), ^{o}R	2560	2560	2474	1547
G.G. Shaft Speed, rpm	68873	53115	34436	34436
P.T. Shaft Speed (Optimum), rpm	66305	62091	40706	-0-
Inlet Airflow, lb/sec	1.062	0.612	0.297	0.379
P1/PA - Inlet Filter Pressure Ratio	0.991	0.997	0.996	0.999
P2/P1 - First Compressor Pressure Ratio	2.687	1.927	1.321	1.316
P3/P2 - Second Compressor Pressure Ratio	1.964	1.571	1.261	1.178
P3A/P2 - Regenerator Cold Side Pressure Ratio	0.970	0.970	0.977	0.969
P4/P3A - Burner Pressure Ratio	0.970	0.967	0.973	0.967
P4/P5 - Compressor Turbine Pressure Ratio	2.426	1.630	1.254	1.382
P5/P6 - Power Turbine Pressure Ratio	1.805	1.631	1.225	1.027
P7/P6 - Exhaust Duct Pressure Ratio	0.969	0.988	0.996	0.997
P8/P7 - Regenerator Hot Side Pressure Ratio	0.926	0.953	0.976	0.982
P9/P8 - Tailpipe Pressure Ratio	0.992	0.998	0.999	0.999
T2, ^{o}R	781	684	603	600
T3, ^{o}R	995	809	660	648
T3A, ^{o}R	1850	2041	2182	1395
T5, ^{o}R	2177	2332	2369	1446
T6, ^{o}R	1940	2124	2280	1446
T8, ^{o}R	1119	931	795	707
Q1 - lb/sec$\sqrt{^{o}R}$/psia	1.734	0.993	0.481	0.614
Q2 - lb/sec$\sqrt{^{o}R}$/psia	0.772	0.577	0.383	0.490
Q4 - lb/sec$\sqrt{^{o}R}$/psia	0.758	0.757	0.644	0.707
Q5 - lb/sec$\sqrt{^{o}R}$/psia	1.696	1.177	0.790	0.944
EC1 - First Compressor Efficiency (Total-to-Total)	0.750	0.805	0.777	0.801
EC2 - Second Compressor Efficiency (Total-to-Static)	0.757	0.748	0.727	0.610
ET1 - Compressor Turbine Efficiency (Total-to-Total)	0.791	0.813	0.807	0.813
ET2 - Power Turbine Efficiency (Total-to-Total)	0.822	0.806	0.794	-0-
EB - Burner Efficiency	0.999	0.999	0.999	0.999
ER - Regenerator Effectiveness	0.905	0.937	0.940	0.936
WL1/W1 - Labyrinth Seal Leakage	0.010	0.010	0.010	0.010
HP1ext - G.G. Shaft Bearing Friction Loss, hp	0.935	0.615	0.316	0.316
HP2ext - Accessory Load Requirement (from G.G. Shaft), hp	1.520	1.137	0.742	0.742
HP3ext - Gearbox Frictional (Bearing) Loss, hp	1.600	1.433	0.729	-0-
HP4ext - Gearbox Gear Loss, hp				

TABLE XXXVIII. ENGINE 8A PERFORMANCE SUMMARY (SI UNITS)

Engine	**8A**			
Compressor Configuration	**R - R**			
TIT @ 100 Percent Power, °K	**1422**			
TIT Control	**VPT**			
Nominal Compressor Pressure Ratio @ 100 Percent Power	**5.28**			
Ta, °K	303	303	303	303
Pa, kPa	99.519	99.519	99.519	99.519
Power, kW	74.6	37.3	7.5	-0-
SFC, kg/kW-h (W_f, kg/h)	0.273	0.232	0.321	(1.41)
T4 (TIT), °K	2100	2100	2058	1121
G.G. Shaft Speed, rpm	67975	52500	33985	33985
P.T. Shaft Speed (Optimum), rpm	65240	60945	40106	-0-
Inlet Airflow, kg/s	0.495	0.286	0.137	0.176
P1/PA - Inlet Filter Pressure Ratio	0.991	0.997	0.999	0.999
P2/P1 - First Compressor Pressure Ratio	2.688	1.931	1.321	1.316
P3/P2 - Second Compressor Pressure Ratio	1.964	1.572	1.262	1.183
P3A/P2 - Regenerator Cold Side Pressure Ratio	0.970	0.970	0.977	0.969
P4/P3A - Burner Pressure Ratio	0.969	0.966	0.972	0.966
P4/P5 - Compressor Turbine Pressure Ratio	2.439	1.643	1.258	1.386
P5/P6 - Power Turbine Pressure Ratio	1.795	1.621	1.220	1.027
P7/P6 - Exhaust Duct Pressure Ratio	0.969	0.988	0.996	0.997
P8/P7 - Regenerator Hot Side Pressure Ratio	0.927	0.954	0.975	0.982
P9/P8 - Tailpipe Pressure Ratio	0.992	0.998	0.999	0.999
T2, °K	434	381	335	334
T3, °K	553	450	367	360
T3A, °K	1028	1134	1234	792
T5, °K	1208	1294	1339	821
T6, °K	1078	1180	1289	821
T8, °K	622	518	444	393
Q1 - (kg/s)($\sqrt{°K}$/kPa)	0.0873	0.0502	0.0241	0.0307
Q2 - (kg/s)($\sqrt{°K}$/kPa)	0.0389	0.0291	0.0192	0.0245
Q4 - (kg/s)($\sqrt{°K}$/kPa)	0.0382	0.0381	0.0326	0.0357
Q5 - (kg/s)($\sqrt{°K}$/kPa)	0.0858	0.0598	0.0401	0.0478
EC1 - First Compressor Efficiency (Total-to-Total)	0.750	0.805	0.777	0.801
EC2 - Second Compressor Efficiency (Total-to-Static)	0.757	0.748	0.727	0.621
ET1 - Compressor Turbine Efficiency (Total-to-Total)	0.790	0.813	0.807	0.812
ET2 - Power Turbine Efficiency (Total-to-Total)	0.822	0.807	0.794	-0-
EB - Burner Efficiency	0.998	0.998	0.998	0.998
ER - Regenerator Effectiveness	0.905	0.937	0.940	0.937
WL1/W1 - Labyrinth Seal Leakage	0.010	0.010	0.010	0.010
HP1ext - G.G. Shaft Bearing Friction Loss, kW	0.746	0.492	0.246	0.246
HP2ext - Accessory Load Requirement (from G.G. Shaft), kW	1.700	1.387	0.865	0.865
HP3ext - Gearbox Frictional (Bearing) Loss, kW	1.119	0.999	0.515	-0-
HP4ext - Gearbox Gear Loss. kW	1.491	0.746	0.149	-0-

TABLE XXXIX. ENGINE 8A PERFORMANCE SUMMARY (ENGLISH UNITS)

Engine	8A			
Compressor Configuration	R - R			
TIT @ 100 Percent Power, °F	2100			
TIT Control	VPT			
Nominal Compressor Pressure Ratio @ 100 Percent Power	5.28			
Ta, °R	545	545	545	545
Pa, psia	14.435	14.435	14.435	14.435
Power, hp	100	50	10	-0-
SFC, lb/hp hr (W_f, lb/hr)	0.448	0.381	0.527	(3.11)
T4 (TIT), °R	2560	2560	2518	1581
G.G. Shaft Speed, rpm	67975	52500	33985	33985
P.T. Shaft Speed (Optimum), rpm	65240	60945	40106	-0-
Inlet Airflow, lb/sec	1.091	0.630	0.303	0.387
P1/PA - Inlet Filter Pressure Ratio	0.991	0.997	0.999	0.999
P2/P1 - First Compressor Pressure Ratio	2.688	1.931	1.321	1.316
P3/P2 - Second Compressor Pressure Ratio	1.964	1.572	1.262	1.183
P3A/P2 - Regenerator Cold Side Pressure Ratio	0.970	0.970	0.977	0.969
P4/P3A - Burner Pressure Ratio	0.969	0.966	0.972	0.966
P4/P5 - Compressor Turbine Pressure Ratio	2.439	1.643	1.258	1.386
P5/P6 - Power Turbine Pressure Ratio	1.795	1.621	1.220	1.027
P7/P6 - Exhaust Duct Pressure Ratio	0.969	0.988	0.996	0.997
P8/P7 - Regenerator Hot Side Pressure Ratio	0.927	0.954	0.975	0.982
P9/P8 - Tailpipe Pressure Ratio	0.992	0.998	0.999	0.999
T2, °R	781	685	603	601
T3, °R	995	810	660	648
T3A, °R	1850	2041	2221	1425
T5, °R	2175	2329	2410	1478
T6, °R	1940	2124	2321	1478
T8, °R	1119	932	799	708
Q1 - lb/sec$\sqrt{°R}$/psia	1.780	1.023	0.491	0.627
Q2 - lb/sec$\sqrt{°R}$/psia	0.793	0.594	0.391	0.500
Q4 - lb/sec$\sqrt{°R}$/psia	0.779	0.778	0.664	0.728
Q5 - lb/sec$\sqrt{°R}$/psia	1.750	1.219	0.817	0.975
EC1 - First Compressor Efficiency (Total-to-Total)	0.750	0.805	0.777	0.801
EC2 - Second Compressor Efficiency (Total-to-Static)	0.757	0.748	0.727	0.621
ET1 - Compressor Turbine Efficiency (Total-to-Total)	0.790	0.813	0.807	0.812
ET2 - Power Turbine Efficiency (Total-to-Total)	0.822	0.807	0.794	-0-
EB - Burner Efficiency	0.998	0.998	0.998	0.998
ER - Regenerator Effectiveness	0.905	0.937	0.940	0.937
WL1/W1 - Labyrinth Seal Leakage	0.010	0.010	0.010	0.010
HP1ext - G.G. Shaft Bearing Friction Loss, hp	1.000	0.660	0.330	0.330
HP2ext - Accessory Load Requirement (from G.G. Shaft), hp	2.280	1.860	1.160	1.160
HP3ext - Gearbox Frictional (Bearing) Loss, hp	1.500	1.340	0.690	-0-
HP4ext - Gearbox Gear Loss, hp	2.000	1.000	0.200	-0-

TABLE XL. ENGINE 8B PERFORMANCE SUMMARY (SI UNITS)

Engine	8B
Compressor Configuration	R - R
TIT @ 100 Percent Power, ^{o}K	1422
TIT Control	VPT
Nominal Compressor Pressure Ratio @ 100 Percent Power	5.28

Ta, ^{o}K	303	303	303	303
Pa, kPa	19.519	19.519	19.519	19.519
Power, kW	54.8	27.4	5.5	-0-
SFC, kg/kW-h (W_f, kg/h)	0.270	0.230	0.251	(1.08)
T4 (TIT), ^{o}K	2100	2100	2100	1155
G.G. Shaft Speed, rpm	78900	61000	39450	39450
P.T. Shaft Speed (Optimum), rpm	75558	70525	46630	-0-
Inlet Airflow, kg/s	0.367	0.213	0.102	0.122
P1/PA - Inlet Filter Pressure Ratio	0.991	0.997	0.999	0.999
P2/P1 - First Compressor Pressure Ratio	2.687	1.933	1.321	1.316
P3/P2 - Second Compressor Pressure Ratio	1.964	1.573	1.262	1.186
P3A/P2 - Regenerator Cold Side Pressure Ratio	0.970	0.970	0.977	0.969
P4/P3A - Burner Pressure Ratio	0.970	0.967	0.973	0.969
P4/P5 - Compressor Turbine Pressure Ratio	2.451	1.654	1.263	1.390
P5/P6 - Power Turbine Pressure Ratio	1.787	1.614	1.217	1.027
P7/P6 - Exhaust Duct Pressure Ratio	0.969	0.987	0.997	0.997
P8/P7 - Regenerator Hot Side Pressure Ratio	0.926	0.953	0.975	0.981
P9/P8 - Tailpipe Pressure Ratio	0.992	0.998	0.999	0.999
T2, ^{o}K	434	381	335	334
T3, ^{o}K	553	450	367	360
T3A, ^{o}K	1028	1134	1254	808
T5, ^{o}K	1208	1293	1360	808
T6, ^{o}K	1078	1180	1311	838
T8, ^{o}K	622	518	446	396
Q1 - (kg/s)($\sqrt{^{o}K}$/kPa)	0.0655	0.0373	0.0178	0.0227
Q2 - (kg/s)($\sqrt{^{o}K}$/kPa)	0.0288	0.0216	0.0141	0.0181
Q4 - (kg/s)($\sqrt{^{o}K}$/kPa)	0.0283	0.0283	0.0242	0.0265
Q5 - (kg/s)($\sqrt{^{o}K}$/kPa)	0.0640	0.0446	0.0300	0.0356
EC1 - First Compressor Efficiency (Total-to-Total)	0.750	0.805	0.776	0.801
EC2 - Second Compressor Efficiency (Total-to-Static)	0.757	0.748	0.726	0.629
ET1 - Compressor Turbine Efficiency (Total-to-Total)	0.790	0.812	0.806	0.812
ET2 - Power Turbine Efficiency (Total-to-Total)	0.822	0.807	0.794	-0-
EB - Burner Efficiency	0.988	0.988	0.988	0.998
ER - Regenerator Effectiveness	0.905	0.937	0.940	0.938
WL1/W1 - Labyrinth Seal Leakage	0.010	0.010	0.010	0.010
HP1ext - G.G. Shaft Bearing Friction Loss, kW	0.559	0.365	0.186	0.186
HP2ext - Accessory Load Requirement (from G.G. Shaft), kW	1.700	1.387	0.865	0.865
HP3ext - Gearbox Frictional (Bearing) Loss, kW	0.843	0.746	0.388	-0-
HP4ext - Gearbox Gear Loss, kW	1.119	0.559	0.112	-0-

TABLE XLI. ENGINE 8B PERFORMANCE SUMMARY (ENGLISH UNITS)

Engine	**8B**			
Compressor Configuration	**R - R**			
TIT @ 100 Percent Power, °F	**2100**			
TIT Control	**VPT**			
Nominal Compressor Pressure Ratio @ 100 Percent Power	**5.28**			
Ta, °R	545	545	545	545
Pa, psia	14.434	14.434	14.434	14.434
Power, hp	73.5	36.8	7.4	-0-
SFC, lb/hp hr (W_f, lb/hr)	0.452	0.386	0.538	(2.37)
T4 (TIT), °R	2560	2560	2560	1615
G.G. Shaft Speed, rpm	78900	61000	39450	39450
P.T. Shaft Speed (Optimum), rpm	75558	70525	46630	-0-
Inlet Airflow, lb/sec	0.810	0.469	0.224	0.286
P1/PA - Inlet Filter Pressure Ratio	0.991	0.997	0.999	0.999
P2/P1 - First Compressor Pressure Ratio	2.687	1.933	1.321	1.316
P3/P2 - Second Compressor Pressure Ratio	1.964	1.573	1.262	1.186
P3A/P2 - Regenerator Cold Side Pressure Ratio	0.970	0.970	0.977	0.969
P4/P3A - Burner Pressure Ratio	0.970	0.967	0.973	0.969
P4/P5 - Compressor Turbine Pressure Ratio	2.451	1.654	1.263	1.390
P5/P6 - Power Turbine Pressure Ratio	1.787	1.614	1.217	1.027
P7/P6 - Exhaust Duct Pressure Ratio	0.969	0.987	0.997	0.997
P8/P7 - Regenerator Hot Side Pressure Ratio	0.926	0.953	0.975	0.981
P9/P8 - Tailpipe Pressure Ratio	0.992	0.998	0.999	0.999
T2, °R	781	685	603	601
T3, °R	995	810	660	648
T3A, °R	1851	2041	2257	1455
T5, °R	2174	2327	2448	1509
T6, °R	1940	2124	2359	1508
T8, °R	1119	933	803	712
Q1 - lb/sec$\sqrt{°R}$/psia	1.332	0.761	0.363	.463
Q2 - lb/sec$\sqrt{°R}$/psia	0.589	0.442	0.289	.70
Q4 - lb/sec$\sqrt{°R}$/psia	0.578	0.578	0.494	0.5[illegible]1
Q5 - lb/sec$\sqrt{°R}$/psia	1.305	0.911	0.611	0.727
EC1 - First Compressor Efficiency (Total-to-Total)	0.750	0.805	0.776	0.801
EC2 - Second Compressor Efficiency (Total-to-Static)	0.757	0.748	0.726	0.629
ET1 - Compressor Turbine Efficiency (Total-to-Total)	0.790	0.812	0.806	0.812
ET2 - Power Turbine Efficiency (Total-to-Total)	0.822	0.807	0.794	-0-
EB - Burner Efficiency	0.998	0.998	0.998	0.998
ER - Regenerator Effectiveness	0.905	0.937	0.940	0.938
WL1/W1 - Labyrinth Seal Leakage	0.010	0.010	0.010	0.010
HP1ext - G.G. Shaft Bearing Friction Loss, hp	0.750	0.490	0.250	0.250
HP2ext - Accessory Load Requirement (from G.G. Shaft), hp	2.280	1.860	1.160	1.160
HP3ext - Gearbox Frictional (Bearing) Loss, hp	1.130	1.000	0.520	-0-
HP4ext - Gearbox Gear Loss, hp	1.500	0.750	0.150	-0-

TABLE XLII. ENGINE 9 PERFORMANCE SUMMARY (SI UNITS)

Engine	9			
Compressor Configuration	R - R			
TIT @ 100 Percent Power, ^{o}K	1505			
TIT Control	Variable Transmission			
Nominal Compressor Pressure Ratio @ 100 Percent Power	5.58			
Ta, ^{o}K	303	303	303	303
Pa, kPa	99.519	99.519	99.519	99.519
Power, kW	74.6	37.3	7.5	-0-
SFC, kg/kW-h (W_f, kg/h)	0.250	0.218	0.308	(1.23)
T4 (TIT), ^{o}K	2250	2250	2106	1149
G.G. Shaft Speed, rpm	79285	61455	40635	39640
P.T. Shaft Speed (Optimum), rpm	79285	61455	40635	39640
Inlet Airflow, kg/s	0.409	0.241	0.127	0.143
P1/PA - Inlet Filter Pressure Ratio	0.991	0.997	0.999	0.999
P2/P1 - First Compressor Pressure Ratio	2.754	2.028	1.367	1.342
P3/P2 - Second Compressor Pressure Ratio	2.027	1.610	1.270	1.194
P3A/P2 - Regenerator Cold Side Pressure Ratio	0.970	0.970	0.971	0.969
P4/P3A - Burner Pressure Ratio	0.970	0.967	0.966	0.967
P4/P5 - Compressor Turbine Pressure Ratio	2.456	2.126	1.437	1.367
P5/P6 - Power Turbine Pressure Ratio	1.886	1.346	1.096	1.075
P7/P6 - Exhaust Duct Pressure Ratio	0.969	0.987	0.996	0.997
P8/P7 - Regenerator Hot Side Pressure Ratio	0.926	0.952	0.974	0.983
P9/P8 - Tailpipe Pressure Ratio	0.992	0.998	0.999	0.999
T2, ^{o}K	442	387	338	336
T3, ^{o}K	568	461	371	363
T3A, ^{o}K	1674	1190	1255	801
T5, ^{o}K	1280	1315	1334	838
T6, ^{o}K	1128	1239	1311	832
T8, ^{o}K	644	536	451	399
Q1 - (kg/s)($\sqrt{^{o}K}$/kPa)	0.0721	0.0422	0.0223	0.0251
Q2 - (kg/s)($\sqrt{^{o}K}$/kPa)	0.0317	0.0235	0.0172	0.0197
Q4 - (kg/s)($\sqrt{^{o}K}$/kPa)	0.0307	0.0307	0.0295	0.0284
Q5 - (kg/s)($\sqrt{^{o}K}$/kPa)	0.0696	0.0552	0.0410	0.0376
EC1 - First Compressor Efficiency (Total-to-Total)	0.729	0.807	0.790	0.802
EC2 - Second Compressor Efficiency (Total-to-Static)	0.758	0.750	0.729	0.628
ET1 - Compressor Turbine Efficiency (Total-to-Total)	0.790	0.780	0.780	0.813
ET2 - Power Turbine Efficiency (Total-to-Total)	0.845	0.838	0.770	0.417
EB - Burner Efficiency	0.998	0.998	0.998	0.998
ER - Regenerator Effectiveness	0.905	0.936	0.940	0.935
XL1/W1 - Labyrinth Seal Leakage	0.010	0.010	0.010	0.010
HP1ext - G.G. Shaft Bearing Friction Loss, kW	0.708	0.047	0.246	0.239
HP2ext - Accessory Load Requirement (from G.G. Shaft), kW	1.141	0.850	0.559	0.552
HP3ext - Gearbox Frictional (Bearing) Loss, kW	1.156	0.761	0.403	0.388
HP4ext - Gearbox Gear Loss, kW				

TABLE XLIII. ENGINE 9 PERFORMANCE SUMMARY (ENGLISH UNITS)

Engine	**9**			
Compressor Configuration	**R - R**			
TIT @ 100 Percent Power, °F	**2250**			
TIT Control	**Variable Transmission**			
Nominal Compressor Pressure Ratio @ 100 Percent Power	**5.58**			
Ta, °R	545	545	545	545
Pa, psia	14.435	14.435	14.435	14.435
Power, hp	100	50	10	-0-
SFC, lb/hp hr (W_f, lb/hr)	0.411	0.358	0.506	(2.72)
T4 (TIT), °R	2710	2710	2566	1609
G.G. Shaft Speed, rpm	79285	61455	40635	39640
P.T. Shaft Speed (Optimum), rpm	79285	61455	40635	39640
Inlet Airflow, lb/sec	0.902	0.531	0.280	0.315
P1/PA - Inlet Filter Pressure Ratio	0.991	0.997	0.999	0.999
P2/P1 - First Compressor Pressure Ratio	2.754	2.028	1.367	1.342
P3/P2 Second Compressor Pressure Ratio	2.027	1.610	1.270	1.194
P3A/P. - Regenerator Cold Side Pressure Ratio	0.970	0.970	0.971	0.969
P4/P3A - Burner Pressure Ratio	0.970	0.967	0.966	0.967
P4/P5 - Compressor Turbine Pressure Ratio	2.456	2.126	1.437	1.367
P5/P6 - Power Turbine Pressure Ratio	1.886	1.346	1.096	1.075
P7/P6 - Exhaust Duct Pressure Ratio	0.969	0.987	0.996	0.997
P8/P7 - Regenerator Hot Side Pressure Ratio	0.926	0.952	0.974	0.983
P9/P8 - Tailpipe Pressure Ratio	0.992	0.998	0.999	0.999
T2, °R	795	696	609	605
T3, °R	1023	829	668	654
T3A, °R	1934	2142	2259	1442
T5, °R	2304	2367	2401	1508
T6, °R	2031	2231	2360	1497
T8, °R	1159	965	811	719
Q1 - lb/sec$\sqrt{°R}$/psia	1.472	0.861	0.454	0.511
Q2 - lb/sec$\sqrt{°R}$/psia	0.646	0.480	0.351	0.401
Q4 - lb/sec$\sqrt{°R}$/psia	0.627	0.627	0.602	0.580
Q5 - lb/sec$\sqrt{°R}$/psia	1.419	1.125	0.836	0.767
EC1 - First Compressor Efficiency (Total-to-Total)	0.729	0.807	0.790	0.802
EC2 - Second Compressor Efficiency (Total-to-Static)	0.758	0.750	0.729	0.628
ET1 - Compressor Turbine Efficiency (Total-to-Total)	0.790	.780	0.780	0.813
ET2 - Power Turbine Efficiency (Total-to-Total)	0.845	838	0.770	0.417
EB - Burner Efficiency	0.998	.998	0.998	0.998
ER - Regenerator Effectiveness	0.905	0.936	0.940	0.935
WL1/W1 - Labyrinth Seal Leakage	0.010	0.010	0.010	0.010
HP1ext - G.G. Shaft Bearing Friction Loss, hp	0.950	0.063	0.330	0.320
HP2ext - Accessory Load Requirement (from G.G. Shaft), hp	1.530	1.140	0.750	0.740
HP3ext - Gearbox Frictional (Bearing) Loss, hp	1.550	1.020	0.540	0.520
HP4ext - Gearbox Gear Loss hp				

TABLE XLIV. ENGINE 10 PERFORMANCE SUMMARY (SI UNITS)

Engine	10
Compressor Configuration	R - R
TIT @ 100 Percent Power, ^{o}K	1422
TIT Control	VPT
Nominal Compressor Pressure Ratio @ 100 Percent Power	5.27

Ta, ^{o}K	303	303	303	303
Pa, kPa	19.519	19.519	19.519	19.519
Power, kW	74.6	37.3	7.5	-0-
SFC, kg/kW-h (W_f, kg/h)	0.287	0.236	0.332	(1.54)
T4 (TIT), ^{o}K	2100	2100	1964	1133
G.G. Shaft Speed, rpm	64772	49483	32386	32386
P.T. Shaft Speed (Optimum), rpm	62084	58573	37615	-0-
Inlet Airflow, kg/s	0.545	0.308	0.157	0.193
P1/PA - Inlet Filter Pressure Ratio	0.991	0.997	0.999	0.999
P2/P1 - First Compressor Pressure Ratio	2.686	1.901	1.320	1.316
P3/P2 - Second Compressor Pressure Ratio	1.964	1.560	1.257	1.183
P3A/P2 - Regenerator Cold Side Pressure Ratio	0.970	0.970	0.976	0.969
P4/P3A - Burner Pressure Ratio	0.970	0.967	0.972	0.967
P4/P5 - Compressor Turbine Pressure Ratio	2.541	1.649	1.271	1.390
P5/P6 - Power Turbine Pressure Ratio	1.724	1.581	1.205	1.026
P7/P6 - Exhaust Duct Pressure Ratio	0.969	0.987	0.997	0.997
P8/P7 - Regenerator Hot Side Pressure Ratio	0.927	0.955	0.976	0.982
P9/P8 - Tailpipe Pressure Ratio	0.992	0.998	0.999	0.999
T2, ^{o}K	434	378	335	334
T3, ^{o}K	553	446	366	360
T3A, ^{o}K	1029	1140	1189	796
T5, ^{o}K	1201	1293	1286	827
T6, ^{o}K	1079	1185	1241	827
T8, ^{o}K	613	500	420	388
Q1 - (kg/s)($\sqrt{^{o}K}$/kPa)	0.0962	0.0541	0.0274	0.0338
Q2 - (kg/s)($\sqrt{^{o}K}$/kPa)	0.0429	0.0318	0.0219	0.0270
Q4 - (kg/s)($\sqrt{^{o}K}$/kPa)	0.0404	0.0404	0.0348	0.0379
Q5 - (kg/s)($\sqrt{^{o}K}$/kPa)	0.0911	0.0636	0.0432	0.0509
EC1 - First Compressor Efficiency (Total-to-Total)	0.749	0.805	0.780	0.801
EC2 - Second Compressor Efficiency (Total-to-Static)	0.757	0.748	0.728	0.622
ET1 - Compressor Turbine Efficiency (Total-to-Total)	0.786	0.813	0.808	0.813
ET2 - Power Turbine Efficiency (Total-to-Total)	0.822	0.805	0.793	-0-
EB - Burner Efficiency	0.998	0.998	0.998	0.998
ER - Regenerator Effectiveness	0.905	0.939	0.940	0.940
WL1/W1 - Labyrinth Seal Leakage	0.050	0.053	0.060	0.050
HP1ext - G.G. Shaft Bearing Friction Loss kW	0.701	0.455	0.239	0.239
HP2ext - Accessory Load Requirement (from G.G. Shaft), kW	1.462	1.081	0.716	0.716
HP3ext - Gearbox Frictional (Bearing) Loss, kW	1.193	1.089	0.537	-0-
HP4ext - Gearbox Gear Loss, kW				

TABLE XLV. ENGINE 10 PERFORMANCE SUMMARY (ENGLISH UNITS)

Engine	10
Compressor Configuration	R - R
TIT @ 100 Percent Power, ^{o}F	2100
TIT Control	VPT
Nominal Compressor Pressure Ratio @ 100 Percent Power	5.27

Ta, ^{o}R	545	545	545	545
Pa, psia	14.435	14.435	14.435	14.435
Power, hp	100	50	10	-0-
SFC, lb/hp hr (W_f, lb/hr)	0.472	0.388	0.546	(3.39)
T4 (TIT), ^{o}R	2560	2560	2424	1593
G.G. Shaft Speed, rpm	64772	49483	32386	32386
P.T. Shaft Speed (Optimum), rpm	62084	58573	37615	-0-
Inlet Airflow, lb/sec	1.202	0.680	0.346	0.426
P1/PA - Inlet Filter Pressure Ratio	0.991	0.997	0.999	0.999
P2/P1 - First Compressor Pressure Ratio	2.686	1.901	1.320	1.316
P3/P2 - Second Compressor Pressure Ratio	1.964	1.560	1.257	1.183
P3A/P2 - Regenerator Cold Side Pressure Ratio	0.970	0.970	0.976	0.969
P4/P3A - Burner Pressure Ratio	0.970	0.967	0.972	0.967
P4/P5 - Compressor Turbine Pressure Ratio	2.541	1.649	1.271	1.390
P5/P6 - Power Turbine Pressure Ratio	1.724	1.581	1.205	1.026
P7/P6 - Exhaust Duct Pressure Ratio	0.969	0.987	0.997	0.997
P8/P7 - Regenerator Hot Side Pressure Ratio	0.927	0.955	0.976	0.982
P9/P8 - Tailpipe Pressure Ratio	0.992	0.998	0.999	0.999
T2, ^{o}R	781	681	603	601
T3, ^{o}R	995	803	658	648
T3A, ^{o}R	1852	2052	2140	1432
T5, ^{o}R	2161	2328	2314	1488
T6, ^{o}R	1942	2133	2234	1488
T8, ^{o}R	1103	900	756	698
Q1 - lb/sec$\sqrt{^{o}R}$/psia	1.961	1.104	0.559	0.690
Q2 - lb/sec$\sqrt{^{o}R}$/psia	0.874	0.649	0.446	0.550
Q4 - lb/sec$\sqrt{^{o}R}$/psia	0.824	0.824	0.710	0.772
Q5 - lb/sec$\sqrt{^{o}R}$/psia	1.858	1.296	0.881	1.037
EC1 - First Compressor Efficiency (Total-to-Total)	0.749	0.805	0.780	0.801
EC2 - Second Compressor Efficiency (Total-to-Static)	0.757	0.748	0.728	0.622
ET1 - Compressor Turbine Efficiency (Total-to-Total)	0.786	0.813	0.808	0.813
ET2 - Power Turbine Efficiency (Total-to-Total)	0.822	0.805	0.793	-0-
EB - Burner Efficiency	0.998	0.998	0.998	0.998
ER - Regenerator Effectiveness	0.905	0.939	0.940	0.940
WL1/W1 - Labyrinth Seal Leakage	0.050	0.053	0.060	0.050
HP1ext - G.G. Shaft Bearing Friction Loss, hp	0.94	0.61	0.32	0.32
HP2ext - Accessory Load Requirement (from G.G. Shaft), hp	1.96	1.45	0.96	0.96
HP3ext - Gearbox Frictional (Bearing) Loss, hp	1.60	1.46	0.72	-0-
HP4ext - Gearbox Gear Loss, hp				

APPENDIX B

CONVERSION FACTORS

TABLE XLVI. CONVERSION OF ENGLISH UNITS TO SI UNITS

PARAMETER	ENGLISH UNIT	MULT. BY TO OBTAIN	SI UNIT
Angle, Unit	degrees (^{o})	$1.7453292519943 \times 10^{-2}$	radians (rad)
Area, Unit	$(feet)^2$ $(ft)^2$ $(inch)^2$ $(in)^2$	9.290304×10^{-2}* 6.4516×10^{0}*	square meter (m(2) square centimeters (cm^2)
Density, Unit	lbm/in^3	2.76799×10^{1}	gram/$centimeter^3$ (g/cm^3)
Energy	Btu (IST)	1.055056×10^{3}	Joule (J)
		NOTE: kilojoules & kilowatts are obvious alternates	
Enthalpy	(Btu/lbm)	2.326000×10^{0}	kilojoule/kilogram (kJ/kg)
Flow Parameter	$\frac{lbm}{s}\ \frac{\sqrt{^oR}}{psia}$	4.90355×10^{-2}	$\frac{kg}{s}\ \frac{\sqrt{^oK}}{kPa}$
Flow Rate, Unit	pounds/hour (lbm/h)	4.5359237×10^{-1}*	kilogram/hour (kg/h)
Force	Lbf/in	1.751268×10^{2}	kilo Newton/meter kN/m
Force, Unit	pound force (lbf)	$4.4482216152605 \times 10^{0}$*	Newton (N)
Gravity, Acceleration of = 9.80621 m/s^2 (32.1725 ft/s^2)			
Length, Unit	Feet (ft) Inch (in)	3.048×10^{-1}* 2.54×10^{0}*	meter (m) centimeter (cm)
	nautical mile (nm)	1.8252×10^{0}*	kilometer (km)
	U.S. statute mile (mi)	1.609344×10^{0}*	kilometer (km)

*Indicates "by definition."

PARAMETER	ENGLISH UNIT	MULT. BY TO OBTAIN	SI UNIT
Mass, Unit	pound mass (lbm)	4.5359237×10^{-1}*	kilogram (kg)
Power	$\frac{\text{ft-lbf}}{\text{s}}$	1.3558179×10^{0}	Watt (W)
Power, Unit	horsepower (hp)	7.4569987×10^{-1}	kiloWatt (kW)
	power $\frac{\text{in-lbf}}{\text{s}}$	1.129848×10^{-1}	Watt (W)
Pressure, Unit	psi (lbf/in^2)	6.8947572×10^{0}	kiloPascal (kPa)
		NOTE: $1\ N/M^2 = 1$ pascal, 1 AT = 101.325 kPa	
Range	nautical mile/gallon (nm/gal)	4.892467×10^{-1}	kilometer/liter (km/l)
	U.S. statute mile/gallon (mpg)	4.251437×10^{-1}	(km/l)
Specific Fuel Comsumption (Power)	BSFC (lbm/hp-h)	6.082774×10^{-1}	kg/kW-h
Specific Fuel Consumption (Thrust)	TSFC (lbm/lbf-h)	$1,01972 \times 10^{-1}$*	kg/N-h
Specific Out-Put Power	$\frac{\text{hp}\cdot\text{s}}{\text{lbm}}$	1.6439869×10^{0}	$\frac{\text{kW}\cdot\text{s}}{\text{kg}}$
Stress, Unit	ksi	6.8947572×10^{0}	Megapascal (MPa)
Temp., Unit	degree Rankine ($^{\circ}R$)	$T_k = \frac{5}{9} T_R$	Kelvin (K)
	degree Fahrenheit ($^{\circ}F$)	$T_k = \frac{5}{9} (T_F + 459.67)$	Kelvin (K)
		NOTE: $T_k = T_{celsius} + 273.15$	
Specific Thrust	(lbf-s/lbm)	9.80665×10^{0}	N-s/kg
Velocity, Unit	feet/minute (ft/min)	3.048×10^{-1}*	meter/minute (m/m)

*Indicates "by definition."

PARAMETER	ENGLISH UNIT	MULT. BY TO OBTAIN	SI UNIT
Velocity, Unit	feet/second (ft/s)	3.048×10^{-1}*	meter/second (m/s)
	knots	1.85200×10^{0}*	kilometer/hour (km/h)
	statute mile/hour (mi/h) (mpr)	1.609344×10^{0}*	kilometer/hour (km/h)
Volume, Unit	$(feet)^3$ (ft^3)	$2.8316846592 \times 10^{-2}$*	cubic meter (m^3)
	$(inch)^3$ (in^3)	1.637064×10^{1}*	cubic centimeter (cm^3)
	gallon (gal.) (U.S. liquid)	$3.785411784 \times 10^{0}$*	liter (l)

*Indicates "by definition."

APPENDIX C

IGT POWERTRAIN PARTS LIST

DATE: 27 NOVEMBER 1978 REVISION

MATERIAL CODE

S	Steel
SS	Stainless Steel
AL	Aluminum
AS	Alloy Steel
I	Insulation
C	Ceramic
B	Bearing
BB	Ball Bearing
V	Viton
G	Gasket
HT	High Temperature Alloy
T	Titanium

Reference - Improved Gas Turbine
Basic Cross Section
P7857 13 September 1978 Revision

GROUP C - GEARBOX

LEVEL	MTRL CODE	QTY	PART NO.	DESCRIPTION
3	-	1	C1	Gearbox Assembly
4	-	1	C2	Hsg, Gearbox - Rear
5	AL	1	C3	Hsg, Gearbox, Rear - Cstg.
4	BB	4	C4	Brg, Pinion Gear (2 on C43 not shown)
4	BB	6	C5	Brg, Acc Drive Gear
4	BB	2	C6	Brg, Power Output Gear
4	-	1	C7	Bushing, Labyrinth Seal
4	S	3	C8	Seal, Acc Drive Gear
4	S	1	C9	Seal, Power Output Gear
4	B	2	C10	Brg, Power Turbine Shaft
4	-	1	C11	CDP Duct Assy
5	-	1	C12	Flange, CDP Duct Assy Mtg
6	S	1	C13	Flange, CDP Duct Assy Mtg - Cstg
5	S	1	C14	CDP Duct Wall - Outer
5	S	1	C15	CDP Duct Wall - Inner
5	-	1	C16	Flange - Vane Control Mtg
6	SS	1	C17	Flange, Vane Control Mtg - Cstg
5	I	AR	C18	Insulation, Exhaust Duct - Outer
5	-	1	C19	Flange, Heat Exchanger Mtg
6	S	1	C20	Flange, Heat Exchanger Mtg - Cstg
4	S	24	C21	Bolt - CDP Assy Mtg
4	-	1	C23	Shroud and Vane Assy - Power Turb
5	-	1	C24	Vane and Shroud - Power Turb
6	SS	1	C25	Vane and Shroud, Power Turb -Cstg
5	SS	1	C27	Support Cyl - Vane and Shroud
5	SS	1	C28	Flange, Support - Vane and Shroud
4	SS	4	C30	Screw - Vane and Shroud Mtg
4	SS	1	C31	Ring - Vane and Shroud Sealing
4	SS	1	C32	Exhaust Duct - Outer Wall
4	B	1	C33	Brg, Power Turb Shaft Thrust - Rear (with pin)
4	B	1	C34	Brg, Power Turb Shaft Thrust - Front (with pin)
4	-	1	C35	Hsg, Turb Shaft Brg
5	S	1	C36	Hsg, Turb Shaft Brg - Cstg
4	S	3	C37	Washer - Turb Shaft Brg Hsg Mtg
4	S	3	C38	Bolt - Turb Shaft Brg Hsg Mtg
4	B	1	C39	Brg, Gasifier Rotor Intermediate
4	-	1	C40	Gear Assy, Drivetrain Inter
5	S	1	C41	Gear, Drivetrain Inter
5	S	1	C42	Pinion, Drivetrain Inter
4	S	1	C43	Gear, Drivetrain Idler (not shown)
4	S	1	C44	Gear, Drivetrain Output
4	-	1	C45	Hsg, Gearbox - Front
5	AL	1	C46	Hsg, Gearbox, Front - Cstg

LEVEL	MTRL CODE	QTY	PART NO.	DESCRIPTION
3	G	1	C53	Gasket, Gearbox Flange
3	S	41	C54	Bolt, Gearbox Hsg
3	S	82	C55	Washer, Gearbox Hsg
3	S	41	C56	Nut, Lock - Gearbox Hsg
3	S	1	C57	Gear, Acc Train Idler
3	-	1	C58	Gear Assy, Acc Train Inter
4	S	1	C59	Gear, Acc Train Inter
4	S	1	C60	Pinion, Acc Train Inter
3	S	1	C61	Gear, Acc Train Output
3	-	1	C62	Tube, Seal - Vane Control
4	SS	1	C63	Tube, Seal - Vane Control Cstg
3	SS	2	C64	Ring, Seal - Vane Control Tube
3	S	36	C66	Bolt, Heat Exchanger Mtg
3	S	1	C67	Plug, Oil Drain
3	S	1	C68	Washer, Oil Drain Plug
4	S	1	C71	Oil Shield - Output Gear

GROUP BD - POWER TURBINE ROTOR

LEVEL	MTRL CODE	QTY	PART NO.	DESCRIPTION
4	-	1	BD1	Power Turbine Rotor Assy
5	-	1	BD2	Rotor, Power Turbine
6	HT	1	BD3	Rotor, Power Turbine - Casting
5	AS	1	BD4	Shaft - Power Turbine
5	S	1	BD6	Washer, Power Turbine Thrust
5	S	1	BD7	Washer, Lock - Power Turbine
5	S	1	BD8	Nut, Pwr Turbine Shaft Assy

GROUP BF - GASIFIER ROTOR

LEVEL	MTRL CODE	QTY	PART NO.	DESCRIPTION
3	-	1	BF1	Rotor Assy, Gasifier Turbine
4	-	1	BF2	Rotor, Turbine, Gasifier
5	HT	1	BF3	Rotor, Turbine, Gasifier - Cstg
4	AS	1	BF4	Shaft, Turbine - Gasifier
4	S	1	BF5	Shaft, Compressor
4	-	1	BF6	Compressor, Centrifugal - No. 2
5	AL	1	BF7	Compressor, Centrifugal, No. 2 - Cstg
4	-	1	BF10	Compressor, Centrifugal - No. 1
5	AL	1	RF11	Compressor, Centrifugal, No. 1 - Cstg
3	S	1	BF14	Washer-Aft Thrust
3	S	1	BF16	Nut, Lock-Turb Shaft
3	S	1	BF17	Washer-Fwd Turb Shaft Thrust
3	S	1	BF18	Sleeve
3	S	1	BF19	Bolt - Gasifier Rotor
3	S	1	BF20	L'washer

GROUP BG - COMPRESSOR STRUCTURES

LEVEL	MTRL CODE	QTY	PART NO.	DESCRIPTION
3	-	1	BG1	Cover, Compressor 2nd
4	AL	1	BG2	Cover, Compressor 2nd - Cstg
3	S	24	BG4	Washer, Compressor Cover Mtg
3	S	24	BG5	Bolt, Compressor Cover Mtg
3	-	1	BG6	Cover, Compressor 1st
4	AL	1	BG7	Cover, Compressor 1st - Cstg
3	B	1	BG11	Brg, Gasifier Rotor Front
3	V	1	BG12	O-Ring - Cap to Cprsr Cover
3	-	1	BG13	Cap - Cprsr Cover
4	AL	1	BG14	Cap, Cprsr Cover - Cstg
3	S	3	BG15	Washer, Cap Mtg
3	S	3	BG16	Bolt, Cap Mtg
3	S	12	BG17	Bolt, Compressor Cover Mtg
3	S	12	BG18	Nut, Compressor Cover Mtg

GROUP F - POWER TURBINE NOZZLE

LEVEL	MTRL CODE	QTY	PART NO.	DESCRIPTION
3	-	1	F1	Power Turb Nozzle Assy
4	-	1	F2	Shroud, Power Turb Nozzle
5	HT	1	F3	Shroud, Power Turb Nozzle - Cstg
4	HT	24	F5	Vane, Power Turb Nozzle
5	HT	24	F6	Vane, Power Turb Nozzle - Cstg
4	SS	24	F7	Gear, PTN Vane
4	-	1	F8	Cover, PTN Vane
5	HT	1	F9	Cover, PTN Vane - Cstg
4	SS	4	F10	Rivet, PTN Vane Cover
4	SS	1	F11	Cylinder, Support-Burst Ring
4	-	1	F12	Burst Ring
5	AS	1	F13	Burst Ring - Cstg
3	-	1	F15	PTN Drive Gear Assy
4	AS	1	F16	Gear - PTN Drive
4	S	1	F17	Coupling - Drive
3	SS	1	F18	Pin - Coupling to Drive Gear
3	SS	1	F24	Brg - Gasifier Rotor
3	-	1	F25	Cover Assy-PTN Drive
3	SS	1	F26	Flange, Fwd-PTN Drive Cover
3	SS	1	F27	Cyl, Support - Nozzle Drive Cover
3	SS	1	F28	Flange, Aft-Nozzle Drive Cover
3	SS	1	F29	Boss, Nozzle Drive Access
3	SS	8	F30	Bolt, Nozzle Drive Cover Mtg
3	SS	2	F33	Ring, Seal-Nozz Assy to Cmbstr
3	SS	1	F34	Cylinder, Support-Seal Ring
3	I	AR	F35	Insulation-Exh Duct - Inner
3	SS	1	F36	Exhaust Duct - Inner Wall

GROUP G - RECUPERATOR

LEVEL	MTRL CODE	QTY	PART NO.	DESCRIPTION
3	-	1	G1	Recuperator
4	C	1	G2	Recuperator - Bonded
3	SS	1	G3	Flange, Recuperator Retaining
3	SS	8	G5	Bolt - Recuperator Mtg
3	-	1	G6	Cover Assy - Recuperator
4	S	1	G7	Flange - Cover Assy Mtg
4	S	1	G8	Duct - Recuperator Cover
4	S	1	G9	Ring, Outer - Heat Exch Seal Mtg
4	SS	1	G10	Ring, Inner - Heat Exch Seal Mtg
4	SS	1	G11	Wall - Inner - Exh Plenum
4	SS	1	G12	Flange - Fuel Injector Hsg Mtg
4	I	AR	G13	Insulation - Heat Exch
4	S	2	G14	Flange, Exhaust Duct-Heat Exch
3	HT	2	G15	Seal, Recuperator Inner
3	HT	2	G16	Seal, Recuperator Outer
3	SS	1	G17	Ring - Pilot and Mtg
4	1	AR	G18	Insulation - Fuel Injector Hsg

GROUP BC - COMBUSTOR

LEVEL	MTRL CODE	QTY	PART NO.	DESCRIPTION
3	-	1	BC1	Combustor Assembly
4	-	19	BC2	Nozzle, Combustor
5	C	19	BC3	Nozzle, Cmbstr - Cstg
4	-	1	BC5	Support, Nozzle, Inner
5	C	1	BC6	Support, Nozzle, Inner-Cstg
4	-	1	BC7	Support, Nozzle - Outer
5	C	1	BC8	Support, Nozzle, Outer-Cstg
4		1	BC9	Catalyst Bed - Combustor
4	-	1	BC10	Support, Catalyst Bed - Cmbstr
5	C	1	BC11	Support, Catalyst Bed, Cmbstr - Cstg
3	SS	1	BC12	Seal, Ring - Injector to Cmbstr
3	-	1	BC13	Fuel Injector Assembly
4	-	1	BC14	Injector, Air - Secondary
5	SS	1	BC15	Injector, Air Secondary - Cstg
4	SS	1	BC16	Injector, Fuel
4	SS	1	BC17	Injector, Air - Primary
4	SS	1	BC18	Nozzle, Fuel
4	SS	1	BC19	Boss, Fuel Inlet
4	-	1	BC20	Housing, Fuel Injector
5	SS	1	BC21	Housing, Fuel Injector - Cstg
3	S	8	BC23	Bolt, Fuel Injector Mtg
3	SS	1	BC24	Hydrogen Generator (not shown)
3		1	BC25	Igniter (not shown)
			BC26	Gasket

REFERENCES

1. Kronogard, S.O. "Turbine Transmission Systems for Automotive and Industrial Traction Applications," SAE Paper No. 660762

2. Kronogard, S.O. "Three-Shaft Automotive Turbine-Transmission Systems of the KTT Type-Performance and Features," ASME Paper No. 77-GT-94

3. Sheiter, M.H., Engineering Consultant to WRC, "The Effect of Transmission Characteristics on Turbine Powered Drive Line Performance," June 15, 1978

4. Rodgers, C. "Variable Geometry Gas Turbine Radial Compressors," ASME Paper 68-GT-63, March 1968

5. AT-6100-R7, "Automobile Gas Turbine Optimization Study," Environmental Protection Agency Contract 68-04-0012, 14 July 1972

6. C. Rodgers and Langworthy, R.A., "Design and Test of a Small Two-Stage High Pressure Ratio Centrifugal Compressor," ASME 74-GT-137, 1973

7. J. O. Wiggins and Waltz, G.L., "Some Experiences in the Scaling of the NASA 9-Stage Transonic Axial Flow Compressor," SAE Paper 720711

8. C.C. Koch and Smith, L.H., Jr., "Loss Sources and Magnitudes in Axial-Flow Compressors," ASME Paper No. 75-WA/GT-6

9. Worth, E.M., "WR33 Low Cost Compressor Aerodynamic Design." WR33-TM1, 3 March 1976

10. Roell, T., "WR33 Six-Stage Axial Compressor Test Results." WR33-TM4, 24 February 1978

11. Wassel, A.B., "Reynolds Number Effects in Axial Compressors," ASME Paper No. 67-WA/GT-2

12. K. Papailiou and Roberts, B., "On the Behavior of Bladings in the Small Reynolds Number Regime," ASME Paper No. 70-WA/GT-11

13. Pampreen, R.C., "Small Turbomachinery Compressor and Fan Aerodynamics," ASME Paper No. 73-GT-6

14. S. Szczecinski et al., "Influence of the Blade Tip Clearance of an Axial Flow Compressor on its Parameters," NASA TT F-12,653, November 1969

15. Roberts, W.B., "A Study of Axial Compressor Blade Optimization for Operation in the Low Reynolds Number Regime," AIAA Paper No. 78-245

16. Heck, R.M., M. Chang, H. Hess and R. Carruba, "Durability Testing at One Atmosphere of Advanced Catalysts and Catalyst Supports for Automotive Gas Turbine Engine Combustors," NASA CR-135132, June 1977.

17. Anderson, D.N., R.R. Tacina, and T.S. Mroz, "Catalytic Combustion for the Automotive Gas Turbine Engine," NASA TM X-73589, April 1977.

18. Wiggins, J.O., and Waltz, G.L., "Some Experiences in the Scaling of the NASA 8-Stage Transonic Axial Flow Compressor," SAE 720711.

19. Riddle, B.C., Davis, R.C., and Castor, J.C., "Automotive Gas Turbine Optimization Study," AiResearch Mfg. Co. of Arizona (APTD-1291, PB-21338910), 1972.

20. Ainley, D.G., and Mathieson, G.C.R., "A Method of Performance Estimation for Axial-Flow Turbines," Report No. R&M 2974, Aeronautical Research Council, Great Britain, 1957.

21. Dunham, J., and Came, P.M., "Improvements to the Ainley-Mathieson Method of Turbine Performance Prediction," ASME Paper No. 70-GT-2.

22. Hamrick, J.T., and Beede, W.L., "Some Investigations with Wet Compression," ASME Transactions Vol. 75, 1953, pp. 409-420.

23. Vanco, M.R., "Fortran Program for Calculating Velocities in the Meridional Plane of a Turbomachine, I - Centrifugal Compressor." NASA TN D-6701, March 1972

24. Hearsey, R.M., "A Revised Computer Program for Axial Compressor Design," ARL 7R 75-0001, January 1975.

25. Smith, S.F., "A Simple Correlation of Turbine Efficiency," Journal R. Aeronautical Science, Vol. 69, 1965, p. 467.